Does building-integrated vegetation provide tangible urban ecosystem services?

By Robert Henry Caesar Fleck

Thesis submitted in fulfilment of the requirements for the degree of Doctor of Philosophy at the University of Technology Sydney under the supervision of Associate Professor Fraser Torpy and Dr. Peter Irga.

This work is a compilation of several published articles where I am the first, or co-first author.

University of Technology Sydney,
Faculty of Science, School of Life Science,
Plants and Environmental Quality Research Group,

Submitted: December 2022.
Revised: March 2023.

Certification of Original Authorship

I, Robert Fleck, declare that this thesis, is submitted in fulfilment of the requirements for the award of Doctor of Philosophy, in the School of Life Sciences at the University of Technology Sydney. This thesis is wholly my own work unless otherwise referenced or acknowledged. In addition, I certify that all information sources and literature used are indicated in the thesis. This document has not been submitted for qualifications at any other academic institution. This research is supported by the Australian Government Research Training Program.

Signature:

Production Note:
Signature removed prior to publication.

Date: 01/12/2022

Acknowledgements

I would like to thank my Supervisors Associate Professor Fraser Torpy and Dr. Peter Irga for giving me the opportunity to do my PhD, giving me the freedom to pursue my research how I thought best, and providing me with the resources and network to develop my professional skills. Over the years, through their mentorship, my academic writing and management skills have improved substantially. I would like to further emphasise my appreciation for the supportive group dynamic they have established. From my perspective, there are many research groups where this is not a priority, and I recognise it is this environment that has helped me grow academically. I'd like to extend my enormous appreciation to Dr. Thomas Pettit for his mentorship, support and patience – and generally being around. Tom, you just being here was a significant driver for me to improve my skills, so thank you for the motivation and one-sided rivalry you probably weren't aware of.

To the rest of the PEQR Research Team, from the interns and capstones I helped supervise, to the Honours and PhD students I have worked with or mentored; Natalie Killingsworth, Ekaterina Arsenteva, Stephanie Sadeeh, Jee Soon Lee, Ky Chau, Gabrielle Duani, Hayden Smith, Stephen Matheson, Luowen Lyu and Raissa Gill. I'd further like to extend my thanks to Dr. Eamon Wooster from the Center for Compassionate Conservation (UTS) for their contributions to our Green Roof projects, as well as Jack Rojahn from the Centre for Conservation Ecology and Genomics (UC). I'd like to thank Nathan Williams from the Ocean Microbiology Group (UTS) for his contributions to my genomic work.

I'd like to thank all of my research collaborators and co-authors for their time and expertise in my exploration of various research topics, often helping me learn something from scratch. I'd like to also thank those academics who helped me understand research topics that I was unable to fully investigate, like the design and synthesis of custom qPCR primers. I would like to acknowledge and express my gratitude to Professor Elena Comino from the Department of Environment, Land, and Infrastructure Engineering (DIATI), Politecnico di Torino (Italy), for creating the link between Australian and Italian research institutions and sending Dr. Laura Dominici to undertake collaborative work with me, contribute to my thesis through the creation of stunning graphics, and for creating such a positive and fun atmosphere to conduct our research.

I'd like to acknowledge my industry partners; Lend Lease, Junglefy, and The City of Sydney for their contributions to this thesis in the form of access, materials, expertise, and funding. Chapters 4, 5 & 6 were conducted with the support of the City of Sydney Environmental Performance - Innovation Grant 2019-20 (2020/037855 / EPI R3 201920005), and the technical expertise and efforts of Mr. Giovanni Cercone, Mr. Martino Masini and Mr. Luke Brown. Most of all, I would like to thank Lucy

Sharman, the Sustainability Manager for Lendlease P/L, without whose management, direction, and facilitation these chapters would have not been possible.

I'd like to thank Dr. Thomas Pettit for his persistent patience and calming demeanour. Tom's guidance and perspective were invaluable, as well as the times we spent in the glasshouse and potting rooms talking things over. Tom's research profile is inspirational, and we all still aim to achieve as much as he did in the few years he was at UTS.

Lastly, I'd like to thank Raissa Gill for her tireless support over the last four years, both academically and personally. As a PhD student your project is never far from your mind and having someone to talk to about your project, work through various ideas and analysis techniques is invaluable, especially when it's past 12am!

Format of Thesis

This thesis is submitted as a *thesis by compilation.* This thesis consists of seven chapters. Chapter 1 is a compilation of two separate peer-reviewed articles (a book chapter and a peer-reviewed conference proceedings), as along with some unpublished material, where Chapters 2-6 represent independent research articles, all of which have been peer-reviewed, accepted, and published in scientific journals. **As such, parts of this thesis are presented verbatim to their published form**, excluding some minor formatting changes to the numbering of figure and table legends, **and with several amendments made as part of the Thesis revision process**; consequently, there is a shift from first person in the introduction and conclusions to third person, and the use of collective terms like "we". There may also be some repetition in regard to themes, style and description of systems. Additionally, the acknowledgements section of each article has been removed and incorporated into the acknowledgements of the thesis.

This thesis is a compilation of my own work, with guidance from my supervisors and others. I conceptualised my research, designed the experiments including choice and development of methods and instrumentation, conducted all data collection and analysis, and wrote the manuscripts. For many of the technical aspects of my project I sought out expertise and was involved in the development of the methodologies and data analysis. My supervisors and co-authors proof-read and edited the final peer reviewed manuscript versions. Publication details are presented at the beginning of each chapter, and co-author contributions are detailed at the end of each chapter.

In respect to formatting, each chapter has been treated as a standalone section, however for the sake of formatting, figures and tables are numbered sequentially. Additionally, this thesis contains a single reference list that encompasses all references used, which is presented at the end of the thesis. This thesis uses the *Journal of Building and Environment* numbered referencing style as the majority of my articles were published in this Journal. As such, references used in the earlier chapters may appear again in the later chapters, and are therefore numbered accordingly. Supplementary material is presented after the references, in separated Chapter-specific sections.

List of peer-reviewed publications contributing to this thesis

Chapter 1:

Fleck. R, Pettit. T.J, Douglas. A.N.J, Irga. P.J, Torpy. F.R, 2020. Chapter 15: Botanical biofiltration for reducing indoor air pollution. *Bio-Based Materials and Biotechnologies for Eco-Efficient Construction*. pp 305-327. doi.org/10.1016/B978-0-12-819481-2.00015-5

Fleck. R, Pettit. T.J, Dominici. L, Gill. R.L, Irga. P.J, Torpy. F.R, 2020. Reducing indoor air pollution through applied botanical biofiltration. *The 16th Conference of the International Society of Indoor Air Quality and Climate: Creative and Smart Solutions for Better Built Environments.* Indoor Air. ISBN: 978-1-7138-2360-5

Chapter 2:

#co-first authors

Dominici. L#, **Fleck. R#**, Gill. R.L, Pettit. T.J, Irga. P.J, Comino. E, Torpy. F.R, 2021. Analysis of lighting conditions of indoor living walls: Effects on CO_2 removal. *Journal of Building Engineering.* 44. doi.org/10.1016/j.jobe.2021.102961

Chapter 3:

Fleck. R, Gill. R.L, Pettit. T.J, Irga. P.J, Williams. N.L.R, Seymour. J.R, Torpy. F.R, 2020. Characterisation of fungal and bacterial dynamics in an active green wall used for indoor air pollutant removal. *Building and Environment.* 179. doi.org/10.1016/j.buildenv.2020.106987

Chapter 4:

Fleck. R, Gill. R.L, Saadeh. S, Pettit. T.J, Wooster. E, Torpy. F.R, Irga. P.J, 2022. Urban green roofs to manage rooftop microclimates: A case study from Sydney, Australia. *Building and Environmen*t. 209. doi.org/10.1016/j.buildenv.2021.108673

Chapter 5:

Fleck. R, Westerhausen. M.T, Killingsworth. N, Ball. J, Torpy. F.R, Irga. P.J, 2022. The hydrological performance of a green roof in Sydney, Australia: A tale of two towers. *Building and Environment*. 221. doi.org/10.1016/j.buildenv.2022.109274

Chapter 6:

Fleck. R, Gill. R.L, Pettit. T.J, Torpy. F.R, Irga. P.J, 2022. Bio-solar green roofs increase solar energy output: the sunny side of integrating sustainable technologies. *Building and Environment.* doi.org/10.1016/j.buildenv.2022.109703

Co-Author Contributions

The contribution of each co-author is stated in the acknowledgements of each chapter. Co-authors have provided their signatures to confirm their contribution in their respective publications as stated in the acknowledgements of each chapter. Associate Professor Fraser Torpy and Dr. Peter Irga formed my supervisory panel (indicated with an Asterix (*)).

Co-Author Name	Signature	Date Signed
Professor Elena Comino	Production Note: Signature removed prior to publication.	11/10/2022
Professor James Ball	Production Note: Signature removed prior to publication.	10/08/2022
Professor Justin Seymour	Production Note: Signature removed prior to publication.	10/10/2022
* Assoc. Prof. Fraser Torpy	Production Note: Signature removed prior to publication.	09/08/2022
Dr. Eamon Wooster	Production Note: Signature removed prior to publication.	10/08/2022
Dr. Laura Dominici	Production Note: Signature removed prior to publication.	13/08/2022
Dr. Mika Westerhausen	Production Note: Signature removed prior to publication.	10/08/2022
* Dr. Peter Irga	Production Note: Signature removed prior to publication.	10/08/2022
Dr. Thomas Pettit	Production Note: Signature removed prior to publication.	09/08/2022
Ashley Douglas	Production Note: Signature removed prior to publication.	09/08/2022
Natalie Killingsworth	Production Note: Signature removed prior to publication.	10/08/2022
Nathan Williams	Production Note: Signature removed prior to publication.	12/08/2022
Raissa Gill	Production Note: Signature removed prior to publication.	09/08/2022
Stephanie Saadeh	Production Note: Signature removed prior to publication.	11/08/2022

Co-author papers published during my Candidature, not included in the thesis

Irga. P.J, **Fleck. R**, Arsenteva. E, Torpy. F.R, 2022. Bio-solar green roofs and ambient air pollution in city centres: mixed results. *Building and Environment. 226.* **doi.org/10.1016/j.buildenv.2022.109712**

Wooster. E, **Fleck. R**, Torpy. F.R, Ramp. D, Irga. P.J, 2022. Urban green roofs promote metropolitan biodiversity: A comparative case study. *Building and Environment.* 207. **doi.org/10.1016/j.buildenv.2021.108458**

Gill. R.L, Collins. S, Argyle. P.A, Larsson. M.E, **Fleck. R**, Doblin. M.A, 2022. Predictability of thermal fluctuations influences functional traits of a cosmopolitan marine diatom. *Proceedings of the Royal Society B.* 289. **doi.org/10.1098/rspb.2021.2581**

Morgan. A.L, Torpy. F.R, Irga. P.J, **Fleck. R**, Gill. R.L, Pettit. T.J, 2022. The botanical biofiltration of volatile organic compounds and particulate matter derived from cigarette smoke. *Chemosphere*. 295. **doi.org/10.1016/j.chemosphere.2022.133942**

Pettit. T.J, Torpy. F.R, Surawski. N.C, **Fleck. R**, Irga. P.J, 2021. Effective reduction of roadside air pollution with botanical biofiltration. *Journal of Hazardous Materials.* 414. **doi.org/10.1016/j.jhazmat.2021.125566**

Co-authored conference presentations

Torpy. F.R, Irga. P.J, **Fleck. R**, Matheson. S, Smith. H, Duani. G, Surawski. N, Douglas. A, Lyu. L, 2022. Phytoremediation of air pollution. *26th International Clean Air and Environment Conference.* Adelaide, Australia.

Irga. P.J, Torpy. F.R, **Fleck. R**, Duani. G, Matheson. S, Douglas. A.N.J, Lyu. L, 2022. The benefits of plants at work. *Workplace Wellness Festival*. Sydney, Australia

Torpy. F.R, Irga. P.J, Wilkinson. S, **Fleck. R**, Pettit. T.J, Douglas. A, 2021. Challenges for the incorporation of food production into functional urban greening systems. *UN Food Systems Summit, Beyond Urban Agriculture section; Yale Center for Ecosystems + Agriculture, Online; 14/09/2021.*

Torpy. F.R, Irga. P.J, Wilkinson. S, Pettit. P.J, **Fleck. R**, Douglas. A, 2021. Plants and urban air pollution in the COVID-19 age. *Presentation to the Green Building Council of Australia.* Sydney, Australia

Table of Contents

Table of Figures

Table of Tables

Abstract

Sustainable urban environments aim to reduce energy consumption, increase localised sustainable production, and provide infrastructure that benefits human health. One method to contribute to sustainable urban environments through the provision of urban ecosystem services is the application of green technologies such as green walls and green roofs. While biophilic design is well-known to have a positive effect on the psychological health of urban dwellers, green walls and green roofs have additional, quantifiable environmental benefits that contribute to health and productivity. In this thesis I explore the benefits and drawbacks of green walls for the indoor environment and green roofs for the outdoor environment and quantify to what extent these technologies provide tangible urban ecosystem services. For example, indoor active green walls have been developed that can remove air pollution emanating from sources such as cooking or the off gassing of toxic chemicals from synthetic materials or cleaning products. Through the addition of active airflow, contaminated airstreams are exposed to the rhizospheric bacterial community within the green wall substrate where pollutants are metabolised as a source of nutrition. However, the combined use of active airflow and botanical material requires strategic design to ensure the efficacy and safety of these systems. As plants rely on lighting to drive photosynthesis, and therefore sustain their biological functions, an inadequately designed lighting system can lead to both decreases in pollution removal performance and the deterioration of plant health. Plant systems that are poorly maintained could potentially lead to the proliferation of pathogenic or allergenic bioaerosols, which coupled with active airflow, could increase the risk of dispersal. Additionally, the sustainability performance of green roofs is significantly under researched in the Australian climate, despite demonstrations in other locations of the range of benefits that this technology can provide. These include improvements to biodiversity, thermal comfort, stormwater filtration and retention, localised air quality and solar performance, and reduced noise pollution and solar reflectance. Additionally, nearly all previous green roof studies have been conducted on an experimental scale, with few studies utilising full-scale buildings nor appropriate controls. In this thesis, I explore several novel aspects of sustainability-oriented green infrastructure, notably the factors that contribute to the health and performance of commercial indoor active green walls, in addition to several services provided by a commercial scale *in-situ* extensive green roof, with an independent control roof free of spatial or temporal confounding factors.

Firstly, I surveyed the *in-situ* lighting conditions of a sample of commercial indoor green walls in Sydney Australia and found the illumination levels to be insufficient for plant health and performance in most instances, leading to this may lead to both poor performance as well as plant health, which has a flow-on effect for maintenance and aesthetics. In this chapter I assessed the

phototropic adaptation potential and CO_2 removal performance of the two plant species that dominated the *in-situ* green walls (*Chlorophytum comosum* and *Spathiphyllum wallisii*). Phototropism (plant movement in response to light) was significant in both plant species, although in most treatments there was little impact of this phenomenon on CO_2 removal performance. However, increased light intensity with optimised lighting direction led to significantly higher CO_2 removal performance than the average lighting scenario observed *in-situ* (up to 30% over a 40-minute period). It was concluded that lighting is a significantly under-addressed factor for the performance of active green walls and that wall design and arrangement of different plant species can influence light availability. Improved lighting could reduce maintenance and improve plant health, which could in turn reduce the potential for the aerolisation of contaminants. This led to the second experiment, involving the assessment of bioaerosol emissions, including potential fungal or bacterial pathogens or allergens, from an *in-situ* active green wall. This study found a significant increase in the fungal aerosol load (120-240 CFU/m^3) proximal to the green wall, however concentrations remained below the WHO guidelines at all times (500 CFU/m^3), and solely consisted of fungal species that posed no allergenic or pathogenic risk. To further understand the pollutant removal capacity of the green wall system, I explored the rhizospheric bacterial community that sustains the VOC degrading potential of active green infrastructure and found the microbial community distribution to be significantly different to those studies previously reported. While no microbial pathogens were detected in the effluent airstream from the system, 16S sequencing results identified the presence of the ubiquitous environmental bacterial genus *Legionella* in the green wall substrate. The abundance of *Legionella* detected was equivalent to previously quantified abundances in environmental soil samples (~1 %). Unfortunately, speciation was not possible with the detection technique, however this finding is unlikely to be a cause for health concern, as substrate bound *Legionella* requires direct contact with mucous membranes after coming into direct contact with contaminated soils, and this phenomenon is very unlikely to occur with an indoor green wall and poses no risk situation different to traditional indoor plant systems.

The proceeding three chapters describe the quantitative benefits of an *in-situ* extensive green roof in the Sydney CBD. The third experiment describes the thermal properties of the green roof and demonstrates a significant reduction in surface temperatures of both rooftop solar panels and roof surfaces, as well as a net reduction in ambient temperatures. The green roof was able to reduce surface temperatures by up to 9.63 and 6.93°C for the solar panels and roof surfaces respectively. There was also an average peak temperature reduction by 8°C on the green roof, which has substantial implications for building thermal comfort. In addition to this, the theoretical heat flow (thermal penetration) through the green roof was significantly improved across all three seasons.

The green roof reduced the average heat flow by 13.37 and 5.37 W/m^2 for Spring and Summer respectively, as well as having a lower average nightly heat flow in Autumn. This indicates that a green roof could reduce building energy consumption for the heating and cooling of air before entering the building, as heat cannot penetration or escape the building envelope as easily as a building with a conventional roof.

The fourth experiment aimed to characterise the stormwater and trace metal retention capacity of the green roof. Green roofs have been documented to have variable stormwater retention capacities, an effect which stems largely from variations in substrate characteristics and depth, and plant species choice and density. In addition, it has been predicted that heavy metal phytoremediation, where plants remediate contaminated soils with high levels of soluble and insoluble trace metals, could occur in green roofs as well as field soils. Here I demonstrate a significant reduction in stormwater flow rates (retention) by up to 60% for storms at a 1 in 10 years severity. Additionally, the green roof achieved a significant reduction in soluble and insoluble copper, chromium, and zinc. These results indicate that a significant increase in green roof coverage in the Sydney CBD could lead to a reduction in flow rates into the urban stormwater management network. It is entirely plausible that the mass adoption of this technology could decrease the severity and duration of semi-frequent flash floods that are experienced in the Sydney CBD as a result of short-lived heavy rain events. Additionally, there are implications for stormwater management where toxic trace metals that stem from vehicle combustion and abrasion can be captured and retained by a green roof, potentially undergoing phytoremediation in the process.

Lastly, it has been predicted that due to plant evapotranspiration on a green roof, there is the potential to passively cool the proximal ambient environment. This reduction in temperature has been previously demonstrated experimentally in pilot-scale studies and has been modelled to be effective for increasing solar performance by reducing the temperature of the panels. However, there are extremely limited studies that demonstrate this effect *in-situ* on a commercial scale roof. In the final experiment I thus monitored a *Bio-solar* roof and a matched conventional solar array for differences in performance. The observed and modelled performance increase provided by the *Bio-solar* roof was significant in both cases, with the *Bio-solar* roof achieving an increased solar power output of 21-107 % depending on the month. Additionally, the modelled performance indicated that an extensive green roof in the Sydney CBD could potentially achieve a 4.5% increase in energy output at *any* given light level. The performance quantified by the *Bio-solar* green roof assessed in this study credentialled the prediction that 13.56 t e-CO_2 greenhouse gasses were mitigated during the course of the project, which equates to the planting of nearly 200 urban trees, and a financial saving of over $4,500 AUD due to savings in energy costs.

Preface: Chapter 1

The following chapter is comprised of text from two peer-reviewed publications (a book chapter and a peer-reviewed conference proceedings) that introduce indoor air quality and green walls, along with some unpublished work on green roofs. Parts have been taken from the two publications verbatim or have been edited to avoid repetition, and new information has been added to create a generalised "green infrastructure" introduction. The Abstract section has been written *de novo* to encompass all of the material presented in this section.

Briefly, with an increasing global urban population, the need for technological innovation that reduces energy consumption and increases sustainability are in growing demand. Green walls and green roofs are ancient technologies that are only recently finding a footing in modern society with a range of published literature describing their many benefits for the indoor and outdoor urban environment [1,2].

Chapter 1

Botanical biofiltration for reducing indoor air pollution

Fleck. R [1], Pettit. T.J [1], Douglas. A.N.J [1], Irga. P.J [2], Torpy. F.R [1]

[1] *Plants and Environmental Quality Research Group, School of Life Science, University of Technology Sydney, Australia*

[2] *Plants and Environmental Quality Research Group, School of Civil and Environmental Engineering, Faculty of Engineering and Information Technology, University of Technology Sydney, Australia*

This article has been published as a Chapter 15 of the book titled Bio-Based Materials and Biotechnologies for Eco-Efficient Construction. Available online at https://doi.org/10.1016/B978-0-12-819481-2.00015-5. Published January 1st, 2020.

Reducing indoor air pollution through applied botanical biofiltration

Fleck. R [1], Pettit. T.J [1], Dominici. L [2], Gill. R.L [1,3], Irga. P.J [4], Torpy. F.R [1]

[1] *Plants and Environmental Quality Research Group, School of Life Science, University of Technology Sydney, Australia*

[2] *Applied Ecology Research Group, Department of Environment, Land and Infrastructure Engineering, Politecnico di Torino, Turin, Italy*

[3] *Coastal Oceanography and Algal Research Team, Faculty of Science, Climate Change Cluster, University of Technology Sydney, Australia*

[4] *Plants and Environmental Quality Research Group, School of Civil and Environmental Engineering, Faculty of Engineering and Information Technology, University of Technology Sydney, Australia*

This article was accepted and presented at the 16th Conference of the International Society of Indoor Air Quality and Climate. Available online at ISBN: 978-1-7138-2360-5. *Volume 2, page 832*. Published January 1st, 2020.

Abstract

Increasing urban populations and behaviour associated with urban lifestyles has led to growing concerns about the sustainability of future cities. Green systems: where the ecosystem services of plants are harnessed to improve the environmental quality and sustainability of urban environments are growing in favour. The two most well-described and developed green systems are green walls and green roofs.

In recent decades there has been an increase in awareness of indoor environmental quality, especially the maintenance and control of indoor air quality (IAQ). Early research into the role of botanical systems for IAQ treatment demonstrated that many common indoor plant species and their potting materials could remove a range of toxic volatile organic compounds (VOCs). It was subsequently established that the predominant mechanism of VOC removal was due to the metabolic action of the substrate microbial community. The rates of removal demonstrated in these early studies, and the numerous laboratory trials that followed, provided evidence that ordinary

potted plants could provide a valuable service within the indoor environment by controlling VOC concentrations. However, limitations to the efficacy of this process have been associate with the slow rate at which potted plants remove pollutants, rendering their practical efficiency in full-scale buildings negligible. Recent developments have fused the removal mechanisms of plants and their substrate with biofiltration technology to create active green walls (botanical biofilters), what have been proven to be highly effective for the removal of gaseous pollutants.

Green roofs are known to provide numerous benefits to building occupants and urban dwellers in the forms of increased biodiversity, contributions to the reduction of stormwater flows, as well as contaminant retention, improvements to the rooftop microclimate, and reductions in thermal penetration, as well as positively influencing the generation of solar energy. While these benefits have been documented and modelled, the performance of these systems varies worldwide. Currently there is very little literature that describes the performance of commercial green roofs in the Australian context, especially for the Eastern Australian Coast, where the majority of the population resides. Not only are there few Australian studies, but the international studies published tend to include internalised controls which may reduce the observable effect of the green roof, depending on the focus of the study. Therefore, the study of Australian green roofs, with the appropriate independent, non-spatially or temporally confounded controls are required to assess the benefits of Australian green infrastructure.

Keywords

Active biofiltration, Active green walls, Air pollution, Bioaerosols, Biological filtration, Green buildings, Green walls, Green roofs, Indoor air quality, Phytoremediation, Volatile organic compounds.

1. Introduction

Air pollution exposure is ranked amongst the most significant health risk factors worldwide, and accounts for up to 5% of the global disease burden [3]. Rapid urbanisation has led to an increase in building occupation time, where on average, urban residents in the developed world spend 90% of their time indoors. In an effort to reduce building energy consumption, natural ventilation has progressively been reduced or eliminated in favour of mechanical ventilation, which has resulted in a substantial decrease in indoor air quality (IAQ). It is well recognised that indoor air is generally more polluted than outdoors [4,5], where indoor spaces are subject to the accumulation of egregious indoor-sourced contaminants which give rise to a range of health issues such as "sick-building-syndrome" and respiratory discomfort. The cost associated with indoor air pollution exposure for developed countries is between 2.1 and 8.4% of the global world product [6].

Common indoor contaminants include volatile organic compounds (VOCs) sourced from off-gassing from synthetic furnishings and cleaning products [7]; particulate matter (PM, [3,8]) from cooking, solid fuel heating, smoking or cleaning activities; and 'criteria' pollutants (CO, NO_2, O_3, SO_2 and CO_2) from heating, smoking, printers and photocopiers, and occupant respiration [9–11]. The concentration of these pollutants across different indoor environments varies due to differences in building filtration technologies, reactivity amongst pollutants, and the presence of indoor sources [12].

Conventionally, commercial spaces are equipped with heating, ventilation and air conditioning (HVAC) systems, that remove PM from ambient air, and modulate its temperature and humidity prior to it entering the building [13]. However, even with the addition of high-efficiency particulate air filters, HVAC systems are still incapable of removing non-particle bound gaseous pollutants such as VOCs in a time-efficient manner [14]. In addition to this shortcoming, the use of HVAC consumes approximately 50% of the urban energy demand [15], and could be responsible for up to 75% of global carbon emissions [16]. Therefore, technologies that reduce occupant exposure to indoor pollutants without increasing the energy demand of the built environment sector are paramount to ensuring safe indoor environments for urban occupants and the development of sustainable cities.

Amongst many eco-efficient technologies, building-integrated vegetation (also known as urban green infrastructure) for both the indoor and outdoor environment provides a multitude of benefits for both building owners and urban residents [17]. There are two distinct formats for building-integrated vegetation, and they are specific to the environments in which they are utilised: Green walls and Green roofs. Green walls are often deployed indoors where they can have the greatest impact on IAQ and building occupants. However, green walls are distinct from green façades [18]

which are often used as cladding on high profile or influential spaces, in that they have a quantifiable effect on the quality of the indoor environment [2] and positive perception of occupants [19]; aspects that are not well quantified for green facades. Green roofs are primarily an outdoor technology, where functional green roofs in commercial spaces are commonly inaccessible to building occupants due to the absence of appropriate building regulation allowing them to function as dedicated recreational spaces [20]. As such, the interaction between building occupants and a green roof are largely indirect, and likely go unnoticed by urban dwellers in many cases.

1.2 Active and passive green walls

Indoor botanical biofiltration, or the use of plants for the remediation of contaminated indoor air, was conceptualised by researchers from the US National Aeronautics and Space Administration (NASA) [29,30] while developing "biological life support systems" as long-term outer space habitation solutions. It was discovered through this research that many common indoor plant species and their potting materials could remove a range of toxic VOCs [30]. I was subsequently established that the predominate mechanism of VOC removal was due to the action of the substrate microbial community [31,32]. The rates of removal demonstrated in these early studies, and the numerous laboratory trials that followed (e.g. [33,34]) provided evidence that ordinary potted plants could provide a valuable service within the indoor environment by controlling VOC concentrations. While more recent research and modelling studies (e.g. [35,36]) have shown that the quantitative pollutant removal rates of potted plants are likely to be inadequate to produce useful air cleaning effects in realistic settings, the proof-of-concept findings provided by the early potted plant research have led directly to the development of active botanical biofilters, which display high-performance pollutant removal efficiencies [11,37].

Active green infrastructure describes any infrastructure that utilises botanical biofilters incorporating some form of active airflow, either through the addition of fans to direct airflow towards the rhizosphere or incorporating botanical material into HVAC systems (Figure 1). One study by Wang et al., [38] described the integration of botanical biofilters into HVAC infrastructure, however while the VOC removal efficiencies recorded in this study were adequate, they are significantly lower than subsequent studies that have tested stand-alone systems. For example, a study conducted by Pettit et al., [21] demonstrated the significant reduction of both TVOC and PM concentrations from a classroom in China with a pilot-scale active green wall [21] at rates that

exceeded those presented by Wang et al., [38]. Additionally, these systems have been found to be capable of removing other gaseous criteria pollutants such as NO_2, CO and CO_2 [10,11,36].

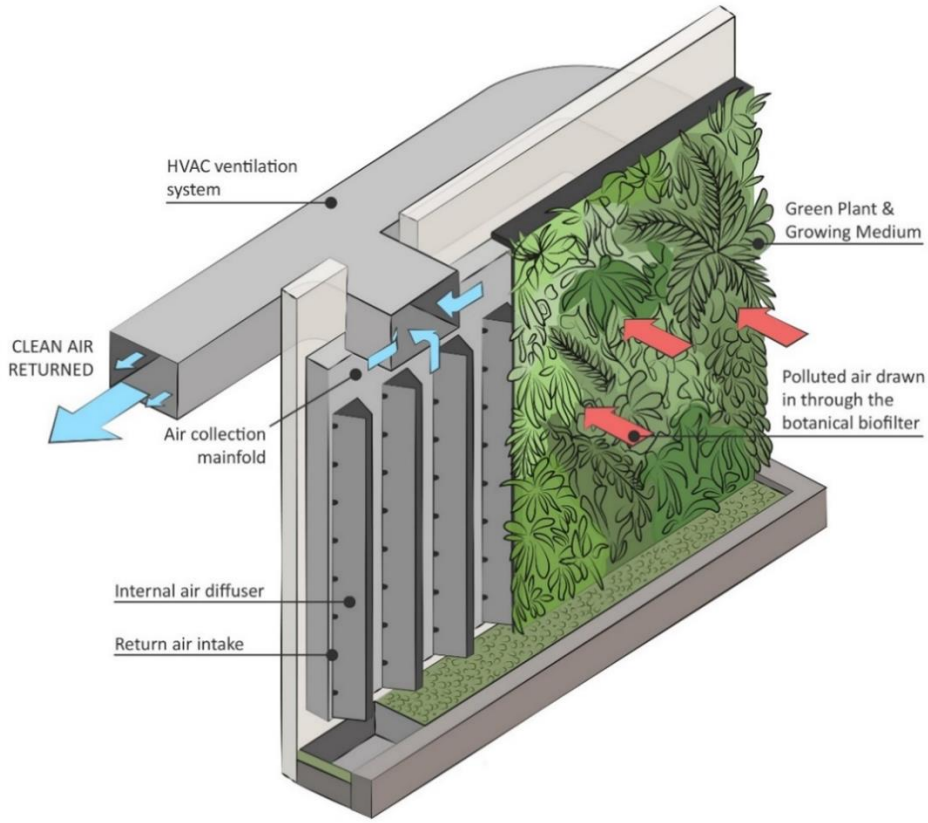

Figure 1. An active green wall incorporated into building HVAC ducting. Air is mechanically forced through the plant foliage, travels through the bioactive substrate, and then returns to the ventilation system through the back of the botanical biofilter modules. Image adapted from [36].

Active systems have been the subject of some system performance development. The exploration of VOC remediation performance based on the modification of the plant species used, substrate composition modifications and the scale of biofilter relative to room volume has been performed, moving these systems beyond the point of proof-of-concept. However, several factors remain that delay the implementation of this technology on larger commercial scales. Currently the capital cost of installation and ongoing maintenance costs are prohibitively high for many commercial consumers [39]. As this technology relies on the natural symbiotic relationship between plants and their rhizospheric microbial community, ensuring optimum plant health through the manipulation of abiotic factors such as light exposure has been shown to ensure sustained VOC removal [40,41], as well as reduce maintenance intervals, and therefore reduce costs [23]. Perhaps more important than performance and cost of active green infrastructure is the validation of biosafety. To date, there are few studies that have explored the biosafety risks associated with the application of active airflow through a biologically active substrate [42]. The dispersal of allergenic or pathogenic fungal

spores has been addressed in some detail, however there is little research available on the speciation of fungal species in these papers [43,44]. Additionally, the use of a soilless substrate does not rule out the proliferation of ubiquitous pathogenic bacteria such as *Legionella* spp. With optimised substrate moisture and active airflow, there is the potential for the aerolisation of pathogenic bacteria from these systems, and to date there is an extremely limited number of studies that address this, let alone quantify the microbial community of *in-situ* commercial active green walls [45,46].

1.3 Green roofs

Green roofs can be characterised by the depth of their substrate, and subsequently the types of plants that can be used. While there is some inconsistency in the literature on the specific definitions of green roof types, there are two main categories of green roofs: *intensive* and *extensive*. Generally, intensive green roofs are defined as those with substrate depths greater than 300 mm. These roof types can host large plant species such as shrubs and trees [47] and are often employed for roofs that are intended to be accessed by building occupants as a recreational space [20,48,49]. Due to the deeper substrate and larger plants, intensive green roofs are substantially heavier than their counterpart, and have higher capital and maintenance costs [50], which reduces their suitability for retrofitting older buildings [51], and discourages many stakeholders. Extensive green roofs, however, are substantially more commonly employed than intensive green roofs [52]. With substrate depths of less than 300 mm, they generally host smaller plant types such as grasses, mosses, wildflowers and succulents [53]. Due to their relative abundance and global distribution, green roof research pertains mostly to extensive green roof designs.

Extensive green roofs are often cited for their biodiversity benefits [26,27,54–56], contributions to the reduction of stormwater flow, as well as contaminant retention [57–60], improvements to the rooftop microclimate and reductions in thermal penetration into the building envelope [61–64], and providing conditions which positively influence the generation of solar energy [65–68]. While these benefits are well documented, there is substantial variation in efficacies reported worldwide, where climate and roof design are appear to be key factors in system performance [69]. To date, the majority of green roof literature describes experimental or pilot-scale installations (Figure 2), with few studies utilising commercial-scale roofs [70]. Due to difficulties associated with establishing non-spatially confounded independent controls, it is common for green roof studies to utilise internalised control roofs that present several methodological problems.

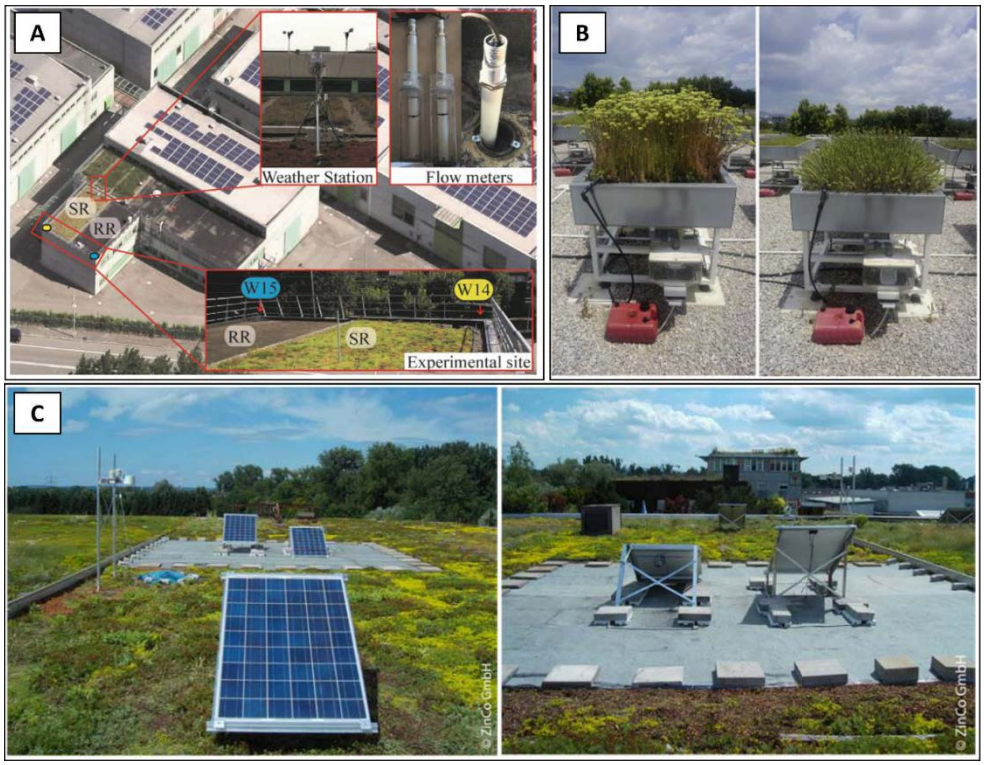

Figure 2. Examples of previous green roof studies. Example [A] describes the hydrological performance of a green roof in a subcontinental climate, image from [71]. *Example [B] describes a simulation of green roof runoff in a Mediterranean climate, image from* [72]. *Example [C] comes from a review of 20 years of green roof research and describes a PV-green roof study in a temperate climate, image from* [56].

For studies that examine biodiversity, thermal effects and solar efficiency, the use of internalised controls may underestimate the observable effect of the green roof due to proximity or carry-over effects. As many of the animal species associated with green roofs are insects and birds, there is the potential for animals to travel through control spaces to reach the planted regions of the roof. Similarly, the evapotranspiration effect of the plant material serves to passively reduce the temperature of a roof space, and may therefore reduce the observable heat flow, or influence the operational temperature of nearby solar installations, increasing performance to an unknown degree. These factors may serve to reduce the effect sizes associated with the green roof effect, and it is therefore essential that green roof studies are conducted on isolated roofs that are not temporally or spatially confounded.

In addition to the lack of effective controls, to date there are an extremely limited number of studies that describe the performance of green roofs in Australia [73–76], with the majority of the research conducted limited to the city of Adelaide [74,75] (Australia's 5th largest city; population 1.4 million [77]). For a country like Australia, with an urban population density of approximately 90% [78] and the 12th largest economy in the world, there is the potential for green roofs to have

substantial impact on the Australian population, especially in the larger cities like Brisbane, Melbourne and Sydney with populations over 2.5, 4.9 and 5.2 million, respectively [77].

1.4 Proceeding Chapters

In Chapter 2 of this thesis I explore both the potential for increased performance and reduced maintenance for green walls through the addition of supplementary lighting based on experimental and *in-situ* measurements. Additionally, in Chapter 3 I present the most comprehensive biosafety assessment of *in-situ* active green walls, as well as the third international study that aims to characterise the microbial population of commercial active green walls. This work is particularly significant as the findings directly relate to the performance of the system for the removal of gaseous contaminants but the current findings have not been confounded by the biostimulation of the system through experimental testing with various VOCs, as has been the case in previous work. The microbial characterisation described in this thesis represents the third ever attempt at characterising the rhizospheric and substrate microbial population of active green walls, with results that vary considerably from those previously reported. I also identify some ubiquitous environmental pathogens and address the risk of aerosolisation from the active green wall design.

In addition, in Chapters 4, 5 and 6 I explore the multifaceted benefits of green roofs in a unique setting. Here I present one of the only studies that have utilised an *in-situ* commercial scale extensive green roof with a non-spatially confounded independent control roof. I quantify the beneficial thermal properties of a green roof as a mechanism for cooling the rooftop microclimate and the potential impacts on building occupants and the urban heat island; the improvements to stormwater runoff in respect to trace metal contamination, as well as reductions in peak stormwater flow with implications for the reduction of flash flood severity in the Sydney CBD; and lastly the effect of a green roof on mediating the temperature below a solar panel array and consequent increase in solar energy output, along with exploring both the environmental and financial benefits of the system. These findings are significant as they represent the most comprehensive study of a green roof to date, and address most of the key aspects of green roof technologies that are critically under addressed in Australia.

Preface: Chapter 2

One key limitation of indoor urban green infrastructure is the inadequate lighting that is often installed by providers. Illumination for indoor living walls is usually limited to ambient lighting through in-room ceiling lights, or horizontal illumination from nearby windows, with the addition of supplementary lighting frequently considered partly as a biological requirement, and partly as a showpiece to demonstrate the aesthetic appeal of the technology. However, even the addition of supplementary lighting may be inadequate for optimal plant health and performance: the provision of insufficient lighting is known to reduce the long-term health of several indoor plant species.

Here I aimed to assess the lighting scenarios experienced by a range of commercial *in-situ* indoor living walls, and to determine the optimum lighting for sustained plant performance and, potentially, health, in an effort to reduce maintenance requirements and therefore costs associated with indoor green wall installations.

The following chapter is comprised of text from a peer-reviewed publication.

Chapter 2: Analysis of lighting conditions of indoor living walls: effects on CO_2 removal

Laura Dominici [1 #*], **Robert Fleck [2 #]**, Raissa L Gill [2,3], Thomas J Pettit [2], Peter J Irga [4], Elena Comino [1], Fraser R Torpy [2]

[1] Applied Ecology Research Group, *Department of Environment, Land, and Infrastructure Engineering (DIATI), Politecnico di Torino, Italy.*
[2] *Plants and Environmental Quality Research Group, School of Life Science, University of Technology Sydney, Australia*
[3] *Coastal Oceanography and Algal Research Team, Climate Change Cluster, Faculty of Science, University of Technology Sydney, Australia*
[4] *Plants and Environmental Quality Research Group, School of Civil and Environmental Engineering, Faculty of Engineering and Information Technology, University of Technology Sydney, Australia*

 # These authors contributed equally to this manuscript.

**Corresponding Author: Laura.Dominici@polito.it*

This article has been published in the Journal of Building Engineering (Q1, Impact factor 7.144 (2022)). Available online at https://doi.org/10.1016/j.jobe.2021.102961. Published July 6th, 2021.

Abstract

Vertical greening systems, or living walls, are becoming increasingly used indoors for improving the sustainability of buildings, including for the mitigation of excess CO_2 levels, derived from human respiration. However, light provision within indoor environments is often insufficient for the efficient functioning of many plant species, leading to low photosynthetic CO_2 removal rates, and the need for supplementary light sources. In this study, we investigated the performance of supplementary lighting employed for indoor living wall systems, and whether optimised lighting conditions could lead to improved CO_2 removal. *In-situ* trials with several medium-large indoor living walls were performed to sample the lighting scenarios currently employed. We concluded that the majority of plants in existing systems were exposed to suboptimal lighting and will have a net-zero CO_2 removal efficiency. Sealed chamber experiments using two common living wall plant species were conducted to explore the effect of varying lighting conditions on CO_2 removal efficiency. Comparisons on optimal and "best case" *in-situ* conditions were carried out, showing that CO_2 removal efficiency was significantly correlated with both leaf and stem angles, which suggest phototropism may influence *in-situ* CO_2 removal. After a ten-day experimental period, the highest CO_2 removal efficiency for both test plant species was observed at 200 $\mu mol \cdot m^{-2} \cdot s^{-1}$ light flux density (~10500 lux) at 15° from the vertical growing surface. Our results indicate that most current lighting systems are inadequate for healthy plant photosynthesis and CO_2 removal, and that modified lighting systems could improve this performance. To reduce maintenance costs, technical guidelines for indoor living wall lighting should be established, and lighting suppliers should recognise the developing niche market for specialised indoor living wall lighting.

Keywords

Green Building, Sustainability, Green wall, Phytoremediation, Indoor air quality, Nature based solutions.

Highlights

- *In-situ* living walls require optimized lighting conditions for high CO_2 removal efficiency.
- Light intensity and directionality influence the CO_2 removal efficiency of indoor living walls.
- Phytosystem selection and design stands to significantly improve indoor CO_2 removal efficiencies.

Graphical Abstract

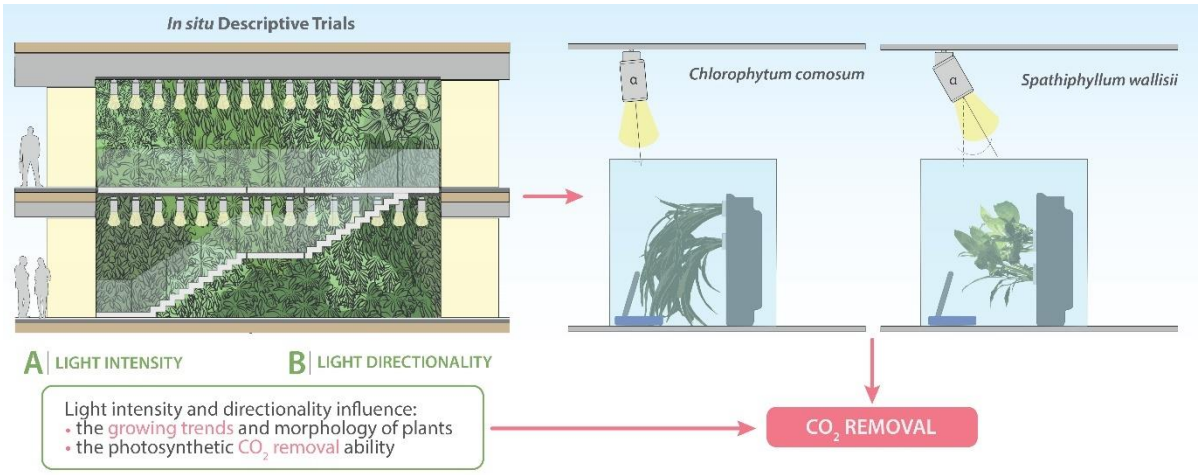

1. Introduction

Densification of cities has led a growing proportion of society becoming urban dwellers, spending approximately 90 % of their time indoors [5,79]. Population exposure to many air pollutants is thus increasingly determined by their concentrations within the indoor environment [80,81], with indoor air quality increasingly recognised as a significant health concern. Carbon dioxide (CO_2), derived mainly from occupant respiration, is a major determinant for the control of indoor environmental air quality. While CO_2 is considered a non-toxic compound at ambient concentrations, elevated CO_2 concentrations have been correlated with negative health effects and reduced working and academic performance in building occupants [9,82,83]. Specifically, reduced decision-making performance was observed as CO_2 concentrations increased from 600 to 2500 ppm [9]. Additionally, high concentrations of CO_2 have been associated with reduced workplace productivity [84,85], decreased school attendance [86], and symptoms of 'sick building syndrome' [87]. Consequently, ASHRAE guidelines indicate that indoor CO_2 concentrations should not exceed 1000–1200 ppm [88], and as such, many heating, ventilation and air conditioning (HVAC) systems increase ventilation rates when indoor CO_2 concentrations reach ~1000 ppm. HVAC operation, however, uses considerable electrical energy, especially when the ambient air requires substantial heating or cooling prior to entering the indoor environment [89]. Thus, there is a need to explore alternative, low-energy-use systems for the maintenance of CO_2 concentrations in indoor environments.

Vertical greening systems, also referred to as green walls or living walls, may be an effective nature-based solution to improve indoor environments and reduce the costs associated with HVAC systems [90,91]. Living walls are characterised by infrastructure that enables ornamental plant species to be grown on, or within, indoor and outdoor wall spaces [92]. The innate biophilic qualities of these systems are often desirable for indoor environments due to their therapeutic psychological effect of building occupants [22,93–95]. However, a commercially underappreciated aspect of living walls is their ability to remove indoor air contaminants such as volatile organic compounds, particulate matter and CO_2 [29,36,96–100]. Through photosynthesis, living walls are able to effectively reduce the concentrations of CO_2 from indoor environments, however lighting conditions have a strong influence on the efficacy of this process [101].

Indoor living walls are often situated in areas where they have the greatest aesthetic impact on building occupants such as hallways, conference rooms or as a backdrop to building lobbies. Consequently, these locations often do not allow for adequate natural sunlight at the plant surfaces [102], and therefore, many systems are illuminated with supplementary artificial lighting. As light is

a fundamental requirement for photosynthesis, the provision of sufficient lighting is essential to maintain plant health and facilitate CO_2 removal [103]. Currently, there has been little research into the provision of optimal lighting for medium to large scale indoor living wall installations [102,104,105].

Various qualitative and quantitative aspects of light affect the photosynthetic activity and photomorphogenesis of indoor plants [106]. Both light intensity (photon flux density) and photoperiod play a vital role in light-sensing and light-acclimatory processes, both of which regulate key physical and chemical plant mechanisms such as disease defense signaling [107] and photosynthesis. Within the indoor environment, light intensities and duration are often designed for human comfort during occupation periods, with light intensities of 500 to 1000 lux (equivalent to photosynthetic photon flux densities of ~10 – 50 $\mu mol \cdot m^{-2} \cdot s^{-1}$) being commonly used [108]. These levels are significantly lower than the photosynthetic requirements of many plant species [109,110], and often do not align with natural diurnal cycles.

Furthermore, the absorption of light and the resulting photosynthetic response are determined by the interaction between light directionality, and leaf orientation [40]. Many plants are able to adapt to dynamic lighting conditions by changing the orientation of their leaves through phototropism, thus maximizing the light irradiance at the leaf surface [111], however there is no existing literature describing the influence of phototropism and the effect of current commercial lighting systems on CO_2 removal for indoor living walls.

The current study seeks to establish a rationale for the development of technical guidelines for lighting designs for indoor living walls through manipulative laboratory experiments informed by *in-situ* observations of current lighting conditions, that aimed to: (i) assess the influence of varying light intensities and light angles on CO_2 reduction by living walls containing two common indoor plant species, and (ii) explore the effect of living wall phototropism on CO_2 removal under varied lighting conditions, reflective of *in-situ* conditions.

2. Materials and Methods

2.1 *In-situ* living wall lighting assessment

Prior to conducting manipulative laboratory experiments, the lighting conditions of four indoor living walls (LW 1 - 4) from multi-story commercial buildings in the Greater Sydney area were

assessed *in-situ*. Indoor living walls one and two (LW 1 & LW 2) each had vertical surface areas of 60 m^2 and were comprised of 240 individual botanical biofilter modules (0.25 m^2), while living walls three and four (LW 3 & LW 4) had vertical surface areas of 27 and 16.25 m^2 and contained 108 and 65 individual botanical biofilter modules respectively (Figure 4).

Botanical biofilter modules used in the commercial systems were made from recycled low-density polyethylene, containing a coconut husk-based growth substrate and designed with 16 front-facing holes into which the following plant species were grown: *Chlorophytum comosum, Spathiphyllum wallisii, Epipremnum aureum, Philodendron xanadu, Peperomia obtusifolia, Nephrolepis exaltata, Neomarica gracilis* and *Gibasis* sp.. The four living walls were selected as they were all installed in environments lacking exposure to natural light and were thus reliant wholly on artificial lighting.

At LW 1, 2 and 4, lighting was supplied by adjustable LED spotlights (COB LED spotlight, model PLD-TL-40W-F1, 130 x 200 cm, 40 W, 60° beam angle, 3000 K warm white, produced by the Huizhou Plamd Lighting Technology Co., China), installed above the living walls at a distance of 0.8 – 1 m from the planted surfaces and 0.2 m from one another. Lighting at LW 3 was supplied by in-ceiling LED downlights, 1 m from the planted surfaces, and 1 m from one another. The intensity of photosynthetically active light (photosynthetically active radiation (PAR); λ = 400 – 700 nm) was measured with a Li-250A light meter (Li-Cor Biosciences, USA) at a distance of 0.5 m from the living wall surface (in front of plant foliage). Light intensity was measured at the wall surface either at 0.5 or 1 m vertical intervals, dependent on wall design (Figure 4).

Lighting devices at LW 1 and 2 were photographed using a Nikon D3200 camera (ISO 100, f. 3.8, t 1/100) to establish the lighting profile and average inclination of luminaries (light angle) relative to the front surface of the walls. Images were taken from the left and right sides of the walls, at a height equal to the luminaries' position. Only LW 1 and 2 were considered for light angle evaluation as they utilised a consistent number of luminaries and represented a larger and more comprehensive lighting design than LW 3 and 4.

Image analysis was performed using Adobe Photoshop CC (Adobe Systems) and AutoCAD 2019 software (Autodesk Inc., USA) to determine the inclination angle between the vertical and the luminary's axis for 50 luminaries (Supplementary Figure 1). Each luminaire was isolated from photographs using Adobe Photoshop CC's (1) [Polygonal Lasso] tool to draw straight-edged segments of the selected luminaire's border, (2) the [Select > Inverse] tool was used to select the background pixels and (3) the [Crop] tool was used to delete background pixels. Luminaries were

imported into the AutoCAD environment featuring a re-created layout setting of LW 1 and 2 for each lighting device. Finally, the [Measure > Angle] tool was used to calculate the luminaire's inclination angle.

2.2 Plant module experimental set up

Chlorophytum comosum and *Spathiphyllum wallisii* were the plant species selected for manipulative examination in this study, as they are frequently used in indoor living wall applications [104,112], were the most prevalent species in *in-situ* observations, and have previously been recommended for the phytomitigation of indoor air pollution [29,101]. While the light requirements of individual plant species differ [113], both *C. comosum* and *S. wallisii* are capable of tolerating low light conditions [101], making them ideal for current indoor living wall designs.

Eight individual plants of each species were housed in open-ended PVC pipes (cassettes: 90 mm external diameter and 120 mm in length) containing coco-husk substrate, similar to the substrate used *in-situ*, as described previously [100]. Plant replicates were adapted to a horizontal growth position at ambient light intensities (~ 6 – 7 $\mu mol \cdot m^{-2} \cdot s^{-1}$; ~235 lux) within a laboratory environment for seven days (temperature 22.0 ± 2.3 °C and relative humidity 65.8 ± 15.8 %). Plants were watered to field capacity weekly and allowed to drain for two days prior to testing. To ensure the plant cassette arrangements were representative of a vertical wall, cassettes were housed in a frame made of rotary molded polyethylene (500 x 500 x 130 mm: Supplementary Figure 2).

During experiments, the rear of the plant cassettes were covered with plastic film to limit respiratory emissions from non-green tissues and microorganisms associated with the growth substrate that would be unrepresentative of living walls with an enclosed growth substrate. [98]. Additionally, *C. comosum* plants were arranged in the upper-central module holes (Supplementary Figure 2). As the experimental test chamber cannot facilitate wall-mounted modules, this arrangement was used to minimise leaf contact with the chamber floor to prevent unrepresentative leaf angles ("floor drag"). Living wall frames with single plant species (henceforth, plant modules) were used to perform subsequent CO_2 removal assessments.

2.3 Chamber experiments

2.3.1 Preliminary study: non-photoadapted CO_2 removal

To determine the effect of lighting conditions on plant specific CO_2 drawdown, a preliminary study was conducted to assess the optimal lighting conditions for each plant species. Plants were placed in a sealed chamber and CO_2 drawdown was monitored under varying conditions. As the plants were given no time to adapt their physiology to the lighting conditions in each treatment, the preliminary study was termed "*non-photoadapted CO_2 removal*". The results from this study were applied over a 10-day period, in which plant species could adjust their physiology to the lighting conditions (*photoadaptation*), similar to how *in-situ* plants would. Prior to CO_2 drawdown assessments, total plant leaf area was determined using plant images in AutoCAD.

CO_2 drawdown assessments for both plant species were conducted in sealed Perspex chambers (216 L), fitted with an 80 mm electric fan (12 V) for air circulation. Lighting was provided by a Parscan circular LED spotlight (12 LEDs, 30 W, 3000K warm white; ERCO Lighting Pty. Ltd., Australia) and an Opton square LED spotlight (6 LEDs, 25 W, 3500K warm white; ERCO Lighting Pty. Ltd., Australia), both equipped with a spherulite optical polymer flood lens (ERCO Lighting Pty. Ltd., Australia). Both luminaries were adjustable through 0° - 90° tilt, light housings were rotatable through 360°, and the luminous flux was dimmable (Parscan luminous flux 200 – 6600 lm; Opton luminous flux 200 – 4920 lm). These light systems were selected due to their similarities to luminaries employed *in-situ,* light manipulation capabilities, low energy consumption, and low radiant heat output [114–117]. Frames were constructed to house luminaries where both spotlights were mounted on a single linear light track power supply (ERCO 3C/DALI, Jadecross, Australia) and positioned adjacent to the test chambers.

Single-species plant modules containing eight plants (Supplementary Figure 2) were placed within the chamber where light angles and intensities were set vertically (Figure 3). Four light inclinations (0°, 15°, 30° and 45° from solar apex) were tested in combination with five light intensities (50, 75, 100, 150, and 200 $\mu mol \cdot m^{-2} \cdot s^{-1}$; ~ 1946, 2919, 3893, 5839, and 7785 lux), providing assessments of CO_2 removal for both plant species under 20 lighting scenarios.

Figure 3. Lighting design for angle and intensity used in Experiment 1 for Spathiphyllum wallisii and Chlorophytum comosum. Species depicted in Figure is S. wallisii.

As indoor CO_2 concentrations trigger many heating, ventilation and air conditioning (HVAC) systems to increase ventilation rates when indoor CO_2 concentrations reach ~1000 ppm [88], we assessed CO_2 drawdown from a starting concentration of ~1000ppm, generated by respiration until chamber concentrations reached this threshold (mean starting concentrations of CO2 were 985ppm ± 90ppm). CO_2 drawdown was measured using an infrared gas analyzer (IAQ-CALC 7525, Tsi Inc., USA; Range 0 – 5000ppm, Accuracy ± 3% or 50ppm, Resolution 1ppm, Response Time 20 seconds) which was sealed within the chamber to monitor the concentration of CO_2 at one-minute intervals over a period of 40-minutes. This instrument was brand new with factory calibration at the time of these

trials. Instrument specifications were: CO_2 Range 0 – 5000 ppm, Accuracy ± 3% or 50 ppm, Resolution 1 ppm, Response Time 20 seconds. These experiments were performed in triplicate with ~5-minute intervals between testing to return chamber CO_2 concentrations to ambient laboratory conditions (baseline global CO_2 concentration of ~410 ppm). Sampling was repeated three times (sample triplicate), with lighting conditions maintained between measurements by measuring the light intensity across plantlet canopies, averaged across four points. Light measurements were taken 150 mm from the module using a LI-250A light meter (Li-Cor Biosciences, USA). Light intensity adjustments between treatments were achieved through modulation of the light dimmers and repositioning of the frame, as necessary.

CO_2 removal efficiency was calculated as percentage removal over the 40-minute period from the 1000 ppm starting concentration after stabilisation. This method accounted for variations in starting CO_2 concentrations among replicates (n = 3). All CO_2 removal data was corrected *post hoc* for chamber leakage (ie. CO_2 decay from the empty chamber without plants), calculated to be 1.24 ± 0.387 % (mean ± SEM) over the 40-minute testing period. Chamber design did not allow for manipulation of temperature and humidity, however these factors did not vary significantly throughout the 40 min experiments.

The results from this experiment informed the optimal lighting angles and intensities required for heightened photosynthetic performance to be assessed in comparison with the conditions observed *in-situ*.

2.3.2 CO_2 removal efficiency and phototropic adaptation study

To determine how prolonged exposure at the optimal light angles and intensities identified during the *in-situ* field assessments and laboratory experiments influences CO_2 removal efficiency and plant morphology (phototropism), single-species plant modules were exposed to the following treatments continuously for ten days:

1. 100 $\mu mol \cdot m^{-2} \cdot s^{-1}$ (~5250 lux) at 15°; this was the highest light intensity detected in the *in-situ* field assessments, and the most common light angle observed in *in-situ* systems,
2. 200 $\mu mol \cdot m^{-2} \cdot s^{-1}$ (~10500 lux) at 15°; this was the optimum lighting combination detected in the laboratory study for non-photoadapted *C. comosum*,
3. 200 $\mu mol \cdot m^{-2} \cdot s^{-1}$ (~10500 lux) at 45°; this was the optimum lighting combination detected in the laboratory study for non-photoadapted *S. wallisii*.

Single-species plant modules containing four plants were assessed in triplicate with a photoperiod of ten hours per day, using the above experimental set up. CO_2 removal was measured daily, and daily movements in leaf and stem angles were measured by taking photographs of four leaves per plant, which were then isolated from the photobank and adjusted to a reference axial system (*xy*) using Adobe Photoshop (Adobe Inc., USA). Variation in leaf and stem angle relative to the axis was measured using AutoCAD 2019 (Autodesk Inc., USA; Figure 7).

A pilot study conducted by the authors indicated that phototropism would be complete after ten days, with negligible leaf/stem angle movement observed after this time thus this trial was performed for 10 days.

2.4. Statistical analysis

Non-photoadapted CO_2 removal was assessed using multiple linear regression to quantify linear associations with plant species, light intensity, and light angle.

To assess whether the observed, linear changes in photoadapted CO_2 removal efficiency through time were significant, a series of linear regression models were generated separately for each plant species and the three, light angle-intensity combination treatments (six in total). Similar models for species and light treatment were conducted to assess whether leaf and stem angle position changed linearly through time (nine total: 6 x leaf angle, 3 x stem angle).

To determine whether photoadapted CO_2 removal efficiency, leaf or stem position on the final day differed significantly between plant species and amongst light treatments, analyses of variance (ANOVA) with Tukey HSD *post hoc* tests were employed independently (three in total). A rank transformation was applied *a priori* to leaf/stem angle data for the ANOVAs only as the data violated parametric data analysis assumptions. As such, these analyses compare differences in median leaf/stem angles.

To investigate whether CO_2 removal efficiency was associated with phototropism, multiple Pearson's correlations were computed between both absolute leaf and stem angle positions, and the net daily movements in these parameters, across the ten-day period. These were performed separately by plant species, both across and within the three light treatments (fifteen in total).

All analyses and graphs were generated using R Project v3.6.2 [118] and using the following packages; “car” [119], “dplyr” [120], “ggplot2” [121], “ggpubr” [122], “multcomp” [123], and “xlsx” [124].

3. Results

3.1 *In-situ* living wall lighting conditions

Field measurements of light intensity for *in-situ* commercial living walls from the Greater Sydney area are presented in Figure 4. All *in-situ* living walls demonstrated non-uniform light distributions across their plant foliage, due to insufficient light provision in both intensity and direction. Additionally, sub-optimal lighting conditions due to inefficient plantscape design and infrastructure was observed (Figure 4). Luminaries were observed to create shade zones, and larger branching plant species (such as *Philodendron xanadu* and *Nephrolepis exaltata*) were observed blocking light to smaller, non-branching species below (such as *Epipremnum aureum, Spathiphyllum wallisii* and *Peperomia obtusifolia*).

Luminary angles of 11–50° were observed *in-situ* at LW 1 and LW 2 no luminaries produced light at angles of between 0–10°, and only 16 % of luminaries were positioned at angles greater than 50° (Supplementary Figure 1).

Of the four living walls measured, no lighting infrastructure was able to achieve light intensities at the plant foliage of 200 $\mu mol \cdot m^{-2} \cdot s^{-1}$ (Supplementary Table 1). In all cases, most plants were exposed to light levels similar to ambient indoor lighting (≤ 10 $\mu mol \cdot m^{-2} \cdot s^{-1}$ and 11–49 $\mu mol \cdot m^{-2} \cdot s^{-1}$ for 35.6 % and 51.8 %, respectively).

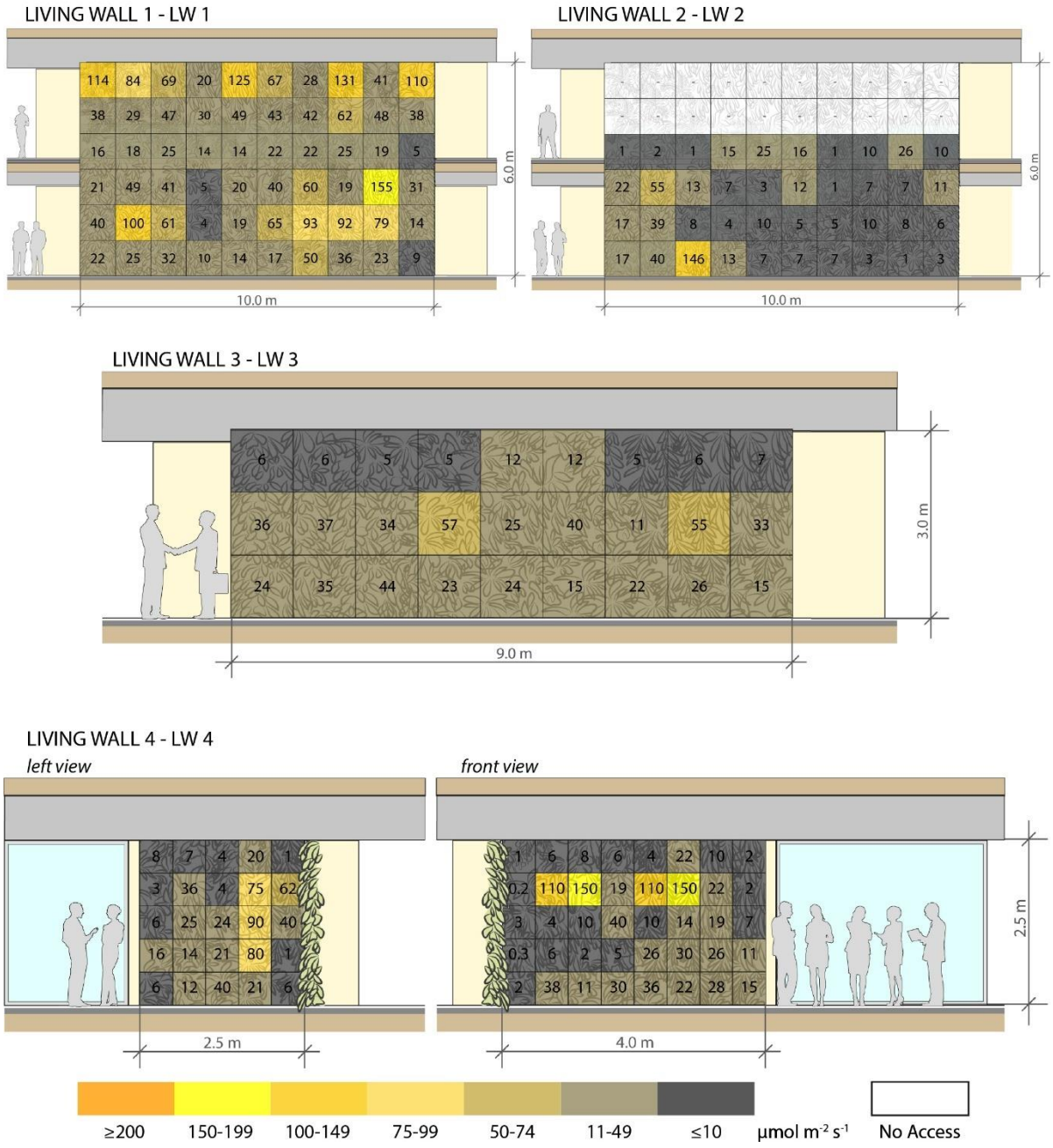

Figure 4. Lightmap of the four Living Walls (LW 1 – 4). Light measurements were taken at 1 m intervals for LW 1-3, and at 0.5 m intervals for LW 4 due to the relative complexity in both design and plant composition. The number within each square represents the average light intensity (µmol·m^{-2}·s^{-1}) available at the plant canopy for each 1 m^2 area of living wall (0.5 m^2 for LW 4). No access was available for light measurements at LW 2 for the upper 20 m^2 due to infrastructure limitations.

3.2 Non-photoadapted plant CO_2 removal

The relationship between non-photoadapted net CO_2 removal over the 40-minute time period, and the combined effects light intensity and angle, was significant in multiple linear regression for both

C. comosum ($F(7,52) = 46.390$, $p < 0.001$, $R^2 = 0.86$) and *S. wallisii* ($F(7,52) = 37.420$, $p < 0.001$, $R^2 = 0.83$).

As expected, higher light intensities displayed significant, positive effects on net CO_2 removal for both plant species ($p < 0.01$ in all cases; Supplementary Table 2). For *C. comosum*, light intensities of 75, 100, 150 and 200 $\mu mol \cdot m^{-2} \cdot s^{-1}$ were associated with a mean increase in net CO_2 removal of 6.8, 11.2, 17.7, and 19.4 % relative to 50 $\mu mol \cdot m^{-2} \cdot s^{-1}$, respectively. *S. wallisii* featured similar associations with intensity, where 75, 100, 150 and 200 $\mu mol \cdot m^{-2} \cdot s^{-1}$ of light were associated with a relative mean increase in CO_2 removal of 4.1, 8.2, 13.1, and 16.7 %, respectively.

For *C. comosum*, there was no difference in net CO_2 removal between light angles of 0 and 15° from the vertical ($p = 0.144$; Supplementary Table 2). Greater angles of 30 and 45° both lead to lower mean net CO_2 removal efficiencies of 4.1 and 6.8 %, relative to 0°, respectively ($p = 0.002$ and $p < 0.001$, respectively). Contrastingly, *S. wallisii* displayed significantly higher net CO_2 removal for all light angles, where inclinations of 15, 30 and 45° from the vertical were associated with a mean increase in net CO_2 removal of 6.1, 4.0, and 5.4 %, relative to 0°, respectively ($p < 0.001$ in all cases; Supplementary Table 2).

Overall, the greatest mean CO_2 removal was observed under the maximum tested light intensity of 200 $\mu mol \cdot m^{-2} \cdot s^{-1}$ for both *C. comosum* and *S. wallisii* at 31.72 ± 3.74 and 30.00 ± 1.14 % (mean ± SD) respectively, and at light angles of 15° and 45° respectively (Figure 5, Supplementary Figure 3).

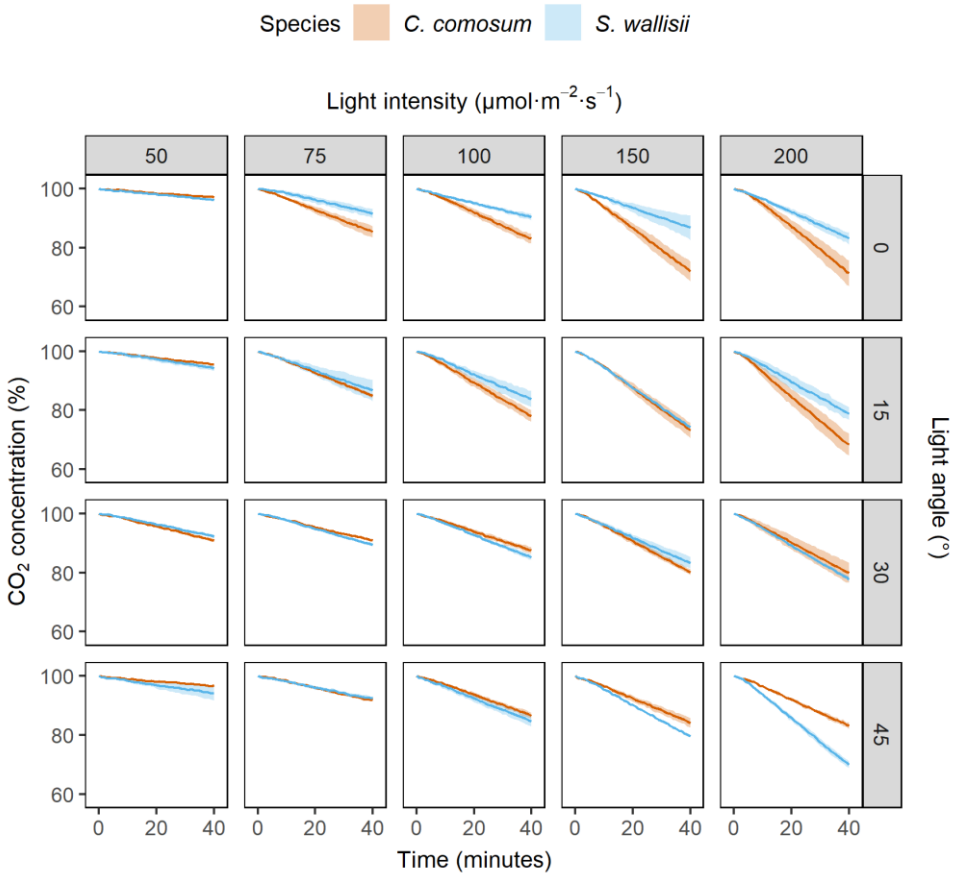

Figure 5. Mean CO_2 removal concentration (%) from input concentration (~1000 ppm) over 40-minute period for C. comosum (orange) and S. wallisii (blue) plant species under various intensities and angles of light. Shaded areas represent SDs (n = 3). CO_2 concentration (%) is expressed as a proportion of the inlet CO_2 at the end of the 40-minute test period.

3.3 Photoadapted CO_2 removal and phototropism

3.3.1 CO_2 draw down performance

Linear regression models of CO_2 removal efficiency across the ten day adaptation periods revealed non-significant relationships for all light treatments except for the 200 µmol·m^{-2}·s^{-1} at 15° treatment (Figure 6), where both models for *C. comosum* and *S. wallisii* were significant (F(1,31) = 15.890, p < 0.001, R^2 = 0.34 and F(1,31) = 13.500, p = 0.001, R^2 = 0.28 respectively). These models show contrasting directional influence of time on CO_2 removal efficiency, where for each additional day, CO_2 removal efficiency decreased on average by 0.92 % for *C. comosum*, whilst it increased by 0.33 % for *S. wallisii* (Supplementary Table 3).

The interaction between species and light treatment had a significant effect on final (day ten) photo-adapted CO_2 removal efficiencies ($F(2,12) = 29.120$, $p < 0.001$), indicating that treatment effects were not equivalent for the two species (Figure 6).

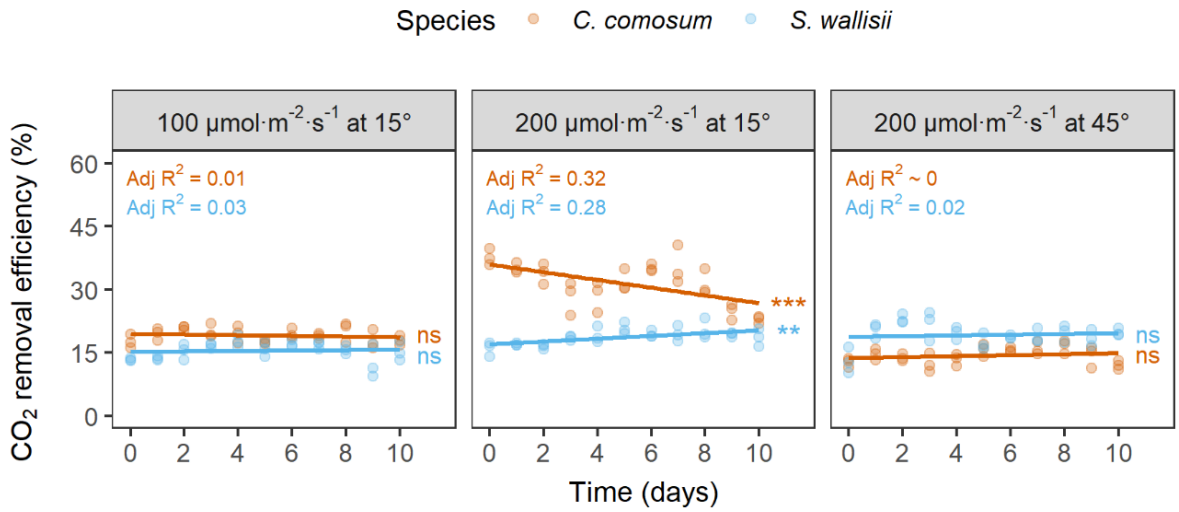

Figure 6. Linear regression models of CO_2 removal efficiency time series in C. comosum (orange) and S. wallisii (blue) species under the three-light angle-intensity treatments. Replicates depict experiments performed in triplicate on single plant modules. Lines of best fit represent fitted models of daily CO_2 removal efficiency through time, where asterisks denote significant relationships (p<0.05; ** p<0.01; *** p<0.001).*

3.3.2 Physiological phototropism

Linear regression models of leaf angle changes with time revealed significant relationships for all light treatments for both plant species ($F(1,130) = 4.623$-42.860, $p < 0.05$ in all cases, $R^2 = 0.03$-0.25), although with contrasting directional trends. *C. comosum* demonstrated an average daily 0.88 to 1.12° decrease in leaf angle from the vertical across treatments, whereas *S. wallisii* demonstrated a 4.2 to 5.2° increase (Figure 7 andFigure 8, Supplementary Table 4). Additionally, linear regression models of *S. wallisii* stem angle changes over time were also significant across all treatments ($F(1,130) = 56.770$-144.900, $p < 0.001$ in all cases, $R^2 = 0.30$-0.53), where stem angle increased on average by 1.5–2.4° per day (Figure 7 andFigure 8, Supplementary Table 4).

The final leaf position at day ten differed significantly amongst the three light treatments ($F(2,63) = 8.564$, $p < 0.001$), which was driven by a single comparison between the 100 µmol·m^{-2}·s^{-1} at 15° and 200 µmol·m^{-2}·s^{-1} at 15° treatments ($p_{adj} = 0.048$). Here, higher leaf angle positions were observed under the 200 µmol·m^{-2}·s^{-1} at 15° treatment for both species (Figure 8). The final leaf position of *S. wallisii* was significantly greater than that of *C. comosum* across treatments ($F(2,63) = 148.308$, $p <$

0.001), ranging on average between 29 to 71° and -17.8 to -30.5°, respectively (Figure 8). There was no significant interaction between treatment and species ($F(2,63) = 0.276$, $p = 0.760$).

The final stem angle position in *S. wallisii* differed significantly across treatments ($F(2,30) = 24.416$, $p < 0.001$), where all treatment comparisons were significant ($p_{adj} < 0.05$ in all cases). The final stem angle for the 200 $\mu mol \cdot m^{-2} \cdot s^{-1}$ at 15° treatment was closest to the vertical at 8.25 ± 7.41° (mean ± SD), followed by the 100 $\mu mol \cdot m^{-2} \cdot s^{-1}$ at 15° and 200 $\mu mol \cdot m^{-2} \cdot s^{-1}$ at 45° treatments at 14.00 ± 12.99° and 23.50 ± 3.87° respectively.

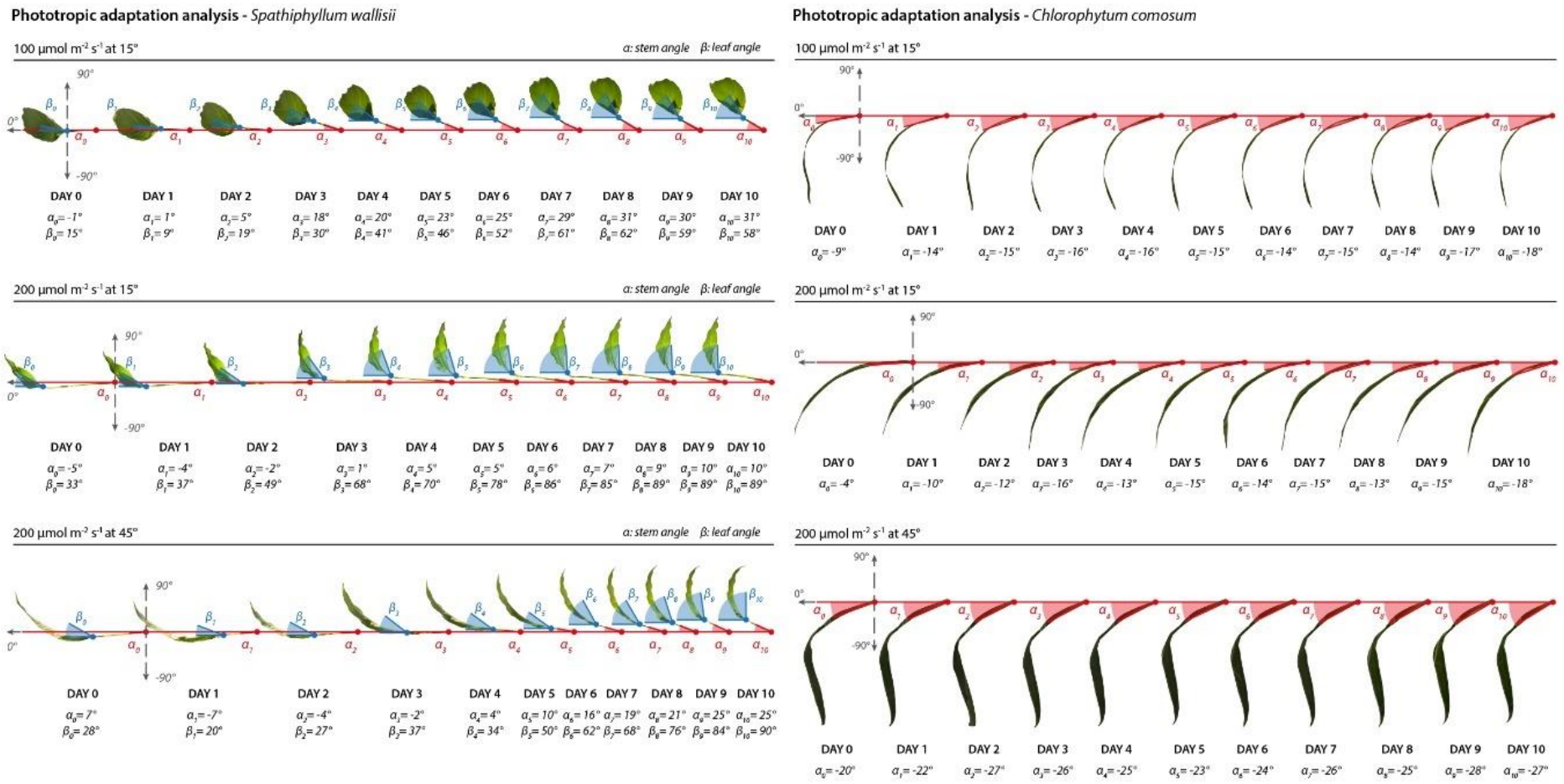

Figure 7. Leaf movement analysis of S. wallissi (left) and C. comosum (right) through time under the three light angle-intensity treatments. Single representative replicates are shown here (n = 4 were used in the trial), where α denotes average leaf angle and β denotes average stem and leaf angle, respectively.

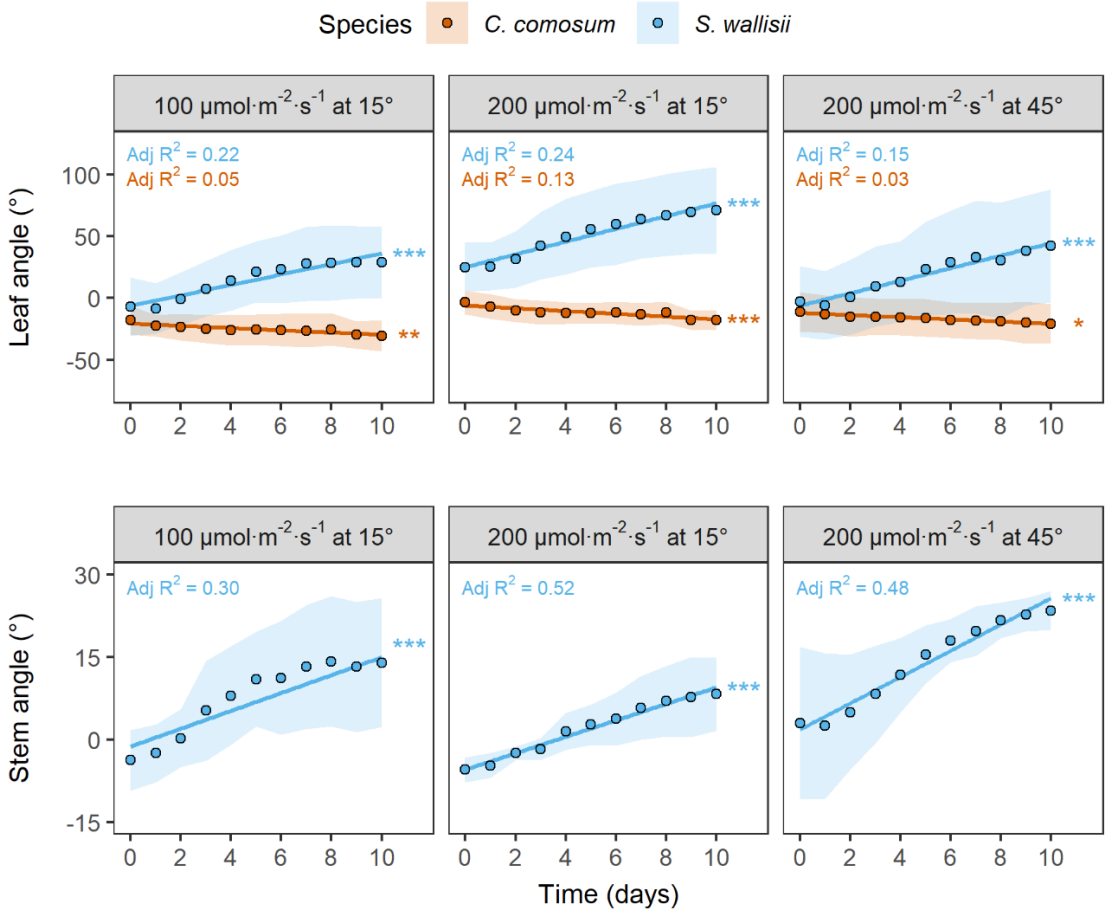

Figure 8. Linear regression models of leaf positions for both C. comosum (orange) and S. wallisii (blue) (top subplots) and stem positions for S. wallisii (bottom subplots) across a 10-day trial under the three light angle-intensity treatments. Points represent the mean leaf/stem angles from the vertical for each day, where the shaded areas depict the SDs (n = 4). Lines of best fit depict fitted models where asterisks denote significant regressions (p < 0.05; ** p < 0.01; *** p < 0.001).*

Leaf position and net daily phototrophic movement had a small effect on CO_2 removal efficiency, with fairly weak correlations observed for both plant species (*C. comosum* leaf position: r = 0.258, $p < 0.001$; *C. comosum* leaf movement: r = -0.027, $p = 0.594$; *S. wallisii* leaf position: r = 0.198, $p < 0.001$; *S. wallisii* leaf movement: r = 0.168, $p = 0.001$). *S. wallisii* stem position and movement was also weakly correlated with CO_2 removal efficiency (*S. wallisii* stem position: r = 0.137, $p = 0.006$; *S. wallisii* stem movement: r = 0.158, $p = 0.002$).

Interestingly, light treatment specific correlations between leaf position and CO_2 removal efficiency yielded comparatively higher correlations for both plant species under the 200 µmol·m^{-2}·s^{-1} at 15° treatment compared to the other two treatments (200 µmol·m^{-2}·s^{-1} at 15° leaf position: r = 0.304-0.323, $p < 0.001$; 100 µmol·m^{-2}·s^{-1} at 15° and 200 µmol·m^{-2}·s^{-1} at 45° leaf positions: r = -0.036-0.109, p = 0.214-0.679; Figure 9). This same trend was also observed for stem position in *S. wallisii* (200 µmol·m^{-}

^{2}·s^{-1} at 15° leaf position: r = 0.437, p < 0.001; 100 µmol·m^{-2}·s^{-1} at 15° and 200 µmol·m^{-2}·s^{-1} at 45° leaf positions: r = 0.001-0.155, p = 0.076-0.991; Figure 9).

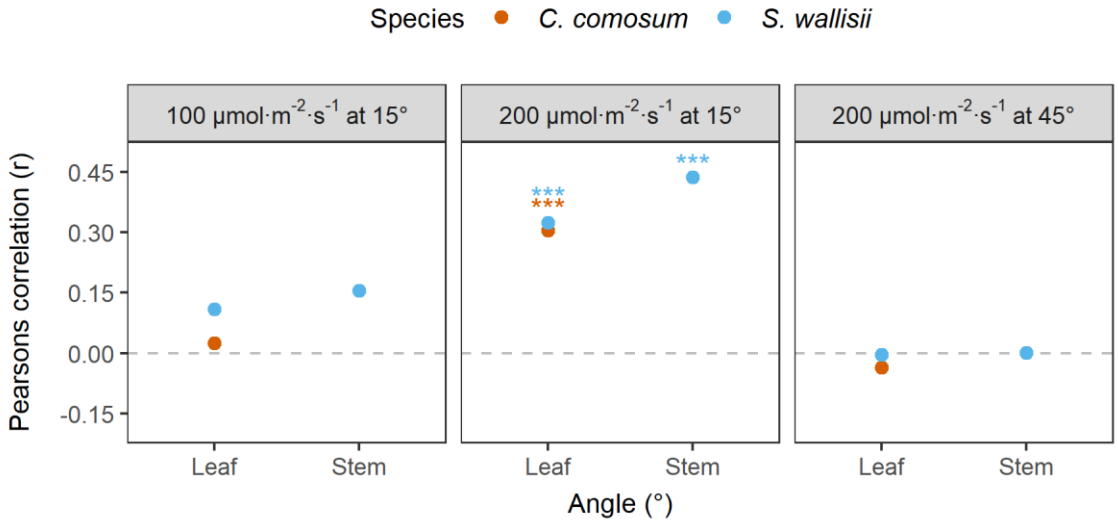

Figure 9. Pearson correlations between CO_2 removal efficiency, and the leaf/stem angle positions throughout the ten-day testing period for each light angle-intensity treatment and plant species. Note, no stem measurements exist for C. comosum due to the physiological nature of the species.

4. Discussion

The angle of incident light, light intensity and photoperiod all influence the photosynthesis and photomorphogenesis of plants, affecting plant metabolism and developmental morphology [114,125]. The indoor environment often provides light that is considerably different to the lighting requirements of most species of plants. Currently, the scientific literature pertaining to optimal lighting for indoor greenery is sparse [99,105,126]. Consequently, commercial suppliers of living wall systems often follow the recommendations provided by lighting suppliers and indoor horticultural practices, which may be based on conditions for human habitability rather than plant health.

In this study, we highlight the reduced efficiency for indoor CO_2 removal under current lighting conditions and demonstrate the practical and ideal lighting conditions for heightened CO_2 removal. By extension, our work also provides direction that may assist in determining the suitability of a given light treatment for plant health, using CO_2 drawdown as a surrogate for photosynthesis and plant metabolic activity.

The lighting conditions observed for the *in-situ* living walls in this study featured relatively low light intensities at a range of inclinations, where ~87 % of all sampled living walls received > 49 µmol·m^{-2}·s^{-1} (Figure 4) at angles of between 11 and 50° (Supplementary Figure 1 and Table 1). Experimentally, these conditions were associated with a mean chamber CO_2 removal efficiency of between 1.68 and 7.95 % of ~1000 ppm over 40-minutes (Figure 5). Non-photoadapted removal efficiencies for *C. comosum* and *S. wallisii* were greatest at a light intensity of 200 µmol·m-2·s-1 and inclinations of 15 and 45° from the vertical respectively, reaching ~30 % CO2 removal over 40-minutes (Figure 5, Supplementary Figure 3). For comparability with existing practices used for indoor environmental quality maintenance in buildings, we have used the CO_2 draw down rates calculated in the current work to estimate the ventilation equivalence that might be possible with the use of indoor living walls using optimised lighting systems *in-situ*. The best performing treatment we found was *C. comosum* at the 200 µmol·m^{-2}·s^{-1} light flux density at 15° from the vertical growing surface. Assuming this CO_2 removal was constant per plant, the extrapolated effects from a reasonably-sized, 5 m^2 passive living wall containing 400 plants in a typical 40 m^3 office can be estimated. Such a system could reduce a 1000 ppm CO_2 concentration to roughly 872 ppm, which has a ventilation equivalence based solely on CO_2 removal to an ACH of 0.21 h^{-1}, assuming an ambient CO_2 concentration of 410 ppm. As stated previously, this light level will be difficult to achieve in practice: an equivalent sized living wall receiving up to 50 µmol·m^{-2}·s^{-1} light flux density will achieve an estimated ACH of only 0.03 h^{-1}.

While no *in-situ* living walls received a light intensity of 200 µmol·m^{-2}·s^{-1}, ~5 % of the sampled walls achieved intensities between 100 and 199 µmol·m^{-2}·s^{-1} (Figure 4 and Supplementary Table 1). If changes to plantscape design or lighting infrastructure could support an average light intensity greater than 100 µmol·m^{-2}·s^{-1}, it may be plausible to increase the rate of elevated indoor CO_2 removal by 1.5–7-fold (Figure 5), and thus reduce building reliance on HVAC ventilation by some degree, if adequately sized living walls can be used. Our findings confirm the positive correlation between light intensity and CO_2 assimilation rates by ornamental plants observed in previous studies [97,98,127] and highlight the need for technical guidelines to be established for the lighting of indoor living walls.

Previous studies highlight the strong influence of the angular distribution of light incident at the leaf surface on the internal absorption profiles and photosynthetic capacity of a plant [128,129]. In low-light environments such as those optimised for human occupation, light intensity and directionality affect the penetration of light through leaf tissues, limiting the effective rate of photosynthesis [130]. Plants respond to this through phototropic and spectral signalling, where leaves will respond to light stimuli by changing their structural features to more efficiently perform their function [129]. Further, phototropism can act synergistically or antagonistically with gravitropic effects to enhance or reduce

plant growth behaviours such as light or gravitational sensing, transduction of signals, and differential growth of organs and tissues [131]. Previous studies have demonstrated that leaf orientation is critical to leaf-level light and that some plant species modify their morphology to increase the light quantity received [9]. In living wall systems, plants are orientated with their apical stems parallel to the ground as opposed to a natural vertical orientation, and thus plant morphology must respond in accordance with gravitropic and spectral signals. During laboratory testing, *S. wallisii* leaves and stems sought to be closer to the light source in all three treatments, while *C. comosum* displayed a downwards trend in response to the light sources over the ten-day testing periods (Figure 7). Differences in plant physiology are likely the key factor in this finding, where *C. comosum* lacks the stem structural integrity to facilitate an increase in inclination over time, leading to a response dominated by gravitropism. However, despite the variance in phototropism between species, both plant species displayed effective CO_2 removal efficiencies over the ten-day test period.

Contrary to our hypothesis, the absolute position of plant leaves and stems and net morphological changes appeared to have weak associations with CO_2 removal efficiency. However, morphological movement did appear to induce some sort of photosynthetic response in specific treatments (Figure 9). Under 200 $\mu mol \cdot m^{-2} \cdot s^{-1}$ at 15° lighting conditions, *S. wallisii* exhibited significant leaf/stem movement in a vertical plane, seeking the light source, of +15° and +56° (leaf and stem respectively; Figure 6 and Figure 7), which exhibited comparatively strong correlations (r = 0.323 and 0.437, respectively; Figure 9) with a CO_2 removal efficiency increase of 0.33 % per day (Figure 6). Similarly, *C. comosum,* under the same conditions, exhibited significant downwards leaf movement (away from the light source) of -14° (Figure 6 and Figure 7), which was also significantly correlated (r = 0.304), compared to the other treatments (Figure 9), with a daily CO_2 removal efficiency reduction of 0.92 % (Figure 6). While there were significant differences observed between species under this treatment, both completed the ten-day period with a CO_2 removal efficiency of ~18 %, which was higher than 100 $\mu mol \cdot m^{-2} \cdot s^{-1}$ at 15° and 200 $\mu mol \cdot m^{-2} \cdot s^{-1}$ at 45°. These findings indicate phototropism should be considered in the decision making process of plantscape design, and could be utilised to optimise light capture, prevent light stress, or to balance the effects of other abiotic factors [111,116], although decisions will inevitably be species specific.

Neither species displayed significant changes in CO_2 removal efficiency under the 100 $\mu mol \cdot m^{-2} \cdot s^{-1}$ at 15° and 200 $\mu mol \cdot m^{-2} \cdot s^{-1}$ at 45° lighting conditions over the ten-day period (Figure 6). These findings indicate these treatments had a generally equivalent effect on final CO_2 removal efficiency, independent of plant species. Variations in plant species performance (Figure 6) could again be

attributed to various physiological characteristics, however it is likely that these results speak to the robust nature of these species and further validates their popularity for species selection in living walls.

Brodersen and Vogelmann [128] notes that at the leaf surface, only illuminated tissues are capable of photosynthesis. As light intensity measurements were taken only across the top of the plant foliage, variations in single leaf light exposure attributed to inclination and orientation may have been overlooked in the current work. nevertheless, from the work conducted, it is evident that light inclination is an important factor in living wall performance and should be considered in future designs or retrofits, such as optimisation of individual species placement to suit the available light.

In many current photosystems used for indoor living walls, static lighting at fixed light inclinations is employed, typically placed ~0.8 – 1 m from the foliage. This 'one size fits all' approach has proven to be suitable for maintaining plant survival between maintenance periods, however it provides little in the way of optimised, plant specific lighting, especially if photosynthetic activity is to be harnessed for indoor environmental quality improvement. Our observations indicate that some living walls are constructed with little forethought for the morphology of specific plant species, giving the impression of a 'set and forget' installation with a reliance on plant cycling and maintenance. In some instances, this approach creates shaded areas across the wall surface, where scrambling plant species such as *Philodendron xanadu* and *Nephrolepis exaltata* block plants below from adequate lighting (Figure 4). This can be overcome only if regular and costly maintenance is performed.

From the *in-situ* measurements performed, up to ~63 % of plant foliage was exposed to light levels less than 10 $\mu mol \cdot m^{-2} \cdot s^{-1}$ (Supplementary Table 1). Previous literature has demonstrated that light intensities below 10–15 $\mu mol \cdot m^{-2} \cdot s^{-1}$ may lead to increased ambient CO_2 concentrations through plant respiration [109,132], and that light levels of 250 $\mu mol \cdot m^{-2} \cdot s^{-1}$ are optimal for highly efficient living walls [109]. It is entirely possible that at the low light levels recorded, the overall effectiveness of living walls could be CO_2 neutral, with plant species exposed to insufficient lighting contributing to indoor CO_2 concentrations.

Insufficient lighting (i.e. below the light compensation point, where plant photosynthetic CO_2 drawdown is greater than respiratory CO_2 emission) provided to living walls may indeed contribute to elevated CO_2 concentrations of an indoor space. Although there is little literature to suggest that this occurs *in-situ,* it might be prudent to assess the costs associated with this inefficiency. Maintenance costs are thought to be the bottleneck in the widespread implementation of air phytoremediation technology worldwide [133], where it is common for maintenance to be conducted purely for 'plant

health management'. With insufficient lighting, ornamental plants are able to sustain biomass, but are unable to properly utilise certain biological functions such as disease defences [107], which in turn leads to the deterioration of plant health, and subsequent increases in the maintenance required. For improved economic management and implementation, designs with sufficient lighting systems for living walls are required. While current systems can provide adequate lighting to limited regions of living walls (Figure 4), there are opportunities in the interior plantscape industry for the development of lighting to provide a more adequate range of illumination.

Recently, light emitting diodes (LEDs) have increased in popularity amongst indoor horticulture applications due to their reduced pricing, operational costs, longevity and energy consumption [115]. LEDs demonstrate remarkable promise as supplementary lighting in terms of luminous flux control due to their low radiant heat output and wavelength specificity [105]. While some capital costs of LEDs may be high, they are characterised by long lifetimes [117] and are more versatile than current indoor lighting systems [134]. They can be easily adjusted to increase photosynthetic photon flux density (PPFD: the proportion of the light spectrum usable by photosynthetic tissues) at the leaf surface, without creating an undesirable glare to building occupants. Additionally, plantscape design is a currently underutilised aspect of indoor living walls, with many suppliers basing plant species placement solely on aesthetics, as opposed to optimal lighting. For example, of the walls observed in this paper, branching species such as *Philodendron Xanadu* and *Nephrolepis exaltata* should be placed towards the base of the LW, to reduce plant-shading. Moreover, plant species with relatively low light compensation points such as *Peperomia obtusifolia* (13 $\mu mol \cdot m^{-2} \cdot s^{-1}$ [109]), may be situated where light intensities are sufficient to ensure photosynthesis. To this extent, future studies that incorporate any form of *in-situ* living wall analysis should take note of the plantscape design employed and monitor the light distribution across the wall.

5. Conclusion

As living walls have become more common for indoor air quality improvement, technical guidelines for lighting design should be developed to promote plant health, enhance phytoremediation potential, and reduce maintenance costs. A systemic design approach that considers plant species responses to supplementary lighting variations would facilitate an understanding of how and where plants should be placed across vertical greening infrastructure to receive optimal lighting conditions.

The current study demonstrates that living wall lighting systems are a crucial yet often neglected consideration to enhance the removal of CO_2 from indoor air. This study simulates the current removal efficiencies of living wall systems to remove CO_2 under commonly used *in-situ* conditions (50 $\mu mol \cdot m^{-2} \cdot s^{-1}$) to be low. Due to the lack of homogenously distributed light observed at the four living walls tested, the shortcomings of the lighting systems employed are clear. To address these shortcomings, commercial suppliers should invest in better lighting systems to increase photosynthesis and reduce maintenance costs associated with plant care and replacement.

This study found the highest CO_2 removal efficiency for both plant species to be in the 200 $\mu mol \cdot m^{-2} \cdot s^{-1}$ at 15° treatment. This, coupled with the enhanced phototropic movements observed, suggests that phototropism at specific light angles may play a significant role in increasing the CO_2 removal efficiency for some plant species. It has been proposed that a permanent lighting schedule could also increase the CO_2 removal by plants indoors due to the elimination of photorespiration that occurs in the dark, however this option is not viable due to the increased energy demand associated with the additional lighting hours. In addition to the power consumption, the impact of the increased net-removal of CO_2 from the indoor environment would be negligible as active green walls are generally only featured in commercial buildings that do not host staff during the night. Instead, the additional CO_2 produced through photorespiration is better dealt with by building ventilation that runs regardless of green wall presence. It would therefore be preferable for commercial suppliers to develop smarter, low energy solutions that cover phototropism, higher light intensities (above 100 $\mu mol \cdot m^{-2} \cdot s^{-1}$) and a plantscape design that considers the morphological parameters of the selected plant species. The intensity and directionality of light will influence the growing trends and morphology of branching species, leading to increased maintenance work when excessive shading occurs (as observed in this study). For this reason, further analysis on plant species growth under *in-situ* conditions, and extended light exposure, may facilitate the design of an appropriate vegetation framework for indoor living walls.

The authors recommend that living wall providers undertake research and development to incorporate not only comprehensive lighting systems, but also a plant-scape design optimised for lighting. This will facilitate the development of more efficient living walls for indoor air pollution removal, rather than those that prioritise aesthetics or ease of access.

Preface: Chapter 3

With the addition of active airflow into the design of botanical biofilters, the rates of removal of gaseous pollutants from both indoor and outdoor air has been significantly increased. However, the addition of airflow raises the question of whether this technology is emitting bioaerosols into the indoor environment. Prior to the current work, this aspect was significantly under addressed in the literature.

Several ubiquitous plant and soil microbes have been associated with significant respiratory symptoms such as the bacterial genus *Legionella* spp. and several fungal genera. The following study aimed to; determine if an existing, commercial indoor active green wall contributed significantly to the indoor fungal load or production/aerosolisation of any *Legionella* species; and to characterise both the bacterial and fungal species diversity associated with the green wall, with particular emphasis placed on the exploration of pathogenic species.

The following chapter is comprised of text from a peer-reviewed publication.

Chapter 3: Characterisation of fungal and bacterial dynamics in an active green wall used for indoor air pollutant removal

Fleck. R [1]*, Gill. R.L. [1,2], Pettit. T [1], Irga. P.J [4], Williams. N [3], Seymour. J [3], Torpy. F.R [1]

[1] Plants and Environmental Quality Research Group, School of Life Sciences, Faculty of Science, University of Technology Sydney, Australia
[2] Coastal Oceanography and Algal Research Team, Faculty of Science, Climate Change Cluster, University of Technology Sydney, Australia
[3] Ocean Microbes and Healthy Oceans, Faculty of Science, Climate Change Cluster, University of Technology Sydney, Australia
[4] Plants and Environmental Quality Research Group, School of Civil and Environmental Engineering, Faculty of Engineering and Information Technology, University of Technology Sydney, Australia

Corresponding Author: Robert.Fleck@uts.edu.au

This article has been published in the Building and Environment (Q1, Impact factor 7.093 (2022)).
Available online at https://doi.org/10.1016/j.buildenv.2020.106987. Published May 18th, 2020.

Abstract

Indoor air quality (IAQ) is of growing public health concern which has prompted the use of plants to phytoremediate air pollution in interior spaces. Active green walls are emerging as a means of reducing indoor contaminants and have demonstrated efficacy comparable to conventional air filtering technologies. However, the use of active airflow through organic substrates has the potential to emit bioaerosols into the surrounding environment, where the potential risk to human health is largely unknown. In this study, we demonstrate that two indoor green walls (with and without active airflow) contribute significantly to the ambient fungal load, however concentrations remained well below WHO safety guidelines. Bacterial dynamics within the rhizosphere/substrate of the operational botanical biofilters displayed variability across plant species. Phyla-wide distribution generally aligned with previous literature; however, differences from those previously reported were observed at the genus level, possibly due to geographic location, substrate composition, or plant species selection. Targeted assessment of *Legionella* aerosol contamination, an under-addressed potential pathogen for these active systems, yielded no positive identification during the sampling period. We conclude that active green walls host a unique bacterial profile and do not emit harmful levels of fungal propagules or pose significant risk of aerosolised *Legionella* species, provided systems are well monitored and maintained.

Keywords

Indoor air quality (IAQ), Active green walls, Botanical biofilter, Bioaerosols, Bacterial characterisation, Legionella.

Highlights

- Green wall bacterial community varied amongst plant species.
- The aerosolised fungal load emitted by green walls did not exceed WHO guidelines.
- No aerosolised *Legionella* species were identified.

Graphical Abstract

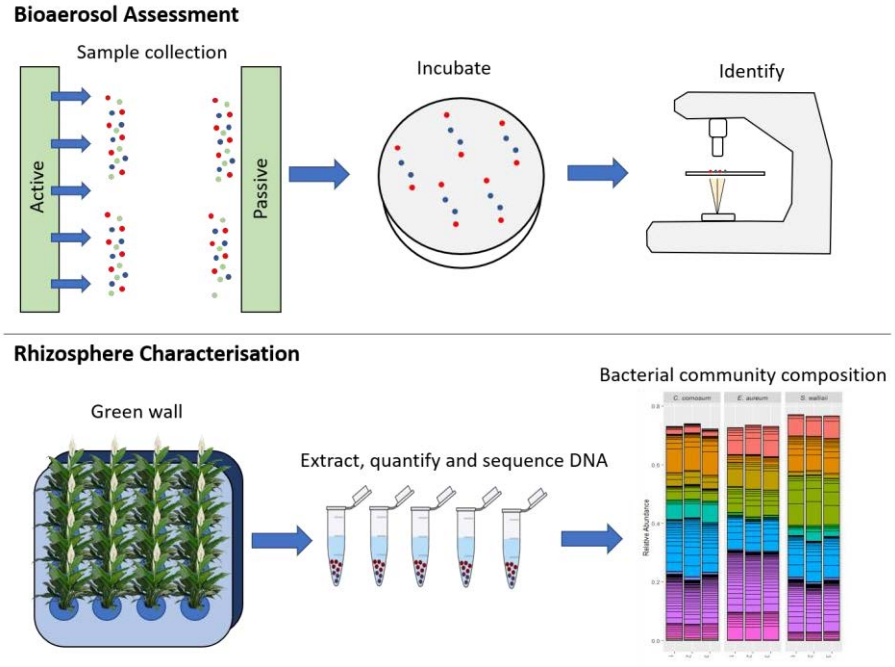

1. Introduction

In modern societies, humans spend up to 80% of their time indoors [45], where air quality is often more polluted than outdoors [4,5]. Due to the accumulation of air pollutants, and the extended duration of exposure associated with an indoor lifestyle [135], domestic and commercial indoor air pollution is responsible for up to 5% of the global disease burden [3], equating to costs of approximately US$90 billion annually [6].

Since the 1980s, the use of plants in interior spaces to phytoremediate air pollution has grown considerably in popularity [29,30]. The efficiency of botanical systems in improving indoor air quality has been significantly enhanced by the development of active botanical biofiltration, or active green wall systems [136]. Active green walls use ornamental plants grown along a vertical plane with the addition of mechanical air induction to actively draw polluted air through the plant growth substrate and foliage [137]. During this process, air pollutants are delivered directly to the rhizosphere where they may be metabolised/sequestered by microbes, the predominant mechanism for contaminant degradation [132,138,139]. Additionally, particulate matter (PM) may be filtered by the substrate and root structures [140].

While botanical biofiltration is still an emerging technology, there is substantial evidence for its practical potential, along with growing commercial interest [2,91,99,141,142]. In their current state, botanical biofilters have comparable removal efficiencies to those of conventional indoor technologies such as MERV (minimum efficiency reporting value) 4, 6, 10, 11 and 13 filters for the removal of PM (PM_{10} and $PM_{2.5}$) [143]. In addition, botanical biofilters are capable of reducing indoor concentrations of volatile organic compounds (VOCs) and other pollutants such as CO and CO_2 [109,144–147], which cannot be removed by most conventional systems, other than by dilution [148].

Despite the benefits of active green wall technologies, there is a potential for systems that use active airflow through biologically active substrates to emit bioaerosols into the surrounding environment [149]. It has indeed been proposed that active green walls may provide a favourable environment for the proliferation of pathogenic fungal or bacterial species, with the use of mechanically assisted air flow increasing the risk of the aerosolisation of water containing microbial bioaerosols. Currently, research which has assessed bioaerosol emissions from active green walls are limited to assessments of total fungal and bacterial loading. While there are no documented cases where harmful levels of fungal [44,150–152] or bacterial aerosols [143,150,152,153] have been detected in active green wall emissions, there is a paucity of research that has comprehensively characterised bioaerosol emissions, and we propose that assessments of this kind are essential to fully understand the implications of biowall systems for indoor air quality (IAQ).

Limited research has specifically investigated the aerosolised release of pathogenic bacteria from green walls [154], such as the ubiquitous bacterial genus *Legionella*. *Legionella* are free-living motile bacteria that can infect other microorganisms or form chemo-resistant biofilms [155–157], and several species are the causative agents of legionellosis [157–159]. *L. pneumophila* serogroup 1 is responsible for up to 90% of infections worldwide, with the exception of in Australia, New Zealand and Thailand, where *L. longbeachae* is the dominant pathogen, and is responsible for up to 40% of infection [160–163]. The dispersal mechanisms of these two species vary significantly [154,164]. Where *L. pneumophila* requires aerosolization through water droplets for infection to occur [154,158,159,165], *L. longbeachae* requires physical contact from contaminated soils with the eyes or mouth [163,164]. Due to the nature of the components used in active green walls, there is some concern that *Legionella* spp. may proliferate within irrigation systems and botanical substrates and become aerosolised in the event of over-watering or physical disturbance.

In this study, we aimed to determine whether an established active green wall in a modern urban office building contributed significantly to the release of fungal and bacterial aerosols, with specific focus on bioaerosols that have implications for IAQ and human health. We assessed the culturable indoor aeromycota, characterised the bacterial community composition using 16S rRNA amplicon sequencing approaches, and performed targeted enumeration of the pathogen *Legionella* spp. to examine potential risks to public health.

2. Methodology

2.1 Site description

Aerosol sampling was conducted on four floors (levels 12 – 14 and 17) of a newly built commercial office building, made of steel and glass near Sydney's Central Business District. The building featured standard heating, ventilation and air conditioning (HVAC) systems with no additional filtration technology. One active and one passive green wall span the interior of two stories (levels 13 and 14), each covering 60 m^2, in a semi-open plan café and meeting/reception space, with a floor space of 2300 m^2. Both green walls consist of several hundred individual plant housings (modules) supporting sixteen plants per module [166]. These house six plant species: *Chlorophytum comosum, Spathiphyllum wallisii, Epipremnum aureum, Gibasis* sp.*, Philodendron xanadu* and *Peperomia obtusifolia*, of which *C. comosum, S. wallisii, E. aureum* represent most of the greenery at the time of sampling.

The active green wall utilises six low-profile 230 V, single-phase, 50 Hz fans operating at 98.96 m^3/h, per fan, when freestanding. These are located at the bottom of the wall to facilitate active air flow

through the plant growth substrate and foliage. Each fan supplies airflow to 9.5 m^2 of active green wall on 15-minute on–off intervals, from 06:00 to 20:00 daily, with a total run time of seven hours per day. The volumetric flow rate of effluent air was recorded as 17.3 m^3/h through the green wall, determined with a VELOCICALC Model 9545-A air velocity meter (TSI Incorporated, USA). Active and passive walls are irrigated every two and four days respectively for eight minutes (two 4-minute watering cycles), with a delivery rate of 5 L/minute. Irrigation is divided into zones, with three irrigation catchments. Runoff falls gravimetrically into large drainage reservoirs at the base of the wall.

To determine the bioparticle density in areas of the building not serviced by the green walls, reference sites were positioned on levels 12 and 17 in thoroughfares within the building, as the open plan office spaces of these floors contained relatively high densities of potted plants (~0.33 potted plants/m^2) which may have also had an effect on indoor bioaerosol levels [13].

Foot traffic was explored by correlation analyses (Pearson's correlation coefficient) to assess its association as a potential influential variable with fungal density [167]. Foot traffic data was sourced from the building reception booking system.

2.2 Bioaerosol assessment

Bioaerosols were sampled over a three-month period from late summer to early autumn (February 28th, March 28th and May 3rd, 2019) between 11:00 and 14:00. Samples were collected with a Reuter Centrifugal Sampler (RCS; Biotest Diagnostics Corp., Denville, NJ, USA), which is comprised of a hand-held cylinder with an impeller that rotates at 4100 rpm. Air is drawn into the sampling head, and aerosolised particles are imbedded on the surface of selective agar strips that encircle the head. The RCS was operated for 2- and 4-minute cycles, sampling 80 and 160 L of air for fungal and bacterial samples respectively. For each green wall, six samples were taken at different locations adjacent to the wall surfaces. On the lower level of each green wall, three samples were taken along the length of the wall 1.8 m above ground and 0.5 m from wall surfaces, clear of any protruding vegetation. This sampling procedure was repeated on the upper level of each green wall. Thus, the sampling locations encompassed the length and height of the green walls, as well as taking air samples from places that were relevant to a person's breathing zone. Reference site samples (six in total) were collected from designated 3 m^2 spaces within the thoroughfares, 1.8 m above ground and 0.5 m from wall surfaces. Sample collection was conducted at each location individually, and all samples were completed within a three-hour window and during the operational period of the active green wall fans.

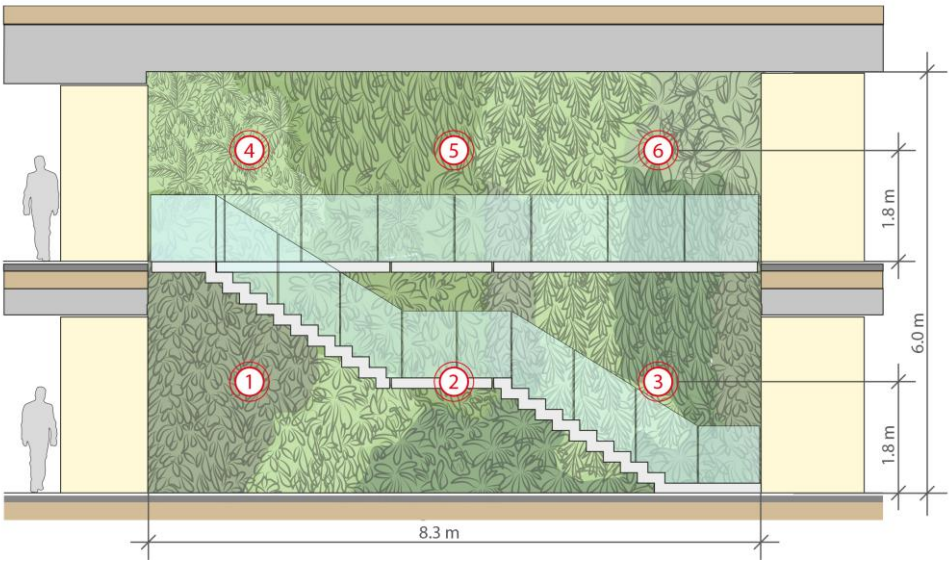

Figure 10. Schematic representation of bioaerosol sampling locations across each green wall site of a newly built commercial office building. Sampling was conducted over two stories, 1.8 m above ground and 0.5 m from protruding vegetation at both sites.

Commercial Rose-Bengal Chloramphenicol (RBC) agar RCS strips and modified RCS strips containing Buffered Charcoal Yeast Extract with L-Cysteine agar (BCYE-cys) were utilised for fungal and *Legionella* sampling respectively. RBC is a pH neutral agar with added Chloramphenicol for the suppression of bacterial growth and allows control of the size and height of mould colonies to prevent luxuriant species growing over slow-growing moulds or yeasts [168]. Bacterial samples were assessed for L*egionella* spp. as per the British Standards Institution (BSI) [169]. Incubated BCYE-Cys agar strips were assessed visually for putative *Legionella* colonies (grey/white in colour) and, if detected, colonies were sub-cultured onto BCYE growth agar, deprived of L-cysteine, where *Legionella* spp. should not grow. BCYE-Cys is a *Legionella* spp. preferential growth media that employs the use of L-Cysteine, soluble ferric pyrophosphate and alpha-ketoglutarate to enhance *Legionella* growth. The use of activated charcoal removes toxic metabolic products and proteins, and other growth nutrients are supplied by yeast extract [170]. All samples were tested against a *Legionella pneumophila* positive control.

Imbedded fungal and bacterial samples were sealed and transported for incubation at room temperature (21–23 °C) and 37 °C respectively in dark, aerobic conditions for five days. Cultured strips were photographed, after which colonies were enumerated. Fungal samples were identified by microscopy using identification guides [171–173]. Colonies that did not have conidial structures or spores were classified as ‘sterile mycelia’.

2.3 Characterisation of bacterial community diversity

Samples from three single-species (*C. comosum, E. aureum* and *S. wallisii*) botanical biofilter modules containing healthy plants were selected randomly from the active green wall. Modules were suspended and flushed with 12 L of Milli-Q water (Ω 18.2; Millipore, Eschborn, Germany) and run-off was collected in pre-sterilised (1:10 sodium hypochlorite, Milli-Q rinsed) natural LDPE plastic bags. Samples were then aseptically transferred to three sodium hypochlorite sterilised 10 L sample containers for filtration. Triplicate 2 L samples were filtered through 0.22 µm GPS sterivex membrane filters (Millipore). Filters were stored at -80 °C prior to DNA extraction.

DNA extraction was performed using the DNeasy PowerWater kit (QUIAGEN) as per the manufacturer's instructions. A Nanodrop-1000 spectrophotometer was used to measure DNA quantity and purity. DNA was sequenced using the 16S rRNA amplicon Illumina MiSeq platform (2 x 300 bp), by the Ramaciotti Centre for Genomics (University of New South Wales, Sydney, Australia), using the V3-V4 region (341f-805r) and 341F and 805R primers.

16S rRNA fastq files were processed using R-Project and the Dada2 (V1.12.1), DECIPHER (V2.12.0), and Biostrings (V2.52.0) packages [174–176]. High quality reads were filtered and trimmed using: trimLeft = c (17,21) to remove primer sequence; truncLen = c (280,210) to trim low-quality tails; and maxEE (2,5) to relax the expected error on the reverse sequence. Taxonomic classification was assigned by aligning amplicon sequence variants (ASVs; equivalent to operational taxonomic units (OTU) at 100% sequence identity) with the Silva SSU r132 database [177]. A grouped mean relative abundance (gmRA) threshold of ≥100 was established as a cut-off for plotting using the phyloseq (V1.28.0) and ggplot2 (V3.2.0) packages [121,178].

2.4 Statistical analysis

Fungal density data was rank transformed prior to analysis to improve homogeneity of variance across treatments. A rank transformation was chosen over a logarithmic function due to the nature of the error distribution in all samples, where variance was highly skewed above the mean, relative to below it. A two-way repeated measures analysis of covariance (2-way RM ANCOVA) was performed to assess differences in rank-transformed fungal bioparticle density (CFU/m^3) between green wall sites and through time, with foot traffic (number of passers-by per sampling period) as a covariate (Pearson's r = 0.651). Tukey's Honest Significant Difference (Tukey's HSD) was performed on significant effects to evaluate comparisons. Further, Shannon's H-Index was calculated to assess fungal diversity between green wall sites and across time points, and a two-way RM ANOVA was performed to analyse

differences. Results were deemed significant at $\alpha = 0.05$. All analyses were performed in R-Project, version 3.6.1 [118].

To assess differences in bacterial community diversity, a non-metric multidimensional scaling (nMDS) biplot was generated (Supplementary Figure 4) using relative abundance taxa data. Observed differences amongst botanical modules with different plant species were then examined with permutational analysis of variance (PERMANOVA), and the contribution of individual phyla to dissimilarities amongst plant species was assessed with analysis of similarity percentages (SIMPER, Bray-Curtis similarity index). These analyses were performed with the Vegan (V2.5.5) package [179] in R-Project.

3. Results

3.1 Fungal bioaerosol assessment

Active and passive green wall sites featured significantly higher fungal densities than the reference sites across the three-month sampling period ($p = 0.001$ and $p = 0.009$ respectively; Figure 11). Temporal differences in fungal density were not significant, nor were interactions amongst factors or with foot traffic ($p > 0.05$). Despite elevated concentrations of aerosolised fungal propagules, total concentrations remained well below the World Health Organisation guideline for indoor air [180] of 500 CFU/m^3 (Figure 11).

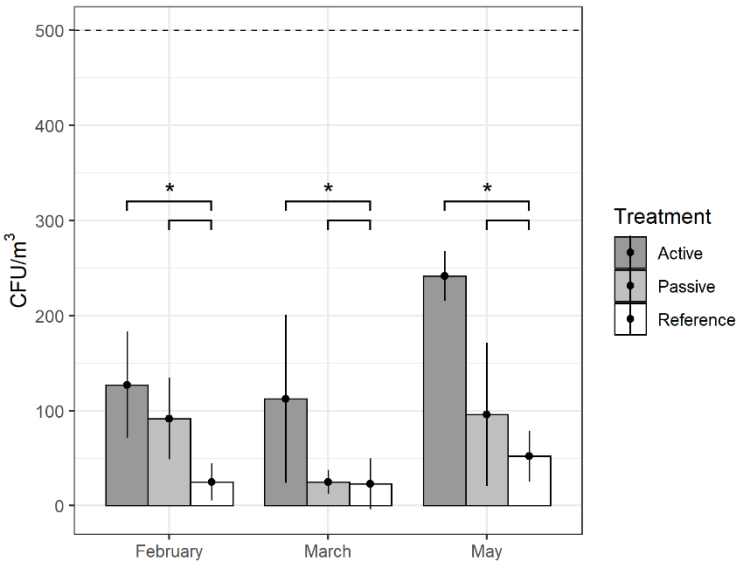

Figure 11. Average aerosolised fungal density (CFU/m3) detected at active and passive green wall sites and reference sites over the three-month sampling period. Error bars represent standard error of the mean. Significant comparisons are indicated by asterisks ($p < 0.05$). Significant WHO Guidelines for safe indoor fungal density is denoted with the dashed line at 500 CFU/m3.

The frequency of generic occurrence, average propagule density and range of detection amongst sites are displayed in Table 1. The most prevalent species was *Aspergillus ochraceus*, at a relative frequency of 83% for the green wall sites and 39% for the reference sites, followed closely by the genus *Wallemia* at 82, 67 and 28% for the active, passive and reference sites, respectively. Despite *A. ochraceus* being the most frequently detected species, the mean densities of *Wallemia* was higher at 40, 45 and 28 CFU/m^3, respectively. Shannon's diversity index ranged between 1.24 and 1.98, where no significant differences were detected amongst sites ($p = 0.098$) or through time ($p = 0.275$).

Table 1. Relative frequency, mean and range of density of aeromycota identified at active and passive green wall and reference sites. Sample measurements across the three time points were pooled for this summary.

	Active			**Passive**			**Reference**		
Species	Frequency (%)	Mean (CFU/m^3)	Range (CFU/m^3)	Frequency (%)	Mean (CFU/m^3)	Range (CFU/m^3)	Frequency (%)	Mean (CFU/m^3)	Range (CFU/m^3)
Wallemia spp.	82	40	ND – 125	67	45	ND – 113	28	5	ND – 25
Aspergillus ochraceus	83	22	ND – 63	83	30	ND – 63	39	8	ND – 63
Penicillium spp.	58	16	ND – 113	58	10	ND – 38	22	3	ND – 25
Paecilomyces spp.	42	14	ND – 75	8	1	ND – 13	22	3	ND – 13
Aspergillus terreus	33	6	ND – 25	33	11	ND – 63	11	2	ND – 25
Sterile mycelia	25	4	ND – 25	25	6	ND – 38	11	3	ND – 25
Basidobolus spp.	17	3	ND – 25	50	7	ND – 25	33	6	ND – 25
Epicoccum spp.	17	3	ND – 25	*ND*	*ND*	*ND*	11	2	ND – 25
Cladosporium spp.	8	2	ND – 25	*ND*	*ND*	*ND*	*ND*	*ND*	*ND*
Rhodotorula spp.	83	1	ND – 13	8	1	ND – 13	11	1	ND – 13

ND not detected

3.2 Characterisation of substrate bacterial communities

16S rRNA amplicon sequencing generated a total of 610,345 high quality reads, distributed across 2,825 Amplicon Sequence Variants (also known as zero-radius Operational Taxonomic Units, where differentiation is made at a single nucleotide to avoid similarity-based clustering). These sequences were classified into 27 phyla, with the 120 ASVs that exceeded the gmRA (grouped mean relative abundance) cut-off accounting for 74.38% of the community composition (Figure 12). The bacterial

community was dominated by Acidobacteria, Acintobacteria, Bacteroidetes, Chlamydiae, Elusimicrobia, Patescibacteria and Proteobacteria, with these phyla contributing to the ten most abundant ASVs (ASV1-10), and accounting for 24.9% of the total bacterial community structure. In order of abundance, Proteobacteria contributed 26.7% of the total bacterial community with 953 individual reads (ASVs), followed by; Patescibacteria (17.6%: 223 reads), Actinobacteria (13.6%: 367 reads), Chlamydiae (12.1%: 206 reads), Acidobacteria (8.3%: 132 reads), Bacteroidetes (6.3%: 204 reads) and Elusimicrobia (2.6%: 11 reads).

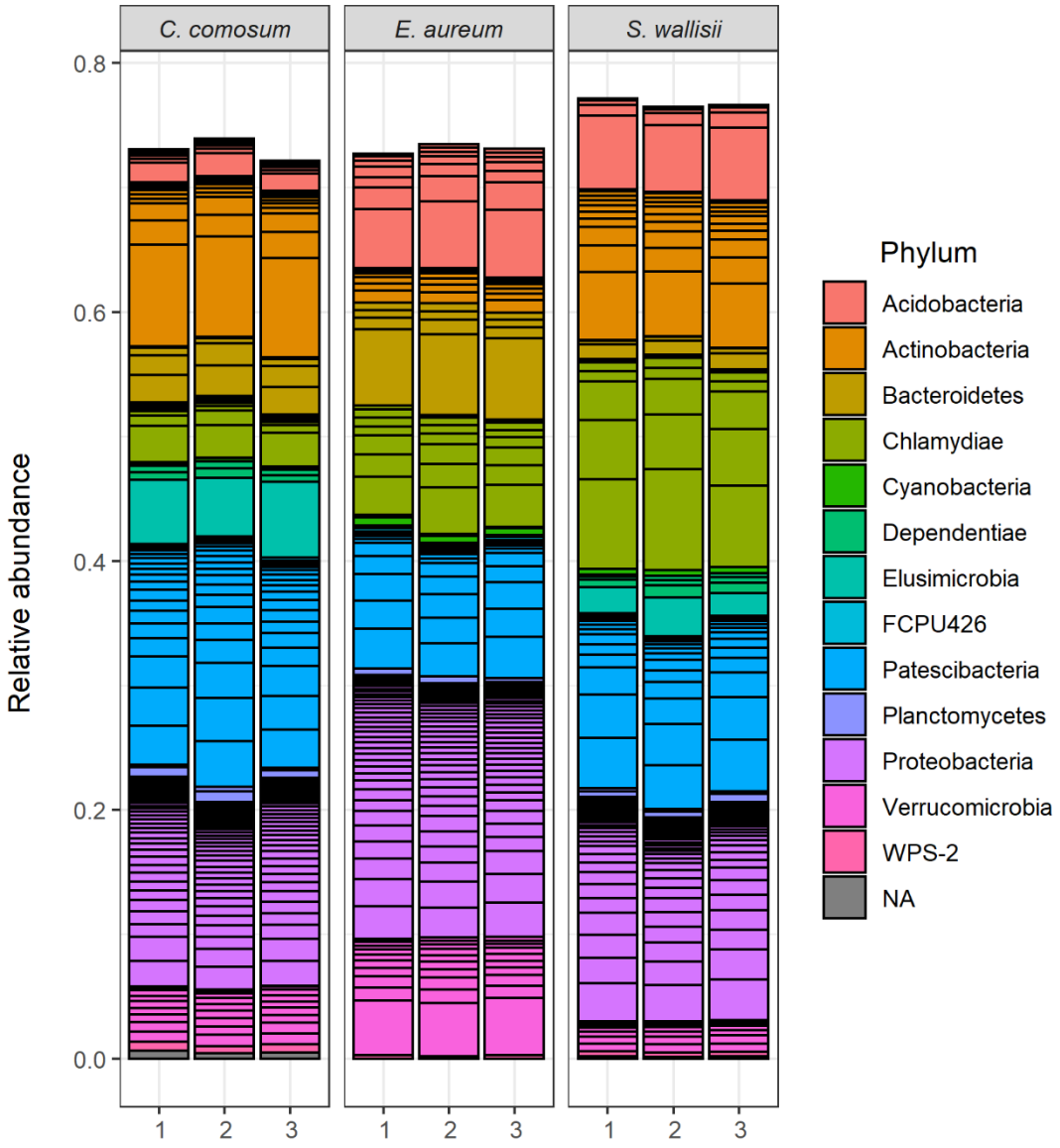

Figure 12. Relative phylum abundance of bacteria associated with the three single- species botanical modules from the active green wall site, showing technical triplicates. The 120 ASVs that exceeded the gmRA cut-off across plant species are displayed (with 2705 ASVs excluded).

PERMANOVA identified significant differences in bacterial community structure among plant species ($p = 0.005$), which was confirmed graphically by an nMDS plot revealing distinct separation of the bacterial community between plant species (Supplementary Figure 4). SIMPER analysis attributed 64.6 – 72.3% of the dissimilarities in bacterial community structure among the three plant species to four phyla (Table 2). Differences between *C. comosum* and *E. aureum* were primarily driven by Patescibacteria (25.5% of the sum dissimilarity between species); *C. comosum* and *S. wallisii* by Chlamydiae (20.8%); and *E. aureum* and *S. wallisii* by Proteobacteria (19.7%).

Table 2. SIMPER analysis results, showing phylum contributions to amongst species differences in bacterial community structure from the three single-species botanical modules from the active green wall site. A dissimilarity contribution threshold of 10% was used for comparisons.

C.comosum - E. aureum		***C.comosum - S. wallisii***		***E. aureum - S. wallisii***	
Phyla	Contribution %	Phyla	Contribution %	Phyla	Contribution %
Patescibacteria	25.47	Chlamydiae	20.82	Proteobacteria	19.72
Actinobacteria	23.01	Proteobacteria	17.61	Chlamydiae	18.82
Proteobacteria	16.2	Patescibacteria	14.76	Actinobacteria	16.92
		Actinobacteria	11.84	Patescibacteria	16.88

Of the 2,825 ASVs sequenced, 33 individual reads were identified as members of the Legionellaceae family (Phylum Gammaproteobacteria), whereby 31 reads were assigned to the genus *Legionella* (Supplementary Table 5). Two ASVs (ASV303 and ASV1316) could not be identified to the genus level but were included as *Legionella* because the Legionellaceae contains only one genus. Interestingly, the distribution of the 28 least abundant *Legionella* reads differed between plant species.

3.3 Bacterial bioaerosol assessment

Aerosolised *Legionella* assessment yielded no indication of presumptive *Legionella* colonies with respect to the *Legionella pneumophila* positive control. Several unknown bacterial colonies grew on the modified RCS strips, but these were morphologically distinct from *Legionella* spp., and were thus not identified further.

4. Discussion

4.1 In-situ bioaerosol analysis

While potting soils have been implicated as a source of human pathogens [181–184], studies documenting the dispersal of aerosolised fungal pathogens from indoor contaminated soils is limited [43]. Several studies have found that neither potted plants nor complex biowall structures contribute significantly to allergenic or pathogenic airborne fungal density [43,185–188], unless considerable physical disturbance or agitation occurs [189]. Nonetheless, as active green wall system circulate air through large volumes of biomass, characterisation of these systems is prudent to assess the likelihood of unfavourable microbial growth and the proliferation of fungal and bacterial aerosols.

Our results demonstrate that both active and passive green walls contributed significantly to ambient fungal aerosol concentration in the tested environments relative to reference sites. However, viable propagule counts at both walls remained well below the World Health Organisation maximum guidelines of 500 CFU/m^3 for indoor fungal spore loads [180], and are classified between very low (50 CFU/m^3) and low (200 CFU/m^3) according to Singh *et al* [190]. A comparative assessment conducted on small scale active green walls by Irga *et al* [43] hypothesised that the use of larger installations may increase the density of bioaerosols [43], however, this was not the case in this study. The results presented here, while higher than those reported by Irga *et al* [43], fell into the same low classification range [190].

No highly pathogenic fungal species were detected (e.g. *Aspergillus fumigatus*) in our analysis, and fungi with known allergenic properties (*Aspergillus, Cladosporium, Epicoccum* and *Penicillium*) were measured in concentrations below their proposed allergenic limits [191]. In line with previous green wall research assessing ambient bioaerosols [43], no dimorphic or systemic pathogens were detected, nor were any dermatophytes. Further, the species identified were comparable to previous active green wall studies in the area [43,192] and generally consisted of common indoor fungi that do not represent health concerns for immunocompetent people. This suggests that while green walls may contribute to an increase in the fungal loading of a space, it does not change the fungal load composition.

4.2 Substrate analysis

Despite the highly variable diversity of bacterial species in soil environments, diversity at the phylum level is remarkably stable world-wide [193]. The substrate bacterial communities detected in this study were similar to previous studies on phytoremediation systems [46,194,195]. However, the

bacterial community composition varied significantly amongst plant species (Figure 12; p = 0.005) with Proteobacteria, Patescibacteria and Actinobacteria driving differences amongst biofilters with different plant species (Table 2).

It is commonly accepted that rhizospheric bacterial communities are controlled by specific assembly rules [196], where factors such as soil type, plant compartment, host genotype/species, plant immune system behaviour, plant trait variation/developmental stage and residence time/season influence bacterial community composition [196]. It is thus likely that differences in root structure and other plant traits are the driving factors for bacterial variances amongst the plant species tested, as there were no other obvious differences between green wall modules. As active green walls utilise a range of botanical species, variations in their natural capacities to host different bacterial communities may, in future, influence their relative success as indoor air phytoremediators.

The prevalence and distribution of Proteobacteria was consistent with earlier rhizospheric studies [45,46,197–199], where Alpha- and Gammaproteobacteria were of almost equal distribution. Within these two classes, the *Acetobacteraceae* (Alpha-) and *Burkholderiaceae* (Gama-) contributed 11.54% and 11.69% of the total Proteobacterial density respectively. These findings align with those of Russel *et al* [45] and Mikkonen *et al* [46], who performed substrate analyses of field-deployed botanical biofilters. Further, the potential VOC-utilising families identified by Mikkonen *et al* [46] (*Nevskiaceae, Patulibacteraceae* and *Xanthobacteraceae*) were also identified in the current study. Interestingly, the genera *Devosia, Prosthecomicrobium* and *Hyphomicrobium*, which are VOC degraders that were found to be abundant in both previous bodies of work, were largely underrepresented in the current study [45,46]. Active green walls equivalent to that tested here have been previously shown to be highly effective VOC remediators [41].

The newly re-classified superphylum Patescibacteria has been estimated to encompass more than 15% of the bacterial domain [200]. Due to their reduced genomic profile and limited metabolic potential, Patescibacteria are believed to be plant-root symbionts [201–204]. In this study, Patescibacteria were dominated by the order Saccharimonadales (56.6%), a vastly understudied group [205]. A recent study by Lemos *et al* [204] found evidence that the Saccharimonadales possess uncharacterised metabolic mechanisms that facilitate nutrient uptake [204]. This discovery may lend support to the theory that these bacteria are endophytic bacterial symbionts in botanical substrates [205]. With little previous research on these bacteria, we hypothesise that variation in Patescibacteria composition amongst plant species may be associated with differences in plant root structure or molecular mechanisms, by which plants favour specific bacterial endophytes [206].

Another driver of dissimilarities in the bacterial communities amongst plant species was the Actinobacteria, a widely distributed environmental taxon, ranging from soil inhabitants (e.g. *Streptomyces* spp.), plant commensals (e.g. *Leifsonia* spp.), nitrogen-fixing symbionts (e.g. *Frankia* spp.) and cellulose metabolisers (*Cytophaga* and *Sporocytophaga* spp.), to animal and plant pathogens (*Mycobacterium* spp.) [207–209]. Approximately 60% of biologically active compounds released in soils are attributed to this taxon, which are noted for the production of plant-growth promoting chemicals [210,211]. For this reason, they are often considered when developing phytoremediation bioaugmentation strategies for pollutants such as heavy metals or pesticides [195,208,210]. Additionally, several other rhizospheric or endophytic Actinobacterial families (Chitinophagaceae, Microbacteriaceae, Solirubrobacteraceae, Sphingobacterium, and Streptosporangiaceae) were detected in comparable concentrations. These families have known properties that may contribute to plant health, environmental sensing, disease regulation or drought resistance [195,209,212,213].

There have been few studies that have characterised the microbial population of deployed commercial botanical biofilters [45,46]. Mikkonen *et al* [46] building on the work of Russel *et al* [45], hypothesised that the genus *Hyphomicrobium* may be a global green wall system inhabitant [46], however, this genus was not detected in this study. Subtle differences in rhizospheric community structure may be attributed to a range of factors such as growth substrate composition, geographical location, or plant species selection, and it is likely that the rhizospheric community structure of botanical biofilters is more dynamic than previously theorised.

4.3 Legionella contamination analysis

While there is a growing body of research that validates the safety of active green walls regarding their contributions to the indoor aeromycota [2,43,44,151], there is less evidence related to the emission of pathogenic bacterial aerosols such as *Legionella* [214]. In Australia, most cases of legionellosis have been attributed to sporadic environmental contamination by either *L. pneumophila* or *L. longbeachae*. However, several major outbreaks by *Legionella pneumophila* sourced from building cooling towers have been documented [158]. In the natural environment, *Legionella* spp. account for less than 1% of the total bacterial community structure [150], which aligns with the levels detected here (Supplementary Table 5). While the density of *Legionella* spp. detected would be considered low, due to the limitations of 16S Illumina Sequencing, this study was unable to speciate the legionellae identified, and thus determine the extent of potential pathogenic species/strains. It is thus suggested that future work makes use of species-specific qPCR to expand on the work conducted here.

Due to the botanical nature of these systems, strict watering regimes should be employed by service providers. The transmission of many pathogens is aerosol dependant [158,215], and it is therefore essential that biofilters are maintained at an optimal water content which is sufficient for normal plant operations, but does not allow water to stagnate within the substrate or harbour biofilms in irrigation catchments [216–218]. In addition to the low concentrations of *Legionella* reported, this active green wall system employed the use of gravimetric drip irrigation – a system that lacks the pressurised components that may lead to active aerosolisation [154,155,159] – making the risk of pathogenic dispersal very low, provided the systems are well maintained.

Briefly, several additional potential pathogens were identified with 16S Sequencing (Supplementary Table 6), however the relative abundance of these bacteria were insufficient to warrant concern [219].

5. Summary and Conclusion

Fungi are ubiquitous soil inhabitants and have strong associations with plants. The installation of botanical material indoors, either as simple potted plants or complex active green walls, is likely to contribute to the ambient fungal load [17,44,188,220]. Fungal aerosols in the ambient indoor environment proximal to active and passive green walls remained well below WHO guidelines and the systems did not release detectable harmful fungal bioaerosols. The concentrations detected were comparative to previously reported literature [43,44,150,153,186], where no pathogenic or allergenic species at symptomatic concentrations were detected.

With an increase in commercial interest in this technology, there is the potential for companies to rush products to market without acceptable research into design and maintenance. In these instances, there is the possibility for poorly maintained systems to provide the niche environments required for an increase in fungal propagation or the formation of harmful bacterial biofilms. In order to prevent this, further scientific research is required on the factors that may influence dispersal of fungal propagules from green technologies. Additionally, more field studies are required of deployed commercial systems in order to validate the research findings presented here and in previous green wall literature.

Whilst the building tested in the current work was new and built to a very high standard, with a concomitant low background fungal diversity, it is possible that less well-maintained structures may experience different effects from the installation of green infrastructure. It is not possible from the current findings to determine whether green walls would make a greater or smaller contribution to

the bioparticle load of a building with a higher background level of contamination, and it is recommended that this issue be addressed in future research.

Phylogenetic distribution of bacterial species provided insight into the composition of the bacterial community in a commercial botanical biofilter deployed in the southern hemisphere. These results differed in some aspects from those previously reported [45,46], inferring that the composition of microbial communities associated with green wall systems may be governed by region, substrate or plant species.

Further, no aerosolised *Legionella* was detected over the three-month monitoring period. Both the abundance of *Legionella* and the pressurised mechanisms required for aerosol dispersal were absent in these systems, and therefore present little risk of a contamination event, provided the systems are maintained at the industry specifications.

This body of work contributes a unique perspective to the microbial state of botanical biofilters situated in the southern hemisphere. The contribution of green walls to the ambient fungal load has been documented, however the bacterial dynamics of these systems is largely understudied. Further work in this area should aim to address the bacterial composition of the rhizosphere of deployed botanical biofilters *in-situ*, as well as the bacterial and fungal aerosols they may generate.

Preface: Chapter 4

Domestically there has been very few peer-reviewed studies that quantify the benefits of green roofs in context with the Australian climate, and to date, most international studies have been undertaken on an experimental scale. Here we provide quantitative evidence for the benefits of green roofs in Australia, primarily the thermal regulatory properties, using a unique experimental method. Due to the comparatively harsh Australian climate, the inclusion of green roofs into building architecture could serve to reduce the thermal burden on HVAC systems for cooling in the summer months, and heating in the winter months, leading to a net reduction in commercial building energy consumption. Green roofs also provide the less easily quantifiable benefit of reducing the Urban Heat Island (UHI) effect through reduced solar reflectance.

In this study we aimed to determine the thermal regulatory effect of an extensive green roof in urban Sydney, Australia, its effects on the rooftop microclimate and the potential benefits of implementing this technology city wide and more broadly. The inclusion of a matched, spatially independent control roof in this study should add objectivity to the dataset and reduce the potential for methodological confounding. This project was run in collaboration with UTS, Lend Lease, Junglefy and the City of Sydney to generate quantitative data to support the City of Sydney 2030 Greening Guide, funded under the City of Sydney Environmental Performance - Innovation Grant 2019-20.

The following chapter is comprised of text from a peer-reviewed publication.

Chapter 4: Urban green roofs to manage rooftop microclimates: A case study from Sydney, Australia

Fleck. R [1*], Gill. R [1, 2], Saadeh. S [3], Pettit. T [1], Wooster. E [4], Torpy. F [1], Irga. P [3]

[1] *Plants and Environmental Quality Research Group, School of Life Sciences, University of Technology Sydney*
[2] *Coastal Oceanography and Algal Research Team, Climate Change Cluster, Faculty of Science, University of Technology Sydney*
[3] *Plants and Environmental Quality Research Group, School of Civil and Environmental Engineering, University of Technology Sydney*
[4] *Centre for Compassionate Conservation, School of Life Sciences, University of Technology Sydney*

**Corresponding Author: Robert.Fleck@uts.edu.au*

This article has been published in the Building and Environment (Q1, Impact factor 7.093 (2022)). Available online at https://doi.org/10.1016/j.buildenv.2021.108673. Published December 8th, 2021.

Abstract

Urbanisation has led to a growing need for sustainable development leading to climate resilient cities. As the urban heat burden increases in severity, technologies to improve the thermal comfort of cities are increasingly required. Green roofs are one such technology that can provide increased building thermal performance. In this study, we investigate two identical buildings, except, one was equipped with a green roof, and the other without. We present the longest-term assessment conducted on an Australian green roof with *in-situ* thermal monitoring coupled with surface temperature assessments. Field measurements were utilised to calculate the thermal buffer potential of the green roof compared to a near-identical conventional roof, over three seasons. Our findings indicated a reduction in rooftop surface temperatures up to 20 °C when ambient temperatures exceeded 40 °C, as well as improvements to heat flow of up to 55.54%. These results indicate that green roofs may contribute to the much-needed reduction in ambient city temperature to alleviate overheating and the costs associated with the urban heat island effect.

Keywords

Green infrastructure, green roof, heat flow, heat transfer, insulation.

Highlights

- Green roof summer panel/roof temperatures reduced by ~9.63 and 6.93 °C.
- Green roof microclimate experienced an average peak temperature reduction of 8 °C.
- Heat flow was 13.37 and 5.37 W/m^2 lower for Spring and Summer, respectively.

1. Introduction

Rapid urbanisation has led to a global move towards climate resilience and sustainable design in commercial properties. Developers and governments are increasingly turning to nature-based solutions (NBS) to address various concerns associated with urban dwellings in an increasingly climate aware environment [221–223]. One emerging urban NBS technology is the addition of green infrastructure such as green walls and green roofs to new or existing buildings [39]. The benefits of these technologies have been well documented, including the provision of ecosystem services [224], absorption of air pollutants [47,225], urban noise reduction [226–228], increases in urban biodiversity [39,229], improved stormwater management and retention [230–232] and an increase in thermal regulation for both indoor and outdoor environments [233–236].

Of these two NBS options, green roofs are often the most actionable, with a significant portion of roofs in urban centres being suitable for retrofitting [51,237–239]. Current roof top real estate is significantly underutilised, with many urban roof tops lacking even solar systems in some countries [240]. As such, there is an opportunity for substantial benefits to be gained for some densely populated urban centres through the addition of green roofs [20]. Green roofs functionally act as urban ecosystems with variable substrate depths, plants, and drainage networks that operate in concert to create a surrogate environment upon the surface of conventional roofs [241]. These provide additional layers to the roof surface, promoting insulation that can reduce both ambient rooftop temperatures and prevent heat penetration into the building envelope. The vegetation can reduce the heat absorbed by the building through evapotranspiration and blocking or reflecting solar radiation [242]. The growth substrate acts as a matrix to retain moisture for plant use, and can function to regulate proximal temperature as well as acting as a physical barrier, in combination with the multiple drainage layers, to reduce heating of the roof surface [243]. The inclusion of green roofs, and therefore vegetation and the associated layers, presents urban designers with an excellent tool to assist in the reduction of the urban heat island (UHI) effect [244] that, in part, stems from ever-dwindling space for vegetated surfaces in urban environments [242].

The effect of the UHI occurs when an increased heat flux from the land surface is moved into the atmosphere near cities [245]. The replacement of vegetated areas for impermeable surfaces such as concrete, stone, glass, steel and bituminous materials leads to a significant reduction in the capacity of urban spaces to regulate temperature, where solar heat is absorbed during the day and radiated overnight as infrared radiation [245,246]. Higher urban temperatures increase the power demand for Heating Ventilation Air Conditioning (HVAC) systems, which leads to a drop in building energy efficiency by approximately 25% [247,248]. As a direct consequence, urban centres increasingly use significant power to heat and cool buildings, with global energy consumption estimates for cooling as

high as 20% [249,250]. To this end, urban greening strategies have raised significant interest at both the academic and urban policy level [245], with urban green roofs presenting a unique opportunity to increase urban green spaces without losing valuable land space.

Green roofs are often classified into two major groups depending on their characteristics: intensive and extensive. Intensive green roofs often have deep substrate depths (> 300 mm) [75] and facilitate large plantings, often being used to create rooftop gardens for human occupation [251]. This leads to requirements for high load-bearing structures and frequent maintenance [252]. Extensive green roofs have shallower substrate depths (< 300 mm) and often utilise grasses and shrubs, and are primarily constructed for environmental benefits [253], with lower maintenance costs than intensive green roofs. Due to the differences in construction costs and maintenance, extensive green roofs are significantly more common in urban spaces than intensive green roofs [52]. Both roof types serve to insulate buildings from solar radiation, leading to a reduction in energy costs [254,255]. In a study conducted by Ascione et al. [256], building energy use amongst five green roof typologies were compared to conventional roofing technology and "cool-painted" roofs across several European climates. This study demonstrated that green roofs could provide a 0 – 11% reduction in energy demand in warm climates, and -1 – 7% reduction in cold climates, with variances owing to differences in solar reflectance amongst locations.

While there are many factors that influence the performance and longevity of green roofs, climate and roof design are of utmost importance. A study conducted by Koroxenidis and Theodosiou [257] evaluated the life cycle impacts of three green roof designs. In their study it was concluded that extensive green roofs would be preferable in warm climates due to the associated economic costs. For colder climates, the selection of green roof type is especially important due to energy consumption costs. A study conducted by Jim and Tsang [252] found that in subtropical climates, the winter energy consumption of the built environment could potentially increase with the introduction of intensive green roofs, as they can create a temperature gradient, effectively drawing heat out of the building through the roof surface due to the upward heat flow demand of the substrate [252]. Additionally, design is an essential aspect of green roof installations. Commercial suppliers must consider a range of environmental factors to facilitate optimal plant species selection. Ideally, a green roof in warmer climates should aim to facilitate a high density of foliage (LAI; leaf area index), while maintaining ease of access and maintenance. Generally, a high LAI serves to increase the evapotranspiration rate of a green roof, and therefore promotes greater cooling potential. However, LAI is often subverted by designers and implementers in favour of plant survivability, ease of maintenance, and pollinator biodiversity to appease stakeholders [56,258].

An additional factor that is often overlooked is the potential to integrate solar systems with green roofs. A study conducted by Zheng and Weng [66] utilised computational models to predict the energy consumption of various commercial properties under climate change scenarios. This study identified considerable net energy use reductions achievable with the inclusion of solar green roofs. They reported reductions in net solar green roof building energy demands of more than 20%, for 11 of the 13 commercial properties modelled in the Los Angeles County, USA [66] .

In addition to roof design, substrate depth, plant selection, and the addition of photovoltaic (PV) panels are all factors that contribute to the thermal regulation of urban rooftops [20]. However, it is difficult to directly and accurately quantify these effects relative to conventional building technologies. Such tests require urban spaces where comparisons between green and conventional roofs can be made without spatial and temporal confounding. To this end, many studies have divided a single roof into multiple sections representing different roofing scenarios [68,259,260], leading to potential problems with sample non-independence (one roof type affecting the other). In the current study, we explore the thermal regulation potential of an extensive green roof in Sydney, Australia with comparisons made against a proximal conventional roof of identical size, construction material and age. Here we aim to quantify the thermal buffer potential of urban green infrastructure in Sydney to reduce the thermal load on buildings and to control the rooftop microclimate.

2. Methodology

2.1 Site Description

This study was conducted on two adjacent roofs atop recently constructed buildings in Barangaroo, Sydney, Australia (33.8643°S, 151.2028°E). Barangaroo is located on the north-western edge of the Sydney Central Business District (CBD), bounded by Sydney Harbour to the west, Barangaroo Central and Headland Park to the north, the Sydney Harbour Bridge approach and northern CBD to the east, and a range of new developments dominated by large CBD commercial tenants to the south (Supplementary Figure 5). Sydney, Australia has a Cfa climate based on the Köppen-Geiger climate classification [261], characterised by warm summers and cool winters [262], receiving 1309 mm of rainfall annually. January is the warmest month, with an average daily air temperature of 23.25 ± 5.19 °C (Mean ± SD). During the study period, the highest recorded temperature was 45.8 °C, and site temperatures exceeded 30 °C on 19 days, with sun hours ranging from 5.21 – 8.95 and evaporation rates of 4.51 to 8.88 mm per day. The study commenced in Spring, 2020 and concluded in Autumn, 2021, with an 8-month / 218-day observational period.

The study utilised the unique opportunity to monitor two buildings of similar age and construction material, one equipped with a green roof, and the other without. The two buildings assessed were the Daramu House (green roof, constructed in 2019) and International House (conventional roof, 2016). Both buildings had similar HVAC/air handling units (AHU) and near-identical rooftop infrastructure, with minor differences associated with building maintenance unit (BMU) design. Daramu House featured a green roof with an integrated, north facing solar array, whereas International House featured an East/West facing solar array (Figure 13).

The construction of the green roof on Daramu House was completed in September 2019 by Junglefy P/L (Australia), during the onset of the spring season. Both the green and conventional roofs are 1,863.35 m^2, with 593.96 m^2 and 567.44 m^2 of PV panel coverage, respectively. The roofs on both buildings featured a 0.8 m thick grey concrete slab as the foundation. The green roof hosted a planted area of 1,460.7 m^2 (78.4% of total roof space) incorporating a selection of native grasses and herbaceous plants chosen to attract a diverse faunal community to the roof. PV panels covered 40.66% of the planted spaces atop the green roof with an average panel height of ~ 1m from substrate. The green roof was host to approximately 15,000 native grasses and herbaceous plants, with an estimated LAI of 4.35 (m^2/m^2) (please see Wooster et al. [28] for detailed information on plant species and succession). This LAI is considered high by most thermal modelling standards [66,263,264], and has been previously reported to reduce heat flow by up to 3 W/m^2 under experimental conditions when compared to a bare roof [265]. A high LAI increases the roof's insulative and cooling potential through greater evapotranspiration [137], which is an extremely desirable trait for Australian urban centres.

The green roof was extensive by design, with a substrate depth of 100-150 mm, and an integrated sub-surface irrigation system. The green roof studied here falls under the R6-L green infrastructure typology proposed by Koc et al. [266] with the following substrate characteristics: Air-Filled porosity: 19%; Water-holding capacity: 47.9%; Saturated repacked density: 1.15 kg/L; Particle size: 48.6% w/w < 2 mm, 48.4% w/w 2 – 10 mm, 2.9% w/w 10 – 20 mm; Permeability: 3769 mm/h; Wettability: AS4419 – 0.03 minutes; and AS4419 Category 1 Dispersibility in water. The roof utilised a sub-surface irrigation system with a variable watering schedule between 3:30 am and 7:30 am. Watering frequency and volume varied with season, with irrigation occurring every second day apart from summer, where watering was conducted each business day. The irrigation system was divided into 10 zones, where each zone received an average 331.6 L of water for each watering cycle, with a water consumption range of 124.92 – 382.33 L per zone. Further, the irrigation system allowed for predictive watering adjustments, where temperature and weather limits can be set to reduce watering frequency and volume.

Unplanted areas on the roof were occupied by rooftop infrastructure or BMU rails, both of which were not included in the temperature analysis on either building. In respect to environmental exposure, both the green and conventional roofs are north facing (Supplementary Figure 5), with approximately equal yearly solar irradiance. Differences in solar irradiance (6% greater on the green roof) are primarily attributed to reflection off surrounding urban geometries. Despite this, the influence of urban geometries on the measurements taken here were eliminated from the surface temperature assessment by ensuring thermal images were captured during similar light hours and included in the subsequent analysis by using continuous monitoring.

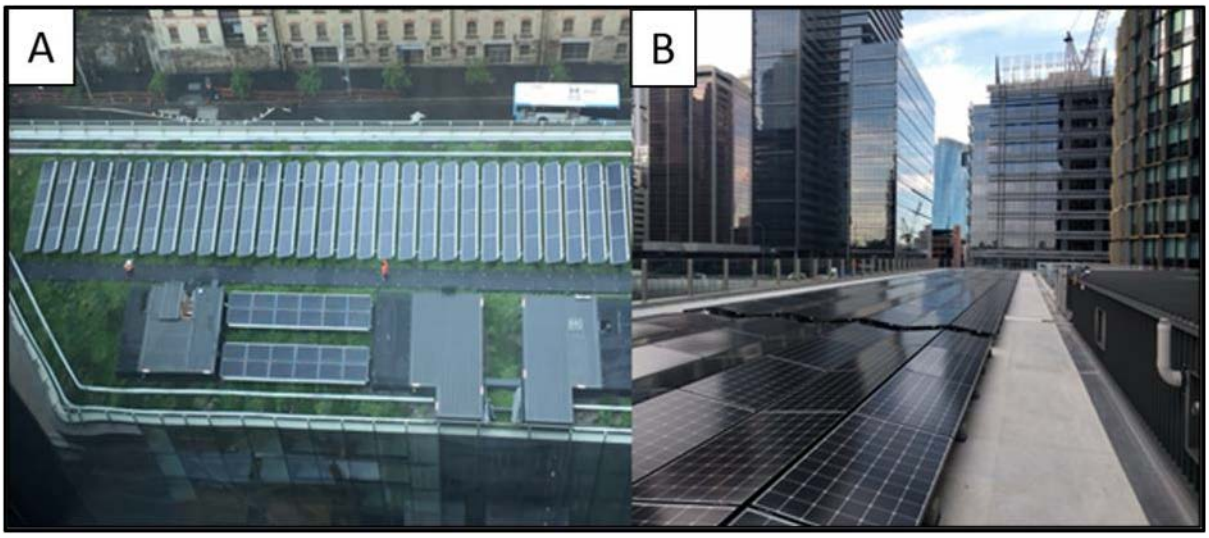

Figure 13. A) Daramu House green roof, top-down view; B) International House rooftop, south facing view.

2.2 Surface temperature

Thermography was utilised to monitor surface temperatures at several points on each roof. Thermal imagery cameras (TG267, FLIR, Australia) were employed to capture surface temperatures of the PV panels (emissivity adjustment 0.80), PV mounting frames (0.60), and rooftop surfaces (0.95 for plants and 0.80 for concrete) across both buildings using a six-point sampling regime. Point-transect sampling was employed along the length of each roof, with a minimum of six points across each transect sampled every two weeks. At each point along the transect, six images were captured; 1) Single PV module surface temperature; 2) plant foliage/ground immediately in front of the single module (Figure 14 C); 3) walkway immediately in front of plant foliage or ground; 4) horizontally across the face of multiple PV modules (Figure 14 A); 5) horizontally across the gap positioned between modules (Figure 14 B); and 6) on the plant foliage or ground immediately below the gap positioned between modules. Images were captured fortnightly at times within 60 minutes between buildings. Due to surrounding urban geometries, images were collected when light conditions were similar between points on the transect.

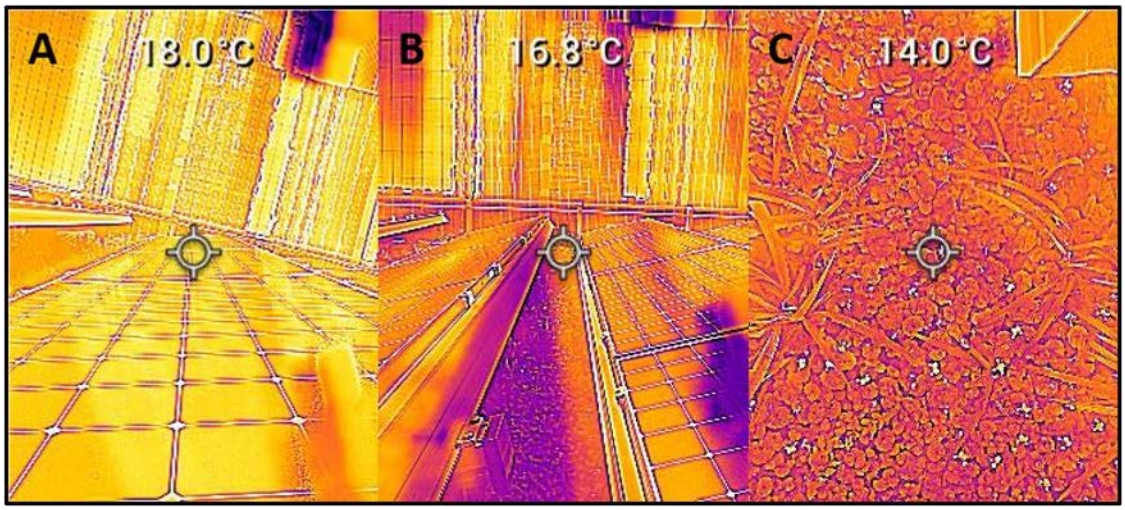

Figure 14. Examples of thermal imagery captured during a sample event. A) horizontal image across the face of multiple modules in direct sunlight; B) horizontal image across the gap positioned between modules; C) plant foliage.

PV panel azimuth differed between buildings, with the green roof utilising a predominantly (~ 75%) North-facing (0°) azimuth and the conventional roof utilising an accordion style East-West (90°/280°) azimuth. This PV panel layout was tailored by building engineers to the specific requirements of the green roof, being planting, maintenance and survival of plant foliage. Both solar irradiation modelling, and on-site observations (not shown here) determined that the global horizontal irradiance experienced on the green roof was only ~ 6% higher than the conventional roof due to the surrounding urban geometries. The effect of urban geometries influencing solar exposure were incorporated into the image sampling method to reduce the effect of panel azimuth and building position on surface temperature. Surface temperature differences were analysed statistically by permutational analysis of variance (PERMANOVA) to determine the significance of roof type, measurement location, and season. Data was unstandardised using a Euclidean distance matrix with 999 permutations. Pairwise PERMANOVA comparisons with a Bonferroni correction were performed separately for each season as its interaction with roof type was significant ($p = 0.001$).

Time and date matched ambient temperatures were calculated using data from the Bureau of Meteorology [267] to determine whether surface temperature differences between roof types were influenced by daily ambient temperatures. Pearson's correlations were performed between ambient temperatures and the difference (°C) between the thermography surface temperatures of the green and conventional roofs.

All analyses and associated graphics were performed using R version 4.1.1 [268] and the following packages: car [119], dplyr [269], ggplot2 [270], pairwiseAdonis [271], tidyr [272], vegan [273] and xlsx [124].

2.3 Rooftop microclimate

Between August 2020 and June 2021, 12 temperature loggers (i-Button model DS1921G, Thermochron, USA) recorded the ambient temperature in 15-minute intervals. i-Buttons have an accuracy of ±1°C between -30°C and 70°C ambient temperature, and measure in 0.5°C increments. i-Buttons were positioned in a vertical alignment to determine the thermal gradient across the roof layers (Figure 15) and were replaced fortnightly (1,334 observations) for continuous monitoring throughout the duration of the experiment. On each roof, sensors were deployed above the PVs (Figure 15; orange arrows), attached to the mounting frames and exposed to direct sunlight to record the ambient unshaded temperatures. Sensors were also deployed below the PVs (Figure 15; blue arrows) to record the ambient shaded temperatures, ~ 100 mm below the underside of the PV panel. Finally, sensors were deployed either beneath the plant substrate (~ 50 mm), or on the concrete floor of the conventional rooftop (Figure 15; white arrows – "substrate/ground"), in complete shade, well out of any sunlight. Sensors were deployed within the substrate layer without being buried to determine the insulative effect of the substrate at half-depth, away from any sub-surface irrigation and largely unshaded by plant foliage (estimated LAI of buried sensor area was < 2). A study conducted by Jim and Tsang [252] examined the diurnal soil temperature change at varying substrate depths, and found it varied by only ~ 0.5 °C between 0 and 900 mm of soil. To facilitate ease of access to the sensor network, a substrate depth of 50 mm (half-substrate depth at that location) was chosen.

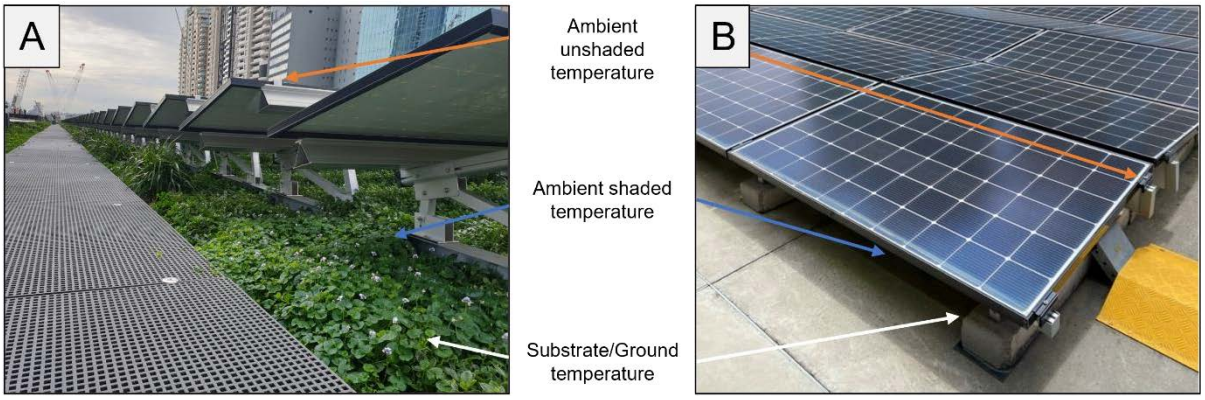

Figure 15. Thermal sensor vertical gradient design. A) Daramu House green roof; B) International House rooftop. On each roof, sensors were deployed above the panels, attached to the mounting frames, and exposed to direct sunlight to record ambient unshaded temperature (orange arrows). Sensors were also deployed below the panels in full shade to record shaded ambient temperature at approximately equal distances from the plant foliage/roof surface (blue arrows). Sensors were also deployed either ~ 50 mm within the growth substrate, or on the ground below the solar panels to determine surface temperatures in complete shade on the rooftop substrate/ground (white arrows).

Daily averages of i-Button temperature data were compiled for subsequent analysis and assessed by PERMANOVA to determine differences associated with the effects of roof type, sensor location, and season. PERMANOVA was run unstandardised based on a Euclidean distance matrix with 999 permutations. Significant effects were investigated by further pairwise PERMANOVA comparisons with a Bonferroni correction. These were performed separately for each sensor location as its interaction with roof type was significant (p = 0.001).

To describe daily variations in sensor temperature, smooth lines were fitted using a generalised additive model (GAM) with cubic splines to each unique combination of roof type x sensor location x season. Splines were used as they reproduced the mean temperature profile very well (Supplementary Figure 6). This was done to aid in visual assessments of whether the differences detected between roof types were distributed equally across a 24-hour period, or whether this was more pronounced at different times of day (particularly in the presence of many data points; $n_{observations}$ = 101,310).

2.4 Heat flow

Most previous studies describing the thermal performance of green roofs have been conducted on small scales or simple model systems that can be easily modified to accommodate various thermal sensors. In this study we present a unique analysis of a recently constructed commercial green roof in Sydney, Australia with a near-identical control roof that presents little spatial confounding. This study was conducted over an 8-month period, with continuous thermal monitoring for heat flow calculations.

To estimate heat flow, calculations utilised the average of the known thermal resistance values for similar plants (Table 3), relative to their abundance on the roof (described previously; see Wooster et al. [28]) as well as *in-situ* time series thermal monitoring data for each roof (T1-T3 below; Figure 15). Theoretical heat flow for each roof was then calculated using the following equation:

$$q = \frac{(T_1 - T_3)}{R_{plant} + R_{substrate}} = \frac{(T_1 - T_2)}{R_{plant}} + \frac{(T_2 - T_3)}{R_{substrate}}$$

Where:

- ***q*** = Heat Flow (W m^{-2})
- ***T1*** = Ambient unshaded temperature
- ***T2*** = Ambient shaded temperature
- ***T3*** = Rooftop surface temperature
- R_{plant} = Thermal resistance of plants
- $R_{substrate}$ = Thermal resistance of substrate

*Table 3. Existing literature relating to the thermal conductivity (λ) and resistance of plant species (Rc) used in the construction of the green roof. Study indicated by * represents the thickness (d), conductivity (λ) and resistance (Rc) of the concrete roofing specific to this study.*

Study	Layers of Green roof	Thickness *d* (m)	Thermal Conductivity λ [W K^{-1} m^{-2}]	Thermal Resistance Rc=d/λ
	Vegetation Layer:	0.1-0.15		
[274]	*Viola hederacea*		1.67	0.09
[275]	*Dichondra repens*		0.5	0.3
[276]	*Crassula multicava*		0.12	1.3
	Aptenia cordifolia		0.05	3.2
	Dianella caerulea		0.14	1.1
	Goodenia ovata		0.56	0.27
	Poa poiformis 'kingsdale'		0.56	0.27
	Themeda australia 'Mingo'		0.56	0.27
[277]	*Myoporum parvifolium*		0.12	1.3
	Brachyscome multifida		0.14	1.1
	Gazania tomentosa		0.14	1.1
[278]	*Carpobrotus glaucescens*		0.79	0.19
[279]	Substrate (Slighted compacted clay loam)	0.1-0.3	0.35 – 0.69	0.29 – 0.57 (*d*=0.2 m)
*	Concrete	0.8	0.14	5.71

3. Results and Discussion

3.1 Surface temperature assessment

One aspect of green roofs that promote thermal efficiencies in urban buildings is their ability to reduce the effect of solar radiation from heating interior spaces [255]. The use of rooftop gardens to lower surface temperatures has been shown to be effective by almost 30 °C [280]. In this study, we monitored the surface temperatures of both the roof areas covered by plant foliage and the PV panels. Each image captured on the green roof was mirrored on the conventional roof within 60 minutes under similar lighting conditions between buildings.

Surface temperatures between buildings were similar during Spring ($p = 0.302$), however in both Summer and Autumn there were significant differences in both panel and roof surface temperatures ($p = 0.001$ in both cases; Figure 16). During the Summer months, average surface temperatures of both solar panels and roof surfaces were 9.63 and 6.93 °C cooler on the green roof building compared to the conventional roof (Supplementary Table 7). For the Autumn months, these average temperature differences were 7.4 and 4.59 °C for solar panels and roof surfaces, respectively. The maximum observed temperature difference between the two roofs for both solar panel and roof surface reached 16.4 and 17 °C in Summer and 2.2 and 7.6 °C in Autumn (Supplementary Table 7). As

expected, there were significant, moderately strong positive correlations between ambient temperatures and the difference in building temperatures in Summer and Autumn (r = 0.59 and 0.67, respectively), which indicates that green roofs perform better in coastal Australian climates at higher ambient temperatures (up to 29 °C).

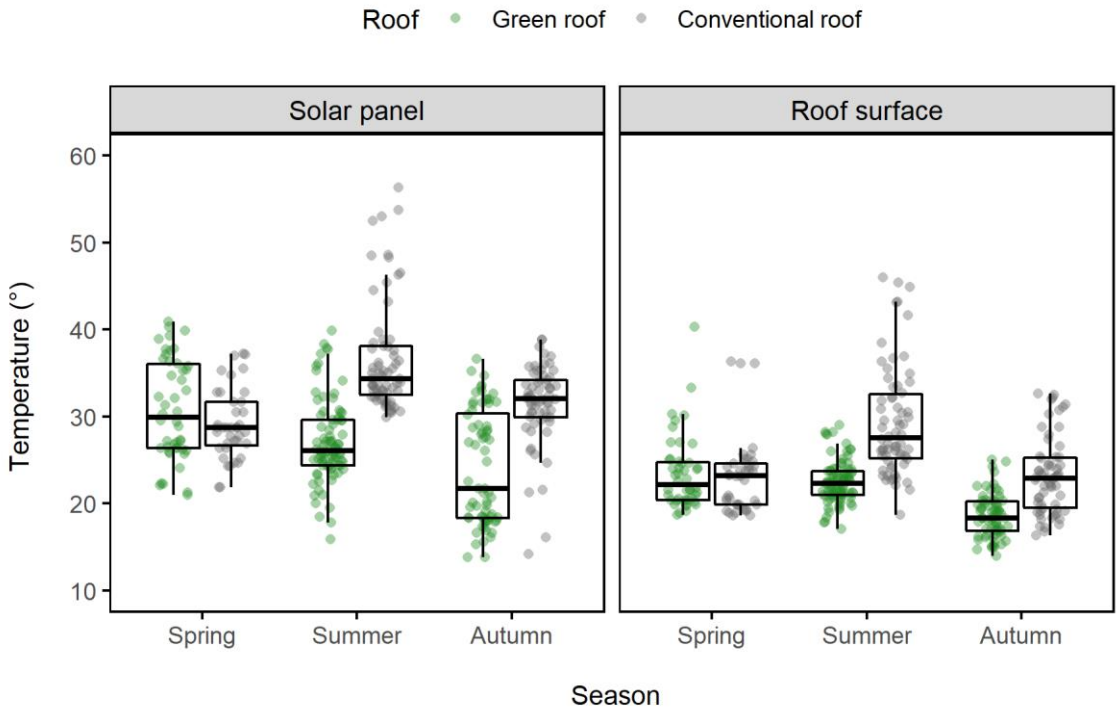

Figure 16. Thermographic surface temperatures recorded on each roof for the PV panels and roof surfaces (plant foliage or concrete) by season (n ≥ 36). Green points = green roof; grey points = conventional roof.

A study conducted by Smalls-Mantey and Montalto [70] on a ~ 27,500 m2 extensive green roof in New York City reported a maximum surface temperature reduction of 18.4 °C. In the current study we observed a maximum daytime surface temperature difference of 16.4 and 17 °C for the roof surface and solar panels respectively. The considerable differences in climate between the sample site of Smalls-Mantey and Montalto [70] and the current work likely led to this difference. Studies conducted by Polo-Labarrios et al. [241] and Ouldboukhitine et al. [63], aimed to assess the surface temperature reduction of a green roof compared to a reference building. Both studies determined that surface temperature was influenced by time of day at equivalent time periods to what is presented here. It is possible that the surface temperature differences observed in this study would exceed those recorded if thermography assessments could have extended to monitor a wider range of seasonal effects. These findings are of substantial significance for urban environments, as the current urban environment is frequently overheated, an effect at least partly attributable to a lack of vegetated space [222].

Reflectance and absorption of solar irradiation by plant surfaces, as well as the evapotranspiration cooling effect, both serve to create a cooler, more resilient climate for increased thermal comfort [242].

3.2 Rooftop microclimate

The i-Button temperatures were used to calculate heat flow (q) and to determine the green roof's influence on the seasonal rooftop microclimate. Daily average temperatures differed significantly between roof types, sensor locations and seasons ($p = 0.001$ in all cases; Figure 17). Ambient unshaded air temperatures did not differ significantly between buildings ($p = 0.382$), indicating that differences in rooftop design, urban geometry, and solar irradiation/reflectance had little effect on these measurements. However, ambient shaded and roof surface temperatures differed significantly between buildings, where average daily green roof temperatures were between 0.42 and 3.1 °C cooler than on the conventional roof, depending on season ($p = 0.001$ in both cases; Supplementary Table 8).

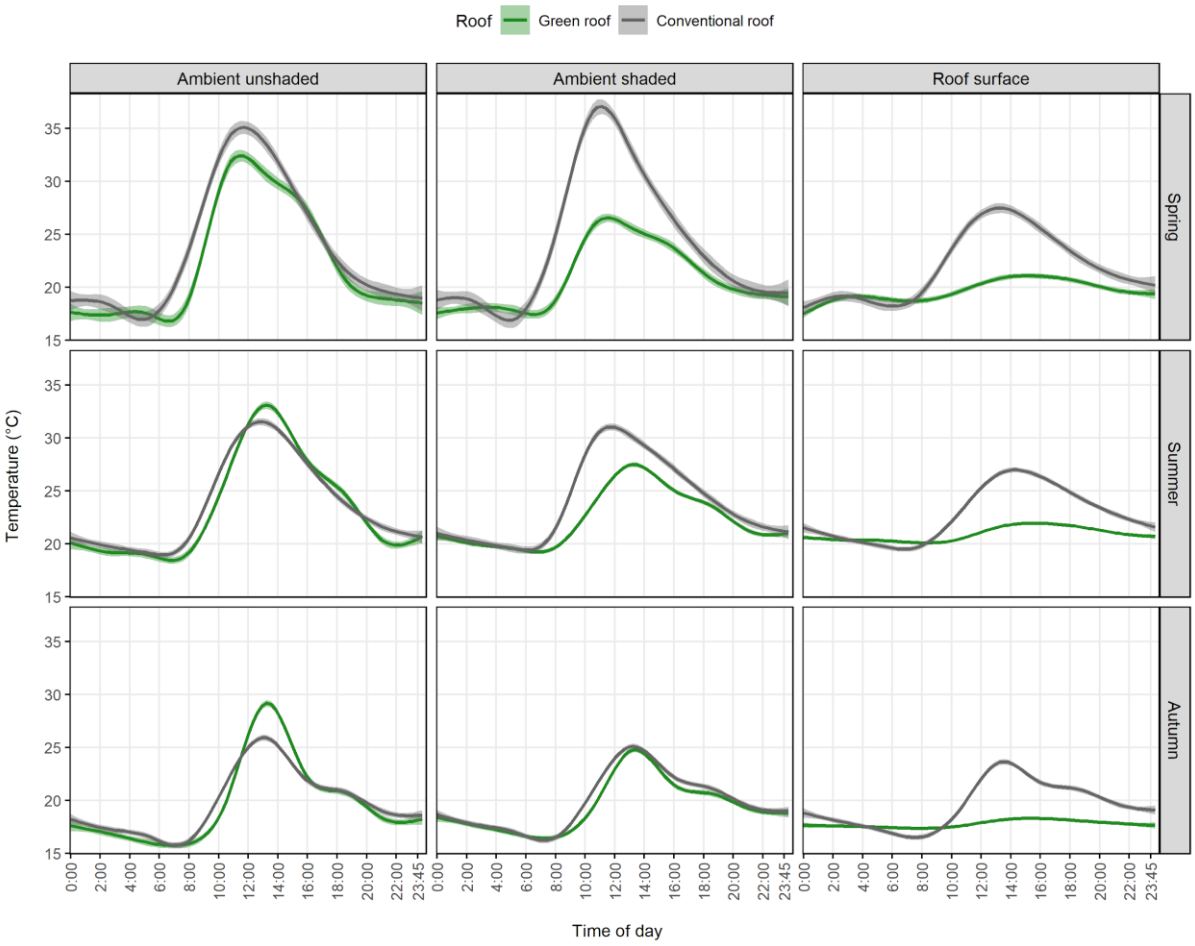

Figure 17. Average daily thermal sensor profiles for the green and conventional roofs, at each location and seasonal period. Curves show fitted generalised additive models (GAMs) with cubic splines, where the lines represent average temperature and shaded areas reflect 95% confidence intervals for the mean. Green lines = green roof; grey lines = conventional roof.

The capacity of the green roof to influence the rooftop microclimate is highlighted by the thermal stability observed relative to the conventional roof for ambient shaded and roof surface temperatures (Figure 17). The ambient shaded temperatures experienced on the conventional roof ranged between 25 °C in Autumn to 33 °C in Spring. During the same time, the green roof experienced an almost constant average peak temperature of 25 °C. These results demonstrate a substantial improvement in thermal stability attributable to the green roof and could contribute to an increase in solar panel performance due to reduced ambient temperature. Differences in the magnitude of temperatures experienced for both green and conventional roof surfaces was significant ($p = 0.001$), with the green roof experiencing an average reduction in peak temperatures in Spring and Summer by ~ 6 °C and ~ 7 °C in Autumn (Figure 17).

The green roof's capacity to regulate the thermal microclimate was further emphasised by the degree in which the roof reduced diurnal temperature fluctuations. Average day and night temperatures were compared between seasons (Table 4). The range of ambient unshaded temperatures experienced on both roofs remained consistent throughout the study, likely due to the similarities in light exposure owed to their similar urban geometries. However, for the ambient unshaded and roof surface temperatures, the green roof was consistently more stable than the conventional roof. For example, the range of temperature on the green roof was 4.05 °C and 0.88 °C for ambient shaded and roof surface locations respectively, which was 55.54 and 78% less variable than the conventional roof (Table 4).

These findings are similar to those previously reported by Eksi et al. [281], who performed a small-scale trial to compare the difference in thermal regulation between green roofs containing Sedum, a low leaf area succulent plant, and a herbaceous green roof. Eksi et al [281] reported an increase in thermal stability on the herbaceous green roof of ~ 11 °C. Differences in thermal stability between the two roof types were credited to an increase in LAI and substrate depth. While Eksi et al. [281] did not include a control, a clear relationship between the density of vegetation and a reduced thermal load of vegetative spaces was identified. It has been suggested that the lack of vegetative spaces and their evapotranspiration potential in Australian city centres may be contributing to urban overheating [282]. It is likely that the differences in rooftop microclimate observed here are due to differences in emissivity and evapotranspiration, where plant foliage often has an observable emissivity of 0.98 [283], and consequently the ability to regulate the microclimate through water transport and evaporative

cooling. Contrastingly, concrete has an emissivity of 0.88 [284], which is likely to retain and re-emit solar heat throughout the day and thus contribute to the urban heat island (UHI) effect [246].

The UHI effect has often been associated with the loss of vegetation in urban spaces, however it is also a product of an increase in heat-absorbing surfaces, inadequate shading, and an increase in heat waste from air-conditioning systems [48]. These factors create a feedback loop, whereby temperatures in urban spaces that are lacking in vegetation rise, and urban dwellers are forced to seek refuge in air-conditioned buildings, which further promotes energy use, and ambient heating. To this end, there is a significant potential for green roofs to reduce the UHI effect of city spaces and increase thermal comfort. This could be achieved by retrofitting under-utilised heat-absorbing areas with functional green spaces [48], thereby mitigating thermal penetration into the building envelope [252] and reducing a proportion of dweller dependency on air-conditioning [66,242].

Table 4. Average diurnal temperatures (°C) and their ranges for each roof, by season.

	Green Roof			Conventional Roof		
	Ambient unshaded	Ambient shaded	Roof surface	Ambient unshaded	Ambient shaded	Roof surface
			Spring			
Day	25.26	22.55	19.99	27.29	27.80	23.63
Night	17.96	18.50	19.11	18.46	18.69	19.63
Range	7.30	4.05	0.88	8.83	9.11	4.00
			Summer			
Day	26.01	23.80	21.14	26.15	26.35	24.05
Night	19.57	20.26	20.54	20.12	20.55	20.95
Range	6.44	3.54	0.60	6.03	5.80	3.10
			Autumn			
Day	22.42	21.09	17.97	21.99	21.79	20.89
Night	17.13	17.91	17.60	17.63	18.06	18.26
Range	5.29	3.18	0.37	4.36	3.73	2.63

Interestingly, the green roof did not demonstrate the same performance in Autumn as it had in the preceding months, with differences between shaded regions on the two roofs being as low as 14.75%. Despite this, the green roof maintained a measurable effect in influencing the rooftop microclimate, even in the cooler months.

3.3 Heat flow

Green roofs are able to reduce the heat flow through the building envelope due to the insulative effect of the growth substrate, plant foliage barrier, and transpiration cooling effect [1,61,285–287].

Due to their ability to reduce heat transport both into and out of buildings, there is the potential for a reduction in building energy consumption for heating and cooling [288]. In a study conducted by Sailor [289], a building energy simulation model predicted the energy savings of a building with a 2000 m2 green roof to be 27.2 to 30.7 GJ/y of electricity and 9.5 to 38.6G J/y of natural gas. It has been estimated that an overall 25% energy saving could be achieved with the large-scale implementation of green roofs in urban spaces due to a reduction in the UHI effect [288–291].

In this study, we compared the thermal performance of similar green and conventional roofs over 218 days. Seasonal heat flow values (q) were calculated (Table 5) across the observed thermal gradients, where positive and negative q values represent heat moving across the rooftop layers and entering or leaving the building envelope, respectively. During the warmer months, the green roof demonstrated an average reduction in the daytime heat flow by 13.37 W/m2 (57%) in Spring and 5.37 W/m2 (39%) in Summer (Table 5), with the largest reductions in heat flow observed in the hot months of November and December (Supplementary Table 9). During the cooler months of Autumn, the green roof had little effect on reducing the average daily heat flow (0.08 W/m2; 2%), possibly due to increased rainfall (average 6.34 mm per day; 48.57 and 40.61% more than Spring and Summer, respectively). Rainfall can have a significant impact on heat flow in urban infrastructure [292]. During the 8-month monitoring period, the average monthly rainfall was 126 mm, where seasonal averages from 2020 to 2021 are 88.7, 112.47 and 166.47 mm for Spring, Summer, and Autumn, respectively.

During the warmer months, the green roof was able to reduce the maximum heat flow through the roof surface by up to 100.9 W/m2, while preventing up to 83.37 W/m2 from exiting the building overnight (Table 5). The results presented here are similar to those previously modelled by Olivieri et al. [293], where an extensive green roof in a Mediterranean coastal city was predicted to reduce Summer heat flow by up to 60% compared to a bare roof. An experimental study conducted by Fioretti et al. [230] assessed the peak solar radiation reduction observed on a single day for an extensive green roof compared to a reference roof, and found an average reduction in solar radiation (W/m2) by 62.55%. An extensive long term monitoring program was established by Spolek [57] in which three small green roofs were assessed for their stormwater and thermal buffering potential. The three green roofs were monitored for ~ 3 years and compared to a control site which was situated within the green roofs. Spolek [57] determined the roofs were able to reduce the heat flow by up to 72% in the prevailing mild and dry Summers.

While these studies detected or modelled slightly greater heat flow effects than the observations made here, this study presents the first long-term continuous green roof monitoring performed in Australia, where an almost identical control building was utilised to eliminate any confounding spatial variables. Differences in climate and LAI of the buildings tested would certainly contribute to the

thermal performance of green roofs, as well as the water loading capacity of individual systems, in addition to the experimental differences amongst studies. For instance, a study conducted by Bevilacqua et al. [294] in Italy aimed to determine the thermal effects of experimental green roof designs (50 m2) where three designs were employed and compared to a reference site. This included two experimental green roof plots with an LAI of 1.5, and a third plot that was unplanted. In substitution of flowering plant species, the third plot was equipped with an additional insulation layer (30 mm) under the water storage layer. The first two plots reduced the average summer-time surface temperatures by 12 °C compared to the control plot. In comparison, the unplanted plot with additional insulation was only able to reduce average summer-time surface temperatures by 4 °C. Differences in thermal performance between plot designs are likely due to differences in evapotranspiration driven by the vegetation on plots 1 and 2. In our study, we observed an average summer-time temperature difference of up to 8 °C, which is substantially lower than Bevilacqua et al.'s observations [294]. This is likely due to differences in observational data collection, where in Bevilacqua et al.'s study [294] described the temperature reduction of a 7-day period with clear skies, high external air temperatures, and an absence of precipitation, whereas our analysis utilised the entire seasonal period of 89 days. It is therefore plausible that the differences observed between these two studies could be attributed to the inclusion of non-clear sky days in the current work, and that the seasonal performance of an Australian green roof (8 °C) could be comparable to the established and well documented green infrastructure in the Mediterranean. The difference in LAI between these two studies suggests that the green roof observed here would have a greater potential for evapotranspiration, and therefore cooling. The significance of substrate water content on evapotranspiration, and therefore the thermal buffer potential of extensive green roofs, is discussed in a study conducted by He et al. [49]. As the heat barrier performance of green roofs is affected by the moisture content of the substrate layer, differences in green roof performance could be directly related to the volume and supply of irrigation [295,296]. It is therefore plausible that current green roofs could integrate optimised irrigation to increase their thermal buffer potential in areas that are not water-limited [297].

Table 5. Seasonal heat flow (q (W/m2)) calculated using thermal resistance values from the literature (Table 1) and in-situ temperatures recorded on each roof over the 8-month monitoring period.

	Green Roof	Conventional Roof
	Spring	
Max	73.10	174.00
Min	-27.59	-32.43
Average	4.93	10.98
Avg Day	10.22	23.59
Avg Night	-2.02	-5.58
	Summer	
Max	78.36	149.21
Min	-10.70	-94.07
Average	3.77	6.77
Avg Day	8.41	13.78
Avg Night	-2.52	-2.69
	Autumn	
Max	57.13	53.07
Min	-7.55	-28.07
Average	1.17	1.81
Avg Day	5.29	5.37
Avg Night	-2.73	-1.56

While the reduction in thermal penetration presented here was significant, there is also the potential for an urban green roof to prevent heat from leaving the building envelope during cool periods, or overnight. During the study, the green roof's average nightly heat flow was higher in Spring (3.56 W/m^2) and lower in Autumn (-1.17 W/m^2), with little difference observed during Summer (0.17 W/m^2) when compared to the conventional roof. However, the minimum heat flow observed on the green roof was consistently higher than that of the conventional roof (differences of -4.84, -83.37 and -20.52 W/m^2 in Spring, Summer and Autumn respectively: Table 5). This suggests that the green roof has some effect on reducing the rate by which heat is able to leave the building envelope [255].

These results demonstrate the potential impact of urban green roofs on regulating building temperature for both heating and cooling in the Australian climate. A comprehensive environmental and economic assessment of green roofs conducted by Koroxenidis and Theodosiou [257] determined that green roofs can contribute a reduction between 8 – 31% of lifecycle energy consumption for

buildings when compared to conventional roofing. It has been further estimated that the HVAC energy consumption of dense urban centres could be reduced by as much as 25%, if only 10% of urban spaces would adopt green roofs or equivalent green infrastructure such as green walls [288–290]. The volume of international green roof research on thermal performances is substantial, however there is a distinct lack of green roof research from Australia where we have a unique climate. Further research should be conducted on Australian green roof design for optimising performance under Australian climate conditions.

3.4 Considerations

In this study we aimed to quantify the thermal buffer potential of a common form of urban green infrastructure in Sydney and assess its influence on the rooftop microclimate. In doing so, we were presented with the unique opportunity to study two near-identical buildings which allowed for building-scale comparisons to be made with little spatial confounding or sample non-independence. However, we did not have the opportunity to install extensive sensor networks such as those used in some previous research. As such, thermal sensors could not be deployed at the full range of depths of the green roof layers. As the two buildings were commercial properties, there were also limitations associated with access timing, building regulations and lightning risk and the inability to install sensor networks within leased interior spaces. Therefore, heat flow calculations can only be made about the thermal penetration of solar radiation across the roof surfaces, and estimates provided for penetration into the building envelope. Any assessment of energy savings associated with these values would be speculative and were therefore avoided.

While the two buildings were of near-identical construction, there were distinct differences in BMU layout, which influenced PV panel arrangement on both roofs. Due to the size of the commercial properties, proximal buildings lead to slight differences in urban geometries affecting the sun pathing, and therefore exposing the roof tops to slightly different solar regimes. While this was found to be non-significant for the ambient unshaded thermal assessments, it must be noted that *in-situ* observations will likely never be able to fully eliminate this effect. Possibly the largest influencing factor that could not be quantified was PV panel layout and orientation. Solar panel azimuth and tilt angle varied between the two roofs, which would affect convection both above and below the panel surfaces. This meant that the affect of evapotranspiration cooling could not be separated from the effect of differential airflow below panels and was therefore treated as a combined affect of the green roof. It should be noted, while differences in panel configuration serve to play an important role in airflow movement across roof spaces, each rooftop was bordered by a 1.3 m tall glass railing, and the

specifications for the green roof panel layout were directly related to considerations for planting. It could be assumed that without the green roof installation, the rooftop on Daramu House (green roof) would have had near-identical panel layout to International House (conventional roof). Nonetheless, the current work provides clear evidence that commercial green roofs can affect the rooftop microclimate compared to conventional roofing in most seasons in the Sydney climate, as well as impact the measurable heat flow across rooftops.

4. Conclusions

Here we present the longest duration Australian green roof study focussing on thermal performance to date. Rooftop surface temperatures were reduced by up to 17 and 20 °C as observed with thermography and temperature sensors, respectively. These findings align with those previously reported, suggesting that Australian green roofs may reduce building heating during Summer and especially severe heatwave conditions. Rooftop microclimate was significantly impacted by the green roof, where ambient shaded temperatures were up to 56% cooler than the conventional roof, likely due to the evapotranspiration of the plant foliage and additional airflow provided by the height and orientation of the PV panels. Calculated heat flow values for each season demonstrate a significant reduction in the thermal energy able to enter or exit the building envelope. The green roof was able to mitigate up to 13.37 W/m^2 more heat from entering the building envelope during Spring than the conventional roof, as well as reducing the heat flow leaving the building by 20.52 W/m^2 during Autumn. These results highlight the potential for energy savings in commercial Australian properties that rely heavily on-air conditioning for cooling during the hotter months and heating during Winter. Future studies should aim to assess the thermal performance of Australian green roofs during the Winter months as this was unachievable here, as well as establishing a robust sensor network prior to green roof installation for ongoing and representative analysis of thermal penetration into the indoor environment.

Preface: Chapter 5

Green roofs provide a range of benefits to the buildings on which they're installed, however the ecosystem services provided by green roofs can potentially extend further than building users. Due to the provision of absorbent substrate and consequent water retention potential of green roofs, a reduction in stormwater flow rates on green roofs compared to conventionally bare surfaces could reduce the city-wide burden of flash flood management. Additionally, green roofs may serve as a detention and remediation basin for sedimented, aerosol trace metals that would otherwise be washed into the basement wastewater management system of city stormwater network.

In this study we aimed to assess the stormwater mitigation potential and quantify the trace metal accumulation and retention capabilities of an extensive green roof in urban Sydney, Australia, in direct comparison to a proximal, conventional rooftop. This work demonstrated a significant reduction in stormwater flow rates into the management network from the green roof, which suggests that mass implementation city-wide *could* serve to reduce the burden on the stormwater management network and reduce the impact and severity of minor-moderate flash flooding in the Sydney CBD, as is common during heavy rain periods. This project was run in collaboration with UTS, Lend Lease, Junglefy and the City of Sydney to generate quantitative data to support the City of Sydney 2030 Greening Guide, funded under a City of Sydney Environmental Performance - Innovation Grant 2019-20.

The following chapter is comprised of text from a peer-reviewed publication.

Chapter 5: The hydrological performance of a green roof in Sydney, Australia: a tale of two towers

Fleck. R [1*], Westerhausen. M.T [2], Killingsworth. N [3], Ball. J [4], Torpy. F.R. [1], Irga. P.J. [4]

[1] Plants and Environmental Quality Research Group, School of Life Sciences, University of Technology Sydney
[2] School of Mathematical and Physical Sciences, University of Technology Sydney
[3] AECOM, Sydney NSW, 2000 Australia
[4] School of Civil and Environmental Engineering, University of Technology Sydney
[5] Plants and Environmental Quality Research Group, School of Civil and Environmental Engineering, University of Technology Sydney

**Corresponding Author: Robert.Fleck@uts.edu.au*

This article has been published in the Journal of Building and Environment (Q1, Impact factor 7.093 (2022)). Available online at https://doi.org/10.1016/j.buildenv.2022.109274. Published June 14th, 2022.

Abstract

This study describes the sister buildings Daramu house and International house in Barangaroo, Sydney (Australia's largest metropolitan city), with and without a green roof, respectively. Trace metal samples were collected from both roofs and analysed using ICP-MS to determine the bioretention potential of the green roof to remediate soluble and particulate stormwater trace metal contamination. Retention of ambient trace metal contamination by the green roof substrate was deemed significant for soluble copper and particulate zinc, chromium and copper. In addition, hydrological models (DRAINS and SWMM) were applied to predict the performance of the green roof to identify its ability to manage stormwater runoff and frequency, as well as to analyse the green roof's performance in complex surface flooding situations where storage or backwater effects occur in overflow routes and surface flows. Our results demonstrate a reduction in peak stormwater flow by 18.29 L/s (~50%) for storms as infrequent as 1 in 5 years, and peak flow reductions up to 90% storms of lower intensities. These results are significant as it demonstrates that a green roof could remediating trace metals contamination, thus reducing the impact on aquatic environments through stormwater runoff. It also highlights their potential to reduce stormwater flow, and utilise this additional water for evapotranspiration, leading to cooler ambient temperatures. Future works should aim to quantify the remediation effect of various planted species on *in-situ* green roofs, as well as determine the specific retention capabilities of various substrate compositions.

Keywords

Green roof, hydrological performance, low impact development, rainfall detention, sustainability, stormwater.

Highlights

- Green roof reduced substrate bound soluble copper
- Reduction in particulate bound zinc, chromium and copper

- Significant reduction of peak flow for severe storms up to 1 in 10 years

1. Introduction

In recent decades there has been a global population shift into highly urbanised areas [1,2]. As a result, many cities worldwide have experienced an increase in the conversion of permeable surfaces to impervious ones. This results in many hydrological issues including; increased flood risk, reduced infiltration, and altered environmental flows [299]. Therefore, solutions that can mitigate the hydrological risk posed by urbanisation are required [300]. In many urban spaces, stormwater drainage is largely achieved using an impervious infrastructure network such as concrete lined gutters, cast iron catchpits, pipe and manhole networks, and canalisation with creeks [301]. These networks inevitably lead to an increase in stormwater runoff volumes, flow and flood peaks downstream. One solution is the implementation of water-sensitive urban design (WSUD), otherwise known as low impact developments (LIDs) in the USA or sustainable urban drainage systems (SUDs) in the UK. These technologies are intended to achieve a 'natural' hydrology through various integrated control measures and site layout [302].

The US EPA describes several LIDs that are effective for the management of stormwater such as biofilter beds, rain gardens, tree filters and permeable pavement [303]. However, many of these solutions require the conversion or use of surface level spaces which may otherwise be occupied by alternative structures. As such, urban green infrastructure, specifically green roofs, have been proposed as an effective tool for managing increase runoff in urban catchments [304]. Green roofs can be installed on new or existing buildings, with relative ease and minimal structural impact [53]. Green roofs provide a myriad of benefits and ecosystem services [224], including the mitigation of air pollutants [47,225], reductions in urban noise [226–228], increases in urban biodiversity [28,39,229], enhanced indoor/outdoor thermal regulation [233–236,305], decreases in building energy consumption [20,306], and improved stormwater management and retention [24–27].

Green roofs typically consist of several layers with varying depths; the uppermost vegetation layer, underlaid by a substrate layer, a root barrier and a drainage/waterproofing layer [307]. These serve to manage the surface water holistically [308], in line with the ideals of sustainable development [52] where surface water can be stored and utilised by plants to reduce runoff and increase retention [72]. Urban stormwater trace metal contamination is often ubiquitous due to diffuse sources such as industrial activity, buildings, vehicular parts and emissions, fuel and oils, and metallic road structures [309–312]. In addition to their water management potential, green roofs are also capable of improving the quality of runoff through the filtration and retention of natural and anthropogenic atmospheric contaminants and leachable roofing materials [313] such as copper, zinc, lead, chromium and

cadmium [309,314–318]. Previous studies have identified green roofs as capable of reducing polycyclic aromatic hydrocarbons in runoff when compared to non-green roofs [319], however there have been some instances with green roofs contributing to the levels of heavy metal contaminants on roof surfaces [319].

Extensive green roofs, those with substrate depths less than 150 mm, have been modelled as an affective mechanism to reduce both building and city-wide stormwater runoff. A study conducted by Mentens et al. [231] predicted 54% and 2.7% reductions in building and city level stormwater runoff if 10% of buildings in Brussels utilised extensive green roofs [231]. However, the actual performance of green roofs varies greatly depending on various factors, including rainfall, green roof coverage, soil media, plant selection, preceding dry periods and roof slope [237,320,321]. Conn et al. [322] proposed that there was a correlation between soil thickness and water retention, and that this may change through time due to soil compaction. Meanwhile, the work of Villarreal and Bengtsson [323] highlighted the effects of roof slope and rainfall intensity on water retention, showing that steeper slopes and greater rainfall intensities both act to lower green roof retention performance.

Many numerical models have been used to further the understanding of the hydrological behaviour of green roofs under varying conditions [324–327]. Numerical modelling is a useful tool for the exploration of theoretical performance in a consistent and comparative manner by removing many of the uncertainties associated with dynamic input variables, thus eliminating the constraints brought on by study location variability [307]. However, even with identical model parameterisation, two numerical models can yield different performance results, leading to inconsistencies in the literature on theoretical performance [328]. Nonetheless, there is currently a lack of research that confirms many of the well understood (but often anecdotal) benefits of green roofs, especially with respect to geographically relevant stormwater management.

There are currently two primary studies that detail the performance of green roofs for stormwater retention in Australia. One study, by Razzaghmanesh and Beecham [75] describes the stormwater retention performance of experimental green roofs in the dry South Australian climate to be up to 74%, which is 12% higher than the global average as estimated by Zheng et al [328]. The second study, conducted by Razzaghmanesh et al aimed to assess quality of stormwater filtrate (soluble fraction) in relation to nutrient content and trace metals. Unfortunately this study did not compare the trace metal profile of the two experimental green roof types to their respective controls, however they did report on the concentrations of Cd, Cu, Pb and Zn being less than average concentrations of surface runoff reported by Göbel et al [329], and attribute what was observed to the organic fertilisers used. Despite these two studies, there is currently a lack of *in-situ* data from large scale commercial green roofs in dense Australian metropolitan areas to confirm their filtration and retention performance.

Currently most empirical green roof studies utilise experimental-scale green roof plots and controls [24,74,230,323,330–338], or larger installations with internal controls, or reference sites [59,313,339–342] which may not be completely representative of the sites tested. To address this, we compare an operational commercial green roof, and a near-identical neighbouring reference roof, with minimal spatial confounding effects. We aim to investigate the potential for extensive green roofs to reduce peak stormwater runoff and mitigate trace metal contamination prior to entering the catchment, in the largest metropolitan city in Australia (Sydney).

2. Methodology

2.1 Site description

This study was conducted on two sister-buildings [343] in Barangaroo, Sydney (33.8643◦S, 151.2028◦E) atop Daramu house and International house (green and conventional, respectively) (Figure 18). Sydney has a humid, subtropical climate, with a median annual rainfall of 1164 mm. Sydney's recent (2017-2022) yearly rainfall distribution is centred around the Summer months [344]. The median rainfall is presented in this instance to more accurately describe Australian rainfall due to the effect of extreme weather events (drought and flooding) from effecting the mean rainfall.

Figure 18. Aerial imagery of study site. Daramu house (green roof) featured in the foreground and International house (conventional roof) featured in the background. Sister buildings are near-identical with differences (excluding greenery) owing to BMU design, rooftop infrastructure, and solar panel layout. Left of image depicts the layering of the green roof, from substrate to insulation layers, as well as a schematic of the stormwater outflow.

Both green and conventional roofs are 1863.35 m^2 with solar arrays covering 593.93 m^2 (~32%), and 567.44 m^2 (~30%) of roof space, respectively. The green and conventional roofs were completed in 2019 and 2017 and each feature a 0.8 m thick, grey concrete slab as the green roof foundation, or roof surface, respectively. Both buildings house rooftop infrastructure such as exhaust vents and machine rooms, with similar layout/positioning.

The green roof employs an extensive design and utilises an integrated subsurface irrigation system. Vegetation on the green roof covered an area of 1460.7 m^2 (78.4% of the roof space), with plant species and distribution being previously described in Wooster et al [28]. The green roof also features a region of loose rocks and a large sand pit that make up an additional 216.15 m^2 (11.6% of roof space). The green roof substrate has a variable depth of 0.1 and 0.12 m, a weight/weight particle size distribution of 48.6% < 2 mm, 48.4% 2-10 mm and 2.9% 10-20 mm, and a permeability of 3769 mm/h. More substrate details are provided in Fleck et al [305].

The two buildings are positioned side-by-side (Figure 18), with little confounding spatial variance. Due to their location, age, dimensions and construction, these two buildings presented a valuable opportunity to compare the *in-situ* performance of green roofs for stormwater flow reductions and trace metal retention/degradation.

2.2 Trace metal analysis

To determine the water quality of runoff from the green roof compared to the conventional roof, trace element analysis was conducted on composite samples collected on each roof. The method employed here is similar to previous work [337,345], with differences owing to the collection and preparation of solid samples, opposed to liquid samples.

Trace element samples were collected fortnightly from the North and South ends of each roof, provided there had been no rainfall in the preceding two-week period (Supplementary Figure 7). Previous literature [346] describes the build-up of contaminants prior to rainfall as achieving an equilibrium load after 10 days. In this instance a 14-day sampling period was deemed sufficient to ensure equilibrium load on each site was reached, provided there were no preceding rain events. Differences in mass collected between sampling events were accounted for by mass correcting the trace metals output prior to analysis. As such, the trace element analysis conducted is representative of the potential trace contaminant load that could enter local stormwater management systems during rain events after a 10+ day dry period. *In-situ* runoff samples were not collected due to safe work procedures preventing roof access in poor weather.

Green roof substrate samples were taken by taking core samples of ~20 grams of substrate, and carefully removing any rocks or fertilizer pellets with plastic tweezers. Samples from the green roof were collected in areas which excluded the sub-surface irrigation to ensure leaching had not occurred prior to collection. Conventional roof samples were collected using a Ryobi One+Hand Vacuum (18V, Ryobi, Australia), where at least three 1 m^2 areas were sampled, per replicate to provide ~1 – 5 g of solid sample. Ten trace metal samples were collected per building over a three-month period (April – June 2021: gross rainfall 162.4 mm). Green roof substrate and conventional roof dust samples were collected, as any anthropogenic sources of trace metal contamination would be contained in the surface dust on rooftops. However, on a green roof there are many deposition surfaces for trace metals to settle. As such, substrate samples were taken as particulate matter would eventually be deposited into the substrate through various mechanisms, and within the substrate there is the potential for bioretention and bioremediation. All samples were deposited into sterilised falcon tubes and transported to the laboratory for analysis.

Samples were dried in a drying oven at 65°C for 36 hours, weighed and transferred to sterile 50 mL falcon tubes and diluted with at least 45 mL of MilliQ water (Ω 18.2; Millipore, Germany). Samples were sonicated using a water bath sonicator for 15-minutes to disrupt any aggregated particles and ensure solubilisation of trace metals. Samples were then centrifuged at 4500 g, and the soluble fraction transferred to a new sterile falcon tube.

The particulate fraction was then digested in 1:1 69% v/v nitric acid and 30% v/v hydrochloric acid and made to volume with MilliQ to prepare for Solution Nebuilisation Induction Coupled Plasma Mass Spectrometry (SN-ICP-MS; 7700cx, Agilent, USA). Samples were processed in technical triplicate. A 12-point calibration curve was made from a 68-element standard (ICP-MS68A-500 Choice Analytical) in 2% HNO_3 / 1% HCl diluent. The calibration points were as follows: 5, 2.5, 1, 0.5, 0.25, 0.1, 0.05, 0.01, 0.005, 0.0025, 0.001 and 0 ppm.

Prior to analysis, samples were again digested in high purity nitric acid (15.6 M) in closed vessels using a microwave apparatus (MARS Xpress, CEM) according to US EPA method 3051A. Analysis of the collected samples focused on particulate phosphorus and the sorbed metals, primarily nickel (Ni), copper (Cu), zinc (Zn), lead (Pb), cadmium (Cd) and chromium (Cr).

All SN-ICP-MS was performed using a 7700cx series ICP-MS (Agilent Technologies, USA) equipped with a micromistTM concentric nebuliser (Glass Expansion, Australia). A Scott type double pass sprat chamber cooled to 2°C was used for sample introduction. Platinum sampling and skimmer cones were used. ICP-MS analysis was controlled using the MassHunter 4.3 software (C.01.03) and all experiments used 99.9995% ultra-high purity liquid argon (Argon 5.0, Coregas Pty Ltd, Australia).

An Agilent integrated autosampler (AIS) was loaded with solutions for analysis. Solutions were transferred to the SN-ICP-MS using a 1.02 mm internal diameter Tygon tubing and a three-channel peristaltic pump. The solution was pumped at a continuous flow of 1.0 $mL.min^{-1}$. A 100 ppb Rhodium solution in 1% HNO_3 was used as an internal standard and introduced into the analyte flow via a T connector post-pump. ICP-MS settings and parameters are detailed in Table 6 below.

Table 6. SN-ICP-MS (7700cx, Agilent, USA) parameters used for trace metal analysis.

Sample Introduction	
RF power (W)	1500
Carrier gas flow rate ($L.min^{-1}$)	0.7
Makeup gas flow rate ($L.min^{-1}$)	0.5
Sample depth, mm	8
Ion lenses	
Extracts 1,2 (V)	3.8,-185
Omega bias, lens (V)	-120, 18
Cell entrance, exit (V)	-30,-40
Octopole parameters	
Octopole RF (V)	190
Octopole bias (V)	-8
Collision gas, flow rate ($mL.min^{-1}$)	0

ICP-MS trace element concentrations were mass corrected and differences between buildings for the soluble and particulate fractions were assessed using individual Mann-Whitney U tests. This analysis was chosen as the data did not satisfy the assumption of parametric testing. Analysis was conducted using R statistical software [268] and the packages; xlsx [124], tidyr [272] and dplyr [269].

Prior to sampling, a literature review (Supplementary Table 10) was conducted to predict the green roof's theoretical performance for the reduction of trace element concentrations. Roadside trace metal concentrations were sourced from the Qantas Drive (Mascot, Sydney [347]) data set, and used as approximations of anthropogenic trace metal concentrations.

2.3 Modelling stormwater peak attenuation performance

Two models were used to assess the potential stormwater attenuation performance of the green roof in this study. The DRAINS Australian Rainfall and Runoff (2019) Initial Loss/Continuing Loss Model [348]

was employed to predict the fluvial mitigation performance of the green roof from a design perspective. The USEPA Storm Water Management Model (SWMM) was employed to quantify the reduction in stormwater flowrates from the green and conventional roofs into the local stormwater management network based on locally sourced data (Observatory Hill, Sydney: Gauge 066062).

For DRAINS, both the green and conventional roofs were divided into four sub catchments representing uniform catchment characteristics of slope, impervious area, and Manning's roughness coefficient (n). The division of the catchments was based on the building hydrology design plans, drainage network information, aerial photographs and the information obtained from onsite field inspections. Pre-burst rainfall data was retrieved from the ARR Data Hub website, using the coordinates -33.8613, 151.2016 and historical rainfall data was sourced from ARR 2019 incremental pattern file and intensity-frequency-duration depth file [349]. Major and minor storms with 5-minute and 2-hour durations were modelled. Simulation parameters are presented in Table 7.

Table 7. Simulated roof top parameters for both the green and conventional roofs for DRAINS.

Model Parameter	Green Roof	Conventional Roof
Catchment Area	.18 ha	.18 ha
Impervious Area	10%	100%
Time of concentration	6 minutes	12 minutes
Impervious area initial loss	1.5	1.5
Impervious area continuing loss	0	0
Suburban pervious area initial loss correction	22.4	NA
Suburban pervious area continuing loss correction	0.64	NA
Sub-catchment areas	4	4
Total catchment areas	8	8
Substrate void space assumption	20%	NA
Detention basin nodes	0.03 m	0.03 m
Drainpipe design	Circular	Circular
K entry/bends	0.5	0.5
Outlet/underdrain pipes diameter	150 mm	150 mm
Weir coefficient C-value	1.75	1.75
Crest length	10 m	10 m
Downstream catchment flow carried by channel	0	0
Channel slope	1%	1%

SWMM is a physically based, spatially distributed model for simulating all aspects of hydrological and water quality cycles, primarily within urban areas [350–352]. The availability of data describing the hydrologic response of urban catchments is extremely limited [353] and due to concurrent construction in the study site area, there was a lack of on-site catchment monitoring data. Therefore, observational data between 1991 and 2010 from Observatory Hill, Sydney (Gauge 066062) was selected for this analysis (Figure 19). Simulation parameters are presented in

Table 8.

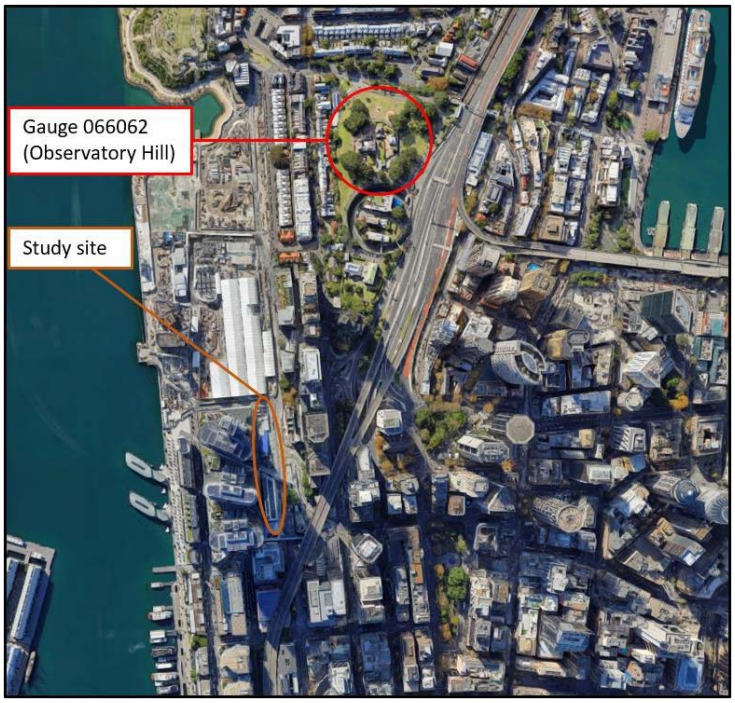

Figure 19. Proximity of Observatory Hill (Gauge 066062) from the study site – approximate linear distance is 590 m.

Table 8. Simulated roof top parameters for both the green and conventional roofs for SWMM.

Model Parameter	Green roof	Conventional roof
Total catchment area	0.09 ha	0.09 ha
Impervious fraction	10%	100%
Impervious depression storage	1 mm	1 mm
Roof slope	1.25%	1.25%
Green roof fraction	90%	N/A
Soil depth	120 mm	N/A

3. Results and Discussion

3.1 Trace element retention

In-situ trace metal analysis detected, on both roofs; Li, Be, Na, Mg, Al, Si, P, K, Ca, Sc, Cr, Mn, Fe, Co, Ni, Cu, Zn, Ga, Ge, As, Se, Rb, Sr, Y, Zr, Ag, Cd, In, Sn, Sb, Cs, Hg, Tl, Pb, Bi, Th. However, there were 21 metals observed above the detection limit solely on the conventional roof ; Ti, V, Nb, Mo, Te, Ba, La, Ce, Pr, Nd, Eu, Gd, Tb, Dy, Er, Tm, Yb, Lu, Ta, W, U. Analysis was conducted on Ni, Cu, Zn, Pb, Cd and Cr due to their prevalence in urban environments and their toxicity to human health and aquatic environments [309].

Results from the *in-situ* trace metal analysis show that the soluble fraction for all trace metals were similar between roofs ($p > 0.05$ in all cases; Figure 20), excluding copper. The concentration of soluble copper on the green roof was 32% lower than that reported on the conventional roof (Cu; $p = 0.022$), not dissimilar to the values predicted by Steusloff [334]. Atmospheric copper can have many sources in urban environments including windblown dust, sea spray, vehicle emissions and mechanical abrasion [354–356]. Due to the proximity of the site to a dense urban centre and major motorway (80,000+ vehicles per day [357]), it is likely the contribution of copper is derived primarily by human activities. A significant reduction in soluble copper on the green roof may be due to the binding to inorganic or organic constituents contained within the green roofs substrate, such as clay, organic matter or sulfides [358]. This reduction in soluble copper indicates green roofs are able to mitigate, to some degree, the impact of soluble trace metal pollution that stems from human activities in dense urban environments.

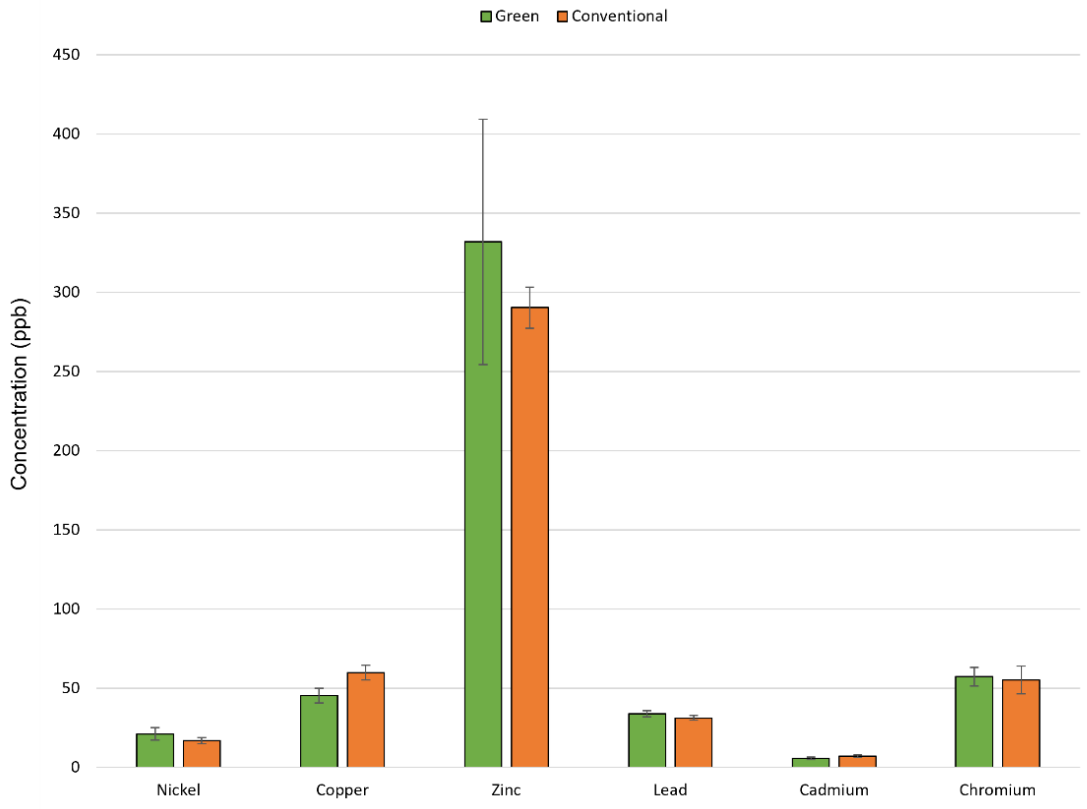

Figure 20. Soluble trace metal fraction for the green roof substrate and conventional roof surface dust. Error bars represent the SEM.

As mentioned previously, an Australian study on experimental green roof plots by Razzaghmanesh et al [74] assessed the soluble trace metal contribution of green roofs to stormwater outflows. Interestingly, the results presented by these authors were substantially lower for both substrate types

tested than those presented here (Cu ~10x; Zn ~17x; Pb ~30x and Cd ~90x), where the trace metal concentrations observed were attributed to organic fertilisers. It is hypothesised by the authors that the concentrations of trace metals presented in the current work are likely aerosolised from anthropogenic sources. Differences in concentrations observed in this study and that of Razzaghmanesh et al [74] are likely due to differences in site specification. The experimental green roofs monitored by Razzaghmanesh et al [74] were situated 22-stories above street level, in a city with 10,523 employed people (2016 census; [359]), compared to the current work in which the green and conventional roofs are 7-stories above street level, in a city with over 124,746 employed people (2016 census; [360]), and both adjacent to and level with an overpass motorway with a daily traffic count of 80,000 vehicles [357].

A similar study by Berndtsson et al [361] estimated that of the green roofs included in that study, one roof type was shown to be capable of retaining 8-93% of the total Zn, Cr and Pb present in precipitation loads. Unfortunately, in the absence of analysing *in-situ* runoff, our study was limited by the measurement of dry-deposition surface trace metals on each roof. This limits the observational power of the study, with our results only detecting a significant different in soluble Cu, possibly attributable to the phytoremediation adsorption and utilisation of trace metals at the root level. It is entirely possible that the analysis of *in-situ* runoff may have elicited a different result.

For particulate trace metals, the phytoremediation of contaminated soils is well documented, and considered to be a cost-effective technology for the remediation of contaminated sites [362]. In the current study, a reduction in particulate trace elements referred to a difference in the concentration (ppb) of each element present in the samples from the sites. In this sense, the green roof demonstrated an ability to significantly reduce particle bound Zn ($p = 0.007$), Cr ($p = 0.012$) and Cu ($p = 0.042$) (Figure 21) by 77.57%, 92.56% and 90.68%, respectively. Previous work carried out by Sun and Davis [315] on experimental bioretention systems for urban pollutants, demonstrated removal efficiencies for Zn, Cu, Pb and Cd of over 88% for low metal loading, and over 93% for high loading. Their study estimated trace metal removal to be 88-97% attributable to the substrate media, and only 0.5-3.3% to accumulation by plant material, over a 230-day period. It is therefore likely that over the lifespan of a green roof, aerosolised trace metals could be deposited and trapped within the substrate media and slowly integrated into plant material through bioretention, rhizofiltration or phytostabilisation [363,364]. Comparatively, the sole mechanism for trace metal removal on conventional roofs is disturbance and aerosolisation back into the atmosphere, or washing into stormwater catchments in storm events [365].

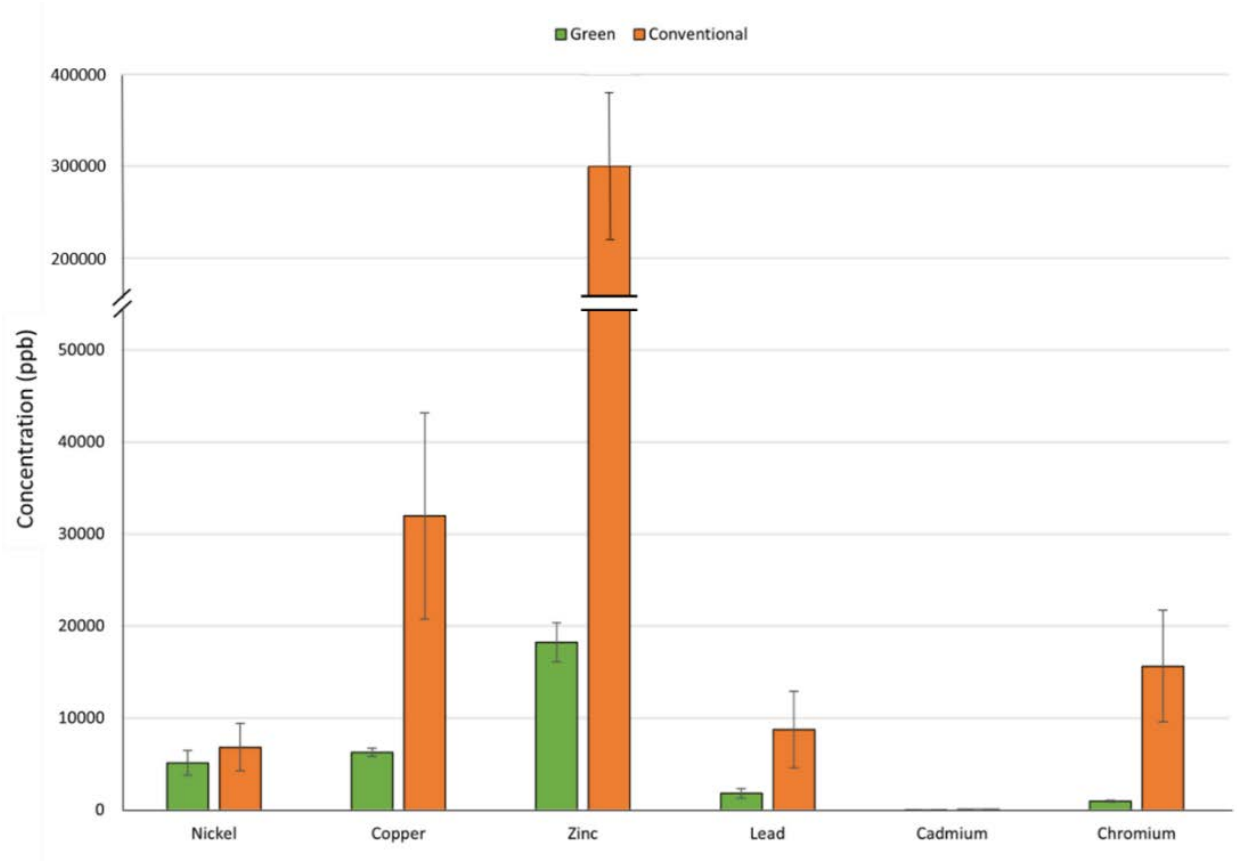

Figure 21. Particulate trace metal fraction for both green roof substrate and conventional roof surface dust. Y-axis break at 50,000 ppb to 200,000 ppb to display particulate Zinc concentrations. Error bars represent the SEM.

The trace metals detected here are common vehicle and industrial pollutants [316,356,366–371] and due to the proximity of the experimental site to a major motorway and extensive urban development, the concentration of dry deposited aerosol pollutants presented here should be considered high. This is reflected by the differences in concentration between the sites (Figure 20 and Figure 21) and the predictive model (Figure 22). Despite the high pollutant loads, the green roof substrate demonstrated an ability to retain significant proportions of ambient particle bound Zn, Cr and Cu, and to remove significant soluble Cu with comparable removal efficiencies to various industrial filter materials [372]. However, the green roof did not significantly reduce the detected concentrations of Pb, Ni, Cd or Cr when compared to the conventional roof. It is possible that under different weather conditions (during or post rainfall) there could be a reduction in runoff concentrations for these contaminants, however this could not be tested in this study. It is also possible that the reduction in both the soluble and particulate concentrations of trace metals observed in the substrate were lower than the conventional roof through the physical barrier provided by the plant leaves. While the dry deposition of aerosolised trace metals onto plant material was untested, the reduction should be considered a function of the green roof. Future analyses should aim to determine the efficiency of green roofs under varying weather events for their removal of trace metal contamination, as well as the

contribution of the above-ground plant matter in respect to trace metal substrate concentration. Additionally, future work should be conducted on the optimisation of substrate depth, composition, and physiochemical properties to positively influence retention times and therefore phytoremediation potential for dry deposition anthropogenic urban trace metals.

Performance estimates of bioremediation and bioretention from the literature only described the total concentration of trace metals that could be removed on each roof, either accumulated in the substrate (green roof) or as surface dust (conventional roof) (Figure 22).

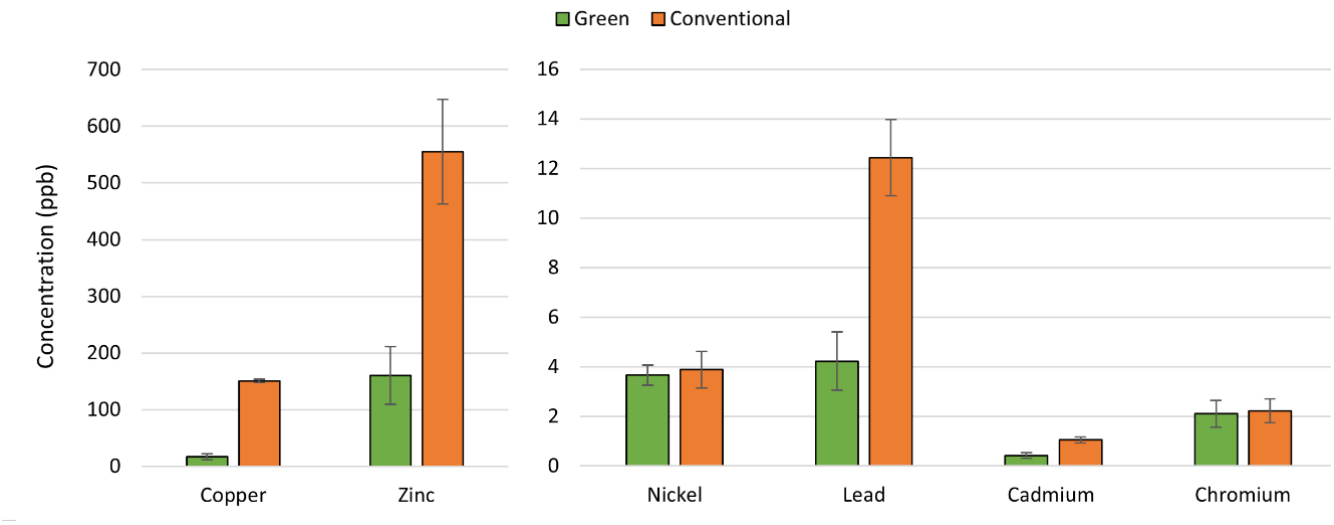

Figure 22. Predicted trace metal concentrations of trace metals to be expected in the substrate of the green roof and surface dust of the conventional roof. Data sourced from Supplementary Table 10. Error bars represent SEM.

Predicted total trace metal concentrations (both soluble and particulate), based on roadside observations showed predicted differences between buildings to be highest for zinc (Zn 71.2%; 395 ppb), copper (Cu 89%; 134 ppb), lead (Pb 66.13%; 8 ppb) and cadmium (Ca 60%; 0.6 ppb). Nickel (Ni) and chromium (Cr) were predicted not to differ between buildings. The predictive results presented here differ significantly to those previously reported. A study conducted by Steusloff [334] described the modelled filtration efficiency of wet deposition trace metals by an extensive green roof (substrate depth 0.1m) and a semi-intensive green roof (substrate depth 0.22m) reporting the removal efficiency of trace metals from runoff filtration to range between 43.7% and 99.8% for copper, depending on season and roof type. Differences in removal efficiency are likely owed to difference in input variables, such as substrate depth or total roof area. The predicted concentrations presented in the current study represent the total trace metal concentration (ppb), similar to the work of Brockbank [347], where Steusloff [334] simply describes the removal of theoretical wet deposition trace metal concentration starting at “100%”.

It should be noted that dry deposition concentrations of trace metals are substantially higher than wet deposition (aerolised pollutants deposited over a period of time vs solubilisation of trace metals during a rain event), but several orders of magnitude lower than road runoff concentrations. Here, the predicted concentrations (Figure 22) differed from the *in-situ* observations (Figure 20 and Figure 21), likely due to differences in source pollution (solubilised roadside runoff from medium density traffic vs long-term accumulation of aerosolised trace metals from extremely high-density traffic). Despite this, the reduction in measurable concentrations were similar for zinc and copper (Zn 72% vs 77%; Cu 89% vs ~91%), but not the other trace metals. It is possible that bioretention and phytoremediation data input from our literature review differed significantly due to species variation, or climatic conditions, or simply the trace metal concentrations. However, both our *in-situ* results and the predictive model demonstrated a functional reduction in urban trace metal contamination on green roofs compared to conventional roofs (Figure 22).

3.2. Modelled stormwater performance

Hydrological models are frequently used for both design and analysis. In this study we present two models, DRAINS and SWMM, to assess differences in design (predictive) and modelled reductions in stormwater flow rates. DRAINS was utilised to predict the effect of the specific green roof design on flow rate, using data from the Australian Rainfall and Runoff (ARR) guide data [349]. Design prediction software relies on a simulated storm burst that has been designed to assist in the transformation of the Intensity–Frequency–Duration (IFD) statistic, which describes the rainfall rate in mm/h, frequency of events and duration into a flow statistic. DRAINS is one of the most commonly used software systems for prediction of design flows and volumes in Australia. SWMM was utilised to determine the specific effect of the green roof for the reduction in peak flow rates using environmental data collected for that specific region (Gauge 066062 [373]). In this instance, SWMM was used with no assumptions made regarding the transformation of rainfall frequency into flow frequency (such as the above simulation of burst rainfall), and therefore can be applied as an analytical tool, rather than a design-oriented tool.

3.2.1 DRAINS

DRAINS was used to calculate the detention nodes, the upper and lower water depths, and flowrate. The estimation of flood characteristics requires the determination of the magnitude of the hazard, and the likelihood of occurrence, referred to as Annual Exceedance Probability (AEP; 1 in x years). Based on an AEP 5 storm event (1 in 5-years), the upper water level was a maximum of 1.04 m for each green

roof catchment area (Figure 23; green text (A)) which indicates there is no risk of overflow (excessive water pooling). Further, the outlet flowrate from the green roof is predicted to be 7 L/s (Figure 23; blue text (C)), which is ~89% reduction in peak stormwater flow rates compared to the conventional roof (63.4L/s; not displayed here).

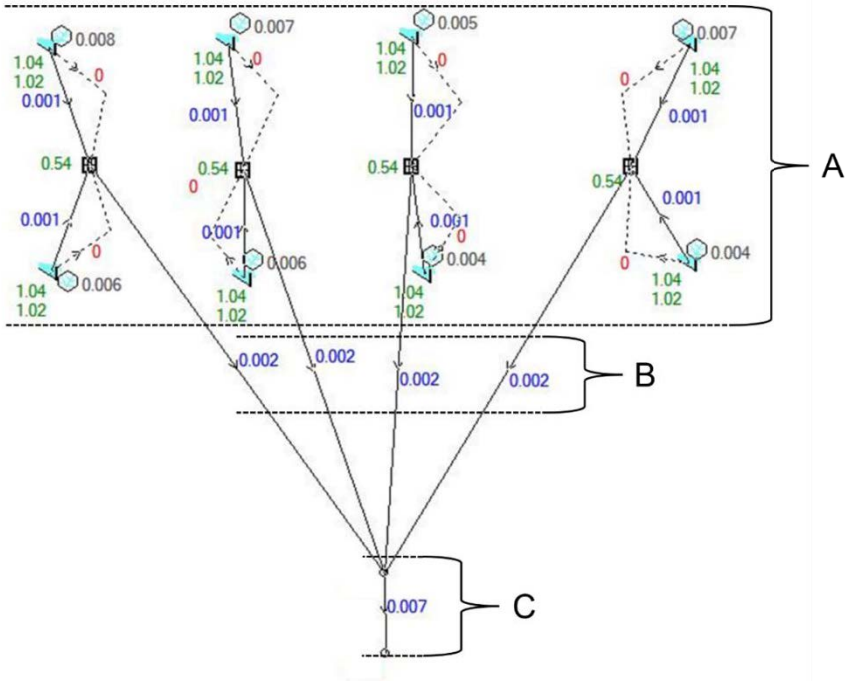

Figure 23. Green roof catchment model output from DRAINS representing an AEP 5 (1 in 5 years) storm event. Figure depicts the catchment areas (A), underdrains (B) and outlet pipe (C) flow rates (blue text; m^3/s). Upper and lower water levels for the catchment areas (A) are also depicted (green text; water height in cm above level (1.0)).

Feitosa and Wilkinson [374] demonstrated an increasing green roof substrate depth yielded greater peak attenuation linearly, with substrate depth having a greater effect on attenuation with an increase in green roof coverage. Based on the results of Feitosa and Wilkinson [374] the green roof in this study should have had a peak attenuation of ~35%, which is significantly lower than the DRAINS output prediction of ~89%. Differences in the predicted and modelled attenuation from the literature are likely owing to the nature of the chosen software (predicted: DRAINS vs modelled: HYDRIUS-1), or the data input parameters. Interestingly, a meta-analysis consolidating results from 75 investigations conducted by Zheng et al [375] describes the average extensive green roof runoff retention attenuation to be 56% [375], noting that the variability across investigations varied very widely (0%-100%).

As DRAINS is predictive modelling software, differences between prediction and observations are expected. Due to the green roof in this study being a commercial installation, we must rely on analytical models to more accurately predict the stormwater flow rates, such as SWMM.

3.2.2. SWMM

Both the theoretical runoff for varying storm conditions, and the depth of surface ponding were determined using the stormwater management model. Here we present the peak flow attenuation potential of an *in-situ* commercial green roof and a control roof within the same catchment with near-identical dimensions and drainage. In our analysis we observed a significant reduction in peak stormwater flow rates for all storm events between AEP 1.01 to 20 (Figure 24). Peak flow rates were predicted to be reduced by 90% (7.5 L/s) to 69% (18.21 L/s) for frequent storm events (1 in 1.01-2 years), and 50% (18 L/s) to 19% (9.2 L/s) for less frequent events: 1 in 5 or 1 in 20 years (Table 9). For storm events less frequent than 1 in 2 years, the SWMM flow rate values more accurately reflect the global averages as reported by Zheng et al [375].

Table 9. SWMM predictive modelling results for peak stormwater flow rate reduction of green and control roofs. AEP indicates the magnitude of a storm event, presented as a likelihood of occurrence.

AEP	Green roof (L/s)	Conventional roof (L/s)	Reduction (L/s)	Reduction (%)
1.01	0.8	8.3	7.5	90
1.5	5.4	21.96	16.56	75
2	8.22	26.43	18.21	69
3	12.44	31.43	18.99	60
5	18.38	36.67	18.29	50
10	27.77	42.75	14.98	35
20	38.89	48.09	9.2	19

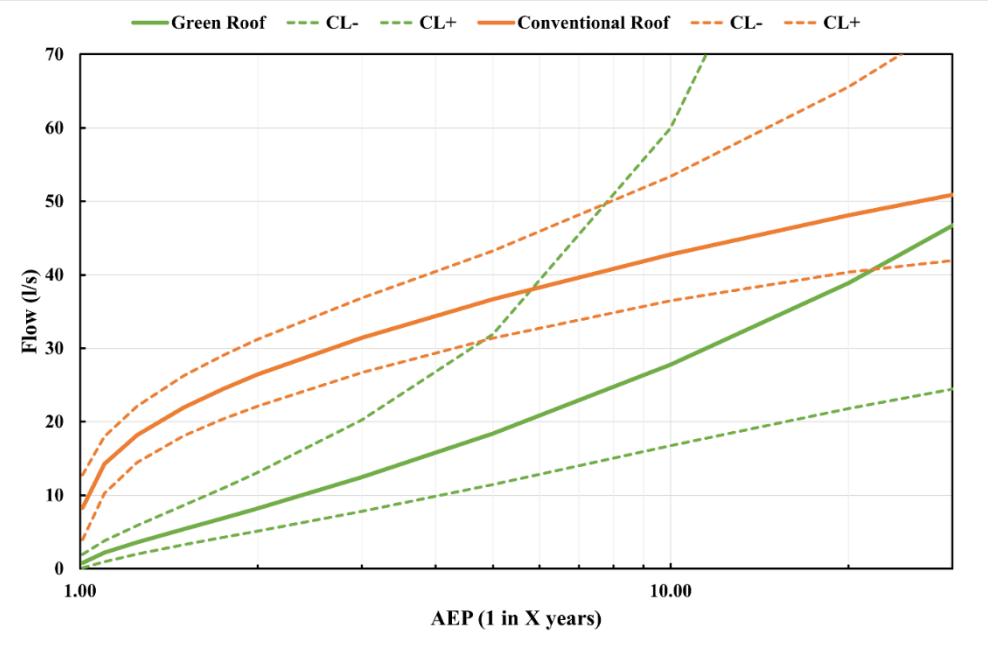

Figure 24. SWMM flood flow prediction model with upper and lower confidence limits for each roof type based on storm event AEP up to 1 in 30 years (log scale).

For AEP 3-, 5- and 10-year storm events, the SWMM results indicate a reduction in peak flow rates by 35%, 50% and 60% respectively (Table 9). These values align with those previously discussed for green roofs with similar sizes and substrate depths [374,375]. A study conducted by Yang et al [376] found urban green roof and LID practises could reduce stormwater peak flow rates by 52.46%, similar to the results presented here for storm events as infrequent as 1 in 5 and 1 in 10 years. Additionally, Palla et al [377] describes both the effectiveness of a case study-sized green roof on the local hydrological response and the catchment-wide impact of retrofitting buildings with green roofs. Palla et al [377] determined that the hydrological performance of retrofitted green roofs could have an impact on the hydrological response for rainfall events with a total depth greater than 32 mm and that at the catchment scale, the use of retrofitting LIDs could significantly contribute to improved storm water runoff management in densely urbanised areas [377].

The results presented here demonstrate the practical use of green roofs to reduce the stormwater runoff from urban buildings in Sydney, Australia for storm events less frequent than 1 in 5 years, with the potential to reduce the runoff for events as severe as 1 in 20 years, although with lower confidence (Figure 24). As Australia experiences unique weather cycles through extreme rainfall and drought, the input data for the annual maximum flows were low, or close to zero, for 30% of the years analysed. Due to this, the degree of confidence the SWMM model can generate for the green roof increases with less frequent storm events, therefore the model output was limited to 30 years. Regions with more stable climates and predictable rainfall could expect significantly less variation in the predicted performance of green roofs. Despite the large confidence interval variation for larger

rainfall event projections, there is clear evidence that green roofs can mitigate the severity of flow rates atop roofs in urban centres.

There is substantial literature available on the suitability of various international cities for the retrofitting of green roofs, and the approximate spaces available [51,224,339,378]. The current findings indicate that it is plausible that the widespread adoption of extensive green roofs in the Sydney metropolitan area could significantly reduce the flood flow of the underground stormwater management network and reduce the impact of short-lived heavy rain events on ground level urban spaces.

4. Conclusion

Here we demonstrate the performance of an *in-situ* commercial extensive green roof for both stormwater peak flow reduction, as well as reductions in both soluble and insoluble trace metals. Our analysis highlights the potential for Sydney urban green roofs to significantly reduce the flow rate of frequent and intermediate storm events through the use of analytical simulations (1 in 5, and 1 in 20 years, respectively), which may reduce contribution of rooftop runoff to over-burdened stormwater networks by up to 60%. The east coast of Australia experiences infrequent flash floods and an overload of the stormwater network, therefore it is plausible that the mass adoption of urban green roofs may reduce the severity of frequent and intermediate storm events and the subsequent effect on the stormwater system, as experienced as recently as March 2022. Additionally, removal efficiencies for soluble copper (32% reduction) were similar to those modelled in previous work, as well as significant reductions in particulate zinc, chromium and copper (77.57, 92.56 and 90.68%, respectively), likely due to substrate retention or entrapment by plant roofs. Future works should assess the substrate composition on flow rate reductions and particle retention, as well as to simulate rain events using realistic dry-deposition *in-situ* trace metal concentrations.

Preface: Chapter 6

A further benefit of green roofs is the potential for synergistic technologies. The installation of solar arrays on green roofs is often referred to as Bio-solar technology. In concept, a Bio-solar roof operates by the addition of additional rooftop layers and plant foliage, which acts as a water reservoir and transport mechanism through which the green roof can regulate rooftop temperatures, as previously shown (Chapter 4). The plant foliage facilitates evapotranspiration to actively cool the rooftop microclimate, leading to lower ambient temperatures which draw heat from the backs of the solar panels installed above the vegetated surface. The synergistic effect of a Bio-solar roof over a conventional solar roof has been shown experimentally [379] to increase the energy output of a solar system by up to 4%, depending on roof specifications and climate type. The implementation of Bio-solar roofs instead of conventional roofs could thus assist in the generation of more efficient, localised sustainable energy.

In this study we aimed to determine the extent to which a Bio-solar roof could increase solar energy outputs when compared to a conventional solar array in Sydney, Australia. This work represents one of the few *in-situ* commercial-scale studies, and the only study to eliminate the confounding effect of an internalised control. Here we observe both *in-situ* and through modelling, an increase in system performance, leading to higher energy generation and subsequently greater monetary savings and reduced greenhouse gas emissions.

This project was run in collaboration with UTS, Lend Lease, Junglefy and the City of Sydney to generate quantitative data to support the City of Sydney 2030 Greening Guide, funded under the City of Sydney Environmental Performance - Innovation Grant 2019-20.

The following chapter is comprised of text from a peer-reviewed publication.

Chapter 6: Bio-solar green roofs increase solar energy output: the sunny side of integrating sustainable technologies

Fleck. R [1*], Gill. R [1, 2], Pettit. T.J [1] Torpy. F.R [1], Irga. P.J [3]

[1] *Plants and Environmental Quality Research Group, School of Life Sciences, University of Technology Sydney*
[2] *Coastal Oceanography and Algal Research Team, Climate Change Cluster, University of Technology Sydney*
[3] *Plants and Environmental Quality Research Group, School of Civil and Environmental Engineering, University of Technology Sydney*

**Corresponding Author: Robert.Fleck@uts.edu.au*

This article has been published in the journal Building and Environment (Q1, Impact factor 7.093 (2022)). Available online at https://doi.org/10.1016/j.buildenv.2022.109703. Published 19th October, 2022.

Abstract

In urban spaces, localised energy generation through rooftop solar has become increasingly popular, and green roofs are often used for a range of services such as thermal insulation. In recent years, the adoption of *Bio-solar* green roofs (BSGR) for both thermal insulation and increased solar energy outputs has increased. Here we present two buildings of the same dimensions and location, similar age and construction material, where one hosts a BSGR, and the other a conventional solar roof (CSR) in Sydney, Australia. Each solar array hosted a range of environmental sensors, including ambient temperature and global horizontal irradiance (GHI). The modelled BSGR average hourly energy output was 4.5% higher than the CSR (seasonal trends observed Spring; 4.14%, Summer; 4.16%, and Autumn; 5.21%) with BSGR producing 14.26 MWh more than the CSR, valued at $4,526.22 AUD, and equal to 11.55 t e-CO_2 greenhouse gas mitigation. Further potential for up to 1.55 t of CO_2 could be mitigated by the plant material on the roof, provided the trimming of plant material during maintenance is conducted responsibly. In this instance, the implementation of a BSGR increased the system's solar output by 23.88 kWh per m^2 of panel coverage, as well as reducing the e-CO_2 emissions by 0.019 t per m^2 over the CSR. When compared to the results of previously reported pilot studies and some simulations, it is evident that the implementation of a BSGR is favourable for maximising energy production and the mitigation of GHGs.

Keywords

Bio-solar roof, green roof, photovoltaic, renewable energy, sustainable infrastructure, urban resilience

Abbreviations

BSGR – Bio-solar green roof

CSR – Conventional solar roof

GHI – Global horizontal irradiance

Highlights

- Average BSGR output 4.5% higher than CSR output across all seasons.
- Average BSGR output (kWh) was 4.14, 4.16 and 5.21**%** higher than CSR for Spring, Summer and Autumn.
- BSGR produced 14.26 MWh more than conventional solar, valued at $4,526.22 AUD.
- BSGR reduced 11.55 t e-CO_2 more than CSR. Up to 1.56 t CO_2 was removed by plant biomass.
- BSGR produced 23.88 kWh and reduced 0.019 t e-CO_2 emissions per m^2 of panel coverage more than CSR.

Graphical Abstract

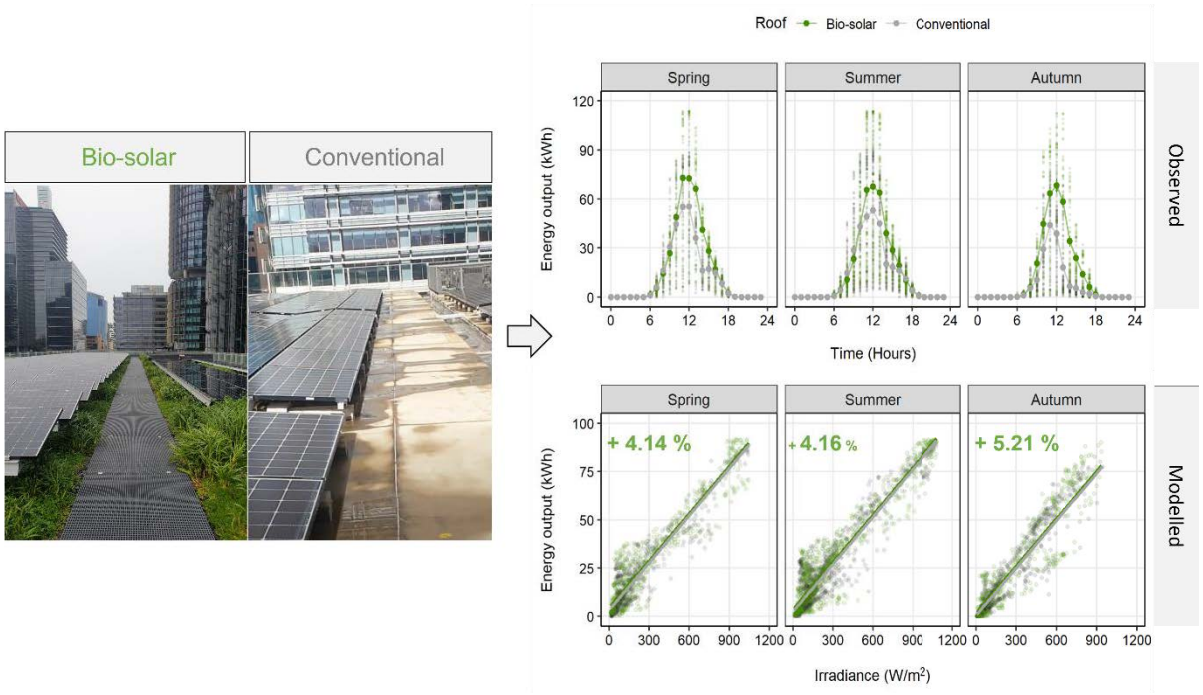

1. Introduction

Non-renewable energy generation, transport and consumption by urban spaces is a significant contributor to greenhouse gas emissions worldwide [380], with urban areas consuming between 67-76% of global energy and generating approximately 75% of the world's carbon emissions [16]. It has been further estimated that 50% of urban energy consumption is attributable to heating, ventilation and air conditioning (HVAC) of buildings [15]. The implementation of a renewable grid will play a major role in reducing future emissions [381], however reducing demand for energy worldwide is often cited as the most effective method to achieve climate targets [382]. In urban spaces, localised energy generation for commercial spaces through rooftop solar has risen in popularity [383], as well as the implementation of various technologies to reduce energy use [384]. For example, green roofs are often used for their range of benefits such as thermal insulation, however in recent years the adoption of *Bio-solar* green roofs (BSGR) for both thermal insulation and increase solar energy outputs has been adopted [70,305,385].

Green roofs are rooftops that have either been purpose built or retrofitted to facilitate the growth of vegetation. Green roof designs vary, however all consist of a vegetation layer, growth substrate layer, drainage layer, root barrier and waterproof membrane [259]. Green roofs are broadly divided into two categories: intensive (substrate depth ≥ 300 mm), and extensive (substrate depth < 300 mm) [75]. Intensive green roofs often utilise large perennial herbaceous plants, shrubs and small trees [225] and are largely implemented for their aesthetic and biophilic properties [251]. Intensive green roofs require high load-bearing structures and frequent maintenance [252] due to soil depth and plant types, which leads to higher construction and maintenance requirements and initial costs [52]. By contrast, extensive green roofs often utilise grasses and perennial plants. Green roofs are known to provide a myriad of ecosystem services [224], including the removal of air pollutants [47,225,246], urban noise reduction [226–228], increases in urban biodiversity [39,229], serving as a slow-release detention basin for stormwater retention [230–232,375] and reducing the thermal loading of buildings [233–236].

Extensive green roofs allow for the integration of solar arrays, which together are often termed *Bio-solar* green roofs or Solar-Green Roofs [56]. Bio-solar roofs are theorised to provide greater energy output than conventional solar arrays due to the evapotranspiration of the vegetation which creates a cooler rooftop microclimate [305,321], reducing solar panel temperatures and increasing performance [386]. Bio-solar roofs can also regulate rooftop temperatures through reduced latent heat and lower solar reflectance than conventional concrete roofs [63].

Several experimental and modelling studies have been conducted to assess the performance of bio-solar roofs compared to conventional solar, with varying results. Pilot-scale sized experiments

conducted by Alshayeb and Chang [68] found an increase in energy production of 1.4% for model bio-solar roofs; where a study by Chemisana and Lamnatou [260] observed an increase in energy production of 1.29 and 3.33% for 5 day pilot scale experiments on *Gazania* sp. and sedum plots, respectively. While there are several pilot-scale studies that complement these works, there are few that employ the use of commercial or full-scale green roofs for energy assessments over longer time periods. One study by Hui and Chan [386] simulated a 2,494 m^2 bio-solar roof with varying physical parameters and predicted a maximum performance increase of 4.3% over conventional solar. However, one of the few scale experiments on bio-solar roofs conducted by Perez et al., [387] observed only a 2% increase in performance compared to a conventional system sharing the same roof-space.

Empirical studies have suggested that the differences between bio-solar and conventional solar system performance is variable. There is the possibility that through the use of internal control roof spaces in some studies, the cooling effect of the green roof on the local microclimate could be influencing the control sites, and therefore reducing the observable effect. In addition to this, there are limited studies that have been conducted on roofs of a commercial scale, with the assessment of bio-solar being largely attributed to small subplots with low plant species diversity or leaf area index (LAI), which is known to have an effect on evapotranspiration and the insulative properties of green infrastructure [277,296]. Here we present the unique opportunity to compare two roofs that are spatially unconfounded, with near identical construction and dimensions, with similar age and rooftop infrastructure. In this study we utilise a commercial scale bio-solar roof, as well as an independent control roof in Sydney, Australia to determine the independent effect of a bio-solar installation through both empirical observations and simulations.

2. Methodology

2.1 Site description

This study aimed to compare the solar energy output of sister buildings [343] in Barangaroo, Sydney, Australia. Daramu House was constructed in 2019 and hosted the bio-solar green roof. International House hosted a conventional solar array and was constructed in 2017. These two buildings are the first multi-story commercial timber office buildings in the country and employed near-identical rooftop infrastructure, with differences owing to building maintenance unit (BMU) model and design, exhaust vent placement and machine room design.

This study commenced in Mid-Spring (October), 2020 and concluded in Autumn (May), 2021 for a total of 237 days. For this period, the Barangaroo district received an average of 6.66 sun hours and 4.08 mm of rain per day, with an average evaporation rate of 5.93 mm/day [267]. Average daily temperatures in this region ranged between 9 and 27.43°C [267] during the study period.

Both roofs had a total rooftop surface area of 1,863.35 m^2, with 593.96 m^2 and 567.44 m^2 of solar panel coverage, for the bio-solar and conventional roofs, respectively. Each building employed 0.8 m thick, grey concrete slabs as the bio-solar roof foundation, or roof surface. The bio-solar roof employed an extensive design with a variable substrate depth of 0.1 to 0.12 m and hosted a planted area of 1,460.7 m^2 (78.4% total roof space). On the bio-solar roof, solar panels covered 40.66% of the planted space (Figure 25).

Figure 25. Aerial image of the study site (centre image). Daramu House (bio-solar; left two panels) and International House (conventional solar; right two panels). Sister buildings were near0identical with the exception of roof surface cover (plant material vs concrete). Plant material covers all regions of below panel areas on the bio-solar roof.

The bio-solar roof hosted over 15,000 individual plants and utilised a selection of native grasses and herbaceous plants to attract a diverse faunal community [28], with an estimated LAI of 4.35 [305]. The bio-solar roof also utilised a sub-surface irrigation system to water the green roof on a varying seasonal schedule between 3:30 pm and 7:30 pm. Specifications for the two roofs in relation to their biodiversity, thermal and stormwater properties have been previously described in [28], [305] and [388], respectively.

2.2 Solar arrays

As construction was completed in 2019 and 2017 for the bio-solar and conventional roofs respectively, the two buildings used different solar panels. Along with other differences between buildings, this

required that a series of corrections were made to the data to facilitate accurate comparisons between buildings.

The bio-solar roof employed 332 MAXEON 3 solar panels (SunPower, Australia; pNom 395W, efficiency 22.6%) and the conventional roof employed 346 NeON2 solar panels (LG, Australia; pNom 320W, efficiency 19.5%; see Supplementary Table 11 for full specifications). The bio-solar and conventional roofs amounted to 131.14 kWp and 110.72 kWp solar systems, respectively. Both buildings utilised four three-phase inverters (27.6k-AU000NNU2, SolarEdge, USA), rated to operate at 98% efficiency.

Prior to construction, each roof was modelled to estimate solar exposure, and the optimal panel layout. Building architects and solar engineers designed differences between panel layouts to account for the presence of the greenery in order to facilitate planting, maintenance and plant survival. On the bio-solar roof, solar panels were divided into several sections. The majority of panels (248) were situated above the main planted area, arranged with an azimuth of 0° (North-facing) and tilt angle of 15°. The remaining panels (84) were arranged between rooftop infrastructure, with an azimuth of 90° (East-facing), and a tilt angle of 2°. On average, the centre of the solar panels were 1 m above the substrate surface (~0.8 m above the leaf zone) due to consideration associated with promotion of plant growth and ease of maintenance.

The CSR did not have the same biological considerations as the green roof; hence the solar panels were arranged accordion-style, with the majority of panels arranged with an azimuth of 90° or 270° towards the centre of the roof space (145 East-facing and 145 West-facing). This layout was chosen by solar engineers to maximise sunlight exposure, as determined by modelling procedures prior to installation, similar to those presented in Section 2.3. Similar to the bio-solar roof, additional panels (56) were positioned between building infrastructure, with an identical layout to those towards the centre of the building. All panels utilised a tilt angle of 5° and were on average the centre of the panels were positioned 0.4 m above the concrete slab surface.

2.3 Solar modelling

Prior to analysis, a 3D model of the Barangaroo district was developed to estimate the average yearly incident solar irradiance on each rooftop (Figure 26) using the Rhino 6 modelling software (Rhino3D, USA) and DAYSIM in Grasshopper's Honeybee plug-in (Grasshopper3D, USA). Solar radiation calculations were based on the Sydney CBD Representative Meteorological Year (RMY) file (Sydney.947680, EnergyPlus, Australia). The model predicted the bio-solar roof would receive 6%

more annual solar radiation than the conventional roof due to the reflectance and shading caused by the local urban geometries (Table 10, consideration 2).

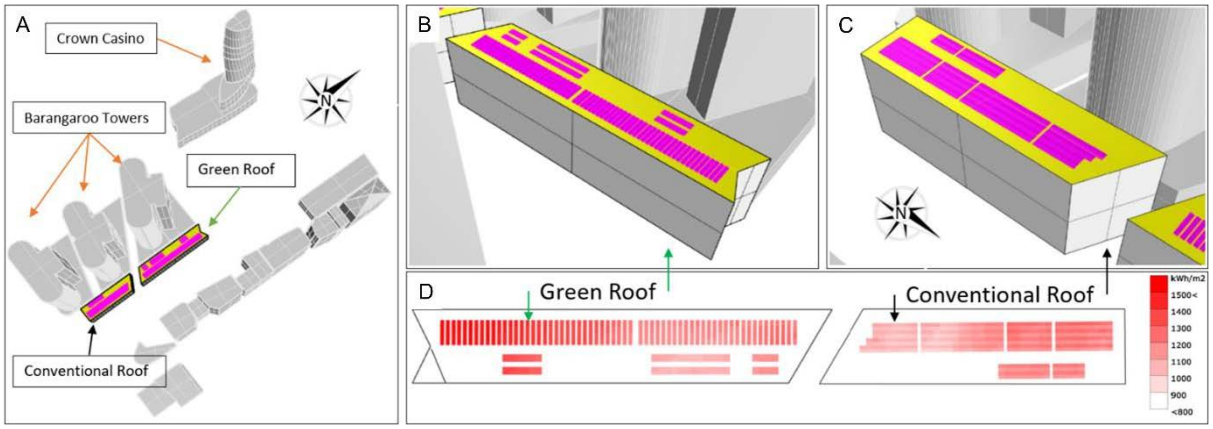

Figure 26. Rhino 3D model of; A) the Barangaroo district to determine the effect of urban geometries on reflectance and shading; B) the as-built bio-solar array; C) the conventional solar array; D) the average annual solar radiation received for each rooftop. Pink regions correspond to the panel layout for each roof, yellow regions represent the roof surface irrespective of plant/concrete coverage. Model dimensions are not to scale.

2.4 Data collection and corrections

Each solar array hosted a range of environmental sensors including ambient temperature and global horizontal irradiance (GHI). All environmental and solar data was uploaded to the SolarEdge monitoring platform for management. This monitoring platform could retrieve time-matched environmental measurements such as temperature from the local NSW Government weather station situated at Observatory Hill (Gauge 066062: approximate 590 linear meters).

Solar energy output data was collected from the SolarEdge monitoring web-platform on a fortnightly basis to coincide with on-site fortnightly onsite inspections. Solar energy outputs were collected for each inverter and summed each fortnight for both buildings. Rooftop pyranometers recorded GHI as the average hourly light intensity for each site.

Four corrections were applied to the gross energy output of the BSGR to account for differences between the two systems, resulting in a total reduction of the recorded energy output of ~19.8%. First, to account for differences in system capacity (BSGR: 131.14; CSR: 110.72 kWp), the BSGR output was reduced by ~15.54% (Table 10; Consideration 1). BSGR outputs were then reduced by a further 1.2% to account for losses associated with the age of the panels that were on CSR (Table 10; Consideration 5), and 3.1% to account for differences in panel efficiency (Table 10; Consideration 6). Output

reductions for efficiency and age were based on the known differences or degradation rates of the two systems, as per the manufacturer specifications. Lastly, to account for differences in the temperature coefficients of the two systems (BSGR: -0.29%/1°C; CSR -0.38%/1°C above 25°C), BSGR energy outputs were reduced by 0.09%/°C for each 1°C panel temperatures were above 25°C (Table 10; Consideration 7) (See Supplementary Figure 8 for an infographic detailing these corrections).

As this study utilised the unique opportunity to analyse an *in-situ* commercial BSGR with a spatially unconfounded CSR of nearly identical size, two considerations involving convection air flow could not be addressed (Table 10; Considerations 8 and 9). Above and below panel convection could potentially influence the cooling potential of the system, and therefore energy output. However, both rooftops were modelled prior to construction, and for each roof the optimal layouts were chosen to maximise energy yield, along with facilitating planting, survival, and ease of maintenance of plant material on the BSGR. Therefore, while this study cannot quantify the effect of above and below panel convection, comparisons were made inclusive of these differences in roof design. It is likely that other commercial scale BSGRs would utilise panel designs based on these criteria. It is also known that in the surrounding region, most CSR solar arrays are designed similarly to the CSR in this study (based on satellite imagery).

*Table 10. List of considerations and variance between buildings/solar arrays. Each consideration was either addressed (Yes), excluded (No), or randomized (N/A) based on the scope of the project. Specific issue is described in **bold** and the response in* italics*.*

Considerations	Addressed	Comments
1. System Capacity	Yes	**The peak nominal power of each roof was different, with a variance in system size of 20.42 kWp (15.54%).** *Bio-solar roof energy output was reduced by ~15.54% to account for the difference between system sizes.*
2. Insolation: Shading	Yes	**Modules across and between roofs will experience shading differently due to urban geometries.** *Solar modelling was employed, and the observed performance was plotted against a standardised light profile through linear regression analysis. This aimed to achieve a standardised performance based on simulated light conditions within the confines of the seasonal light observed for each site.*
3. Insolation: Soiling	Yes	**Modules were impacted by soiling differently due to tilt, age and cleaning routines.** *Each roof was visually inspected fortnightly for the duration of the study and soiling was monitored. In instances where soiling was observed, building management organised cleaning which was conducted prior to the proceeding fortnight's inspection.*
4. Insolation: Array layout	Yes	**Module azimuth of each roof resulted in different insolation that PV panels were exposed to.** *Panel azimuth could not be changed for this study, however building architects and engineers consulted solar models to determine the optimal layout for each building with respect to the physical properties of each roof. Differences in azimuth and tilt were attributed by design teams to the specific physiological requirements of the green roof.*
5. Module: Degradation losses	Yes	**System age differed between roofs and the calculated efficiency of each system varied between manufacturers.** *The panel age difference between systems was accounted for by reducing the output of the panels on the green roof (~1.2%) for equivalence with the conventional roof.*
6. Module: Panel efficiency	Yes	**Module efficiency differed between solar arrays.** *The modules used on the green roof were rated 22.6% efficient compared to 19.6% on the conventional roof. As such, green roof outputs were reduced by ~3.1%.*
7. Module: Temperature coefficients	Yes	**Modules will respond to temperature fluctuations differently**. *The temperature coefficients of the BSGR and CSR modules were -0.29%/°C and -0.38%/°C, respectively for temperatures over 25°C. In instances where BSGR panel temperatures exceeded 25°C, output was reduced by the difference in temperature coefficients (0.09%/°C) to simulate output losses similar to the panels deployed on the conventional roof.*
8. Convection: Below panel	No	**Module azimuth (Green roof: North ballast layout; Conventional roof: East-West accordion layout) resulted in different convective heat transfer opportunities on the rear surface of the panels. Module temperatures will be impacted by this.** *The effect of convective heat transfer was not specifically addressed in this instance, and therefore the comparisons made can only be representative of the two solar arrays as built. Temperature variation of panels attributable to building design has been previously explored and directly linked to the function of the green roof through evapotranspiration* [305].
9. Convection: Above panel	No	**Module tilt (Green roof: 15° and 2°; Conventional roof: 5°) resulted in different convective heat transfer opportunities on the front surface of the panels. Module temperatures will be impacted by this.** *Module tilt could not be manipulated in this study and therefore convective heat transfer could not be equalised. Therefore, convective heat transfer owing to tilt was not assessed. The comparisons made are thus representative of the two solar arrays as built.*
10. Mismatch Losses	N/A	**No two modules will be electrically identical which incurs mismatch losses. These will limit the PV performance.** *Electrical mismatch losses are inherent in a multi-panel system. It is assumed in this study, and all studies on commercial systems, that mismatch losses would be randomly distributed across the roofs and any effects associated with panel mismatch were therefore be randomised within this design.*

2.5 Analysis

2.5.1 On-site measurements

Both solar exposure (expressed as GHI), as well as temperature were recorded locally for each roof. Both roofs were equipped with pyranometers, as well as ambient and panel temperature sensors. GHI was recorded for each building on a continuous timescale and averaged hourly. Both panel and ambient temperatures were recorded on a continuous timescale and averaged hourly. All on-site data was collected weekly though the online SolarEdge monitoring platform.

2.5.2 Regression analysis

To determine the theoretical performance of each roof under a standardised lighting scenario, a multiple linear regression model was generated for hourly energy output using GHI, roof, and season as predictors. The model was as follows: Energy output (kWh) = (GHI × 0.0817) + (Bio-solar Roof × 0.978) + (Spring × 2.682) + (Summer × 2.009) + 0.613 (Intercept), with an R^2 of 0.90 ($p < 0.0001$) (R^2 or coefficient of determination represents the proportion of variance in energy output that is explained by the predictors of the model, on a scale of 0-1). The model output was then used to compare the estimated performance of each roof under standardised on-site conditions. Input GHI spanned from 25 W/m^2 (minimum daytime irradiance) to the maximum shared irradiance for both roofs per season (745, 796, and 752 W/m^2 for Spring, Summer and Autumn respectively). Results were deemed significant at $\alpha = < 0.05$ (α or significance level represents the probability of the analysis yielding a Type I error, that is the risk of a false-positive result).

2.5.3 Alternative performance metrics

In addition to energy production, solar systems are often described in respect to their economic and environmental/social benefits. In this sense, the energy outputs of both buildings can be described in relation to the energy savings in dollars, as well as the mitigation of e-CO_2 (carbon dioxide equivalent greenhouse gasses) emissions related to the use of renewable energy as opposed to energy from a fossil fuel powered grid. Additionally, plant matter on a green roof could also contribute to the removal of ambient CO_2 through photosynthesis and biomass growth, with the total CO_2 removal/mitigation being relatable to the CO_2 abatement from planting of urban trees.

To calculate the financial value generated through the use of the solar arrays on each building, the net output of each roof was multiplied by the retail energy costs (AUD $317.5 MWh) as described by the

Australian Energy Regulator (AER) for the time period [389]. The mitigation of greenhouse gas emissions was calculated using the NSW National Greenhouse Accounts Factor of 0.81 kg e-CO2/kWh [390], and the CO_2 removal potential of the plant material on the bio-solar roof was estimated according to Shafique et al., [391]. A translation of clean energy produced to "trees planted" equivalents was calculated using the ratio of 0.0117:1 trees per kWh as outlined by US EPA [392].

3. Results and Discussion

3.1 Observed difference between Bio- and Conventional solar

The Rhino 3D solar model predicted an annual GHI exposure difference between the BSGR and CSR of 6% due to surrounding buildings both blocking and reflecting light. However, during the 237 days of this study, the measured light exposure was both greater than the Rhino model predicted, and varied significantly between seasons. On average, the BSGR received 4.37 and 61.31% more GHI than the CSR in Spring and Autumn respectively, whilst receiving 5.67% less GHI in Summer (Figure 3A). While the current analysis did not incorporate the Winter months, or the full date range of Spring, the observed solar exposure was more than double (15.72%) that predicted by the Rhino 3D predictive model. It is therefore evident that conducting on-site monitoring for environmental variables such as GHI and temperature, which are two key factors in solar energy outputs, are paramount for these types of assessments.

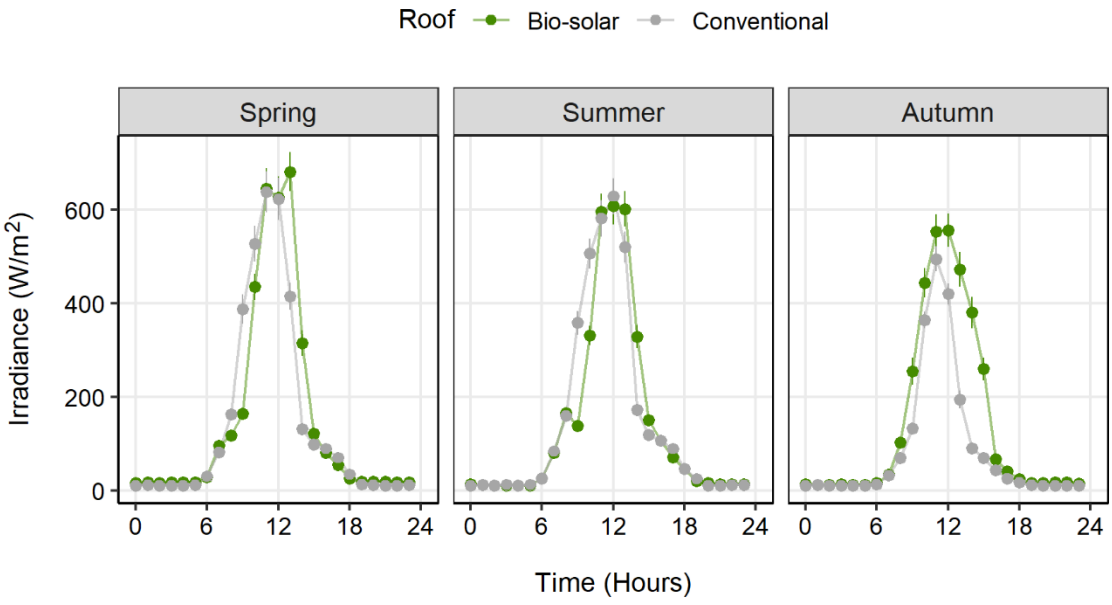

Figure 27. Mean ± SEM hourly GHI reported by on-site pyranometers during each season for both roofs. Within season variance in light availability are largely attributed to urban geometries, and between season variance to seasonal day-arc. During Spring and Autumn, the

BSGR received an average of 4.37% and 61.31% more GHI than the CSR, however in Summer the CSR received an average of 5.67% more GHI than the BSGR.

For the duration of this study, the BSGR maintained an average ambient temperature 1.00, 1.12 and 0.72°C cooler than the CSR (Figure 28A) for Spring, Summer and Autumn respectively. However, during peak GHI hours (11 am-2 pm inclusive (Figure 27)), the BSGR ambient temperatures were only 0.44, 0.95 and 0.26°C cooler than the CSR (28A). Despite ambient roof temperature not being substantially different between buildings, a previous study conducted by Fleck et al., [305] on the same two roofs found a significant difference between the two rooftop microclimates (the temperature gradient ~1m from the surface of the roof/plant foliage). One unexplored aspect from this previous study was the potential cooling effect of the BSGR on the solar array. Below-panel temperatures were up to 6 and 11°C cooler on the BSGR than the CSR during Spring and Summer, respectively. In this study however we observed a substantial reduction in solar panel temperature during peak GHI hours, which aligns with the previously reported below-panel temperatures [305]. This effect is more likely due to the evapotranspiration and reduced latent heat/solar reflectance of the plant material than panel orientation, where plant foliage may apply a foliage-specific drag coefficient [393], slowing or reducing the total airflow beneath panels, and thus reducing the effect of below-panel convection to some degree. However, as this was not specifically measured in the current study the effect of below-panel convection cannot be excluding as a contributing factor.

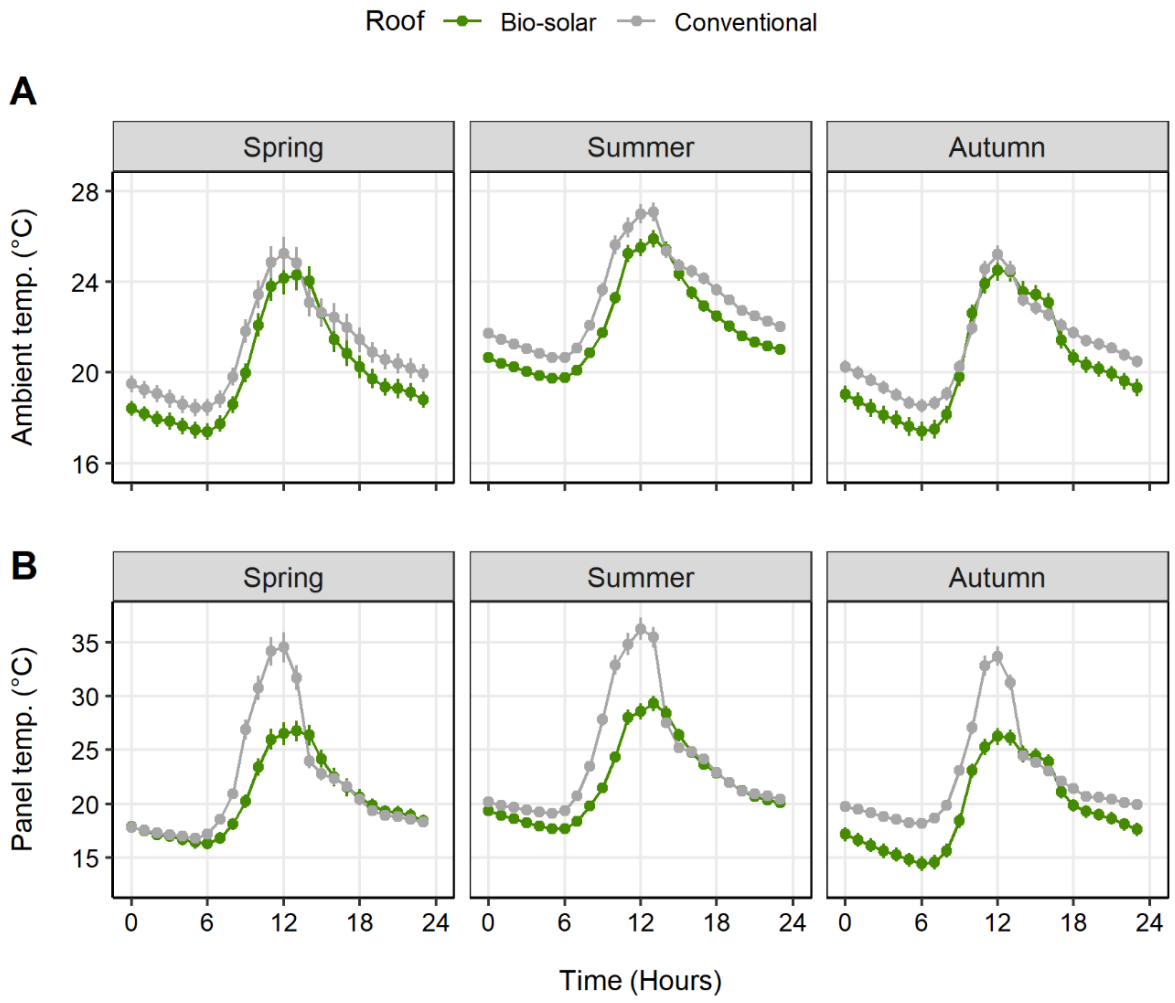

Figure 28. Mean ± SEM hourly ambient (A) and panel temperatures (B) reported by on-site temperature sensors during each season for both roofs. The ambient rooftop and panel temperatures of the BSGR were on average 1.00, 1.12 and 0.72°C and 1.50, 2.10 and 2.88°C cooler than the CSR in Spring, Summer and Autumn, respectively. During peak GHI hours (11:00 to 14:00 inclusive), ambient and panel temperatures on the BSGR was on average 0.44, 0.95 and 0.26°C and 4.68, 4.95 and 4.98°C cooler than the CR in Spring, Summer and Autumn, respectively.

The BSGR panel temperatures were 1.50, 2.10 and 2.88°C cooler than those on the CSR in Spring, Summer and Autumn, respectively, however during peak GHI hours, the BSGR was 4.68, 4.95 and 4.98°C cooler for the same time period (28B). These temperature reductions are significant as solar panel performance decreases above 25°C [277]. In this study, the temperature coefficients of the BSGR and CSR were -0.29 and -0.38% for each 1°C above 25°C. It is therefore evident that the BSGR was able to mitigate performance loss due to temperature by 1.36, 1.44 and 1.44% during peak GHI hours in Spring, Summer and Autumn respectively.

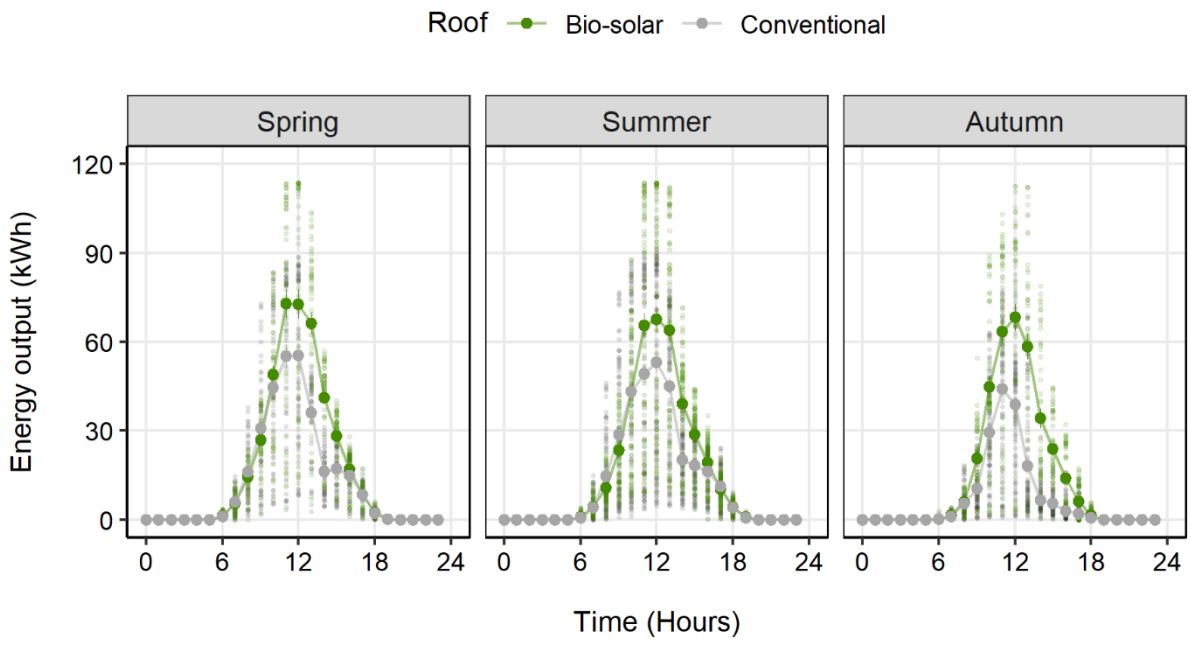

Figure 29. Mean ± SEM hourly energy output (kWh) during each season for both roofs. The BSGR generated an average 32.52, 21.25 and 107.29% more kWh than the CSR during Spring, Summer and Autumn, respectively. Differences between BSGR and CSR maximum power outputs were 25.14, 20.35 and 29.8 kWh for Spring, Summer and Autumn respectively.

For each season, the average hourly energy output for the BSGR was 16.85 ± 0.76 (SEM), 15.66 ± 0.58 and 14.30 ± 0.74 kWh, whereas the CSR outputs were 12.71 ± 0.58, 12.92 ± 0.48 and 6.90 ± 0.32 kWh (Figure 29), although it appears that these performance differences are predominantly driven by solar exposure (Figure 27). However, despite the variance in GHI exposure between seasons, and the clear effect of the urban geometry (which can be seen in Figure 27: Spring; 8 am-10 am and 1 pm-3 pm, Summer; 9 am-11 am and 1 pm-3 pm, Autumn; 8 am-3 pm), in instances where the solar exposure was approximately equal, the energy output of the BSGR was substantially higher than the CSR. The BSGR produced an average of 17.71 and 17.32 (Spring), and 16.45 and 14.47 (Summer) kWh more energy than the CSR (Figure 29) at 11 am and 12 pm, respectively. This was likely due to differences in panel temperature, caused by the evapotranspiration effect of the BSGR and the resulting cooler microclimate [305,394] (Figure 28). Differences in solar irradiance aside (Figure 27), the BSGR in this study had a LAI of 4.35, which would likely have increased the cooling potential of the BSGR to a higher degree than those BSGRs studied previously [260,395]. However, due to the discrepancies in solar exposure, it is difficult to isolate the primary causative effect for the increased energy output of the BSGR, where the BSGR produced an average of 32.52, 21.25 and 107.29% more energy for Spring, Summer, and Autumn, respectively (Figure 29). As such, the observed system performance of both systems was modelled under standardised lighting conditions to eliminate the effect of the increased solar exposure recorded on the BSGR.

3.2 Modelled difference between Bio-solar and Conventional solar

To eliminate variability caused by the effect of urban geometries and seasonal day arc, a multiple linear regression model was employed using GHI, roof and season as predictors (Figure 30). Under standardised lighting scenarios, the BSGR outperformed the CSR by 4.14, 4.16 and 5.21% for Spring, Summer and Autumn, respectively. For the duration of the study, on average, the BSGR produced 4.5% more energy than the CSR at any given light level.

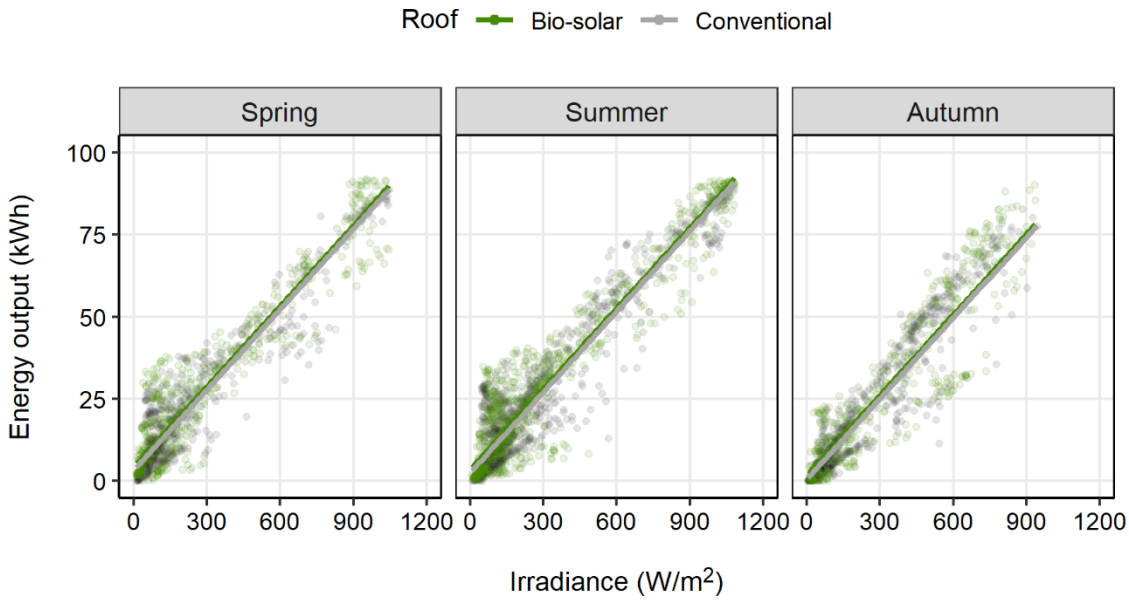

Figure 30. Daytime irradiance versus energy output reported by on-site sensors during each season for both roofs. Lines depict fitted multiple linear regression model: Energy output (kWh) = (GHI x 0.0817) + (BSGR x 0.978) + (Spring x 2.009) + 0.613 (Intercept) with $R^2 = 0.90$ ($p < 0.0001$).

Previous literature comparing PV system performance varies in the metrics by which system efficiencies have been reported, with authors reporting either total energy output for a given period, or the average difference in system performance for a specified period (Table 11). Most studies have been conducted on small experimental or pilot scale systems, with few testing *in-situ* commercial scale BSGRs with the appropriate controls. The performance differences presented here are higher than those previously reported from both experimental and pilot scale studies BSGR (Table 11).

The study that achieved the closest average system performance to ours was conducted by Hui and Chan [386] in Hong Kong (Köppen climate type Cfa), who reported a 4.3% increase in performance by a BSGR when compared to an internal control roof. This study used simulations and modelling to estimate the performance increase of a commercial BSGR, reporting an increase of 8.3% in the total energy output compared to a simulated CSR [386]. While the average performance difference

between Hui and Chan's study and the efficiencies reported here are similar, the total energy produced varies substantially.

Table 11. Comparison of previous literature to this study in respect to; study location, Köppen climate classification, study type, study duration, bio-solar array size/panel coverage (m^2), comparison made, and difference in solar energy output between treatments. Results are reported as total energy output (tot) or average difference in system performance (sys).

Study	Location	Köppen	Type	Duration	Size	Comparison	Result
This study	***Sydney, Australia***	***Cfa***	***Experimental & Simulation***	***8 months (237 days)***	***593.96 m^2***	***Commercial bio-solar vs independent conventional PV***	***4.5% (sys) 23.83% (tot)***
Nagengast et al., [379]	Pittsburgh, USA	Cfa	Experimental & Simulation	16 months	87 m^2	Model bio-solar vs internal PV-black roof	0.8-1.5% (tot)
Köhler et al., [396]	Germany	Cfb	Pilot Experiment	12 months	Undisclosed	Variable model bio-solar vs internal PV-bitumen roofs	6.5% (tot)
Perez et al., [387]	New York City, USA	Cfa	Pilot Experiment & Simulation	10 months	Undisclosed	Bio-solar vs internal PV gravel	2.42% (tot)
Hui & Chan, [386]	Hong Kong	Cfa	Pilot Experiment & Simulation	1 days 12 months	Undisclosed *2,494 m^2*	Bio-solar vs internal conventional PV	4.3% (sys) 8.3% (tot)
Chemisana & Lamnatou, [260]	Spain	BSk	Pilot Experiment	5 days	1.69 m^2	Model bio-solar vs internal PV gravel	1.29-3.33% (tot)
Osma-Pinto & Ordóñez-Plata [65]	Colombia	Af	Pilot Experiment	Undisclosed	15 m^2	Model bio-solar vs internal PV-black roof	0.9-1.7% (sys)
Ogaili & Sailor, [259]	Portland, USA	Csb	Pilot Experiment	3 months	6.6 m^2	Model bio-solar vs internal PV-black/white roof	0.8-1.2% (sys)
Alshayeb & Chang, [68]	Kansas, USA	BSk	Pilot Experiment	12 months	14.7 m^2	Model bio-solar vs internal PV-black roof	3.3% (sys) 1.4% (tot)
Kaewpraek et al, [397]	Thailand	Am	Pilot Experiment	1 months	13.58 m^2	Model bio-solar vs internal PV-grey roof	2% (sys) 5% (tot)

Differences between previous findings and the results presented here may be influenced by study duration or plant selection. For many studies ([379], [396], [387], [68]), the inclusion of the winter months may have reduced the difference in system performance either due to the cooler weather reducing the impact of the BSGR, or reduced solar exposure reducing the performance of both systems. It is potentially possible that the inclusion of winter months in the current study would have also reduced the average system performance and possibly the total energy output difference. However, for the Spring, Summer and Autumn months, our reported average efficiencies are higher than previously reported. Additionally, many past studies have utilised plants from the genus *Sedum* for their experimental BSGRs [260,386]. This Crassulacean species has substantially lower LAI and practical planting densities [28] than many commercial *in-situ* systems, such as the one tested in the current study. A higher LAI and planting density would substantially increase the evapotranspiration effect, reduce latent heat, and increase the solar reflectance of the BSGR [277,296], thus improving the thermal regulation properties of the space [64].

It is therefore plausible that the installation and use of BSGRs in similar regions and climates of the world to the current work would stand to gain substantial increases in electrical energy generation BSGR, as well as benefit from the numerous additional services that BSGRs provide to building occupants. As such, while the results presented here are directly representative of the Eastern Australian coast and similar Cfa climates, the quantified benefits of a BSGR to provide a cooler microclimate for sustained increases in solar energy output can be applied globally.

3.3 Alternative Performance Metrics

For the period observed, the BSGR and CSR produced 74.05 and 59.80 MWh of renewable energy, with the BSGR producing 23.83% more energy than the CSR. Based on the retail consumer market price outlined by the AER [389], the BSGR and CSR offset the purchase price of energy by $23,511.52 and $18,985.29 AUD, respectively. The implementation of a green roof therefore served to increase the economic benefits of the solar array by 23.84**%** ($4,526.22 AUD; Figure 31).

While these values may appear small when compared to the scale and capital cost of the two commercial systems tested, there is a significant push by governments worldwide for the adoption of localised renewable energy within urban environments [398]. In the short term, it is expected that the financial savings gained through the use of a solar or bio-solar roof would increase from what was observed here due to growing insecurities in the energy market, especially in countries with unstable energy markets [399].

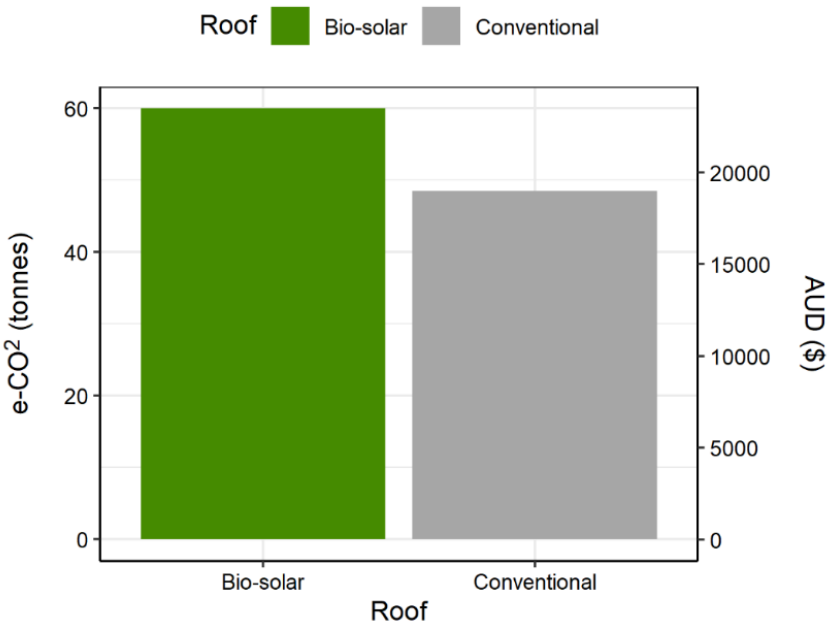

Figure 31. Performance difference between BSGR and CSR using alternative metrics. Axis-Y1 demonstrates the e-CO_2 mitigation of each system (BSGR; 59.98 t e-CO_2, CSR; 48.43 t e-CO_2), and Axis-Y2 demonstrates the price offset (BSGR; $23,511.52, CSR; $18,985.29, in $AUD) of each system. The BSGR and CSR roofs are represented in green and grey, respectively.

Based on the total energy generated by each roof, the bio-solar and conventional roofs were able to mitigate greenhouse gas (GHG) emissions of 59.98 and 48.43 t e-CO_2 respectively, based on the Australian National Greenhouse Accounts Factor (NGAF) [390]. The increase in bio-solar energy production equates to an e-CO_2 offset of 11.55 t greater than that associated with the conventional roof (Figure 7). These GHG emission calculations are based on the consumption of purchased electricity or loss from the grid, and therefore localised energy generation for each building would offset these emissions by reducing reliance on the grid. Additionally, the bio-solar roof hosted over 15,000 individual plants, which innately remove CO_2 from the atmosphere through photosynthesis during growth. Estimates derived from the literature [391,400] suggest that the green-components of the BSGR could have removed up to 1.56 t of CO_2 from the atmosphere and stored this carbon in the form of biomass gain over the duration of the study (237 days). This would increase the e-CO_2 mitigation potential of a similarly sized bio-solar roof to 13.10 t for the same period. Colloquially, the mitigation of GHG emissions is often reported as an equivalent to number of "trees planted". Here we observe equivalent tree plantings of 866.41 and 699.62 trees for the bio-solar and conventional roofs, respectively. With the inclusion of the photosynthetic removal of atmospheric carbon, the BSGR has an equivalent carbon capture/abatement to planting 192.49 urban trees and growing them for 10 years.

The inclusion of photosynthetic removal of atmospheric CO_2 in the calculation of GHG mitigation potential of green and bio-solar roofs will, however, be reduced by biomass management by green roof maintenance. The removal of atmospheric CO_2 through photosynthesis is primarily driven by biomass accumulation, both above and below ground [401]. However, for commercial green roofs, maintenance is usually performed whereby plant material is maintained at certain heights, especially when grown around solar modules. The removal of plant biomass, and the disposal of plant material will largely determine the CO_2 removal potential of a green roof, where biomass burning or composting will lead to the reemission of a proportion of the stored carbon [402]. Additionally, some carbon is sequestered by the plant roots into the substrate, and made available to rhizospheric microbes [401], and thus transferred to the substrate's labile carbon pool. From the labile carbon pool, there is the potential for microbial biomass to consume this carbon and respire or emit volatile organic compounds back into the atmosphere [401,403]. It is therefore essential that further research be conducted on how green and bio-solar roof biomass management will affect the carbon sequestration potential of this promising technology.

Lastly, a factor unexplored here that would serve to increase the e-CO_2 emission performance of bio-solar roofs is the inherent ability of green and bio-solar roofs to insulate buildings [305,391,403]. The thermal insulation effect of green and bio-solar roofs has been shown in experimental studies to have the potential to reduce annual building energy consumption by 15.1% in warm Mediterranean climates [404]. To date, few studies have successfully determined the energy saving potential of green and bio-solar roofs from experimental studies on commercial systems, and it is therefore recommended that further research be conducted on medium-large scale commercial projects to determine this effect across a range of climates.

4. Conclusions

Here we present the largest known commercial BSGR solar energy study to date. BSGR average energy output was 4.5% greater than the CSR, and the total energy output was 23.83% higher. The BSGR served to reduce the greenhouse gas emissions of the building through off-setting fossil fuel powered energy consumption by an additional 11.55 t e-CO_2, with the potential for up to 1.55 t of additional CO_2 being mitigated by the plants on the roof. This increase in energy output equates to $4,526.22 AUD and an equivalent of 192.49 “trees planted” and grown over 10 years in an urban setting. The inclusion of a green roof over a conventional solar array served to increase the energy output of the system by 23.88 kWh, reduce the GHG emissions by 0.019 t e-CO2 and produced an additional $7.62 AUD per m^2 of solar panels deployed for the duration of the study. The effect of the BSGR during the winter months, however, is unknown, and it is therefore recommended that future studies along the Eastern Australian coastline, or similar climates, conduct long term monitoring studies on *in-situ* commercial scale BSGRs and CSRs.

Declaration of competing interest

The authors declare that they have no known competing financial interests or personal relationships that could have appeared to influence the work reported in this paper.

Chapter 7: Summary and Conclusion

Green walls and green roofs are promising technologies that could make considerable contributions to the development of sustainable urban centres by providing functional benefits to building occupants, owners, and residents. Here I have demonstrated a range of variables and considerations for the sustained health and performance of indoor green walls for increased occupant comfort and safety, as well as the multifaceted benefits of green roofs in urban Sydney.

7.1 Green walls

The benefits of green walls have been well documented, with extensive laboratory testing demonstrating quantitative air quality benefits backed by survey data to quantify the psychological benefits provided to building occupants, however the exploration of the operational requirements of green walls, such as light exposure, are often overlooked. While there is substantial laboratory testing on phytoremediation performance, there is comparatively little of direct relevance to *in-situ* green walls. The work presented here on light optimisations, while conducted under laboratory conditions, has significant impacts for the future design and implementation of *in-situ* walls by identifying optimal, technically achievable conditions for growth and sustained photosynthesis. This would be expected to lead to reduced maintenance costs, as well as a healthier, more functional systems overall. Additionally, the work described in this thesis addressed the importance of appropriate plantscape design, where *in-situ* walls were observed to be poorly optimised with respect to plant species placement in relationship to their associated morphological conditions, and how this affects light availability. As this study focussed on the effects of lighting on phototropism and CO_2 removal, the findings may be of significant value to future research where phytosystems are to be incorporated into HVAC for indoor CO_2 maintenance and energy savings. It is also plausible that optimised lighting could provide beneficial circumstances for the plant rhizosphere due to a reduction in stress hormone production from the plants, which could potentially have effects in regulating the microbial community for sustained VOC remediation. This hypothesis would be worthy of future study. Long-term testing under varied lighting conditions with different plant species should thus be conducted to isolate the effect of lighting for long-term plant health and performance, both for CO_2 removal as well as VOC remediation.

An additional aspect of indoor green walls behaviour that is often overlooked in both the research and commercial spheres are biosafety aspects. As described previously, the addition of active airflow through a biological medium, especially one with moisture and nutrients, has the hypothetical potential to lead to the proliferation and dispersal of harmful bioaerosols. This thesis provides preliminary data to verify the biosafety of green walls in respect to both the aerosolisation of fungal

and bacterial particles. It is unlikely that indoor green walls will significantly contribute to the proliferation of pathogenic fungal species that carry significant impacts on human health, although this circumstance is not entirely impossible, given the variety of green wall designs and maintenance practices used worldwide. Future studies should thus be conducted globally to assess the aerosolisation of fungal and bacterial species of concern commonly associated with plants and moist/substrate environments such as *Aspergillus* spp. and *Legionella* spp. under a broad range of design and maintenance conditions. From the work conducted here however, the large, commercial indoor green wall tested produced levels of fungal propagules that were well below the World Health Organisation guidelines and posed no threat in respect to the production of pathogenic fungal species. In addition, no aerosolised *Legionella* spp. were detected. This work furthered the understanding of the green wall microbiome with the addition of 16S sequencing of an *in-situ* green wall. This work was the 3rd study of its type to be conducted worldwide, and the results obtained differed significantly both between plant species currently tested and the findings of previous work, with the previously hypothesised [45,46] "globally distributed green wall bacterial species" not present in the systems tested (*Devosia, Hyphomicrobium* and *Prosthecomicrobium*). This indicates that the rhizospheric bacterial community is significantly more diverse than previously hypothesised. The current experiment should thus be replicated both domestically on various green walls and green infrastructure, as well as globally, especially in functional systems with active airflow that are deployed for their air quality benefits.

7.2 Green roofs

In this thesis I present the most comprehensive body of work published to date on Australian green roof ecosystem services. The analysis conducted covered the thermal, hydrological, and renewable energy benefits of an extensive green roof in urban Sydney, however the research project also covered biodiversity and air quality benefits, the findings of which have been published separately. In the current study I monitored and took field measurements on an extensive green roof for up to 237 days, spanning three distinct seasons and capturing continuous data for the period. The significance of this project may not be limited to the Australian east coast but may also have applicability to climatic regions that share the *Cfa* Köppen climate type. In addition, this project is one of very few that have utilised an independent control roof of nearly identical dimensions, age, and construction materials, thus providing robust control over spatial or temporal confounding factors. This aspect of this study provides novelty, as it allows for a direct comparison with conventional infrastructure and serves to isolate the effect of the green roof more effectively than previous studies that have employed internalised controls.

The thermal performance of green roofs is well documented; however, performance estimates vary worldwide depending on climate type, LAI and other factors. Green roofs appear to be well-suited for *Cfa* climate types, such as the Eastern Australian Coast, provided they have suitable irrigation. The thermal properties presented in this thesis are indicative of high performance for the Australian climate, however hardier, drought resistant plants may be better suited for the long-term survival of the green roof due to the severe drought seasons frequently experienced outside of the (current) *La Niña* climate cycle. Conversely, the adoption of a predominantly Australian native (plant species) green roof could reduce the LAI, and therefore alter the thermal properties t from those reported here. It is nonetheless recommended that any future Australian studies should focus on assessing the thermal properties of a predominantly Australian native plant species roof, and globally, studies should focus on the assessment of extensive green roofs with different LAIs to provide a better understanding of the impact of LAI on thermal performance at the commercial scale. Additionally, if given the opportunity, future studies should be established prior to the construction of commercial systems so as to facilitate the full range of sensors required to calculate the true thermal penetration potential and assess the potential energy savings achieved through the regulation of the indoor environment (which could not be achieved here due to building design). Further, thermal assessments should be conducted on both extensive and intensive green roofs to determine if the additional substrate depth contributes to performance linearly, or if substrate depth yields diminishing results for the indoor environment. It would also be worthy of research to assess how the plant species associated with different substrate depths affect thermal performance, along with providing a cost-benefit analysis for thermal performance and roof type. These studies should preferably be carried out on a multi-year scale to accurately reflect the temporal variation in weather and climate conditions to further explore the thermal buffer potential of green infrastructure in the urban environment.

Here I have contributed to our understanding of the trace metal and stormwater retention potential of green roofs. In this study I demonstrated the ability of a green roof to mitigate anthropogenic vehicle emissions transported locally throughout the city via dry deposition. I observed a significant reduction in both soluble copper and insoluble (particle bound) copper, zinc and chromium. These metals were likely transported onto the roofs from the Sydney Harbour Bridge overpass, which carries 80,000+ cars daily, and is a significant contributor to ambient air pollution levels in the Barangaroo area. It was theorised that the dry deposited trace metals were trapped in the substrate of the green roof and thus potentially remediated through phyto-or-microbial remediation, opposed to being re-aerosolised or washed into stormwater drainage systems as would invariably occur on conventional roofing. Reductions in dry-deposited trace metals leads to a reduction in trace metal contamination entering marine systems, which has significant impacts on bioaccumulation through the natural food

webs found there. In addition to these findings, stormwater modelling was conducted, indicating that the green roof could reduce the severity of stormwater flows for rain events as infrequent as 1 in 10 years, and possibly up to 1 in 20 years. A significant reduction in stormwater flow is a substantial finding for a city like Sydney which experiences short-frequency intense flash flooding in the CBD. As roof spaces occupy up to 40% of available city space, the mass adoption of green roofs could reduce the burden on the stormwater management network in cities and reduce the intensity and frequency of these short-frequency flash floods, leading to reduced traffic congestion and less flood damage in the CBD during rain events. Through this work it is evident that green roofs have tangible benefits for both pollution mitigation and stormwater management in the Sydney CBD, however future studies should be conducted on longer time scales and should also incorporate post-rain events to determine the trace metal background prior to dry deposition. Additionally, stormwater flow rate modelling should be conducted again after the current *La Niña* cycle in Australia to include the additional environmental data (current historical data is heavily skewed by long drought seasons) and to assess how green roofs might manage less frequent stormwater volumes and flows.

Lastly, in this thesis I present the largest scale, comparative *in-situ* commercial Bio-solar green roofs. The results presented here represent amongst the highest performance demonstrated in any study worldwide, with the *Bio-solar* roof (a green roof with integrated solar arrays) producing an ***average of 4.5% more electricity at any given light level***. The observed performance difference between the Bio-solar and conventional roofs ranged from 20–107% increase in energy output, depending on the season. The results presented here are significant both for the generation of sustainable energy, but also as a demonstration that building owners/stakeholders should not have to choose between either a green roof or a solar roof, rather that there and many benefits for *Bio-solar* green roofs. The increase in energy generation can also be considered from other perspectives, with the *Bio-solar* roof energy saving equivalent to the planting of an additional 200 urban trees (grown over 10 years) when compared to the conventional roof based on CO_2 mitigation, generating over $4,500 AUD more electricity (in the given 9-month study period), and contributing to the mitigation of CO_2 emissions by an additional 13.11 t e-CO_2 mitigation, however, requires the responsible disposal of plant biomass during maintenance, as burning biomass will re-release some of the CO_2 captured during photosynthesis. The sustainable use of plant-cuttings from urban forestry is an aspect not addressed in the current work, but one which clearly has a strong bearing on the sustainability performance of any green initiative. Future studies that utilise modelling should ensure that the input data comes from a seasonally robust dataset, preferably collected over several years. In addition, future studies should aim to manipulate, or monitor roofs with varied LAIs to assess the effect of LAI on evapotranspiration and how it impacts *Bio-solar* energy output on a commercial scale.

In Chapters 2 and 3 of this thesis, I have determined and tested best practise lighting conditions for sustained plant performance within the indoor environment, as well as demonstrating the potential for different biosafety risks associated with indoor green infrastructure. The thesis further contributes to indoor green infrastructure research with the 3rd ever global study (and 1st study in the Southern hemisphere) describing the microbial community of a commercial active green wall, with results that contrast with previous studies. Further, Chapters 4, 5 and 6 demonstrate the wide array of services that can be provided by extensive green roofs in the Sydney context. The potential reduction in energy consumption through heat regulation by green roofs could be substantial, as well as the reduced reliance on the conventional energy grid through increase power output from *Bio-solar* systems, which could in turn significantly increase the sustainability of built urban spaces. My work also demonstrates the significance of green infrastructure through contributions to the regulation of the stormwater network, which could serve to decrease damage and inconvenience to urban dwellers during the regular short frequency, semi-intensive flash flooding commonly experienced in the Sydney CBD. These studies indicate the potential benefits of the mass implementation of green infrastructure throughout Sydney, and similar Australian cities, which are essential if Australians are to meet their local and global sustainability targets, like the United Nations Sustainable Development Goals, specifically SDG 11 ("Sustainable cities and communities"). The critical component of my research presented in this thesis is the study of commercial systems *in-situ* to represent the quantification of real-world benefits that green infrastructure currently provide. If future developments in the Sydney region can be designed with the sustainability aspects described here, a large contribution to future sustainability would be possible, potentially making Sydney the driving force for sustainable cities in Australia.

References

[1] N.H. Wong, Y. Chen, C.L. Ong, A. Sia, Investigation of thermal benefits of rooftop garden in the tropical environment, Build. Environ. 38 (2003) 261–270. https://doi.org/10.1016/S0360-1323(02)00066-5.

[2] T. Pettit, P.J.J. Irga, F.R.R. Torpy, Towards practical indoor air phytoremediation: A review, Chemosphere. 208 (2018) 960–974. https://doi.org/10.1016/j.chemosphere.2018.06.048.

[3] A.J. Cohen, M. Brauer, R. Burnett, H.R. Anderson, J. Frostad, K. Estep, K. Balakrishnan, B. Brunekreef, L. Dandona, R. Dandona, V. Feigin, G. Freedman, B. Hubbell, A. Jobling, H. Kan, L. Knibbs, Y. Liu, R. Martin, L. Morawska, C.A. Pope, H. Shin, K. Straif, G. Shaddick, M. Thomas, R. van Dingenen, A. van Donkelaar, T. Vos, C.J.L. Murray, M.H. Forouzanfar, Estimates and 25-year trends of the global burden of disease attributable to ambient air pollution: an analysis of data from the Global Burden of Diseases Study 2015, Lancet. 389 (2017) 1907–1918. https://doi.org/10.1016/S0140-6736(17)30505-6.

[4] R. Barro, J. Regueiro, M. Llompart, C. Garcia-Jares, Analysis of industrial contaminants in indoor air: Part 1. Volatile organic compounds, carbonyl compounds, polycyclic aromatic hydrocarbons and polychlorinated biphenyls, J. Chromatogr. A. 1216 (2009) 540–566. https://doi.org/10.1016/j.chroma.2008.10.117.

[5] N.E. Klepeis, W.C. Nelson, W.R. Ott, J.P. Robinson, A.M. Tsang, P. Switzer, J. V. Behar, S.C. Hern, W.H. Engelmann, The National Human Activity Pattern Survey (NHAPS): A resource for assessing exposure to environmental pollutants, J. Expo. Anal. Environ. Epidemiol. 11 (2001) 231–252. https://doi.org/10.1038/sj.jea.7500165.

[6] G. Hutton, Air pollution: global damage costs from 1900 to 2050, Cambridge University Press, Cambridge, 2013. https://doi.org/10.1017/CBO9781139225793.

[7] C. Jia, S. Batterman, C. Godwin, VOCs in industrial, urban and suburban neighborhoods-Part 2: Factors affecting indoor and outdoor concentrations, Atmos. Environ. 42 (2008) 2101–2116. https://doi.org/10.1016/j.atmosenv.2007.11.047.

[8] K. Balakrishnan, S. Dey, T. Gupta, R.S. Dhaliwal, M. Brauer, A.J. Cohen, J.D. Stanaway, G. Beig, T.K. Joshi, A.N. Aggarwal, Y. Sabde, H. Sadhu, J. Frostad, K. Causey, W. Godwin, D.K. Shukla, G.A. Kumar, C.M. Varghese, P. Muraleedharan, A. Agrawal, R.M. Anjana, A. Bhansali, D. Bhardwaj, K. Burkart, K. Cercy, J.K. Chakma, S. Chowdhury, D.J. Christopher, E. Dutta, M. Furtado, S. Ghosh, A.G. Ghoshal, S.D. Glenn, R. Guleria, R. Gupta, P. Jeemon, R. Kant, S. Kant, T. Kaur, P.A. Koul, V. Krish, B. Krishna, S.L. Larson, K. Madhipatla, P.A. Mahesh, V. Mohan, S. Mukhopadhyay, P. Mutreja, N. Naik, S. Nair, G. Nguyen, C.M. Odell, J.D. Pandian, D. Prabhakaran, P. Prabhakaran, A. Roy, S. Salvi, S. Sambandam, D. Saraf, M. Sharma, A. Shrivastava, V. Singh, N. Tandon, N.J. Thomas, A. Torre, D. Xavier, G. Yadav, S. Singh, C. Shekhar, T. Vos, R. Dandona, K.S. Reddy, S.S. Lim, C.J.L. Murray, S. Venkatesh, L. Dandona, The impact of air pollution on deaths, disease burden, and life expectancy across the states of India: the Global Burden of Disease Study 2017, Lancet Planet. Heal. 3 (2019) e26–e39. https://doi.org/10.1016/S2542-5196(18)30261-4.

[9] U. Satish, M.J. Mendell, K. Shekhar, T. Hotchi, D. Sullivan, Concentrations on Human Decision-Making Performance, Environ. Health Perspect. 120 (2012) 1671–1678.

[10] L. Zuo, D. Wu, L. Yu, Y. Yuan, Phytoremediation of formaldehyde by the stems of Epipremnum aureum and Rohdea japonica, Environ. Sci. Pollut. Res. 29 (2022) 11445–11454. https://doi.org/10.1007/s11356-021-16571-x.

[11] T. Pettit, P.J. Irga, N.C. Surawski, F.R. Torpy, An assessment of the suitability of active green walls for NO2 reduction in green buildings using a closed-loop flow reactor, Atmosphere (Basel). 10 (2019) 1–17. https://doi.org/10.3390/ATMOS10120801.

[12] B. Mitchell, Building materials can be a major source of indoor air pollution, 2013.

[13] G. Liu, M. Xiao, X. Zhang, C. Gal, X. Chen, L. Liu, S. Pan, J. Wu, L. Tang, D. Clements-Croome, A review of air filtration technologies for sustainable and healthy building ventilation, Sustain. Cities Soc. 32 (2017) 375–396. https://doi.org/10.1016/j.scs.2017.04.011.

[14] G. Hernandez, S.L. Wallis, I. Graves, S. Narain, R. Birchmore, T.A. Berry, The effect of ventilation on volatile organic compounds produced by new furnishings in residential buildings, Atmos. Environ. X. 6 (2020) 100069. https://doi.org/10.1016/j.aeaoa.2020.100069.

[15] L. Pérez-Lombard, J. Ortiz, C. Pout, A review on buildings energy consumption information, Energy Build. 40 (2008) 394–398. https://doi.org/10.1016/j.enbuild.2007.03.007.

[16] Intergovernmental Panel on Climate Change, Climate Change 2014: Mitigation of Climate Change, Cambridge University Press, 2015. https://doi.org/10.1017/CBO9781107415416.

[17] A. Medl, R. Stangl, F. Florineth, Vertical greening systems – A review on recent technologies and research advancement, Build. Environ. 125 (2017) 227–239. https://doi.org/10.1016/j.buildenv.2017.08.054.

[18] R.W.F. Cameron, J.E. Taylor, M.R. Emmett, What's "cool" in the world of green façades? How plant choice influences the cooling properties of green walls, Build. Environ. 73 (2014) 198–207. https://doi.org/10.1016/j.buildenv.2013.12.005.

[19] T.A. Moya, A. van den Dobbelsteen, M. Ottelé, P.M. Bluyssen, A review of green systems within the indoor environment, Indoor Built Environ. 28 (2019) 298–309. https://doi.org/10.1177/1420326X18783042.

[20] P. Bevilacqua, The effectiveness of green roofs in reducing building energy consumptions across different climates. A summary of literature results, Renew. Sustain. Energy Rev. 151 (2021) 111523. https://doi.org/10.1016/j.rser.2021.111523.

[21] T. Pettit, P.J. Irga, F.R. Torpy, The in situ pilot-scale phytoremediation of airborne VOCs and particulate matter with an active green wall, 1 (2019) 33–44.

[22] S. Tifferet, I. Vilnai-Yavetz, Phytophilia and Service Atmospherics: The Effect of Indoor Plants on Consumers, Environ. Behav. 49 (2017) 814–844. https://doi.org/10.1177/0013916516669390.
[23] K.M. Zielinska-Dabkowska, J. Hartmann, C. Sigillo, LED light sources and their complex set-up for visually and biologically effective illumination for ornamental indoor plants, Sustain. 11 (2019). https://doi.org/10.3390/su11092642.
[24] J. Wang, A. Garg, N. Liu, D. Chen, G. Mei, Experimental and numerical investigation on hydrological characteristics of extensive green roofs under the influence of rainstorms, Environ. Sci. Pollut. Res. (2022). https://doi.org/10.1007/s11356-022-19609-w.
[25] A. Bellazzi, B. Barozzi, M.C. Pollastro, I. Meroni, Thermal resistance of growing media for green roofs: To what extent does the absence of specific reference values potentially affect the global thermal resistance of the green roof? An experimental example, J. Build. Eng. 28 (2020). https://doi.org/10.1016/j.jobe.2019.101076.
[26] B.Y. Schindler, L. Blank, S. Levy, G. Kadas, D. Pearlmutter, L. Blaustein, Integration of photovoltaic panels and green roofs: review and predictions of effects on electricity production and plant communities, Isr. J. Ecol. Evol. 62 (2016) 68–73. https://doi.org/10.1080/15659801.2015.1048617.
[27] B.Y. Schindler, L. Blaustein, R. Lotan, H. Shalom, G.J. Kadas, M. Seifan, Green roof and photovoltaic panel integration: Effects on plant and arthropod diversity and electricity production, J. Environ. Manage. 225 (2018) 288–299. https://doi.org/10.1016/j.jenvman.2018.08.017.
[28] E.I.F. Wooster, R. Fleck, F. Torpy, D. Ramp, P.J. Irga, Urban green roofs promote metropolitan biodiversity: A comparative case study, Build. Environ. 207 (2022) 108458. https://doi.org/10.1016/j.buildenv.2021.108458.
[29] B.C. Wolverton, A. Johnson, K. Bounds, Interior landscape plants for indoor air pollution abatement, 1989.
[30] B.C. Wolverton, R.C. McDonald, E.A. Watkins Jr, Foliage plants for removing indoor air pollutants from energy-efficient homes, Econ. Bot. (1984) 224–228.
[31] R. Orwell, R. Wood, J. Tarran, F. Torpy, M. Burchett, Removal of benzene by the indoor plant/substrate microcosm and implications for air quality, Water, Air Soil Pollut. 157 (2004) 193–207.
[32] R.A. Wood, R.L. Orwell, J. Tarran, F. Torpy, M. Burchett, Potted-plant/growth media interactions and capacities for removal of volatiles from indoor air, J. Hortic. Sci. Biotechnol. 77 (2002) 120–129. https://doi.org/10.1080/14620316.2002.11511467.
[33] K.J. Kim, M. Il Jeong, D.W. Lee, J.S. Song, H.D. Kim, E.H. Yoo, S.J. Jeong, S.W. Han, S.J. Kays, Y.-W. Lim, H.-H. Kim, Variation in Formaldehyde Removal Efficiency among Indoor Plant Species, HortScience. 45 (2010) 1489–1495. https://doi.org/10.21273/HORTSCI.45.10.1489.
[34] K. Kim, H. Kim, M. Khalekuzzaman, E. Yoo, H. Jung, H. Jang, Removal ratio of gaseous toluene and xylene transported from air to root zone via the stem by indoor plants, Environ. Sci. Pollut. Res. 23 (2016) 6149–6158. https://doi.org/10.1007/s11356-016-6065-y.
[35] D. Llewellyn, M. Dixon, Can Plants Really Improve Indoor Air Quality?, Second Edi, Elsevier B.V., 2011. https://doi.org/10.1016/B978-0-08-088504-9.00325-1.
[36] G. Soreanu, M. Dixon, A. Darlington, Botanical biofiltration of indoor gaseous pollutants - A mini-review, Chem. Eng. J. 229 (2013) 585–594. https://doi.org/10.1016/j.cej.2013.06.074.
[37] G. Soreanu, 12 - Biotechnologies for improving indoor air quality, in: Smart Eco-Efficient Built Environ., 2016: pp. 301–328.
[38] Z. Wang, J.S. Zhang, Characterization and performance evaluation of a full-scale activated carbon-based dynamic botanical air filtration system for improving indoor air quality, Build. Environ. 46 (2011) 758–768. https://doi.org/10.1016/j.buildenv.2010.10.008.
[39] F. Mayrand, P. Clergeau, Green roofs and greenwalls for biodiversity conservation: A contribution to urban connectivity?, Sustain. 10 (2018). https://doi.org/10.3390/su10040985.
[40] J.M. Posada, R. Sievänen, C. Messier, J. Perttunen, E. Nikinmaa, M.J. Lechowicz, Contributions of leaf photosynthetic capacity, leaf angle and self-shading to the maximization of net photosynthesis in Acer saccharum: a modelling assessment., Ann. Bot. 110 (2012) 731–741. https://doi.org/10.1093/aob/mcs106.
[41] M. Dela Cruz, J.H. Christensen, J.D. Thomsen, R. Müller, Can ornamental potted plants remove volatile organic compounds from indoor air? — a review, Environ. Sci. Pollut. Res. 21 (2014) 13909–13928. https://doi.org/10.1007/s11356-014-3240-x.
[42] P.J. Irga, P. Abdo, M. Zavattaro, F.R. Torpy, An assessment of the potential fungal bioaerosol production from an active living wall, Build. Environ. 111 (2017) 140–146. https://doi.org/10.1016/j.buildenv.2016.11.004.
[43] P.J. Irga, P. Abdo, M. Zavattaro, F.R. Torpy, An assessment of the potential fungal bioaerosol production from an active living wall, Build. Environ. 111 (2017) 140–146. https://doi.org/10.1016/j.buildenv.2016.11.004.
[44] D. Tudiwer, A. Korjenic, The effect of an indoor living wall system on humidity, mould spores and CO2-concentration, Energy Build. 146 (2017) 73–86. https://doi.org/10.1016/j.enbuild.2017.04.048.
[45] J. Russell, Y. Hu, L. Chau, M. Pauliushchyk, I. Anastopoulos, S. Anandan, M. Waring, Indoor-biofilter growth and exposure to airborne chemicals drive similar changes in plant root bacterial communities, Appl. Environ. Microbiol. 80 (2014) 4805–4813. https://doi.org/10.1128/AEM.00595-14.
[46] A. Mikkonen, T. Li, M. Vesala, J. Saarenheimo, V. Ahonen, S. Kärenlampi, J.D. Blande, M. Tiirola, A. Tervahauta, Biofiltration of airborne VOCs with green wall systems—Microbial and chemical dynamics, Indoor Air. 28 (2018) 697–707. https://doi.org/10.1111/ina.12473.
[47] B.A. Currie, B. Bass, Estimates of air pollution mitigation with green plants and green roofs using the UFORE model, Urban Ecosyst. 11 (2008) 409–422. https://doi.org/10.1007/s11252-008-0054-y.

[48] S. Sattler, I. Zluwa, D. Österreicher, The “PV Rooftop Garden”: Providing Recreational Green Roofs and Renewable Energy as a Multifunctional System within One Surface Area, Appl. Sci. 10 (2020) 1791. https://doi.org/10.3390/app10051791.
[49] Y. He, H. Yu, N. Dong, H. Ye, Thermal and energy performance assessment of extensive green roof in summer: A case study of a lightweight building in Shanghai, Energy Build. 127 (2016) 762–773. https://doi.org/10.1016/j.enbuild.2016.06.016.
[50] P. Rosasco, K. Perini, Selection of (green) roof systems: A sustainability-based multi-criteria analysis, Buildings. 9 (2019). https://doi.org/10.3390/buildings9050134.
[51] S.J. Wilkinson, C. Rose, V. Glenis, J. Lamond, Modelling a green roof retrofit in the Melbourne Central Business District, WIT Trans. Ecol. Environ. 184 (2014) 125–135. https://doi.org/10.2495/FRIAR140111.
[52] D.B. Rowe, K.L. Getter, The role of extensive green roofs in sustainable development, HortScience. 41 (2006) 1276–1285.
[53] M. Manso, I. Teotónio, C.M. Silva, C.O. Cruz, Green roof and green wall benefits and costs: A review of the quantitative evidence, Renew. Sustain. Energy Rev. 135 (2021). https://doi.org/10.1016/j.rser.2020.110111.
[54] S.E. Clemants, J. Marinelli, G. Moore, E. Peters, N. Dunne, J. Blackburn, B. Botanic, G. Website, A. Dorfman, D. Allen, Managing Editor Copy Editor Publisher The Center for Urban Restoration Ecology A collaboration between Rutgers University and Brooklyn Botanic Garden, Urban Habitats. 4 (2006) 1–26. http://www.urbanhabitats.org/v04n01/urbanhabitats_v04n01_pdf.pdf.
[55] R.A. Francis, J. Lorimer, Urban reconciliation ecology: The potential of living roofs and walls, J. Environ. Manage. 92 (2011) 1429–1437. https://doi.org/10.1016/j.jenvman.2011.01.012.
[56] R. Ciriminna, F. Meneguzzo, M. Pecoraino, M. Pagliaro, Solar Green Roofs: A Unified Outlook 20 Years On, Energy Technol. 7 (2019) 1–7. https://doi.org/10.1002/ente.201900128.
[57] G. Spolek, Performance monitoring of three ecoroofs in Portland, Oregon, Urban Ecosyst. 11 (2008) 349–359. https://doi.org/10.1007/s11252-008-0061-z.
[58] K.R. Ayub, Green Roof Performance for Stormwater Management in Malaysia, 2020. https://www.researchgate.net/profile/Aminuddin_Ab_Ghani/publication/346668637_GREEN_ROOF_PERFORMANCE_FOR_STORMWATER_MANAGEMENT_IN_MALAYSIA/links/5fcd9a7aa6fdcc697be87166/GREEN-ROOF-PERFORMANCE-FOR-STORMWATER-MANAGEMENT-IN-MALAYSIA.pdf.
[59] J.Y. Lee, M.J. Lee, M. Han, A pilot study to evaluate runoff quantity from green roofs, J. Environ. Manage. 152 (2015) 171–176. https://doi.org/10.1016/j.jenvman.2015.01.028.
[60] K. Charalambous, A. Bruggeman, M. Eliades, C. Camera, L. Vassiliou, Stormwater retention and reuse at the residential plot level-green roof experiment and water balance computations for long-term use in Cyprus, Water (Switzerland). 11 (2019) 1–11. https://doi.org/10.3390/w11051055.
[61] E. Palomo Del Barrio, Analysis of the green roofs cooling potential in buildings, Energy Build. 27 (1998) 179–193. https://doi.org/10.1016/s0378-7788(97)00029-7.
[62] S.M. dos Santos, J.F.F. Silva, G.C. dos Santos, P.M.T. de Macedo, S. Gavazza, Integrating conventional and green roofs for mitigating thermal discomfort and water scarcity in urban areas, J. Clean. Prod. 219 (2019) 639–648. https://doi.org/10.1016/j.jclepro.2019.01.068.
[63] S.E. Ouldboukhitine, R. Belarbi, I. Jaffal, A. Trabelsi, Assessment of green roof thermal behavior: A coupled heat and mass transfer model, Build. Environ. 46 (2011) 2624–2631. https://doi.org/10.1016/j.buildenv.2011.06.021.
[64] E. Grala da Cunha, C. Maria Brito Correa, R. Peil, V. Mülech Ritter, D. Hohn, H. Maieves, J. Neila González, M. Estima Silva, R. Karini Leitzke, Characterizing leaf area index of rooftop farm to assess thermal-energy performance by simulation, Energy Build. 241 (2021) 110960. https://doi.org/10.1016/j.enbuild.2021.110960.
[65] G. Osma-Pinto, G. Ordóñez-Plata, Measuring factors influencing performance of rooftop PV panels in warm tropical climates, Sol. Energy. 185 (2019) 112–123. https://doi.org/10.1016/j.solener.2019.04.053.
[66] Y. Zheng, Q. Weng, Modeling the Effect of Green Roof Systems and Photovoltaic Panels for Building Energy Savings to Mitigate Climate Change, Remote Sens. 12 (2020) 2402. https://doi.org/10.3390/rs12152402.
[67] M. Shafique, X. Luo, J. Zuo, Photovoltaic-green roofs: A review of benefits, limitations, and trends, Sol. Energy. 202 (2020) 485–497. https://doi.org/10.1016/j.solener.2020.02.101.
[68] M.J. Alshayeb, J.D. Chang, Variations of PV panel performance installed over a vegetated roof and a conventional black roof, Energies. 11 (2018). https://doi.org/10.3390/en11051110.
[69] E. Burszta-Adamiak, J. Stańczyk, J. Łomotowski, Hydrological performance of green roofs in the context of the meteorological factors during the 5-year monitoring period, Water Environ. J. 33 (2019) 144–154. https://doi.org/10.1111/wej.12385.
[70] L. Smalls-Mantey, F. Montalto, The seasonal microclimate trends of a large scale extensive green roof, Build. Environ. 197 (2021) 107792. https://doi.org/10.1016/j.buildenv.2021.107792.
[71] S.S. Cipolla, M. Maglionico, I. Stojkov, A long-term hydrological modelling of an extensive green roof by means of SWMM, Ecol. Eng. 95 (2016) 876–887. https://doi.org/10.1016/j.ecoleng.2016.07.009.
[72] K.X. Soulis, J.D. Valiantzas, N. Ntoulas, G. Kargas, P.A. Nektarios, Simulation of green roof runoff under different substrate depths and vegetation covers by coupling a simple conceptual and a physically based hydrological model, J. Environ. Manage. 200 (2017) 434–445. https://doi.org/10.1016/j.jenvman.2017.06.012.
[73] R. Castiglia Feitosa, S.J. Wilkinson, Small-scale experiments of seasonal heat stress attenuation through a combination of green roof and green walls, J. Clean. Prod. 250 (2020) 119443. https://doi.org/10.1016/j.jclepro.2019.119443.

[74] M. Razzaghmanesh, S. Beecham, F. Kazemi, Impact of green roofs on stormwater quality in a South Australian urban environment, Sci. Total Environ. 470–471 (2014) 651–659. https://doi.org/10.1016/j.scitotenv.2013.10.047.
[75] M. Razzaghmanesh, S. Beecham, The hydrological behaviour of extensive and intensive green roofs in a dry climate, Sci. Total Environ. 499 (2014) 284–296. https://doi.org/10.1016/j.scitotenv.2014.08.046.
[76] M.G. Rasul, L.K.R. Arutla, Environmental impact assessment of green roofs using life cycle assessment, Energy Reports. 6 (2020) 503–508. https://doi.org/10.1016/j.egyr.2019.09.015.
[77] Australian Bureau of Statistics, Regional Population, 2022. https://www.abs.gov.au/statistics/people/population/regional-population/latest-release#key-statistics.
[78] Australian Bureau of Statistics, Historical Population, 2019. https://www.abs.gov.au/statistics/people/population/historical-population/latest-release.
[79] Z. Liu, W. Li, Y. Chen, Y. Luo, L. Zhang, Review of energy conservation technologies for fresh air supply in zero energy buildings, Appl. Therm. Eng. 148 (2019) 544–556. https://doi.org/10.1016/j.applthermaleng.2018.11.085.
[80] S.B. Molloy, M. Cheng, I.E. Galbally, M.D. Keywood, S.J. Lawson, J.C. Powell, R. Gillett, E. Dunne, P.W. Selleck, Indoor air quality in typical temperate zone Australian dwellings, Atmos. Environ. 54 (2012) 400–407. https://doi.org/10.1016/j.atmosenv.2012.02.031.
[81] J.E. Riviere, Dermal Absorption Modelling, Springer, 2010. https://doi.org/10.1007/978-90-481-8663-1_7.
[82] C.A. Erdmann, M.G. Apte, Mucous membrane and lower respiratory building related symptoms in relation to indoor carbon dioxide concentrations in the 100-building BASE dataset, Indoor Air, Suppl. 14 (2004) 127–134. https://doi.org/10.1111/j.1600-0668.2004.00298.x.
[83] T. Vehviläinen, H. Lindholm, H. Rintamäki, R. Pääkkönen, A. Hirvonen, O. Niemi, J. Vinha, High indoor CO2 concentrations in an office environment increases the transcutaneous CO2 level and sleepiness during cognitive work, J. Occup. Environ. Hyg. 13 (2016) 19–29. https://doi.org/10.1080/15459624.2015.1076160.
[84] O. Seppänen, W.J. Fisk, Q.H. Lei, Ventilation and performance in office work, Indoor Air. 16 (2006) 28–36. https://doi.org/10.1111/j.1600-0668.2005.00394.x.
[85] D.K. Milton, Risk of sick leave associated with outdoor air supply rate, humidification, and occupant complaints, Indoor Air. 10 (2000) 212–221. https://doi.org/10.1034/j.1600-0668.2000.010004212.x.
[86] S. Gaihre, S. Semple, J. Miller, S. Fielding, S. Turner, Classroom carbon dioxide concentration, school attendance, and educational attainment, J. Sch. Health. 84 (2014) 569–574. https://doi.org/10.1111/josh.12183.
[87] M.J. Jafari, A.A. Khajevandi, S.A.M. Najarkola, M.S. Yekaninejad, M.A. Pourhoseingholi, L. Omidi, S. Kalantary, Association of sick building syndrome with indoor air parameters, Tanaffos. 14 (2015) 55–62.
[88] T. Lawrence, A. Darwich, J. Means, ASHRAE GreenGuide, 2018.
[89] T. Ben-David, M.S. Waring, Impact of natural versus mechanical ventilation on simulated indoor air quality and energy consumption in offices in fourteen U.S. cities, Build. Environ. 104 (2016) 320–336. https://doi.org/10.1016/j.buildenv.2016.05.007.
[90] D. Pearlmutter, D. Theochari, T. Nehls, P. Pinho, P. Piro, A. Korolova, S. Papaefthimiou, M.C.G. Mateo, C. Calheiros, I. Zluwa, U. Pitha, P. Schosseler, Y. Florentin, S. Ouannou, E. Gal, A. Aicher, K. Arnold, E. Igondová, B. Pucher, Enhancing the circular economy with nature-based solutions in the built urban environment: green building materials, systems and sites, Blue-Green Syst. 2 (2020) 46–72. https://doi.org/10.2166/bgs.2019.928.
[91] P.J. Irga, N.J. Paull, P. Abdo, F.R. Torpy, An assessment of the atmospheric particle removal efficiency of an in-room botanical biofilter system, Build. Environ. 115 (2017) 281–290. https://doi.org/10.1016/j.buildenv.2017.01.035.
[92] J. Newton, D. Gedge, P. Early, S. Wilson, Building greener : guidance on the use of green roofs, green walls and complementary features on buildings, Construction Industry Research & Information Association (CIRIA), London, 2007.
[93] T. Bringslimark, T. Hartig, G.G. Patil, The psychological benefits of indoor plants: A critical review of the experimental literature, J. Environ. Psychol. 29 (2009) 422–433. https://doi.org/10.1016/j.jenvp.2009.05.001.
[94] A.E. van den Berg, J.E. Wesselius, J. Maas, K. Tanja-Dijkstra, Green Walls for a Restorative Classroom Environment: A Controlled Evaluation Study, Environ. Behav. 49 (2017) 791–813. https://doi.org/10.1177/0013916516667976.
[95] E. Montacchini, S. Tedesco, T. Rondinone, Greenery for a university campus: Does it affect indoor environmental quality and user well-being?, Energy Procedia. 122 (2017) 289–294. https://doi.org/10.1016/j.egypro.2017.07.324.
[96] A. Aydogan, L.D. Montoya, Formaldehyde removal by common indoor plant species and various growing media, Atmos. Environ. 45 (2011) 2675–2682. https://doi.org/10.1016/j.atmosenv.2011.02.062.
[97] G.S. Oh, G.J. Jung, M.H. Seo, Y. Bin Im, Experimental study on variations of CO2 concentration in the presence of indoor plants and respiration of experimental animals, Hortic. Environ. Biotechnol. 52 (2011) 321–329. https://doi.org/10.1007/s13580-011-0169-6.
[98] C. Gubb, T. Blanusa, A. Griffiths, C. Pfrang, Can houseplants improve indoor air quality by removing CO2 and increasing relative humidity?, Air Qual. Atmos. Heal. 11 (2018) 1191–1201. https://doi.org/10.1007/s11869-018-0618-9.
[99] T. Moya, A. van den Dobbelsteen, M. Ottelé, P. Bluyssen, A review of green systems within the indoor environment, Indoor Built Environ. 0 (2018) 1420326X1878304. https://doi.org/10.1177/1420326X18783042.
[100] T. Pettit, P.J. Irga, F.R. Torpy, Functional green wall development for increasing air pollutant phytoremediation: Substrate development with coconut coir and activated carbon, J. Hazard. Mater. 360 (2018) 594–603. https://doi.org/10.1016/j.jhazmat.2018.08.048.
[101] F. Torpy, M. Zavattaro, P. Irga, Green wall technology for the phytoremediation of indoor air: a system for the reduction of high CO2 concentrations, Air Qual. Atmos. Heal. 10 (2017) 575–585. https://doi.org/10.1007/s11869-

016-0452-x.
[102] C.L. Tan, N.H. Wong, P.Y. Tan, M. Ismail, L.Y. Wee, Growth light provision for indoor greenery: A case study, Energy Build. 144 (2017) 207–217. https://doi.org/10.1016/j.enbuild.2017.03.044.
[103] S. Pennisi, M. van Iersel, Quantification of Carbon Assimilation by Indoor Plants in Simulated and In Situ Environments, Hortscience. 45 (2012) S94–S94.
[104] G. Egea, L. Pérez-Urrestarazu, J. González-Pérez, A. Franco-Salas, R. Fernández-Cañero, Lighting systems evaluation for indoor living walls, Urban For. Urban Green. 13 (2014) 475–483. https://doi.org/10.1016/j.ufug.2014.04.009.
[105] M.P. Kaltsidi, R. Fernández-Cañero, L. Pérez-Urrestarazu, Assessment of different LED lighting systems for indoor living walls, Sci. Hortic. (Amsterdam). 272 (2020) 109522. https://doi.org/10.1016/j.scienta.2020.109522.
[106] K.R. Cope, M.C. Snowden, B. Bugbee, Photobiological interactions of blue light and photosynthetic photon flux: Effects of monochromatic and broad-spectrum light sources, Photochem. Photobiol. 90 (2014) 574–584. https://doi.org/10.1111/php.12233.
[107] S. Karpinski, H. Gabrys, A. Mateo, B. Karpinska, P.M. Mullineaux, Light perception in plant disease defence signalling, Curr. Opin. Plant Biol. 6 (2003) 390–396. https://doi.org/10.1016/S1369-5266(03)00061-X.
[108] European committee for standardization, BSI Standards Publication Light and lighting — Lighting of work places Part 1 : Indoor work places, (2011) 1–57.
[109] F. Torpy, P. Irga, M. Burchett, Profiling indoor plants for the amelioration of high CO 2 concentrations, Urban For. Urban Green. Urban Green. 13 (2014) 227–233.
[110] J. Kim, S.W. Kang, C.H. Pak, M.S. Kim, Changes in leaf variegation and coloration of english ivy and polka dot plant under various indoor light intensities, Horttechnology. 22 (2012) 49–55. https://doi.org/10.21273/horttech.22.1.49.
[111] A. Goyal, B. Szarzynska, C. Fankhauser, Phototropism: At the crossroads of light-signaling pathways, Trends Plant Sci. 18 (2013) 393–401. https://doi.org/10.1016/j.tplants.2013.03.002.
[112] L. Pérez-Urrestarazu, R. Fernández-Cañero, A. Franco, G. Egea, Influence of an active living wall on indoor temperature and humidity conditions, Ecol. Eng. 90 (2016) 120–124. https://doi.org/10.1016/j.ecoleng.2016.01.050.
[113] Ü. Niinemets, The controversy over traits conferring shade-tolerance in trees: Ontogenetic changes revisited, J. Ecol. 94 (2006) 464–470. https://doi.org/10.1111/j.1365-2745.2006.01093.x.
[114] R.C. Morrow, LED lighting in horticulture, HortScience. 43 (2008) 1947–1950. https://doi.org/10.21273/hortsci.43.7.1947.
[115] N. Yeh, J.P. Chung, High-brightness LEDs-Energy efficient lighting sources and their potential in indoor plant cultivation, Renew. Sustain. Energy Rev. 13 (2009) 2175–2180. https://doi.org/10.1016/j.rser.2009.01.027.
[116] T. Ouzounis, E. Rosenqvist, C.O. Ottosen, Spectral effects of artificial light on plant physiology and secondary metabolism: A review, HortScience. 50 (2015) 1128–1135. https://doi.org/10.21273/hortsci.50.8.1128.
[117] P.M. Pattison, J.Y. Tsao, G.C. Brainard, B. Bugbee, LEDs for photons, physiology and food, Nature. 563 (2018) 493–500. https://doi.org/10.1038/s41586-018-0706-x.
[118] R Core Team, R: A language and environment for statistical computer, (2019). www.R-project.org.
[119] J. Fox, S. Weisberg, An (R) Companion to Applied Regression, 3rd ed., Sage, Thousand Oaks, CA, 2019. socialsciences.mcmaster.ca/jfox/books/companion/.
[120] H. Wickham, R. François, L. Henry, K. Müller, dplyr: A Grammar of Data Manipulation, (2019). CRAN.R-project.org/package=dplyr.
[121] H. Wickham, ggplot2: Elegant Graphics for Data Analysis., Springer-Verlag New York, 2016. ggplot2.tidyverse.org.
[122] A. Kassambara, ggpubr: “ggplot2” Based Publication Ready Plots, (2019). CRAN.R-project.org/package=ggpubr.
[123] T. Hothorn, F. Bretz, P. Westfall, Simultaneous Inference in general Parametric Models, Biometrical J. 50 (2008) 346–363.
[124] A. Dragulescu, C. Arendt, 2018, xlsx: Read, Write, Format Excel 2007 and Excel 97/2000/2003 Files, (2020). CRAN.R-project.org/package=xlsx.
[125] K.M. Folta, K.S. Childers, Light as a growth regulator: Controlling plant biology with narrow-bandwidth solid-state lighting systems, HortScience. 43 (2008) 1957–1964. https://doi.org/10.21273/hortsci.43.7.1957.
[126] K. Gunawardena, K. Steemers, Living walls in indoor environments, Build. Environ. 148 (2019) 478–487. https://doi.org/10.1016/j.buildenv.2018.11.014.
[127] M. Cetin, H. Sevik, Measuring the impact of selected plants on indoor CO2 concentrations, Polish J. Environ. Stud. 25 (2016) 973–979. https://doi.org/10.15244/pjoes/61744.
[128] C.R. Brodersen, T.C. Vogelmann, Do changes in light direction affect absorption profiles in leaves?, Funct. Plant Biol. 37 (2010) 403. https://doi.org/10.1071/FP09262.
[129] W.K. Smith, T.C. Vogelmann, E.H. DeLucia, D.T. Bell, K.A. Shepherd, Leaf Form and Photosynthesis, Bioscience. 47 (1997) 785–793. https://doi.org/10.2307/1313100.
[130] C.R. BRODERSEN, T.C. VOGELMANN, W.E. WILLIAMS, H.L. GORTON, A new paradigm in leaf-level photosynthesis: direct and diffuse lights are not equal, Plant. Cell Environ. 31 (2007) 071120025305001-??? https://doi.org/10.1111/j.1365-3040.2007.01751.x.
[131] M.J. Correll, J.Z. Kiss, Interactions between gravitropism and phototropism in plants, J. Plant Growth Regul. 21 (2002) 89–101. https://doi.org/10.1007/s003440010056.
[132] C. Treesubsuntorn, P. Thiravetyan, Botanical biofilter for indoor toluene removal and reduction of carbon dioxide emission under low light intensity by using mixed C3 and CAM plants, J. Clean. Prod. 194 (2018) 94–100. https://doi.org/10.1016/j.jclepro.2018.05.141.
[133] K. Perini, P. Rosasco, Cost-benefit analysis for green façades and living wall systems, Build. Environ. 70 (2013) 110–

121. https://doi.org/10.1016/j.buildenv.2013.08.012.
[134] M. Rehman, S. Ullah, Y. Bao, B. Wang, D. Peng, L. Liu, Light-emitting diodes: whether an efficient source of light for indoor plants?, Environ. Sci. Pollut. Res. 24 (2017) 24743–24752. https://doi.org/10.1007/s11356-017-0333-3.
[135] R.D. Brook, S. Rajagopalan, C.A. Pope, J.R. Brook, A. Bhatnagar, A. V. Diez-Roux, F. Holguin, Y. Hong, R. V. Luepker, M.A. Mittleman, A. Peters, D. Siscovick, S.C. Smith, L. Whitsel, J.D. Kaufman, Particulate matter air pollution and cardiovascular disease: An update to the scientific statement from the american heart association, Circulation. 121 (2010) 2331–2378. https://doi.org/10.1161/CIR.0b013e3181dbece1.
[136] T. Pettit, M. Bettes, A.R. Chapman, L.M. Hoch, N.D. James, P.J. Irga, F.R. Torpy, The botanical biofiltration of VOCs with active airflow: is removal efficiency related to chemical properties?, Atmos. Environ. 214 (2019). https://doi.org/10.1016/j.atmosenv.2019.116839.
[137] L. Pan, S. Wei, P.Y. Lai, L.M. Chu, Effect of plant traits and substrate moisture on the thermal performance of different plant species in vertical greenery systems, Build. Environ. 175 (2020) 106815. https://doi.org/10.1016/j.buildenv.2020.106815.
[138] A. Mikkonen, T. Li, M. Vesala, J. Saarenheimo, V. Ahonen, S. Kärenlampi, J.D. Blande, M. Tiirola, A. Tervahauta, Biofiltration of airborne VOCs with green wall systems—Microbial and chemical dynamics, Indoor Air. 28 (2018) 697–707. https://doi.org/10.1111/ina.12473.
[139] F. Torpy, N. Clements, M. Pollinger, A. Dengel, I. Mulvihill, C. He, P. Irga, Testing the single-pass VOC removal efficiency of an active green wall using methyl ethyl ketone (MEK), Air Qual. Atmos. Heal. 11 (2018) 163–170. https://doi.org/10.1007/s11869-017-0518-4.
[140] T. Pettit, P. Irga, P. Abdo, F. Torpy, Do the plants in functional green walls contribute to their ability to filter particulate matter?, Build. Environ. 125 (2017) 299–307. https://doi.org/10.1016/j.buildenv.2017.09.004.
[141] I.Z. Ibrahim, W.T. Chong, S. Yusoff, The design of the botanical indoor air biofilter system for the atmospheric particle removal, MATEC Web Conf. 192 (2018) 1–4. https://doi.org/10.1051/matecconf/201819202035.
[142] J.J. McArthur, C. Powell, Health and wellness in commercial buildings: Systematic review of sustainable building rating systems and alignment with contemporary research, Build. Environ. 171 (2020) 106635. https://doi.org/10.1016/j.buildenv.2019.106635.
[143] P. Irga, T. Pettit, F. Torpy, The phytoremediation of indoor air pollution: a review on the technology development from the potted plant through to functional green wall biofilters, Rev. Environ. Sci. Bio/Technology. 17 (2018) 395–415. https://doi.org/10.1007/s11157-018-9465-2.
[144] J. Tarran, F. Torpy, M. Burchett, Use of living pot-plants to cleanse indoor air - Research review, in: Proc. Sixth Int. Conf. Indoor Air Quaity, Vent. Energy Conserv. Build. - Sustain. Built Environ., 2007: pp. 249–256.
[145] X. Wei, S. Lyu, Y. Yu, Z. Wang, H. Liu, Phylloremediation of air pollutants: exploiting the potential of plant leaves and leaf-associated microbes, Front. Plant Sci. 8 (2017) 1–23. https://doi.org/10.3389/fpls.2017.01318.
[146] P. Irga, F. Torpy, Indoor air pollutants in occupational buildings in a sub-tropical climate: Comparison among ventilation types, Build. Environ. 98 (2016) 190–199. https://doi.org/10.1016/j.buildenv.2016.01.012.
[147] G. Munz, M. Dixon, A. Darlington, The removal of carbon monoxide by botanical systems, SAE Tech. Pap. (2002). https://doi.org/10.4271/2002-01-2265.
[148] R. Fleck, T.. Pettit, A.N.J. Douglas, P.J. Irga, F.R. Torpy, Botanical biofiltration for reducing indoor air pollution, in: Bio-Based Mater. Biotechnol. Eco-Efficient Constr., Woodhead Publishing, 2020: pp. 305–327.
[149] F.M. Chegini, A.N. Baghani, M.S. Hassanvand, A. Sorooshian, S. Golbaz, R. Bakhtiari, A. Ashouri, M.N. Joubani, M. Alimohammadi, Indoor and outdoor airborne bacterial and fungal air quality in kindergartens: Seasonal distribution, genera, levels, and factors influencing their concentration, Build. Environ. 175 (2020) 106690. https://doi.org/10.1016/j.buildenv.2020.106690.
[150] J. Mallany, A. Darlington, M. Dixon, BIOAEROSOL PRODUCTION FROM INDOOR AIR BIOFILTERS, (2002) 1038–1043.
[151] M.B. McCullough, M.D. Martin, M.A. Sajady, Implementing green walls in schools, Front. Psychol. 9 (2018) 1–5. https://doi.org/10.3389/fpsyg.2018.00619.
[152] I. Cheung, Impact of Interior Living Walls on Indoor Air Quality : Study in a Dynamic Environment by, 2017.
[153] F. Torpy, P. Irga, M. Burchett, Reducing indoor air pollutants through biotechnology, in: Biotechnol. Biomimetics Civ. Eng., 2015: pp. 1–437. https://doi.org/10.1007/978-3-319-09287-4.
[154] A. Prussin, D. Schwake, L. Marr, Ten questions concerning the aerosolization and transmission of Legionella in the built environment, Build. Environ. 123 (2017) 684–695. https://doi.org/10.1016/j.buildenv.2017.06.024.
[155] A. Abu Khweek, A.O. Amer, Factors mediating environmental biofilm formation by Legionella pneumophila, Front. Cell. Infect. Microbiol. 8 (2018) 1–10. https://doi.org/10.3389/fcimb.2018.00038.
[156] H. Wang, S. Masters, M.A. Edwards, J.O. Falkinham, A. Pruden, Effect of disinfectant, water age, and pipe materials on bacterial and eukaryotic community structure in drinking water biofilm, Environ. Sci. Technol. 48 (2014) 1426–1435. https://doi.org/10.1021/es402636u.
[157] Mekkour, Driss, Tai, Cohen, Legionella pneumophila: An Environmental Organism and Accidental Pathogen, Int. J. Sci. Technol. 2 (2013) 187–196.
[158] C. MacIntyre, A. Dyda, C. Bui, A. Chughtai, Rolling epidemic of Legionnaires' disease outbreaks in small geographic areas article, Emerg. Microbes Infect. 7 (2018). https://doi.org/10.1038/s41426-018-0051-z.
[159] I. Pepper, C. Gerba, Risk of infection from Legionella associated with spray irrigation of reclaimed water, Water Res. 139 (2018) 101–107. https://doi.org/10.1016/j.watres.2018.04.001.
[160] A. Doleans, H. Aurell, M. Reyrolle, G. Lina, J. Freney, F. Vandenesch, J. Etienne, S. Jarraud, Clinical and Environmental Distributions of Legionella Strains in France Are Different, J. Clin. Microbiol. 42 (2004) 458–460.

https://doi.org/10.1128/JCM.42.1.458-460.2004.
[161] H.K. Lee, J.I. Shim, H.E. Kim, J.Y. Yu, Y.H. Kang, Distribution of legionella species from environmental water sources of public facilities and genetic diversity of L. pneumophila serogroup 1 in South Korea, Appl. Environ. Microbiol. 76 (2010) 6547–6554. https://doi.org/10.1128/AEM.00422-10.
[162] E. van Heijnsbergen, A. van Deursen, M. Bouwknegt, J.P. Bruin, A.M. de Roda Husman, J.A.C. Schalk, Presence and persistence of viable, clinically relevant Legionella pneumophila bacteria in garden soil in the Netherlands, Appl. Environ. Microbiol. 82 (2016) 5125–5131. https://doi.org/10.1128/AEM.00595-16.
[163] NSW Health, NSW Health Notifiable Conditions Information Management System (NCIMS), Commun. Dis. Branch Cent. Epidemiol. Evid. (2019).
[164] H. Whiley, R. Bentham, Legionella longbeachae and legionellosis, Emerg. Infect. Dis. 17 (2011) 579–583. https://doi.org/10.3201/eid1704.100446.
[165] L.M. Massis, M.A. Assis-Marques, F.V.S. Castanheira, Y.J. Capobianco, A.C. Balestra, P. Escoll, R.E. Wood, G.Z. Manin, V.M.A. Correa, J.C. Alves-Filho, F.Q. Cunha, C. Buchrieser, M.C. Borges, H.J. Newton, D.S. Zamboni, Legionella longbeachae is immunologically silent and highly virulent in vivo, J. Infect. Dis. 215 (2017) 440–451. https://doi.org/10.1093/infdis/jiw560.
[166] P.J. Irga, T. Pettit, R.F. Irga, N.J. Paull, A.N.J. Douglas, F.R. Torpy, Does plant species selection in functional active green walls influence VOC phytoremediation efficiency?, Environ. Sci. Pollut. Res. 26 (2019) 12851–12858. https://doi.org/10.1007/s11356-019-04719-9.
[167] R.I. Adams, S. Bhangar, W. Pasut, E.A. Arens, J.W. Taylor, S.E. Lindow, W.W. Nazaroff, T.D. Bruns, Chamber bioaerosol study: Outdoor air and human occupants as sources of indoor airborne microbes, PLoS One. 10 (2015) 1–18. https://doi.org/10.1371/journal.pone.0128022.
[168] Thermo Scientific, Rose-Bengal Chloramphenicol Agar Base (Dehydrated), (2019) 1. https://www.thermofisher.com/order/catalog/product/CM0549B.
[169] European Committee for Standardisation, BSI Standards Publication Water quality — Enumeration of Legionella, 2017.
[170] Hardy Diagnostics, Buffered Charcoal Yeast Extract (BCYE) Agar, (1996) 1. https://catalog.hardydiagnostics.com/cp_prod/Content/hugo/BCYEAgar.htm.
[171] M. Klich, J. Pitt, A laboratory guide to the common aspergillus species and their teleomorphs, CSIRO, Sydney, 1988.
[172] C.J. Alexopoulos, M. Blackwell, C.W. Mims, Introductory mycology, 4th ed., Wiley, New York, 1996.
[173] D. Ellis, S. Davis, H. Alexiou, R. Handke, R. Bartley, Descriptions of medical fungi, 2nd ed., Authors, Adelaide, 2007.
[174] B.J. Callahan, P.J. McMurdie, M.J. Rosen, A.W. Han, A.J.A. Johnson, S.P. Holmes, DADA2: High-resolution sample inference from Illumina amplicon data, Nat. Methods. 13 (2016) 581–583. https://doi.org/10.1038/nmeth.3869.
[175] H. Pagès, P. Aboyoun, R. Gentleman, S. DebRoy, Biostrings: Efficient manipulation of biological strings., (2019).
[176] E.S. Wright, Using DECIPHER v2.0 to Analyze Big Biological Sequence Data in R, R J. 8 (2016) 352–359.
[177] C. Quast, E. Pruesse, P. Yilmaz, J. Gerken, T. Schweer, P. Yarza, J. Peplies, F.O. Glöckner, The SILVA ribosomal RNA gene database project: Improved data processing and web-based tools, Nucleic Acids Res. 41 (2013) 590–596. https://doi.org/10.1093/nar/gks1219.
[178] P.J. McMurdie, S.P. Holmes, phyloseq: An R package for reproducible interactive analysis and graphics of microbiome census data., PLoS One. 8 (2013) e61217. dx.plos.org/10.1371/journal.pone.0061217.
[179] J. Oksanen, F. Guillaume Blanchet, M. Friendly, R. Kindt, P. Legendre, D. McGlinn, P. Minchin, R. O'Hara, G. Simpson, P. Solymos, M. Stevens, E. Szoecs, H. Wagner, vegan: Community Ecology package, (2019). https://cran.r-project.org/package=vegan.
[180] World Health Organisation (WHO), Indoor air quality: biological contaminants, Copenhagen, 1990.
[181] M.T. Hedayati, A. Mohseni-Bandpi, S. Moradi, A survey on the pathogenic fungi in soil samples of potted plants from Sari hospitals, Iran, J. Hosp. Infect. 58 (2004) 59–62. https://doi.org/10.1016/j.jhin.2004.04.011.
[182] C. Lass-Flörl, P.M. Rath, D. Niederwieser, G. Kofler, R. Würzner, A. Krezy, M.P. Dierich, Aspergillus terreus infections in haematological malignancies: Molecular epidemiology suggests association with in-hospital plants, J. Hosp. Infect. 46 (2000) 31–35. https://doi.org/10.1053/jhin.2000.0799.
[183] S. Engelhart, E. Rietschel, M. Exner, L. Lange, Childhood hypersensitivity pneumonitis associated with fungal contamination of indoor hydroponics, Int. J. Hyg. Environ. Health. 212 (2009) 18–20. https://doi.org/10.1016/j.ijheh.2008.01.001.
[184] F. Staib, B. Tompak, D. Thiel, A. Blisse, Aspergillus fumigatus and aspergillus niger in two potten ornamental plants, cactus (Epiphyllum truncatum) and Clivia (Clivia miniata). Biological and Epidemiological aspects, Mycopathologia. 66 (1978) 27–30.
[185] F. Torpy, P. Irga, J. Brennan, M. Burchett, Do indoor plants contribute to the aeromycota in city buildings ?, Aerobiologia (Bologna). 29 (2013) 321–331. https://doi.org/10.1007/s10453-012-9282-y.
[186] A. Darlington, M. Chan, D. Malloch, C. Pilger, M.A. Dixon, The biofiltration of indoor air: implications for air quality., Indoor Air. 10 (2000) 39–46. https://doi.org/10.1034/j.1600-0668.2000.010001039.x.
[187] H.A. Burge, W.R. Solomon, M.L. Muilenberg, Evaluation of indoor plantings as allergen exposure sources, J. Allergy Clin. Immunol. 70 (1982) 101–108. https://doi.org/10.1016/0091-6749(82)90236-6.
[188] J. Mallany, A. Darlington, M. Dixon, The biofiltration of indoor air II: microbial loading of the indoor space, … Conf. Biofiltration Air …. (2000) 5–10. http://biostem.ca/files/Darlington Indoor II.PDF.
[189] T. Reponen, M. Lehtonen, T. Raunemaa, Effect of indoor sources on fungal spore concentrations and size distributions, J. Aerosol Sci. 19 (1992) 463–466. https://doi.org/10.20595/jjbf.19.0_3.

[190] J. Singh, C.W.F. Yu, J.T. Kim, Building pathology, investigation of sick buildings - Toxic moulds, Indoor Built Environ. 19 (2010) 40–47. https://doi.org/10.1177/1420326X09358808.
[191] W.R. Lin, Y.H. Chen, M.F. Lee, L.Y. Hsu, C.J. Tien, F.M. Shih, S.C. Hsiao, P.H. Wang, Does spore count matter in fungal allergy?: The role of allergenic fungal species, Allergy, Asthma Immunol. Res. 8 (2016) 404–411. https://doi.org/10.4168/aair.2016.8.5.404.
[192] P. Irga, F. Torpy, A survey of the aeromycota of Sydney and its correspondence with environmental conditions: grass as a component of urban forestry could be a major determinant, Aerobiologia (Bologna). 32 (2016) 171–185. https://doi.org/10.1007/s10453-015-9388-0.
[193] H. Wei, C. Peng, B. Yang, H. Song, Q. Li, L. Jiang, G. Wei, K. Wang, H. Wang, S. Liu, X. Liu, D. Chen, Y. Li, M. Wang, Contrasting Soil Bacterial Community, Diversity, and Function in Two Forests in China, Front. Microbiol. 9 (2018). https://doi.org/10.3389/fmicb.2018.01693.
[194] L. Cheng, Q. Zhou, B. Yu, Responses and roles of roots, microbes, and degrading genes in rhizosphere during phytoremediation of petroleum hydrocarbons contaminated soil, Int. J. Phytoremediation. 0 (2019) 1–9. https://doi.org/10.1080/15226514.2019.1612841.
[195] N. Weyens, S. Thijs, R. Popek, N. Witters, A. Przybysz, J. Espenshade, H. Gawronska, J. Vangronsveld, S. Gawronski, The role of plant–microbe interactions and their exploitation for phytoremediation of air pollutants, Int. J. Mol. Sci. 16 (2015) 25576–25604. https://doi.org/10.3390/ijms161025576.
[196] M.A. Hassani, P. Durán, S. Hacquard, Microbial interactions within the plant holobiont, Microbiome. 6 (2018) 58. https://doi.org/10.1186/s40168-018-0445-0.
[197] M. Dhote, A. Kumar, A. Jajoo, A. Juwarkar, Study of microbial diversity in plant–microbe interaction system with oil sludge contamination, Int. J. Phytoremediation. 20 (2018) 789–795. https://doi.org/10.1080/15226514.2018.1425668.
[198] C. Knief, N. Delmotte, S. Chaffron, M. Stark, G. Innerebner, R. Wassmann, C. Von Mering, J.A. Vorholt, Metaproteogenomic analysis of microbial communities in the phyllosphere and rhizosphere of rice, ISME J. 6 (2012) 1378–1390. https://doi.org/10.1038/ismej.2011.192.
[199] J. Kim, S.H. Kang, K.A. Min, K.S. Cho, I.S. Lee, Rhizosphere microbial activity during phytoremediation of diesel-contaminated soil, J. Environ. Sci. Heal. - Part A Toxic/Hazardous Subst. Environ. Eng. 41 (2006) 2503–2516. https://doi.org/10.1080/10934520600927658.
[200] C.T. Brown, L.A. Hug, B.C. Thomas, I. Sharon, C.J. Castelle, A. Singh, M.J. Wilkins, K.C. Wrighton, K.H. Williams, J.F. Banfield, Unusual biology across a group comprising more than 15% of domain Bacteria, Nature. 523 (2015) 208–211. https://doi.org/10.1038/nature14486.
[201] M. Sánchez-Osuna, J. Barbé, I. Erill, Comparative genomics of the DNA damage-inducible network in the Patescibacteria, Environ. Microbiol. 19 (2017) 3465–3474. https://doi.org/10.1111/1462-2920.13826.
[202] W.C. Nelson, J.C. Stegen, The reduced genomes of Parcubacteria (OD1) contain signatures of a symbiotic lifestyle, Front. Microbiol. 6 (2015) 1–14. https://doi.org/10.3389/fmicb.2015.00713.
[203] R. León-Zayas, L. Peoples, J.F. Biddle, S. Podell, M. Novotny, J. Cameron, R.S. Lasken, D.H. Bartlett, The metabolic potential of the single cell genomes obtained from the Challenger Deep, Mariana Trench within the candidate superphylum Parcubacteria (OD1), Environ. Microbiol. 19 (2017) 2769–2784. https://doi.org/10.1111/1462-2920.13789.
[204] L.N. Lemos, J.D. Medeiros, F. Dini-Andreote, G.R. Fernandes, A.M. Varani, G. Oliveira, V.S. Pylro, Genomic signatures and co-occurrence patterns of the ultra-small Saccharimonadia (phylum CPR/Patescibacteria) suggest a symbiotic lifestyle, Mol. Ecol. (2019) 4259–4271. https://doi.org/10.1111/mec.15208.
[205] M. Herrmann, C.E. Wegner, M. Taubert, P. Geesink, K. Lehmann, L. Yan, R. Lehmann, K.U. Totsche, K. Küsel, Predominance of Cand. Patescibacteria in groundwater is caused by their preferential mobilization from soils and flourishing under oligotrophic conditions, Front. Microbiol. 10 (2019) 1–15. https://doi.org/10.3389/fmicb.2019.01407.
[206] S. Kandel, P. Joubert, S. Doty, Bacterial Endophyte Colonization and Distribution within Plants, Microorganisms. 5 (2017) 77. https://doi.org/10.3390/microorganisms5040077.
[207] M. Ventura, C. Canchaya, A. Tauch, G. Chandra, G.F. Fitzgerald, K.F. Chater, D. van Sinderen, Genomics of Actinobacteria: Tracing the Evolutionary History of an Ancient Phylum, Microbiol. Mol. Biol. Rev. 71 (2007) 495–548. https://doi.org/10.1128/mmbr.00005-07.
[208] A. Alvarez, J.M. Saez, J.S. Davila Costa, V.L. Colin, M.S. Fuentes, S.A. Cuozzo, C.S. Benimeli, M.A. Polti, M.J. Amoroso, Actinobacteria: Current research and perspectives for bioremediation of pesticides and heavy metals, Chemosphere. 166 (2017) 41–62. https://doi.org/10.1016/j.chemosphere.2016.09.070.
[209] M. Taillefer, M.Ø. Arntzen, B. Henrissat, P.B. Pope, J. Larsbrink, Proteomic Dissection of the Cellulolytic Machineries Used by Soil-Dwelling Bacteroidetes, MSystems. 3 (2018) 1–16. https://doi.org/10.1128/msystems.00240-18.
[210] M.Z. Simón Solá, N. Lovaisa, J.S. Dávila Costa, C.S. Benimeli, M.A. Polti, A. Alvarez, Multi-resistant plant growth-promoting actinobacteria and plant root exudates influence Cr(VI) and lindane dissipation, Chemosphere. 222 (2019) 679–687. https://doi.org/10.1016/j.chemosphere.2019.01.197.
[211] M. McGuinness, D. Dowling, Plant-associated bacterial degradation of toxic organic compounds in soil, Int. J. Environ. Res. Public Health. 6 (2009) 2226–2247. https://doi.org/10.3390/ijerph6082226.
[212] C.R. Fitzpatrick, J. Copeland, P.W. Wang, D.S. Guttman, P.M. Kotanen, M.T.J. Johnson, Assembly and ecological function of the root microbiome across angiosperm plant species, Proc. Natl. Acad. Sci. U. S. A. 115 (2018) E1157–E1165. https://doi.org/10.1073/pnas.1717617115.

[213] X. Huang, D. Pinto, G. Fritz, T. Mascher, Environmental sensing in Actinobacteria: A comprehensive survey on the signaling capacity of this phylum, J. Bacteriol. 197 (2015) 2517–2535. https://doi.org/10.1128/JB.00176-15.
[214] M. Zavattaro, P.J. Irga, M.D. Burchett, Assessing the air quality remediation capacity of the Junglefy breathing wall modular plant wall system, 2015.
[215] A.C. Llewellyn, C.E. Lucas, S.E. Roberts, E.W. Brown, B.S. Nayak, B.H. Raphael, J.M. Winchell, Distribution of Legionella and bacterial community composition among regionally diverse US cooling towers, PLoS One. 12 (2017) 1–16. https://doi.org/10.1371/journal.pone.0189937.
[216] S. Adcock, F. Graham, G. Jackson, C. Lease, L. Fitzgerald, P. Bartley, V. Garnys, T. Hale, J. Noonan, W. Keep, B. George, N. Disney, N. Young, E. Hartland, C. Lucas, H. Psarras, A. Vickers, Guidelines for Legionella control, 2015.
[217] British Standards Institution, Water quality - risk assessments for Legionella control - Code of Practice, 2012.
[218] N. Messonnier, P. Breysse, Developing a water management program to reduce Legionella growth & spread in buildings, 2017.
[219] J.L. Baron, A. Vikram, S. Duda, J.E. Stout, K. Bibby, Shift in the microbial ecology of a hospital hot water system following the introduction of an on-site monochloramine disinfection system, PLoS One. 9 (2014) 1–9. https://doi.org/10.1371/journal.pone.0102679.
[220] R. Cameron, J. Taylor, M. Emmett, What's "cool" in the world of green façades? How plant choice influences the cooling properties of green walls, Build. Environ. 73 (2014) 198–207. https://doi.org/10.1016/j.buildenv.2013.12.005.
[221] A.E. van den Berg, J. Maas, R.A. Verheij, P.P. Groenewegen, Green space as a buffer between stressful life events and health, Soc. Sci. Med. 70 (2010) 1203–1210. https://doi.org/10.1016/j.socscimed.2010.01.002.
[222] A. Panno, G. Carrus, R. Lafortezza, L. Mariani, G. Sanesi, Nature-based solutions to promote human resilience and wellbeing in cities during increasingly hot summers, Environ. Res. 159 (2017) 249–256. https://doi.org/10.1016/j.envres.2017.08.016.
[223] N. Kabisch, M. van den Bosch, R. Lafortezza, The health benefits of nature-based solutions to urbanization challenges for children and the elderly – A systematic review, Environ. Res. 159 (2017) 362–373. https://doi.org/10.1016/j.envres.2017.08.004.
[224] M. Shafique, R. Kim, M. Rafiq, Green roof benefits, opportunities and challenges – A review, Renew. Sustain. Energy Rev. 90 (2018) 757–773. https://doi.org/10.1016/j.rser.2018.04.006.
[225] J. Yang, Q. Yu, P. Gong, Quantifying air pollution removal by green roofs in Chicago, Atmos. Environ. 42 (2008) 7266–7273. https://doi.org/10.1016/j.atmosenv.2008.07.003.
[226] T. Van Renterghem, D. Botteldooren, Reducing the acoustical façade load from road traffic with green roofs, Build. Environ. 44 (2009) 1081–1087. https://doi.org/10.1016/j.buildenv.2008.07.013.
[227] T. Van Renterghem, D. Botteldooren, In-situ measurements of sound propagating over extensive green roofs, Build. Environ. 46 (2011) 729–738. https://doi.org/10.1016/j.buildenv.2010.10.006.
[228] T. Van Renterghem, M. Hornikx, J. Forssen, D. Botteldooren, The potential of building envelope greening to achieve quietness, Build. Environ. 61 (2013) 34–44. https://doi.org/10.1016/j.buildenv.2012.12.001.
[229] S.E. Clemants, J. Marinelli, G. Moore, E. Peters, N. Dunne, J. Blackburn, B. Botanic, G. Website, A. Dorfman, D. Allen, Green Roofs and Biodiversity, Urban Habitats. 4 (2006) 1–26. http://www.urbanhabitats.org/v04n01/urbanhabitats_v04n01_pdf.pdf.
[230] R. Fioretti, A. Palla, L.G. Lanza, P. Principi, Green roof energy and water related performance in the Mediterranean climate, Build. Environ. 45 (2010) 1890–1904. https://doi.org/10.1016/j.buildenv.2010.03.001.
[231] J. Mentens, D. Raes, M. Hermy, Green roofs as a tool for solving the rainwater runoff problem in the urbanized 21st century?, Landsc. Urban Plan. 77 (2006) 217–226. https://doi.org/10.1016/j.landurbplan.2005.02.010.
[232] K. Vijayaraghavan, F.D. Raja, Design and development of green roof substrate toimprove runoff water quality: Plant growth experiments and adsorption, Water Res. 63 (2014) 94–101. https://doi.org/10.1016/j.watres.2014.06.012.
[233] R.C. Feitosa, S.J. Wilkinson, Attenuating heat stress through green roof and green wall retrofit, Build. Environ. 140 (2018) 11–22. https://doi.org/10.1016/j.buildenv.2018.05.034.
[234] R.C. Feitosa, S.J. Wilkinson, Small-scale experiments of seasonal heat stress attenuation through a combination of green roof and green walls, J. Clean. Prod. 250 (2020) 119443. https://doi.org/10.1016/j.jclepro.2019.119443.
[235] C. Rosenzweig, W. Solecki, L. Parshall, S. Gaffin, B. Lynn, R. Goldberg, J. Cox, S. Hodges, Mitigating New York City's heat island with urban forestry, living roofs, and light surfaces, in: 86th AMS Annu. Meet., 2006.
[236] K.R. Smith, P.J. Roebber, Green roof mitigation potential for a proxy future climate scenario in Chicago, Illinois, J. Appl. Meteorol. Climatol. 50 (2011) 507–522. https://doi.org/10.1175/2010JAMC2337.1.
[237] V.R. Stovin, S.L. Moore, M. Wall, R.M. Ashley, The potential to retrofit sustainable drainage systems to address combined sewer overflow discharges in the Thames Tideway catchment, Water Environ. J. 27 (2013) 216–228. https://doi.org/10.1111/j.1747-6593.2012.00353.x.
[238] H.F. Castleton, V. Stovin, S.B.M. Beck, J.B. Davison, Green roofs; Building energy savings and the potential for retrofit, Energy Build. 42 (2010) 1582–1591. https://doi.org/10.1016/j.enbuild.2010.05.004.
[239] C.M. Silva, I. Flores-Colen, M. Antunes, Step-by-step approach to ranking green roof retrofit potential in urban areas: A case study of Lisbon, Portugal, Urban For. Urban Green. 25 (2017) 120–129. https://doi.org/10.1016/j.ufug.2017.04.018.
[240] S. Izquierdo, M. Rodrigues, N. Fueyo, A method for estimating the geographical distribution of the available roof surface area for large-scale photovoltaic energy-potential evaluations, Sol. Energy. 82 (2008) 929–939. https://doi.org/10.1016/j.solener.2008.03.007.
[241] M.A. Polo-Labarrios, S. Quezada-Garciá, H. Sánchez-Mora, M.A. Escobedo-Izquierdo, G. Espinosa-Paredes,

Comparison of thermal performance between green roofs and conventional roofs, Case Stud. Therm. Eng. 21 (2020). https://doi.org/10.1016/j.csite.2020.100697.
[242] M. Taleghani, Outdoor thermal comfort by different heat mitigation strategies- A review, Renew. Sustain. Energy Rev. 81 (2018) 2011–2018. https://doi.org/10.1016/j.rser.2017.06.010.
[243] A. Bellazzi, B. Barozzi, M.C. Pollastro, I. Meroni, Thermal resistance of growing media for green roofs: To what extent does the absence of specific reference values potentially affect the global thermal resistance of the green roof? An experimental example, J. Build. Eng. 28 (2020) 101076. https://doi.org/10.1016/j.jobe.2019.101076.
[244] M. Köhler, D. Kaiser, Evidence of the climate mitigation effect of green roofs-A 20-year weather study on an Extensive Green Roof (EGR) in Northeast Germany, Buildings. 9 (2019). https://doi.org/10.3390/buildings9070157.
[245] S.S. Alcazar, F. Olivieri, J. Neila, Green roofs: Experimental and analytical study of its potential for urban microclimate regulation in Mediterranean–continental climates, Urban Clim. 17 (2016) 304–317. https://doi.org/10.1016/j.uclim.2016.02.004.
[246] D. Suszanowicz, A. Kolasa-Więcek, The impact of green roofs on the parameters of the environment in urban areas-review, Atmosphere (Basel). 10 (2019). https://doi.org/10.3390/ATMOS10120792.
[247] A.M. Rizwan, L.Y.C. Dennis, C. Liu, A review on the generation, determination and mitigation of Urban Heat Island, J. Environ. Sci. 20 (2008) 120–128. https://doi.org/10.1016/S1001-0742(08)60019-4.
[248] M. Santamouris, Cooling the cities - A review of reflective and green roof mitigation technologies to fight heat island and improve comfort in urban environments, Sol. Energy. 103 (2014) 682–703. https://doi.org/10.1016/j.solener.2012.07.003.
[249] T. Randazzo, E. De Cian, M.N. Mistry, Air conditioning and electricity expenditure: The role of climate in temperate countries, Econ. Model. 90 (2020) 273–287. https://doi.org/10.1016/j.econmod.2020.05.001.
[250] International Energy Agency (IEA), The Future of Cooling Opportunities for energy- efficient air conditioning, 2018. www.iea.org.
[251] J. Yang, Z.H. Wang, Physical parameterization and sensitivity of urban hydrological models: Application to green roof systems, Build. Environ. 75 (2014) 250–263. https://doi.org/10.1016/j.buildenv.2014.02.006.
[252] C.Y. Jim, S.W. Tsang, Biophysical properties and thermal performance of an intensive green roof, Build. Environ. 46 (2011) 1263–1274. https://doi.org/10.1016/j.buildenv.2010.12.013.
[253] R. Liu, R.L. Stanford, Y. Deng, D. Liu, Y. Liu, S.L. Yu, The influence of extensive green roofs on rainwater runoff quality: a field-scale study in southwest China, Environ. Sci. Pollut. Res. 27 (2020) 12932–12941. https://doi.org/10.1007/s11356-019-06151-5.
[254] A. Naranjo, A. Colonia, J. Mesa, H. Maury, A. Maury-Ramírez, State-of-the-art green roofs: Technical performance and certifications for sustainable construction, Coatings. 10 (2020) 1–14. https://doi.org/10.3390/coatings10010069.
[255] J. Schade, S. Lidelöw, J. Lönnqvist, The thermal performance of a green roof on a highly insulated building in a sub-arctic climate, Energy Build. 241 (2021) 110961. https://doi.org/10.1016/j.enbuild.2021.110961.
[256] F. Ascione, N. Bianco, F. de' Rossi, G. Turni, G.P. Vanoli, Green roofs in European climates. Are effective solutions for the energy savings in air-conditioning?, Appl. Energy. 104 (2013) 845–859. https://doi.org/10.1016/j.apenergy.2012.11.068.
[257] E. Koroxenidis, T. Theodosiou, Comparative environmental and economic evaluation of green roofs under Mediterranean climate conditions – Extensive green roofs a potentially preferable solution, J. Clean. Prod. 311 (2021) 127563. https://doi.org/10.1016/j.jclepro.2021.127563.
[258] J. MacIvor, O. Starry, S. Brenneisen, N. Baumann, G. Grant, K. Gyondover, M. Kohler, J. Lundholm, Introduction: "Looking up" to green roofs to understand urban biodiversity: a decade on, in: Urban Nat., 2018.
[259] H. Ogaili, D.J. Sailor, Measuring the Effect of Vegetated Roofs on the Performance of Photovoltaic Panels in a Combined System, J. Sol. Energy Eng. Trans. ASME. 138 (2016) 1–8. https://doi.org/10.1115/1.4034743.
[260] D. Chemisana, C. Lamnatou, Photovoltaic-green roofs: An experimental evaluation of system performance, Appl. Energy. 119 (2014) 246–256. https://doi.org/10.1016/j.apenergy.2013.12.027.
[261] M.C. Peel, B.L. Finlayson, T.A. McMahon, Updated world map of the Köppen-Geiger climate classification, Hydrol. Earth Syst. Sci. 11 (2007) 1633–1644. https://doi.org/10.5194/hess-11-1633-2007.
[262] M. Santamouris, S. Haddad, F. Fiorito, P. Osmond, L. Ding, D. Prasad, X. Zhai, R. Wang, Urban heat island and overheating characteristics in Sydney, Australia. An analysis of multiyear measurements, Sustain. 9 (2017). https://doi.org/10.3390/su9050712.
[263] S. Cascone, J. Coma, A. Gagliano, G. Pérez, The evapotranspiration process in green roofs: A review, Build. Environ. 147 (2019) 337–355. https://doi.org/10.1016/j.buildenv.2018.10.024.
[264] G. Peri, G. Rizzo, G. Scaccianoce, M. La Gennusa, P. Jones, Vegetation and soil – related parameters for computing solar radiation exchanges within green roofs: Are the available values adequate for an easy modeling of their thermal behavior?, Energy Build. 129 (2016) 535–548. https://doi.org/10.1016/j.enbuild.2016.08.018.
[265] R. Kumar, S.C. Kaushik, Performance evaluation of green roof and shading for thermal protection of buildings, Build. Environ. 40 (2005) 1505–1511. https://doi.org/10.1016/j.buildenv.2004.11.015.
[266] C.B. Koc, P. Osmond, A. Peters, A Green Infrastructure Typology Matrix to Support Urban Microclimate Studies, Procedia Eng. 169 (2016) 183–190. https://doi.org/10.1016/j.proeng.2016.10.022.
[267] Bureau of Meteorology, Bureau of Meteorology, Aust. Gov. (2021). bom.gov.au/nsw.
[268] R Core Team, R: A language and environment for statistical computing, (2021). www.R-project.org.
[269] H. Wickham, R. Fracois, L. Henry, K. Muller, dplyr: A Grammar of Data Manipulation, (2021). https://cran.r-project.org/package=dplyr.

[270] H. Wickham, Elegant Graphics for Data Analysis, Springer-Verlag, New York, 2016. https://ggplot2.tidyverse.org.
[271] P.M. Azbizu, pairwiseAdonis: Pairwise Multilevel Comparison using Adonis., (2017).
[272] H. Wickham, tidyr: Tidy Messy Data, (2021). https://cran.r-project.org/package=tidyr.
[273] J. Oksanen, F. Guillaume Blanchet, M. Friendly, R. Kindt, P. Legendre, D. McGlinn, P.R. Minchin, R.B. O'Hara, G.L. Simpson, P. Solymos, H. Stevens, E. Szoecs, H. Wagner, vegan: Community Ecology Package, (2020). https://cran.r-project.org/package=vegan.
[274] K. Perini, M. Ottelé, A.L.A. Fraaij, E.M. Haas, R. Raiteri, Vertical greening systems and the effect on air flow and temperature on the building envelope, Build. Environ. 46 (2011) 2287–2294. https://doi.org/10.1016/j.buildenv.2011.05.009.
[275] L. Libessart, M.A. Kenai, Measuring thermal conductivity of green-walls components in controlled conditions, J. Build. Eng. 19 (2018) 258–265. https://doi.org/10.1016/j.jobe.2018.05.016.
[276] M. Ottelé, K. Perini, Comparative experimental approach to investigate the thermal behaviour of vertical greened façades of buildings, Ecol. Eng. 108 (2017) 152–161. https://doi.org/10.1016/j.ecoleng.2017.08.016.
[277] L. Bianco, V. Serra, F. Larcher, M. Perino, Thermal behaviour assessment of a novel vertical greenery module system: first results of a long-term monitoring campaign in an outdoor test cell, Energy Effic. 10 (2017) 625–638. https://doi.org/10.1007/s12053-016-9473-4.
[278] D. Morau, T. Libelle, F. Garde, Performance evaluation of green roof for thermal protection of buildings in reunion Island, Energy Procedia. 14 (2012) 1008–1016. https://doi.org/10.1016/j.egypro.2011.12.1047.
[279] N.H. Abu-Hamdeh, A.I. Khdair, R.C. Reeder, Comparison of two methods used to evaluate thermal conductivity for some soils, Int. J. Heat Mass Transf. 44 (2001) 1073–1078. https://doi.org/10.1016/S0017-9310(00)00144-7.
[280] S. Onmura, M. Matsumoto, S. Hokoi, Study on evaporative cooling effect of roof lawn gardens, Energy Build. 33 (2001) 653–666. https://doi.org/10.1016/S0378-7788(00)00134-1.
[281] M. Eksi, D.B. Rowe, I.S. Wichman, J.A. Andresen, Effect of substrate depth, vegetation type, and season on green roof thermal properties, Energy Build. 145 (2017) 174–187. https://doi.org/10.1016/j.enbuild.2017.04.017.
[282] H.S. Khan, M. Santamouris, P. Kassomenos, R. Paolini, P. Caccetta, I. Petrou, Spatiotemporal variation in urban overheating magnitude and its association with synoptic air-masses in a coastal city, Sci. Rep. 11 (2021) 1–15. https://doi.org/10.1038/s41598-021-86089-2.
[283] C. Chen, Determining the Leaf Emissivity of Three Crops by Infrared Thermometry, Sensors. 15 (2015) 11387–11401. https://doi.org/10.3390/s150511387.
[284] M.M. Elbadry, A. Ghali, Temperature Variations in Concrete Bridges, J. Struct. Eng. 109 (1983) 2355–2374. https://doi.org/10.1061/(asce)0733-9445(1983)109:10(2355).
[285] Q. Meng, W. Hu, Roof cooling effect with humid porous medium, Energy Build. 37 (2005) 1–9. https://doi.org/10.1016/j.enbuild.2003.11.004.
[286] T. Takakura, S. Kitade, E. Goto, Cooling effect of greenery cover over a building, Energy Build. 31 (2000) 1–6. https://doi.org/10.1016/S0378-7788(98)00063-2.
[287] T.G. Theodosiou, Summer period analysis of the performance of a planted roof as a passive cooling technique, Energy Build. 35 (2003) 909–917. https://doi.org/10.1016/S0378-7788(03)00023-9.
[288] K.L. Getter, D.B. Rowe, J.A. Andresen, I.S. Wichman, Seasonal heat flux properties of an extensive green roof in a Midwestern U.S. climate, Energy Build. 43 (2011) 3548–3557. https://doi.org/10.1016/j.enbuild.2011.09.018.
[289] D.J. Sailor, A green roof model for building energy simulation programs, Energy Build. 40 (2008) 1466–1478. https://doi.org/10.1016/j.enbuild.2008.02.001.
[290] H. Akbari, S. Konopacki, Calculating energy-saving potentials of heat-island reduction strategies, Energy Policy. 33 (2005) 721–756. https://doi.org/10.1016/j.enpol.2003.10.001.
[291] P. Bevilacqua, R. Bruno, N. Arcuri, Green roofs in a Mediterranean climate: energy performances based on in-situ experimental data, Renew. Energy. 152 (2020) 1414–1430. https://doi.org/10.1016/j.renene.2020.01.085.
[292] S. Vujovic, B. Haddad, H. Karaky, N. Sebaibi, M. Boutouil, Urban Heat Island: Causes, Consequences, and Mitigation Measures with Emphasis on Reflective and Permeable Pavements, CivilEng. 2 (2021) 459–484. https://doi.org/10.3390/civileng2020026.
[293] F. Olivieri, C. Di Perna, M. D'Orazio, L. Olivieri, J. Neila, Experimental measurements and numerical model for the summer performance assessment of extensive green roofs in a Mediterranean coastal climate, Energy Build. 63 (2013) 1–14. https://doi.org/10.1016/j.enbuild.2013.03.054.
[294] P. Bevilacqua, D. Mazzeo, R. Bruno, N. Arcuri, Experimental investigation of the thermal performances of an extensive green roof in the Mediterranean area, Energy Build. 122 (2016) 63–79. https://doi.org/10.1016/j.enbuild.2016.03.062.
[295] D. Kaiser, M. Köhler, M. Schmidt, F. Wolff, Increasing Evapotranspiration on Extensive Green Roofs by Changing Substrate Depths, Construction, and Additional Irrigation, Buildings. 9 (2019) 173. https://doi.org/10.3390/buildings9070173.
[296] M.G. Gomes, C.M. Silva, A.S. Valadas, M. Silva, Impact of vegetation, substrate, and irrigation on the energy performance of green roofs in a Mediterranean climate, Water (Switzerland). 11 (2019). https://doi.org/10.3390/w11102016.
[297] M. Kazemi, L. Courard, J. Hubert, Heat transfer measurement within green roof with incinerated municipal solid waste aggregates, Sustain. 13 (2021). https://doi.org/10.3390/su13137115.
[298] Y. Zhou, Y. Kong, H. Wang, F. Luo, The impact of population urbanization lag on eco-efficiency: A panel quantile approach, J. Clean. Prod. 244 (2020) 118664. https://doi.org/10.1016/j.jclepro.2019.118664.

[299] P.C.D. Milly, R.T. Wetherald, K.A. Dunne, T.L. Delworth, Increasing risk of great floods in a changing climate, Nature. 415 (2002) 514–517. https://doi.org/10.1038/415514a.
[300] I. Teotónio, C.M. Silva, C.O. Cruz, Economics of green roofs and green walls: A literature review, Sustain. Cities Soc. 69 (2021). https://doi.org/10.1016/j.scs.2021.102781.
[301] M. Vice, Century City as a case study for sustainable drainage systems (SuDS) in South Africa, 2011.
[302] T.D. Fletcher, W. Shuster, W.F. Hunt, R. Ashley, D. Butler, S. Arthur, S. Trowsdale, S. Barraud, A. Semadeni-Davies, J.L. Bertrand-Krajewski, P.S. Mikkelsen, G. Rivard, M. Uhl, D. Dagenais, M. Viklander, SUDS, LID, BMPs, WSUD and more – The evolution and application of terminology surrounding urban drainage, Urban Water J. 12 (2015) 525–542. https://doi.org/10.1080/1573062X.2014.916314.
[303] US EPA, Managing Stormwater with Low Impact Development Practices., (2009) 7. https://www3.epa.gov/region1/npdes/stormwater/assets/pdfs/AddressingBarrier2LID.pdf.
[304] Z. Kalantari, C.S.S. Ferreira, S. Keesstra, G. Destouni, Nature-based solutions for flood-drought risk mitigation in vulnerable urbanizing parts of East-Africa, Curr. Opin. Environ. Sci. Heal. 5 (2018) 73–78. https://doi.org/10.1016/j.coesh.2018.06.003.
[305] R. Fleck, R.L. Gill, S. Saadeh, T. Pettit, E. Wooster, F. Torpy, P. Irga, Urban green roofs to manage rooftop microclimates: A case study from Sydney, Australia, Build. Environ. 209 (2022) 108673. https://doi.org/10.1016/j.buildenv.2021.108673.
[306] T. Susca, Green roofs to reduce building energy use? A review on key structural factors of green roofs and their effects on urban climate, Build. Environ. 162 (2019) 106273. https://doi.org/10.1016/j.buildenv.2019.106273.
[307] N. She, J. Pang, Physically Based Green Roof Model, J. Hydrol. Eng. 15 (2010) 458–464. https://doi.org/10.1061/(asce)he.1943-5584.0000138.
[308] A.S. Castro, J.A. Goldenfum, A.L. da Silveira, A.L.B. DallAgnol, L. Loebens, C.F. Demarco, D. Leandro, W.C. Nadaleti, M.S. Quadro, The analysis of green roof's runoff volumes and its water quality in an experimental study in Porto Alegre, Southern Brazil, Environ. Sci. Pollut. Res. 27 (2020) 9520–9534. https://doi.org/10.1007/s11356-019-06777-5.
[309] G. Sakson, A. Brzezinska, M. Zawilski, Emission of heavy metals from an urban catchment into receiving water and possibility of its limitation on the example of Lodz city, Environ. Monit. Assess. 190 (2018). https://doi.org/10.1007/s10661-018-6648-9.
[310] M.C. Gromaire, S. Garnaud, M. Saad, G. Chebbo, Contribution of different sources to the pollution of wet weather flows in combined sewers, Water Res. 35 (2001) 521–533. https://doi.org/10.1016/S0043-1354(00)00261-X.
[311] J.N. Brown, B.M. Peake, Sources of heavy metals and polycyclic aromatic hydrocarbons in urban stormwater runoff, Sci. Total Environ. 359 (2006) 145–155. https://doi.org/10.1016/j.scitotenv.2005.05.016.
[312] A.E. Barbosa, J.N. Fernandes, L.M. David, Key issues for sustainable urban stormwater management, Water Res. 46 (2012) 6787–6798. https://doi.org/10.1016/j.watres.2012.05.029.
[313] T. van Seters, L. Rocha, D. Smith, G. MacMillan, Evaluation of green roofs for runoff retention, runoff quality, and leachability, Water Qual. Res. J. Canada. 44 (2009) 33–47. https://doi.org/10.2166/wqrj.2009.005.
[314] S. Bae, X.C. Pan, S.Y. Kim, K. Park, Y.H. Kim, H. Kim, Y.C. Hong, Exposures to particulate matter and polycyclic aromatic hydrocarbons and oxidative stress in schoolchildren, Environ. Health Perspect. 118 (2010) 579–583. https://doi.org/10.1289/ehp.0901077.
[315] X. Sun, A.P. Davis, Heavy metal fates in laboratory bioretention systems, Chemosphere. 66 (2007) 1601–1609. https://doi.org/10.1016/j.chemosphere.2006.08.013.
[316] R. Świetlik, A. Molik, M. Molenda, M. Trojanowska, J. Siwiec, Chromium(III/VI) speciation in urban aerosol, Atmos. Environ. 45 (2011) 1364–1368. https://doi.org/10.1016/j.atmosenv.2010.12.001.
[317] W.F. Hunt, A.R. Jarrett, J.T. Smith, L.J. Sharkey, Evaluating Bioretention Hydrology and Nutrient Removal at Three Field Sites in North Carolina, J. Irrig. Drain. Eng. 132 (2006) 600–608. https://doi.org/10.1061/(asce)0733-9437(2006)132:6(600).
[318] C. Chapman, R.R. Horner, Performance Assessment of a Street-Drainage Bioretention System, Water Environ. Res. 82 (2010) 109–119. https://doi.org/10.2175/106143009x426112.
[319] F.J. Knoche, Quality of roof runoff from green roofs, in: Proc. 8th Int. Conf. Urban Storm Drain., American Society of Civil Engineers, Sydney, Australia, 1999.
[320] J. Czemiel Berndtsson, Green roof performance towards management of runoff water quantity and quality: A review, Ecol. Eng. 36 (2010) 351–360. https://doi.org/10.1016/j.ecoleng.2009.12.014.
[321] Z. Zhang, C. Szota, T.D. Fletcher, N.S.G. Williams, J. Werdin, C. Farrell, Influence of plant composition and water use strategies on green roof stormwater retention, Sci. Total Environ. 625 (2018) 775–781. https://doi.org/10.1016/j.scitotenv.2017.12.231.
[322] R. Conn, J. Werdin, J.P. Rayner, C. Farrell, Green roof substrate physical properties differ between standard laboratory tests due to differences in compaction, J. Environ. Manage. 261 (2020) 110206. https://doi.org/10.1016/j.jenvman.2020.110206.
[323] E.L. Villarreal, L. Bengtsson, Response of a Sedum green-roof to individual rain events, Ecol. Eng. 25 (2005) 1–7. https://doi.org/10.1016/j.ecoleng.2004.11.008.
[324] Z. Peng, V. Stovin, Independent Validation of the SWMM Green Roof Module, J. Hydrol. Eng. 22 (2017) 04017037. https://doi.org/10.1061/(asce)he.1943-5584.0001558.
[325] S.S. Cipolla, M. Maglionico, I. Stojkov, A long-term hydrological modelling of an extensive green roof by means of SWMM, Ecol. Eng. 95 (2016) 876–887. https://doi.org/10.1016/j.ecoleng.2016.07.009.
[326] S. Browne, A. Lintern, B. Jamali, J.P. Leitão, P.M. Bach, Stormwater management impacts of small urbanising towns:

The necessity of investigating the 'devil in the detail,' Sci. Total Environ. 757 (2021) 143835. https://doi.org/10.1016/j.scitotenv.2020.143835.
[327] S. Musa, M. Arish, N. Arshad, M. Jalil, H. Kasmin, Potential of Storm Water Capacity Using Vegetated Roofs in Malaysia, in: Int. Conf. Civ. Eng. Pract. 08, 2011. http://eprints.uthm.edu.my/275/.
[328] X. Zheng, Y. Zou, A.W. Lounsbury, C. Wang, R. Wang, Green roofs for stormwater runoff retention: A global quantitative synthesis of the performance, Resour. Conserv. Recycl. 170 (2021) 105577. https://doi.org/10.1016/j.resconrec.2021.105577.
[329] P. Göbel, C. Dierkes, W.G. Coldewey, Storm water runoff concentration matrix for urban areas, J. Contam. Hydrol. 91 (2007) 26–42. https://doi.org/10.1016/j.jconhyd.2006.08.008.
[330] C. Loiola, W. Mary, L. Pimentel da Silva, Hydrological performance of modular-tray green roof systems for increasing the resilience of mega-cities to climate change, J. Hydrol. 573 (2019) 1057–1066. https://doi.org/10.1016/j.jhydrol.2018.01.004.
[331] M. Uhl, L. Schiedt, Green roof storm water retention–monitoring results, in: … Urban Drainage, Edinburgh, Scotland, UK, 2008: pp. 1–10. http://www.ecotelhado.com.br/InformacoesInterna/Green Roof Storm Water Retention.pdf.
[332] K.L. Getter, D.B. Rowe, J.A. Andresen, Quantifying the effect of slope on extensive green roof stormwater retention, Ecol. Eng. 31 (2007) 225–231. https://doi.org/10.1016/j.ecoleng.2007.06.004.
[333] Y. Gong, X. Zhang, J. Li, X. Fang, D. Yin, P. Xie, L. Nie, Factors affecting the ability of extensive green roofs to reduce nutrient pollutants in rainfall runoff, Sci. Total Environ. 732 (2020) 139248. https://doi.org/10.1016/j.scitotenv.2020.139248.
[334] S. Steusloff, Input and Output of Airborne Aggressive Substances on Green Roofs in Karlsruhe, Urban Ecol. (1998) 144–148. https://doi.org/10.1007/978-3-642-88583-9_24.
[335] A.F. Speak, J.J. Rothwell, S.J. Lindley, C.L. Smith, Rainwater runoff retention on an aged intensive green roof, Sci. Total Environ. 461–462 (2013) 28–38. https://doi.org/10.1016/j.scitotenv.2013.04.085.
[336] C. Brandão, M. do R. Cameira, F. Valente, R. Cruz de Carvalho, T.A. Paço, Wet season hydrological performance of green roofs using native species under Mediterranean climate, Ecol. Eng. 102 (2017) 596–611. https://doi.org/10.1016/j.ecoleng.2017.02.025.
[337] Q. Zhang, L. Miao, X. Wang, D. Liu, L. Zhu, B. Zhou, J. Sun, J. Liu, The capacity of greening roof to reduce stormwater runoff and pollution, Landsc. Urban Plan. 144 (2015) 142–150. https://doi.org/10.1016/j.landurbplan.2015.08.017.
[338] V. Stovin, G. Vesuviano, H. Kasmin, The hydrological performance of a green roof test bed under UK climatic conditions, J. Hydrol. 414–415 (2012) 148–161. https://doi.org/10.1016/j.jhydrol.2011.10.022.
[339] M. Shafique, R. Kim, K. Kyung-Ho, Green roof for stormwater management in a highly urbanized area: The case of Seoul, Korea, Sustain. 10 (2018) 1–14. https://doi.org/10.3390/su10030584.
[340] D.J. Bliss, R.D. Neufeld, R.J. Ries, Storm Water Runoff Mitigation Using a Green Roof, Environ. Eng. Sci. 26 (2009) 407–418. https://doi.org/10.1089/ees.2007.0186.
[341] E.L. Villarreal, A. Semadeni-Davies, L. Bengtsson, Inner city stormwater control using a combination of best management practices, Ecol. Eng. 22 (2004) 279–298. https://doi.org/10.1016/j.ecoleng.2004.06.007.
[342] H. Yin, F. Kong, I. Dronova, Hydrological performance of extensive green roofs in response to different rain events in a subtropical monsoon climate, Landsc. Ecol. Eng. 15 (2019) 297–313. https://doi.org/10.1007/s11355-019-00380-z.
[343] A. Brambilla, E. Gasparri, Hygrothermal behaviour of emerging timber-based envelope technologies in Australia: A preliminary investigation on condensation and mould growth risk, J. Clean. Prod. 276 (2020) 124129. https://doi.org/10.1016/j.jclepro.2020.124129.
[344] Bureau of Meteorology, Sydney Monthly Rainfall, Aust. Gov. (2022).
[345] A.F. Speak, J.J. Rothwell, S.J. Lindley, C.L. Smith, Metal and nutrient dynamics on an aged intensive green roof, Environ. Pollut. 184 (2014) 33–43. https://doi.org/10.1016/j.envpol.2013.08.017.
[346] J.E. Ball, R. Jenks, D. Aubourg, An assessment of the availability of pollutant constituents on road surfaces, Sci. Total Environ. 209 (1998) 243–254. https://doi.org/10.1016/S0048-9697(97)00319-7.
[347] C.I. Brockbank, G.E. Batley, J.E. Ball, J.H. Tilley, Investigation Report ET/IR98: Metals and Hydrocarbons in Stormwater runoff from urban roads, 1998.
[348] WaterCom, DRAINS: Stormwater Drainage System design and analysis software for Australian practise, (2021). watercom.com.au.
[349] Australia Rainfall and Runoff Data Hub, (2021). data.arr-software.org.
[350] L.A. Rossman, Storm water management model user's manual, version 5.0, (2010).
[351] N. Sun, M. Hall, B. Hong, L. Zhang, Impact of SWMM Catchment Discretization: Case Study in Syracuse, New York, J. Hydrol. Eng. 19 (2014) 223–234. https://doi.org/10.1061/(asce)he.1943-5584.0000777.
[352] I. Broekhuizen, G. Leonhardt, J. Marsalek, M. Viklander, Event selection and two-stage approach for calibrating models of green urban drainage systems, Hydrol. Earth Syst. Sci. 24 (2020) 869–885. https://doi.org/10.5194/hess-24-869-2020.
[353] B. Hicks, S. Gray, J. Ball, A Critical Review of the Urban Rational Method, in: Proc. H2009 32nd Hydrol. Water Resour. Symp., 2009: pp. 1424–1433.
[354] B.E. Davies, P.C. Elwood, J. Gallacher, R.C. Ginnever, J. Gallachert, R.C. Ginnever, The relationships between heavy metals in garden soils and house dusts in an old lead mining area of North Wales, Great Britain, Environ. Pollution. Ser. B, Chem. Phys. 9 (1985) 255–266. https://doi.org/10.1016/0143-148X(85)90002-3.
[355] P.G. Georgopoulos, A. Roy, M.J. Yonone-Lioy, R.E. Opiekun, P.J. Lioy, Environmental copper: Its dynamics and human exposure issues, J. Toxicol. Environ. Heal. - Part B Crit. Rev. 4 (2001) 341–394.

https://doi.org/10.1080/109374001753146207.
[356] A.G. Jiries, H.H. Hussein, Z. Halaseh, The quality of water and sediments of street runoff in Amman, Jordan, Hydrol. Process. 15 (2001) 815–824. https://doi.org/10.1002/hyp.186.
[357] The NSW Government, Traffic Volume Viewer, (2019). roads-waterays,transport.nsw.gov.au.
[358] K.J. Rader, R.F. Carbonaro, E.D. van Hullebusch, S. Baken, K. Delbeke, The Fate of Copper Added to Surface Water: Field, Laboratory, and Modeling Studies, Environ. Toxicol. Chem. 38 (2019) 1386–1399. https://doi.org/10.1002/etc.4440.
[359] Australian Bureau of Statistics, 2016 Census QuickStats - Adelaid City, (2016).
[360] Australia Bureau of Statistics, 2016 Census QuickStats - Sydney (LC), (n.d.).
[361] J.C. Berndtsson, T. Emilsson, L. Bengtsson, The influence of extensive vegetated roofs on runoff water quality, Sci. Total Environ. 355 (2006) 48–63. https://doi.org/10.1016/j.scitotenv.2005.02.035.
[362] Y. Sun, Q. Zhou, Y. Xu, L. Wang, X. Liang, Phytoremediation for co-contaminated soils of benzo[a]pyrene (B[a]P) and heavy metals using ornamental plant Tagetes patula, J. Hazard. Mater. 186 (2011) 2075–2082. https://doi.org/10.1016/j.jhazmat.2010.12.116.
[363] A.G. Khan, Role of soil microbes in the rhizospheres of plants growing on trace metal contaminated soils in phytoremediation, J. Trace Elem. Med. Biol. 18 (2005) 355–364. https://doi.org/10.1016/j.jtemb.2005.02.006.
[364] J. Kim, S.H. Kang, K.A. Min, K.S. Cho, I.S. Lee, Rhizosphere microbial activity during phytoremediation of diesel-contaminated soil, J. Environ. Sci. Heal. - Part A Toxic/Hazardous Subst. Environ. Eng. 41 (2006) 2503–2516. https://doi.org/10.1080/10934520600927658.
[365] L. Thouron, C. Seigneur, Y. Kim, C. Legorgeu, Y. Roustan, B. Bruge, Simulation of trace metals and PAH atmospheric pollution over Greater Paris: Concentrations and deposition on urban surfaces, Atmos. Environ. 167 (2017) 360–376. https://doi.org/10.1016/j.atmosenv.2017.08.027.
[366] M.Y. Hanfi, M.Y.A. Mostafa, M. V. Zhukovsky, Heavy metal contamination in urban surface sediments: sources, distribution, contamination control, and remediation, Environ. Monit. Assess. 192 (2020). https://doi.org/10.1007/s10661-019-7947-5.
[367] H. Arslan, Heavy metals in street dust in bursa, turkey, J. Trace Microprobe Tech. 19 (2001) 439–445. https://doi.org/10.1081/TMA-100105058.
[368] E. De Miguel, J.F. Llamas, E. Chacón, L.F. Mazadiego, Sources and pathways of trace elements in urban environments: A multi-elemental qualitative approach, Sci. Total Environ. 235 (1999) 355–357. https://doi.org/10.1016/S0048-9697(99)00234-X.
[369] M. Salim Akhter, I.M. Madany, Heavy metals in street and house dust in Bahrain, Water, Air, Soil Pollut. 66 (1993) 111–119. https://doi.org/10.1007/BF00477063.
[370] S. Jamil, P.C. Abhilash, A. Singh, N. Singh, H.M. Behl, Fly ash trapping and metal accumulating capacity of plants: Implication for green belt around thermal power plants, Landsc. Urban Plan. 92 (2009) 136–147. https://doi.org/10.1016/j.landurbplan.2009.04.002.
[371] Z. Li, L.M. Shuman, Heavy metal movement in metal contaminated soil profiles, Soil Sci. 161 (1996) 656–666.
[372] K.R. Reddy, T. Xie, S. Dastgheibi, Removal of heavy metals from urban stormwater runoff using different filter materials, J. Environ. Chem. Eng. 2 (2014) 282–292. https://doi.org/10.1016/j.jece.2013.12.020.
[373] Bureau of Meteorology, Bureau of Meteorology - Sydney, Observatory Hill, (2022). http://www.bom.gov.au/products/IDN60901/IDN60901.94768.shtml.
[374] R. Feitosa, S. Wilkinson, Modelling green roof stormwater response for different soil depths, Landsc. Urban Plan. 153 (2016) 170–179. https://doi.org/10.1016/j.landurbplan.2016.05.007.
[375] X. Zheng, Y. Zou, A.W. Lounsbury, C. Wang, R. Wang, Green roofs for stormwater runoff retention: A global quantitative synthesis of the performance, Resour. Conserv. Recycl. 170 (2021) 105577. https://doi.org/10.1016/j.resconrec.2021.105577.
[376] W. Yang, J. Zhang, S. Mei, P. Krebs, Impact of antecedent dry-weather period and rainfall magnitude on the performance of low impact development practices in urban flooding and non-point pollution mitigation, J. Clean. Prod. 320 (2021) 128946. https://doi.org/10.1016/j.jclepro.2021.128946.
[377] A. Palla, I. Gnecco, P. La Barbera, Assessing the hydrologic performance of a green roof retrofitting scenario for a small urban catchment, Water (Switzerland). 10 (2018). https://doi.org/10.3390/w10081052.
[378] L. Aye, J. Blair, T. Blanusa, R. Cameron, R. Castiglia Feitosa, S. Ghosh, A. Giovanangeli, D. Hes, M. Irger, C. Jensen, S. Kemp, J. Lamond, T. Latty, P. Osmond, D. Proverbs, F. Torpy, I. Vanni, M. Vaz Monterio, Green Roof Retrofit, Sussex, 2016.
[379] A.L. Nagengast, C. Hendricksen, H.S. Matthews, Energy Performance Impacts from Competing Low-slope Roofing Choices and Photovoltaic Technologies, 2012. http://search.proquest.com/docview/1313752974?accountid=14556%5Cnhttp://vv6tt6sy5c.search.serialssolutions.com/?ctx_ver=Z39.88-2004&ctx_enc=info:ofi/enc:UTF-8&rfr_id=info:sid/ProQuest+Dissertations+%26+Theses+Global&rft_val_fmt=info:ofi/fmt:kev:mtx:disser.
[380] O. Schneising, M. Reuter, M. Buchwitz, J. Heymann, H. Bovensmann, J.P. Burrows, Terrestrial carbon sink observed from space: variation of growth rates and seasonal cycle amplitudes in response to interannual surface temperature variability, Atmos. Chem. Phys. 14 (2014) 133–141. https://doi.org/10.5194/acp-14-133-2014.
[381] D. Gielen, F. Boshell, D. Saygin, M.D. Bazilian, N. Wagner, R. Gorini, The role of renewable energy in the global energy transformation, Energy Strateg. Rev. 24 (2019) 38–50. https://doi.org/10.1016/j.esr.2019.01.006.
[382] S. Sorrell, Reducing energy demand: A review of issues, challenges and approaches, Renew. Sustain. Energy Rev. 47

(2015) 74–82. https://doi.org/10.1016/j.rser.2015.03.002.
[383] T.N. Thanh, P.V. Minh, K.D. Trung, T. Do Anh, Study on performance of rooftop solar power generation combined with battery storage at office building in northeast region, vietnam, Sustain. 13 (2021). https://doi.org/10.3390/su131911093.
[384] M. Fadzli Haniff, H. Selamat, R. Yusof, S. Buyamin, F. Sham Ismail, Review of HVAC scheduling techniques for buildings towards energy-efficient and cost-effective operations, Renew. Sustain. Energy Rev. 27 (2013) 94–103. https://doi.org/10.1016/j.rser.2013.06.041.
[385] M. Taleghani, Outdoor thermal comfort by different heat mitigation strategies- A review, Renew. Sustain. Energy Rev. 81 (2018) 2011–2018. https://doi.org/10.1016/j.rser.2017.06.010.
[386] S.C.M. Hui, S.C. Chan, Integration of green roof and solar photovoltaic systems, in: Jt. Symp. 2011 Integr. Build. Des. New Era Sustain., 2011: pp. 1–12.
[387] M.J.R. Perez, N.T. Wight, V.M. Fthenakis, C. Ho, Green-roof integrated pv canopies-an empirical study and teaching tool for low income students in the South Bronx, in: World Renew. Energy Forum, WREF 2012, Incl. World Renew. Energy Congr. XII Color. Renew. Energy Soc. Annu. Conf., 2012: pp. 4046–4052.
[388] R. Fleck, M.T. Westerhausen, N. Killingsworth, J. Ball, F.R. Torpy, P.J. Irga, The hydrological performance of a green roof in Sydney, Australia: A tale of two towers, Build. Environ. (2022) 109274. https://doi.org/10.1016/j.buildenv.2022.109274.
[389] AER, Annual retail markets report 2019–20, 2020.
[390] DISER, National Greenhouse Accounts Factors October 2020, 2020. https://www.industry.gov.au/data-and-publications/national-greenhouse-accounts-factors-2020.
[391] M. Shafique, X. Xue, X. Luo, An overview of carbon sequestration of green roofs in urban areas, Urban For. Urban Green. 47 (2020) 126515. https://doi.org/10.1016/j.ufug.2019.126515.
[392] Greenhouse Gas Equivalencies Calculator, United States Environ. Prot. Agency. (2021).
[393] V. Etminan, R.J. Lowe, M. Ghisalberti, A new model for predicting the drag exerted by vegetation canopies, Water Resour. Res. 53 (2017) 3179–3196. https://doi.org/10.1002/2016WR020090.
[394] C. Lamnatou, D. Chemisana, A critical analysis of factors affecting photovoltaic-green roof performance, Renew. Sustain. Energy Rev. 43 (2015) 264–280. https://doi.org/10.1016/j.rser.2014.11.048.
[395] T. Baumann, H. Nussbaumer, M. Klenk, A. Dreisiebner, F. Carigiet, F. Baumgartner, Photovoltaic systems with vertically mounted bifacial PV modules in combination with green roofs, Sol. Energy. 190 (2019) 139–146. https://doi.org/10.1016/j.solener.2019.08.014.
[396] M. Kohler, R. Feige, W. Wiartalla, Interaction between PV-systems and extensive green roofs, in: 5th Annu. Int. Green. Rooftops Sustain. Communities Conf. Award. Trade Show, Green Roofs for Healthy Cities, Minneapolis, 2007.
[397] C. Kaewpraek, L. Ali, M.A. Rahman, M. Shakeri, M.S. Chowdhury, M.S. Jamal, M.S. Mia, J. Pasupuleti, L.K. Dong, K. Techato, The effect of plants on the energy output of green roof photovoltaic systems in tropical climates, Sustain. 13 (2021) 1–10. https://doi.org/10.3390/su13084505.
[398] City of Sydney, Greening Sydney Strategy, 2021. https://www.cityofsydney.nsw.gov.au/-/media/corporate/files/publications/strategies-action-plans/greening-sydney-strategy/greening-sydney-strategy.pdf?download=true.
[399] J. Polcyn, Y. Us, O. Lyulyov, T. Pimonenko, A. Kwilinski, Factors influencing the renewable energy consumption in selected european countries, Energies. 15 (2022) 1–27. https://doi.org/10.3390/en15010108.
[400] T. Kuronuma, H. Watanabe, T. Ishihara, D. Kou, K. Toushima, M. Ando, S. Shindo, CO2 Payoff of Extensive Green Roofs with Different Vegetation Species, Sustainability. 10 (2018) 2256. https://doi.org/10.3390/su10072256.
[401] C. Jansson, C. Faiola, A. Wingler, X.G. Zhu, A. Kravchenko, M.A. de Graaff, A.J. Ogden, P.P. Handakumbura, C. Werner, D.M. Beckles, Crops for Carbon Farming, Front. Plant Sci. 12 (2021) 1–12. https://doi.org/10.3389/fpls.2021.636709.
[402] P. Prosperi, M. Bloise, F.N. Tubiello, G. Conchedda, S. Rossi, L. Boschetti, M. Salvatore, M. Bernoux, New estimates of greenhouse gas emissions from biomass burning and peat fires using MODIS Collection 6 burned areas, Clim. Change. 161 (2020) 415–432. https://doi.org/10.1007/s10584-020-02654-0.
[403] M.R. Seyedabadi, U. Eicker, S. Karimi, Plant selection for green roofs and their impact on carbon sequestration and the building carbon footprint, Environ. Challenges. 4 (2021) 100119. https://doi.org/10.1016/j.envc.2021.100119.
[404] M. Foustalieraki, M.N. Assimakopoulos, M. Santamouris, H. Pangalou, Energy performance of a medium scale green roof system installed on a commercial building using numerical and experimental data recorded during the cold period of the year, Energy Build. 135 (2017) 33–38. https://doi.org/10.1016/j.enbuild.2016.10.056.
[405] A.P. Davis, M. Shokouhian, H. Sharma, C. Minami, Laboratory Study of Biological Retention for Urban Stormwater Management, Water Environ. Res. 73 (2001) 5–14. https://doi.org/10.2175/106143001x138624.
[406] A.P.; Davis, M.; Shokouhian, H.; Sharma, C.; Minami, D. Winogradoff, Water quality improvement through bioretention: Lead, copper, and zinc removal, n.d.
[407] C.H. Hsieh, A.P. Davis, Evaluation of Bioretention for Treatment of Urban Storm Water Runoff, World Water Environ. Resour. Congr. 131 (2003) 141–148. https://doi.org/10.1061/40685(2003)281.
[408] C. Glass, S. Bissouma, Evaluation of a Parking Lot Bioretention Cell for Removal of Stormwater Pollutants, WIT Trans. Ecol. Environ. 81 (2005) 699–708.
[409] X. Sun, A.P. Davis, Heavy metal fates in laboratory bioretention systems, Chemosphere. 66 (2007) 1601–1609. https://doi.org/10.1016/j.chemosphere.2006.08.013.
[410] R.M. Roseen, T.P. Ballestero, J.J. Houle, P. Avelleneda, R. Wildey, J. Briggs, Storm water low-impact development, conventional structural, and manufactured treatment strategies for parking lot runoff: Performance evaluations

under varied mass loading conditions, Transp. Res. Rec. (2006) 135–147. https://doi.org/10.3141/1984-15.
[411] A.P. Davis, Field performance of bioretention: Water quality, Environ. Eng. Sci. 24 (2007) 1048–1064. https://doi.org/10.1089/ees.2006.0190.
[412] W.F. Hunt, J.T. Smith, S.J. Jadlocki, J.M. Hathaway, P.R. Eubanks, Pollutant Removal and Peak Flow Mitigation by a Bioretention Cell in Urban Charlotte, N.C., J. Environ. Eng. 134 (2008) 403–408. https://doi.org/10.1061/(asce)0733-9372(2008)134:5(403).

SUPPLEMENTARY MATERIAL

Chapter 2

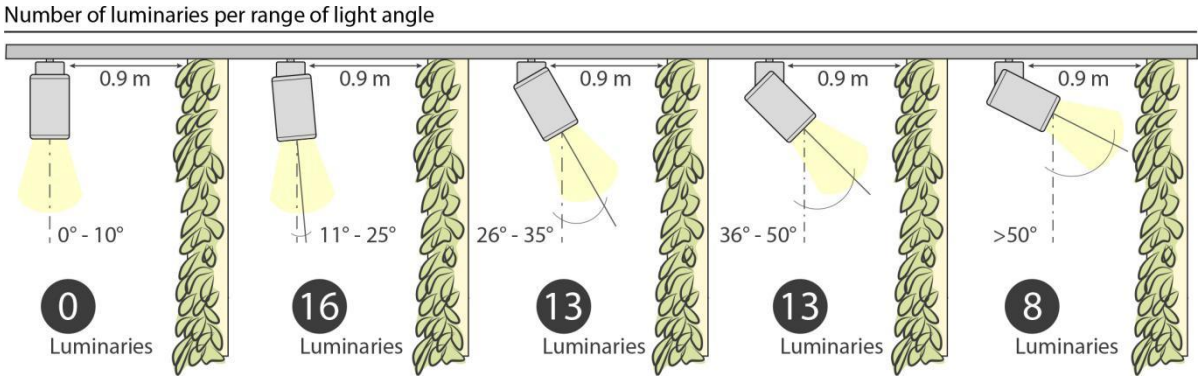

Supplementary Figure 1. Range of luminary angles as observed for the 50 units isolated from on-site image assessment of LW 1 and LW2.

Supplementary Figure 2. Design layout of *Chlorophytum comosum* and *Spathiphyllum wallisii* modules used during Experiment 2.2 (Plant response to light angle/intensity) and 2.3 (Phototropism and plant response).

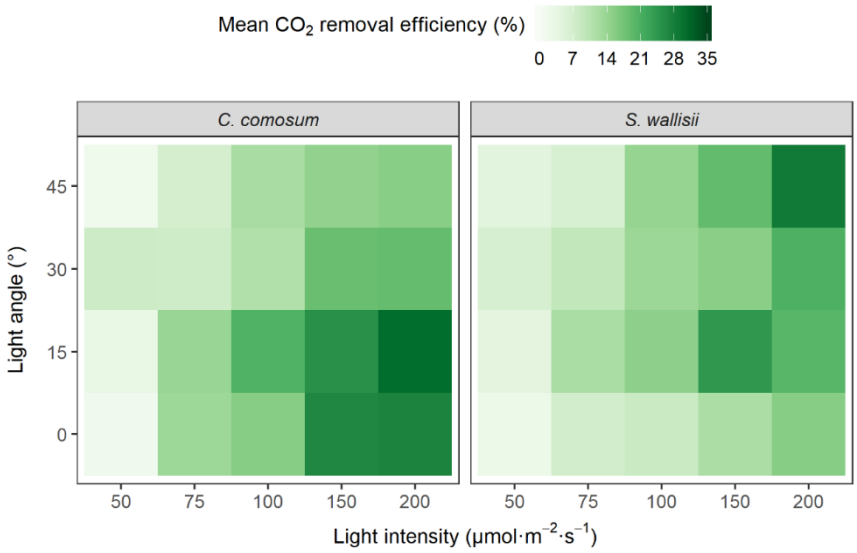

Supplementary Figure 3. Mean CO_2 removal efficiency (%) from input concentration (~1000 ppm) over 40-minute period for *C. comosum* and *S. wallisii* species under various intensities and angles of light (n = 3).

Supplementary Table 1. Average light availability at the proportion of the total plant foliage area at the four *in situ* living walls.

Light intensity (µmol·m^{-2}·s^{-1})	LW 1	LW 2	LW 3	LW 4	Average
≤ 10	6.7 %	62.5 %	26 %	44.6 %	35 %
11–49	65 %	32.5 %	66.6 %	43.1 %	51.8 %
50–74	11.6 %	2.5 %	7.4 %	1.5 %	5.8 %
75–99	6.7 %	0 %	0 %	4.6 %	2.8 %
100–149	8.3 %	2.5 %	0 %	3.1 %	3.4 %
150–199	1.7 %	0 %	0 %	3.1 %	1.2 %

Supplementary Table 2. Statistical output of multiple linear regression models for net non-photoadapted CO_2 removal over 40-minutes across levels of light intensity and light angle, for both *Chlorophytum comosum* ("*C.*com") and *Spathiphyllum wallisii* ("*S.wal*") models. Variable levels listed are in reference to 50 $\mu mol \cdot m^{-2} \cdot s^{-1}$ for light intensity effects, and 0° for light angle effects.

Variable	Coefficient	SE	*t*-value	*p*-value
***C.com*:**	$F(7,52) = 46.390$, $p < 0.001$, $R^2 = 0.86$, Adj $R^2 = 0.84$			
Intercept	7.189	1.237	5.812	< 0.001
Intensity				
75 $\mu mol \cdot m^{-2} \cdot s^{-1}$	6.816	1.383	4.929	< 0.001
100 $\mu mol \cdot m^{-2} \cdot s^{-1}$	11.228	1.383	8.119	< 0.001
150 $\mu mol \cdot m^{-2} \cdot s^{-1}$	17.702	1.383	12.801	< 0.001
200 $\mu mol \cdot m^{-2} \cdot s^{-1}$	19.375	1.383	14.010	< 0.001
Angle				
15°	1.836	1.237	1.484	0.144
30°	-4.115	1.237	-3.327	0.002
45°	-6.755	1.237	-5.461	< 0.001
S.wal:	$F(7,52) = 37.420$, $p < 0.001$, $R^2 = 0.83$, Adj $R^2 = 0.81$			
Intercept	1.993	1.127	1.769	0.083
Intensity				
75 $\mu mol \cdot m^{-2} \cdot s^{-1}$	4.137	1.260	3.284	0.002
100 $\mu mol \cdot m^{-2} \cdot s^{-1}$	8.153	1.260	6.472	< 0.001
150 $\mu mol \cdot m^{-2} \cdot s^{-1}$	13.119	1.260	10.413	< 0.001
200 $\mu mol \cdot m^{-2} \cdot s^{-1}$	16.712	1.260	13.265	< 0.001
Angle				
15°	6.068	1.127	5.385	< 0.001
30°	4.013	1.127	3.561	0.001
45°	5.408	1.127	4.799	< 0.001

Supplementary Table 3. Statistical output of linear regression models for photoadapted CO_2 removal efficiency time series in *Chlorophytum comosum* ("*C.com*") and *Spathiphyllum wallisii* ("*S.wal*").

Variable	Coefficient	SE	*t*-value	*p*-value
***C.com*: 100 µmol·m^{-2}·s^{-1} at 15°**	$F(1,31) = 0.779$, $p = 0.384$, $R^2 = 0.03$, Adj $R^2 = 0.01$			
Intercept	19.455	0.549	35.468	< 0.001
Days	-0.082	0.093	-0.882	0.384
***C.com*: 200 µmol·m^{-2}·s^{-1} at 15°**	$F(1,31) = 15.890$, $p < 0.001$, $R^2 = 0.34$, Adj $R^2 = 0.32$			
Intercept	35.980	1.368	26.303	< 0.001
Days	-0.922	0.231	-3.987	< 0.001
***C.com*: 200 µmol·m^{-2}·s^{-1} at 45°**	$F(1,31) = 1.143$, $p = 0.293$, $R^2 = 0.04$, Adj $R^2 \sim 0.00$			
Intercept	13.699	0.632	21.680	< 0.001
Days	0.114	0.107	1.069	0.293
***S.wal*: 100 µmol·m^{-2}·s^{-1} at 15°**	$F(1,31) = 0.195$, $p = 0.662$, $R^2 = 0.01$, Adj $R^2 = 0.03$			
Intercept	15.173	0.704	21.547	< 0.001
Days	0.053	0.119	0.442	0.662
***S.wal*: 200 µmol·m^{-2}·s^{-1} at 15°**	$F(1,31) = 13.500$, $p = 0.001$, $R^2 = 0.30$, Adj $R^2 = 0.28$			
Intercept	16.967	0.537	31.622	< 0.001
Days	0.333	0.091	3.674	0.001
***S.wal*: 200 µmol·m^{-2}·s^{-1} at 45°**	$F(1,31) = 0.264$, $p = 0.611$, $R^2 = 0.01$, Adj $R^2 = 0.02$			
Intercept	18.739	0.979	19.133	0.024
Days	0.085	0.166	0.514	0.611

Supplementary Table 4. Statistical output of linear regression models for photoadapted leaf and stem position time series in *Chlorophytum comosum* ("*C.com*") and *Spathiphyllum wallisii* ("*S.wal*").

Variable	Coefficient	SE	*t*-value	*p*-value
Leaf angle in *C.com*: 100 µmol·m^{-2}·s^{-1} at 15°				
$F(1,130) = 8.083$, $p = 0.005$, $R^2 = 0.06$, Adj $R^2 = 0.05$				
Intercept	-20.682	1.892	-10.933	< 0.001
Days	-0.909	0.320	-2.842	0.005
Leaf angle in *C.com*: 200 µmol·m^{-2}·s^{-1} at 15°				
$F(1,130) = 21.200$, $p < 0.001$, $R^2 = 0.14$, Adj $R^2 = 0.13$				
Intercept	-6.068	1.443	-4.207	< 0.001
Days	-1.123	0.244	-4.604	< 0.001
Leaf angle in *C.com*: 200 µmol·m^{-2}·s^{-1} at 45°				
$F(1,130) = 4.623$, $p = 0.033$, $R^2 = 0.03$, Adj $R^2 = 0.03$				
Intercept	-12.080	2.408	-5.018	< 0.001
Days	-0.875	0.407	-2.150	0.033
Leaf angle in *S.wal*: 100 µmol·m^{-2}·s^{-1} at 15°				
$F(1,130) = 36.770$, $p < 0.001$, $R^2 = 0.22$, Adj $R^2 = 0.22$				
Intercept	-6.136	4.125	-1.488	0.139
Days	4.227	0.697	6.064	< 0.001
Leaf angle in *S.wal*: 200 µmol·m^{-2}·s^{-1} at 15°				
$F(1,130) = 42.860$, $p < 0.001$, $R^2 = 0.25$, Adj $R^2 = 0.24$				
Intercept	25.239	4.656	5.421	< 0.001
Days	5.152	0.787	6.547	< 0.001
Leaf angle in *S.wal*: 200 µmol·m^{-2}·s^{-1} at 45°				
$F(1,130) = 24.420$, $p < 0.001$, $R^2 = 0.16$, Adj $R^2 = 0.15$				
Intercept	-6.034	6.054	-0.997	0.321
Days	5.057	1.023	4.942	< 0.001
Stem angle in *S.wal*: 100 µmol·m^{-2}·s^{-1} at 15°				
$F(1,130) = 56.770$, $p < 0.001$, $R^2 = 0.30$, Adj $R^2 = 0.30$				
Intercept	-2.023	1.520	-1.330	0.186
Days	1.936	0.257	7.534	< 0.001
Stem angle in *S.wal*: 200 µmol·m^{-2}·s^{-1} at 15°				
$F(1,130) = 144.900$, $p < 0.001$, $R^2 = 0.53$, Adj $R^2 = 0.52$				
Intercept	-5.455	0.735	-7.421	< 0.001
Days	1.496	0.124	12.036	< 0.001
Stem angle in *S.wal*: 200 µmol·m^{-2}·s^{-1} at 45°				
$F(1,130) = 124.000$, $p < 0.001$, $R^2 = 0.49$, Adj $R^2 = 0.48$				
Intercept	1.841	1.271	1.449	0.150
Days	2.391	0.215	11.133	< 0.001

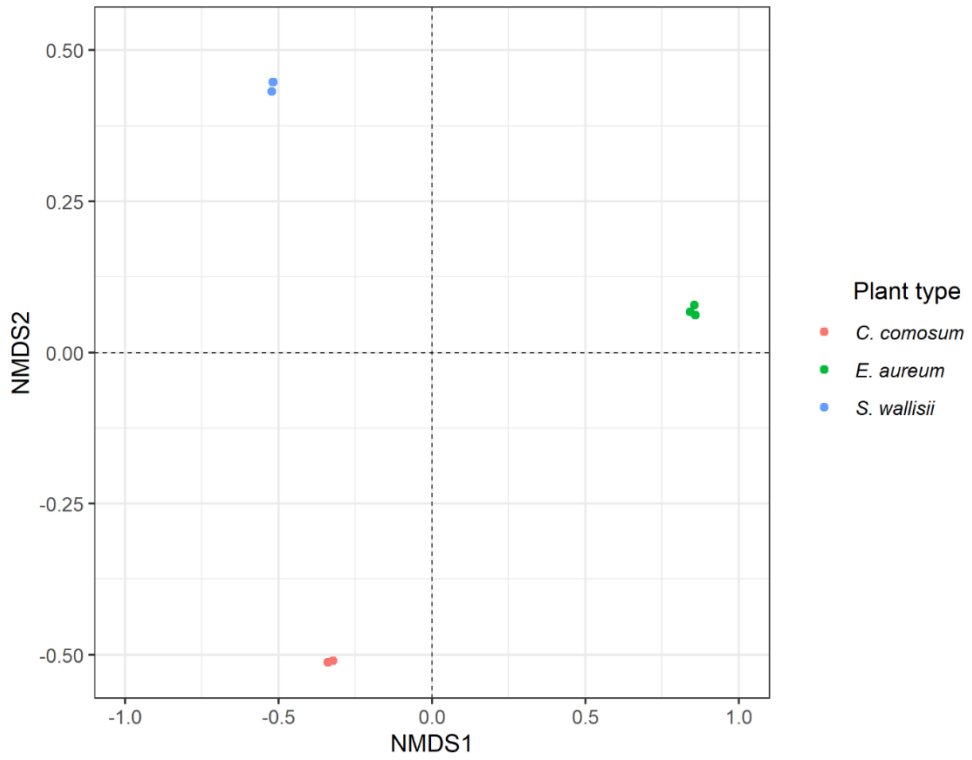

Supplementary Figure 4. nMDS plot showing dissimilarities in bacterial community structure amongst active green wall plant species, with significant differences detected between species (PERMANOVA; p = 0.005; R = 0.977; stress = < 0.01).

Supplementary Table 5. Average abundance (concentration/100 mL) ± SEM of individual Legionella ASVs for each plant species. Three ASVs (52, 108, 116) exceed the grouped mean relative abundance (gmRA) cut-off and were included in Figure 3. Percentage population abundance (PPA) is listed as function of its contribution to the total bacterial community composition (Legionella <1 % of total bacterial community).

ID	Genus	*C.comosum*	*E. aureum*	*S. wallisii*	gmRA	PPA (%)
ASV52	*Legionella*	22.9 ± 1.6	90.9 ± 32.5	4.2 ± 1.1	250.0	0.378
ASV108	*Legionella*	10 ± 0.9	42 ± 14.8	1.5 ± 1.5	112.2	0.17
ASV116	*Legionella*	45.1 ± 3.8	11.3 ± 4.4	17.7 ± 4.4	101.9	0.154
ASV224	*Legionella*	17.2 ± 2.8	4.4 ± 2	10.3 ± 2.8	43.4	0.066
ASV317	*Legionella*	9.1 ± 1	3.3 ± 1.2	7.1 ± 1.1	28.3	0.043
ASV439	*Legionella*		7.4 ± 2.6		16.6	0.025
ASV511	*Legionella*	5.9 ± 0.7	2.4 ± 0.9		12.1	0.018
ASV553	*Legionella*	2.5 ± 1.4		5.6 ± 1.9	10.1	0.015
ASV664	*Legionella*	0.9 ± 0.5	0.2 ± 0.2	4.2 ± 1.1	6.9	0.01
ASV802	*Legionella*	2.3 ± 0.5	0.6 ± 0.4		4.3	0.007
ASV844	*Legionella*			2.9 ± 0.6	4.0	0.006
ASV863	*Legionella*			2.9 ± 1	3.8	0.006
ASV940	*Legionella*			2.4 ± 0.7	3.1	0.005
ASV1259	*Legionella*	1.1 ± 0.6			1.2	0.002
ASV1279	*Legionella*			0.8 ± 0.6	1.2	0.002
ASV1281	*Legionella*			0.5 ± 0.5	1.2	0.002
ASV1317	*Legionella*		0.2 ± 0.2		1.1	0.002
ASV1321	*Legionella*			0.9 ± 0.9	1.11	0.002
ASV1348	*Legionella*	0.8 ± 0.8			1.00	0.002
ASV1412	*Legionella*		0.1 ± 0.1		0.89	0.001
ASV1554	*Legionella*		0.1 ± 0.1		0.67	0.001
ASV1594	*Legionella*			0.7 ± 0.7	0.67	0.001
ASV1616	*Legionella*	0.5 ± 0.5			0.56	0.001
ASV1619	*Legionella*	0.5 ± 0.5			0.56	0.001
ASV1638	*Legionella*		0.3 ± 0.3		0.56	0.001
ASV1652	*Legionella*		0.1 ± 0.1		0.56	0.001
ASV1695	*Legionella*			0.6 ± 0.6	0.56	0.001
ASV2447	*Legionella*		0.1 ± 0.1		0.22	0.00
ASV2538	*Legionella*				0.22	0.00
ASV2580	*Legionella*		0.1 ± 0.1		0.22	0.00
ASV2669	*Legionella*			0.2 ± 0.2	0.22	0.00
ASV303	NA	1 ± 0.5	11.6 ± 3.2		29.89	0.045
ASV1316	NA		0.7 ± 0.4		1.11	0.002
Total	*Legionellaceae*	119.8 ± 55.56	175.8 ± 122.15	62.5 ± 35.32	–	0.969%

Supplementary Table 6. Additional bacterial genera (identities/100 mL ± SD) containing opportunistic human pathogens described by Baron *et al* [219]. Relative abundances presented here are insufficient to warrant concern or sterilisation. [219].

ID	Class	Genus	*C. comosum*	*E. aureum*	*S. wallisii*	gmRA
ASV75	Actinobacteria	Mycobacterium	12.7 ± 2.4	1.3 ± 1.1	122.6 ± 27.9	181.4
ASV134	Actinobacteria	Mycobacterium	5.2 ± 1	1.1 ± 0.9	54.1 ± 13.5	81.2
ASV268	Actinobacteria	Mycobacterium	5.5 ± 1.3	7.2 ± 2.9	9.9 ± 2.1	35.4
ASV355	Actinobacteria	Mycobacterium	12.7 ± 0.8	0.7 ± 0.5	5.9 ± 2.7	23.9
ASV495	Actinobacteria	Mycobacterium	3.6 ± 2.1	3.0 ± 3.0	3.2 ± 3.2	12.6
ASV656	Actinobacteria	Mycobacterium		3.7 ± 1.7		7.1
ASV728	Actinobacteria	Mycobacterium			3.4 ± 2.0	5.7
ASV759	Actinobacteria	Mycobacterium			3.7 ± 0.6	5.1
ASC880	Actinobacteria	Mycobacterium	2.9 ± 1.5			5.1
ASC954	Actinobacteria	Mycobacterium	2.5 ± 1.3			2.9
ASC981	Actinobacteria	Mycobacterium	2.2 ± 1.1			2.7
ASC1079	Actinobacteria	Mycobacterium			1.6 ± 1.1	2.1
ASC1220	Actinobacteria	Mycobacterium			0.8 ± 0.5	1.4
ASC1318	Actinobacteria	Mycobacterium		0.2 ± 0.2		1.1
ASC1697	Actinobacteria	Mycobacterium			0.6 ± 0.6	0.6
ASV385	Alphaproteobacteria	Sphingomonas	14.2 ± 0.4		3.4 ± 1.1	21.0
ASV782	Alphaproteobacteria	Sphingomonas	2.1 ± 2.1	1.2 ± 1.2		4.7
ASV987	Alphaproteobacteria	Sphingomonas	2.1 ± 2.1			2.7
ASV1084	Alphaproteobacteria	Sphingomonas	1.9 ± 1.9			2.0
ASV1299	Alphaproteobacteria	Sphingomonas	1.0 ± 1.0			1.1
ASV1674	Alphaproteobacteria	Sphingomonas			0.4 ± 0.4	0.6
ASV561	Bacteroidetes	Chryseobacterium	8.7 ± 2.5			9.9
ASV644	Bacteroidetes	Chryseobacterium			5.6 ± 1.4	7.4
ASV742	Bacteroidetes	Chryseobacterium	4.6 ± 0.6			5.3
ASV890	Bacteroidetes	Chryseobacterium		0.2 ± 0.2	2.5 ± 1.0	3.6
ASV1350	Bacteroidetes	Chryseobacterium	0.8 ± 0.8			1.0
ASV2237	Bacteroidetes	Chryseobacterium	0.2 ± 0.2			0.2
ASV470	Gammaproteobacteria	Pseudomonas		4.4 ± 1.3	2.8 ± 1.1	14.2
ASV623	Gammaproteobacteria	Pseudomonas		3.9 ± 1.6		8.1
ASV1135	Gammaproteobacteria	Pseudomonas		0.6 ± 0.4		1.8
ASV1257	Gammaproteobacteria	Pseudomonas	1.1 ± 1.1			1.2
ASV959	Gammaproteobacteria	Acinetobacter		1.2 ± 0.3		2.9
ASV2045	Gammaproteobacteria	Acinetobacter				0.3
ASV529	Gammaproteobacteria	Stenotrophomonas	9.4 ± 0.1			10.9
ASV2587	Gammaproteobacteria	Stenotrophomonas		0.1 ± 0.1		0.2

Supplementary Figure 5. Aerial view (Google Earth) of the site and the surrounding geography. Satellite images pre-date the construction of the green roof, however the conventional roof is on display. Substantial development has occurred to the north and west of the site since the images were taken, however the southern and eastern urban geometries remain largely unchanged.

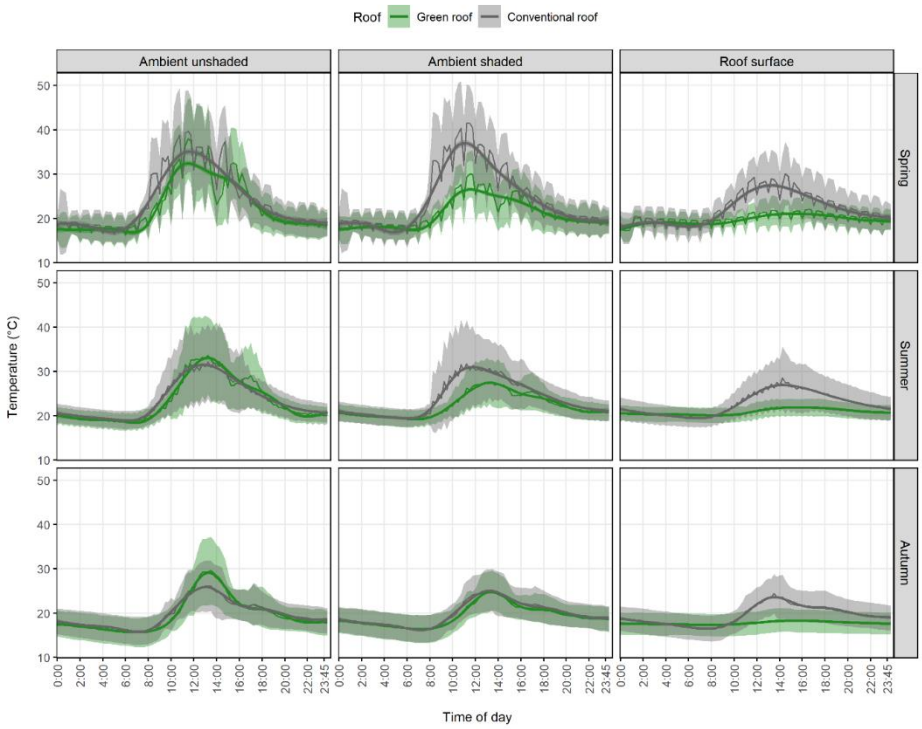

Supplementary Figure 6. Daily thermal sensor profile comparison between fitted generalised additive model (GAM) curves with cubic splines, and mean ± SD. Green lines = green roof; grey lines = conventional roof.

Supplementary Table 7. Summary of seasonal thermography surface temperatures (°C) for each roof type by season and location. Comparisons are drawn between PV panel and roof surface temperatures (plant foliage or concrete).

	Panel		Roof Surface	
	Green	Conventional	Green	Conventional
		Spring		
Mean	30.77	29.11	23.47	23.19
SD	5.8	4.04	4.24	4.44
Max.	40.9	37.2	40.3	36.3
Min.	21	21.9	18.7	18.6
		Summer		
Mean	27.07	36.7	22.47	29.4
SD	4.71	6.45	2.44	6.35
Max.	39.9	56.3	29	46
Min.	15.9	29.9	17.1	18.7
		Autumn		
Mean	24.05	31.45	18.62	23.21
SD	6.52	4.7	2.5	4.39
Max.	36.6	38.8	25	32.6
Min.	13.8	14.2	14	13.6

Supplementary Table 8. Summary of seasonal rooftop temperatures (°C) as recorded by thermal sensors for each roof type by sensor location. Values are daily averages across each season.

Sensor Location	Green Roof			Conventional Roof		
	Ambient unshaded	Ambient shaded	Roof surface	Ambient unshaded	Ambient shaded	Roof surface
			Spring			
Mean	22.15	20.82	19.61	23.53	23.92	21.93
SD	7.78	5.12	2.79	8.69	8.98	5.48
Max.	56.00	43.50	31.50	61.00	63.00	43.50
Min.	12.00	12.00	14.00	11.50	12.00	12.00
			Summer			
Mean	23.31	22.32	20.89	23.63	23.92	22.75
SD	6.76	4.03	1.89	6.31	6.27	4.45
Max.	58.00	44.00	32.50	56.00	53.50	52.50
Min.	14.00	14.50	16.00	14.50	14.50	16.00
			Autumn			
Mean	19.70	19.45	17.78	19.75	19.87	19.54
SD	5.56	3.95	2.55	4.70	4.26	3.85
Max.	53.00	40.00	24.50	51.00	38.00	37.00
Min.	8.50	10.00	11.00	9.50	10.00	10.00

Supplementary Table 9. Monthly heat flow (q; W m-2) values calculated using thermal resistance data from previous literature and in-situ temperatures recorded on each roof over the 8-month monitoring period.

	October	November	December	January	February	March	April	May
				Green roof				
Max	46.93	73.10	59.59	78.36	51.36	57.13	48.97	35.56
Min	-27.59	-7.22	-8.92	-10.70	-7.22	-6.97	-7.55	-7.39
Average	3.43	5.26	4	4.39	3.02	1.88	1.48	18.18
Avg Day	7.59	10.77	8.64	9.81	7.12	5.67	6.12	2.25
Avg Night	-1.47	-2.15	-2.29	-3.01	-2.3	-1.89	-3.03	-3.59
				Conventional roof				
Max	133.43	174	202.07	110.79	79.29	53.07	32.93	43.36
Min	-10.93	-32.43	-14.29	-25.36	-94.07	-20.00	-28.07	-9.07
Average	4.30	12.47	10.89	5.82	5.14	3.22	0.27	2.69
Avg Day	11.92	26.06	20.86	12.93	10.26	7.57	2.89	7.01
Avg Night	-4.66	-5.8	-2.64	-3.90	-1.51	-1.13	-2.28	-0.76

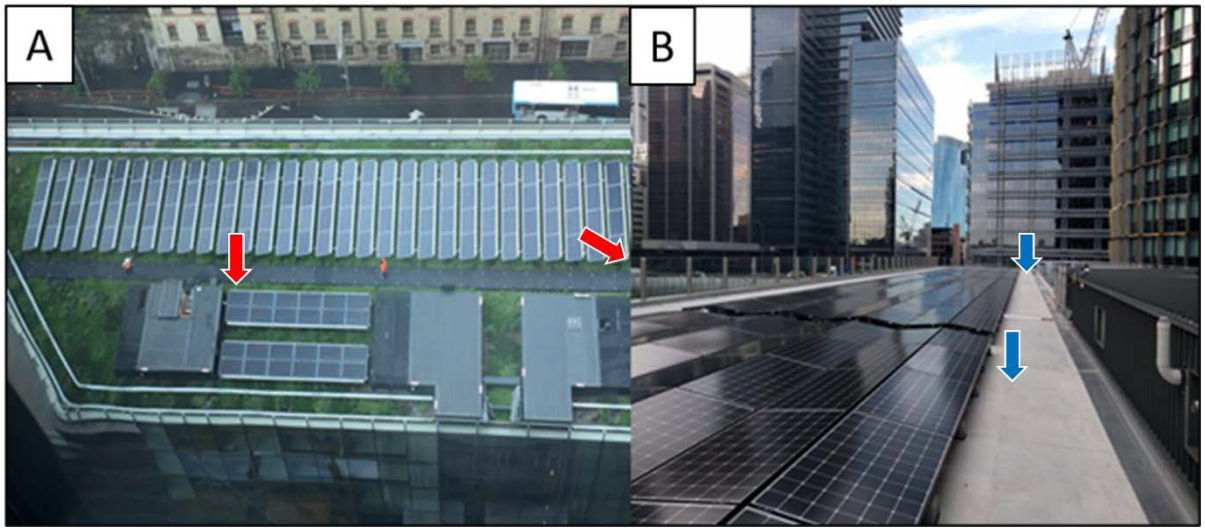

Supplementary Figure 7. Image of both green and conventional roofs (A and B, respectively), including indicators for trace metal sampling locations. Sampling was conducted on the North and South ends of each building, with substrate and surface dust samples being collected for the green and conventional roofs, respectively.

Supplementary Table 10. Examined literature relating to the bioretention of trace metals from stormwater and impervious surfaces.

Study	Investigation	Location
Davis et al. [405]	Laboratory experiment	USA
Davis et al. [406]	Laboratory experiment	USA
Hsieh & Davis [407]	Laboratory experiment	USA
Glass & Bissouma [408]	Field observations	Washington DC, USA
Sun & Davis [409]	Laboratory experiment	USA
Hunt et al. [317]	Field observations	North Carolina, USA
Roseen et al. [410]	Field observations	New Hampshire, USA
Davis [411]	Field observations	Maryland, USA
Hunt et al. [412]	Field observations	North Carolina, USA
Chapman & Horner [318]	Field observations	Washing, USA

Chapter 6

Supplementary Table 11. Specifications of the photovoltaic panels used on the BSGR and CSR.

Roof type	Bio-solar	Conventional
Panel model	SPR-MAX3-395	LG320N1K-V5
Manufacturer	Maxeon	LG
Solar Cells	104 Monocrystalline Gen 3	60 Monocrystalline / N-type
Dimensions (mm)	1046 x 1690 x 40 mm	1016 x 1686 x 40 mm
Nominal Power (pNom in W)	395	320
Power Tolerance (%)	+5/0	+3/0
Panel Efficiency (%)	22.3	19.2
Rated Voltage (V)	65.4	33.3
Rated Current (A)	6.04	9.62
Open-Circuit Voltage (V)	75.6	40.8
Short-Circuit Current (A)	6.57	10.19
Power Temp Coefficient (%)	−0.29 /°C	-0.38 /°C
Voltage Temp Coefficient (%)	−0.236 /°C	-0.28 /°C
Current Temp Coefficient (%)	0.058 /°C	0.03 /°C

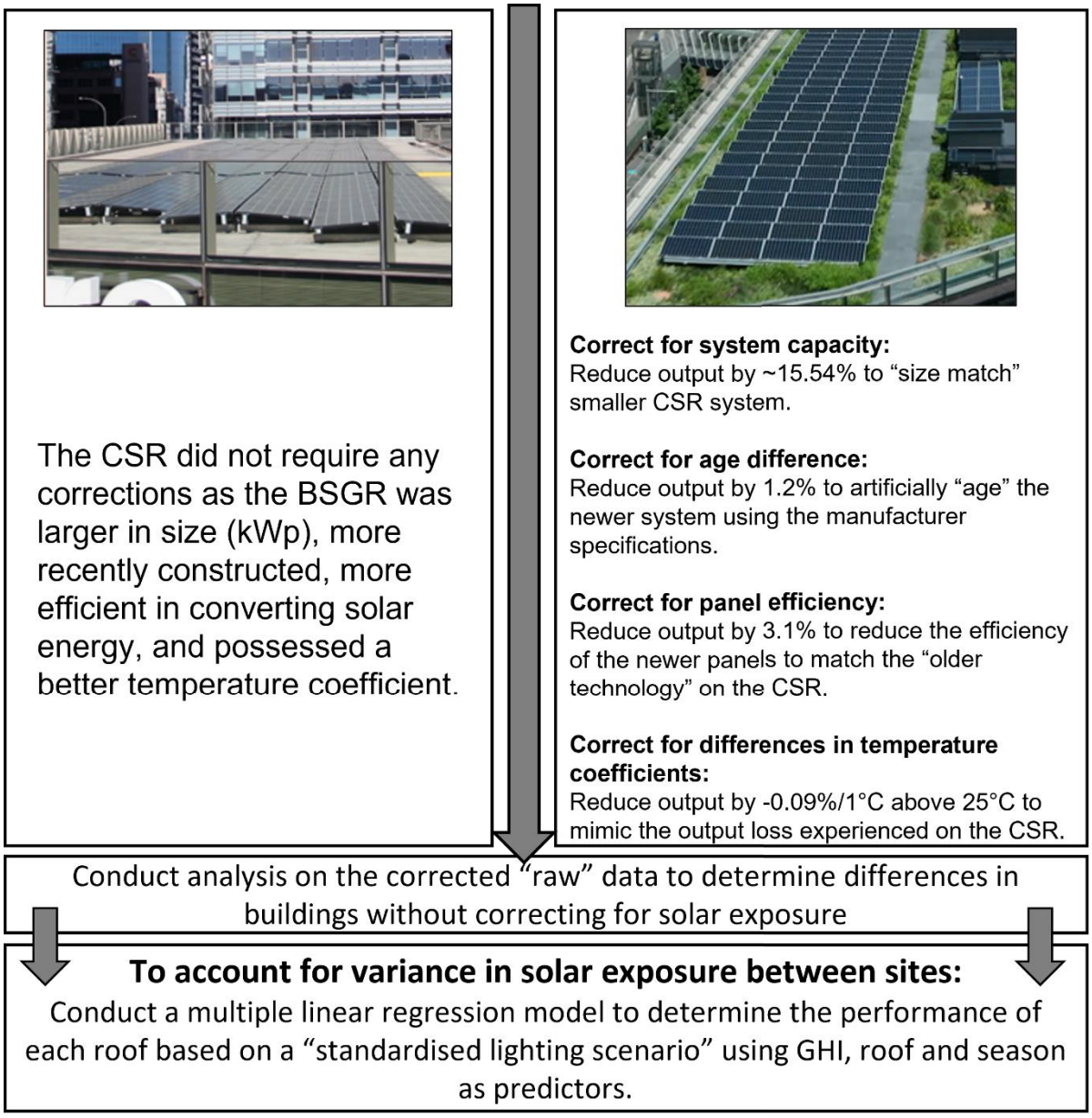

Supplementary Figure 8. Methodological infographic depicting the sequence of corrections applied to the BSGR to reduce the raw energy output to a state in which it is representative of the CSR energy output based on various factors and differences in system design.